1958

Anchorage and bond in pretensioned prestressed concrete members, (Progress Report No. 19), Lehigh University, (December 1958)

G. A. Dinsmore

P. L. Deutsch

J. L. Montemayor

Prestressed Concrete Bridge Members

Progress Report 19

ANCHORAGE AND BOND IN PRETENSIONED PRESTRESSED CONCRETE MEMBERS

by

George A. Dinsmore

Peter L. Deutsch

Jose L. Montemayor

Fritz Engineering Laboratory
LEHIGH UNIVERSITY
Bethlehem, Pennsylvania

Fritz Laboratory Report 223-19

December, 1958

ACKNOWLEDGEMENTS

The research described in this report was carried out in Fritz Laboratory under the auspices of the Institute of Research of Lehigh University as a part of the program sponsored by the Lehigh Prestressed Concrete Committee. The Committee is composed of representatives from the following organizations: The Pennsylvania Department of Highways; The U.S. Bureau of Public Roads; The Reinforced Concrete Research Council; Concrete Products Company of America, Division of the American Marietta Company; American Steel and Wire Division of U.S. Steel Corporation; John A. Roebling's Sons Corporation; and Lehigh University.

The reinforcing strand was donated by the John A. Roebling's Sons Corporation.

Dr. Carl E. Ekberg, Jr., Chairman of the Concrete Division at Fritz Laboratory directs the research program in prestressed concrete. Professor William J. Eney is Director of the laboratory and head of the Department of Civil Engineering.

The valued counsel of Professor Ekberg and the generous assistance of the members of the Division is acknowledged with sincere appreciation.

TABLE OF CONTENTS

TABLE OF CONTENTS (cont'd.)

LIST OF TABLES

LIST OF FIGURES

LIST OF FIGURES (cont'd.)

I INTRODUCTION

A pretensioned concrete beam may fail in one of three ways: flexure, shear or bond. Numerous acceptable methods for predicting ultimate strength in flexure are presently available and considerable current research is devoted to the problem of shear capacity. As yet no practical method of analyzing the bond capacity of a member has been presented. The various analyses of shear and flexure all assume that bond failure will not occur first. Because test data for bond show great statistical variation it is generally agreed that design should be based on flexure and shear and that requirements for bond be so severe as to preclude the possibility of failure in bond.

A member may be said to fail in bond when bond inadequacy results in a significant reduction in the ultimate capacity of the member in flexure or shear. This would occur if the reinforcement slipped--i.e. pulled in from the end of the member with an attendent loss of prestress--or, if the bond in the interior of the member were broken down to the extent that the condition of an unbonded, post-tensioned member were approached. The first case would be considered an anchorage failure, the second a failure in flexural bond.

Flexural bond is much less critical in prestressed than in conventional design because cracking is severly restricted under normal service conditions. The prestressing strands in general use in this country, have large contact surfaces and excellent mechanical bonding action. A failure in flexural bond would require the distruction of the grooves in the concrete at the contact surface over a considerable portion of the member's length. No such failures have been reported.

Numerous tests have indicated the dangers of anchorage bond failures, however. The purpose of this paper is to explore this problem and to report laboratory findings on the bond capacity of 7/16" strands leading to recommendations of a form for design criteria.

To develop the problem in an orderly manner the mechanics of prestress transfer will be considered first. Then the bonding action at the interior of a member as the result of flexure will be explored. Finally the subject of anchorage will be analyzed and the experimental work reported.

II MECHANICS OF PRESTRESS TRANSFER

A. Bonding Action of Smooth Wires

To facilitate this discussion of bond developed at release of prestress, a simple case, that of a prism centrally prestressed by a single smooth wire, will be considered.

In Figure 1a equidistant cross-sectional planes have been arbitrarily selected and labeled aa, bb, etc., starting from the end of the member. Any cross-section unrestricted as to location will be designated xx.

The deformations resulting from release of prestress are idealized in Figure 1b. The member as a whole is shortened by the elastic compression of the concrete. It is assumed for clarity that the prestress transferred between the end of the member and the section under consideration is uniformly distributed over the section except for a local warping or dishing effect in the immediate vicinity of the prestressing tendon. The original sections aa, bb, xx after release are then AA, BB, XX respectively. At the interface between the concrete and steel the concrete has shifted to positions A', B', X' as a result of the local warping. The steel has moved to A", B", X" as a result of the warping and also relative movement of the steel with respect to the concrete.

In the region where the adhesive bond has not been destroyed the displacement of the steel and concrete are necessarily the same, i.e. X' and X" coincide. This region has been termed the "elastic zone". In a sense this is a misnomer. There is no assurance that the concrete at the interface is not stressed beyond the elastic range in the portion adjacent to the friction zone. However, the bond capacity does vary as the stress-strain characteristics of the concrete rather than with a friction coefficient and so may be termed "elastic" in that context.

The region in which adhesion is destroyed giving rise to relative movement between the steel and concrete is termed the "friction zone". Bond transfer in this portion is dependent upon the frictional coefficient of the two

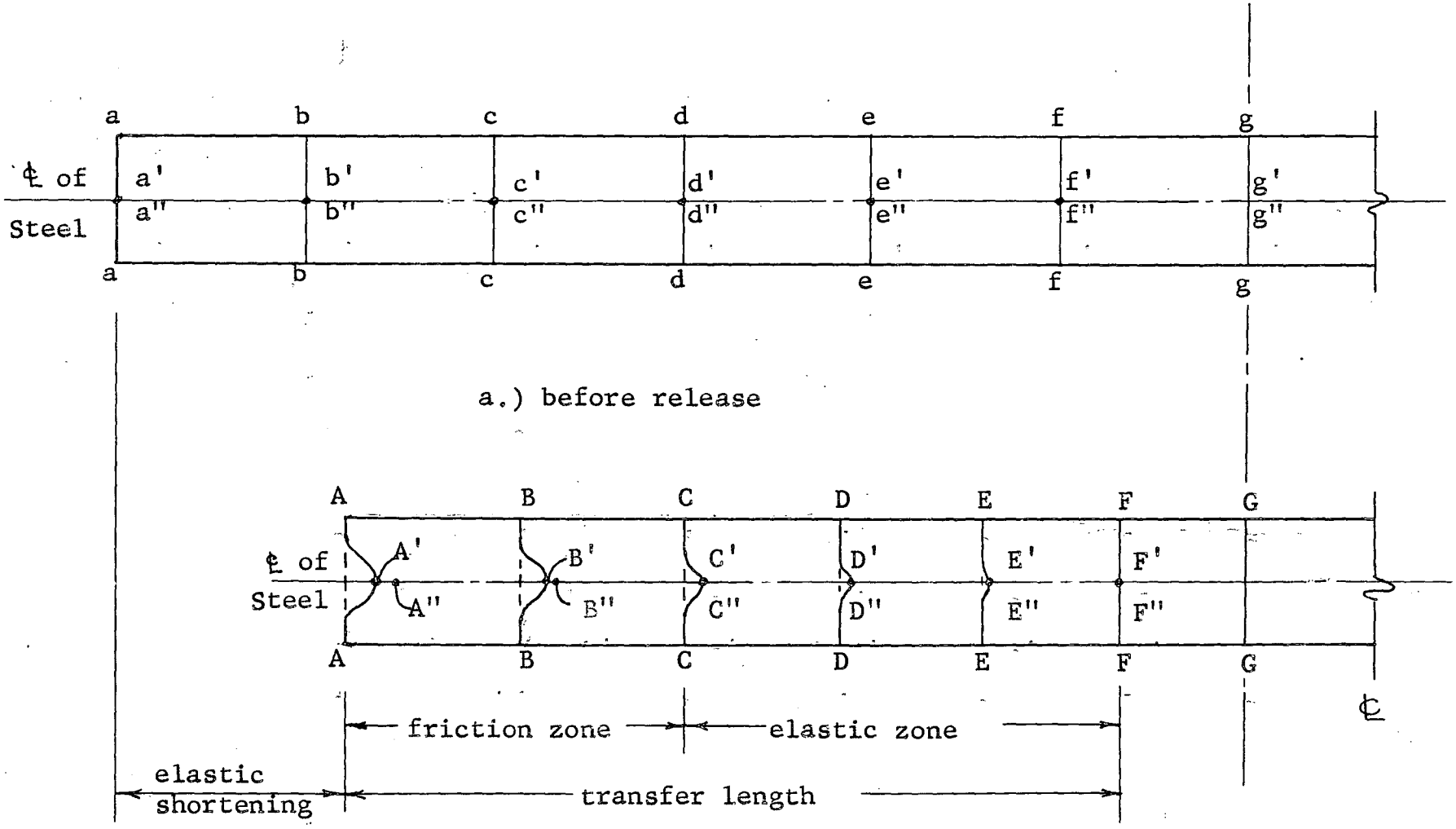

Figure 1. Transfer Zone Deformations Due to Released Prestress

materials and the radial pressure at the interface. A notation for displacements in the elastic and friction zones is established in Figure 2. The portion of the prestress transferred by each of the zones is primarily dependent upon the adhesive bond capacity. For lubricated tendons the transfer would be entirely frictional while for low levels of prestress it might well be entirely elastic.

The bonding phenomena is localized at the interface and can be properly evaluated only by direct observation of the contact surfaces. This is a complex instrumentation problem especially for members with stranded tendons, so most investigations have attempted to evaluate bond stresses from strains measured at the surface of the concrete. There are limitations to this procedure that must be understood.

Suppose for example, an investigator chooses to assume that initially plane sections in the transfer zone remain plane after transfer. This would require in Figure 2 that $g_\chi = 0$ and that Section CC in Figure 1 be the limit of the transfer zone. The transfer would necessarily be entirely frictional. Or, suppose he makes the assumption upon which Figure 1 is based--that prestress transferred between the end of the member and the section being considered is uniformly distributed over the section. On this assumption the end of the transfer zone observed by surface strains should be at section FF.

Actually, of course, FF does mark the end of transfer at the interface but this would be reflected by surface strains at some additional distance from the end of the member, a distance which must be dependent upon the cross-sectional dimensions. All apparent transfer lengths measured at the surface are greater than the actual and the greater the cover, the greater is the error.

Similarly, the use of the curve obtained by plotting surface strains against distance from the end of the specimen in the quantitative evaluation of bond stress can be misleading because the maximum slope of the indicated curve is necessarily less than the slope of a similar curve obtained at the interface. Results obtained by measurements of surface strains are thus seen to be relative, and are comparable only for specimens having the same cover.

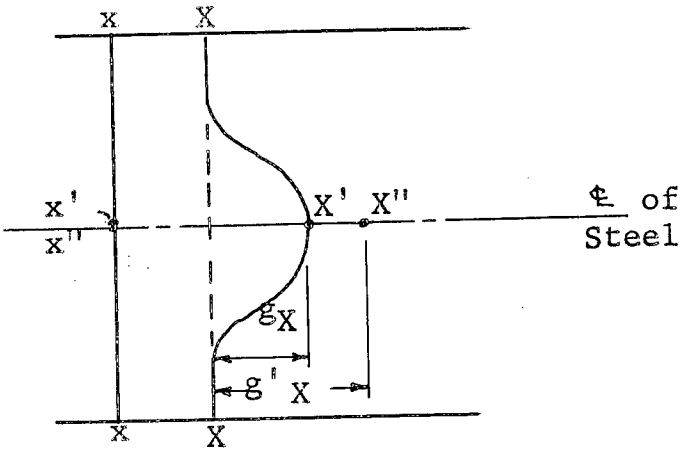

a.) friction zone

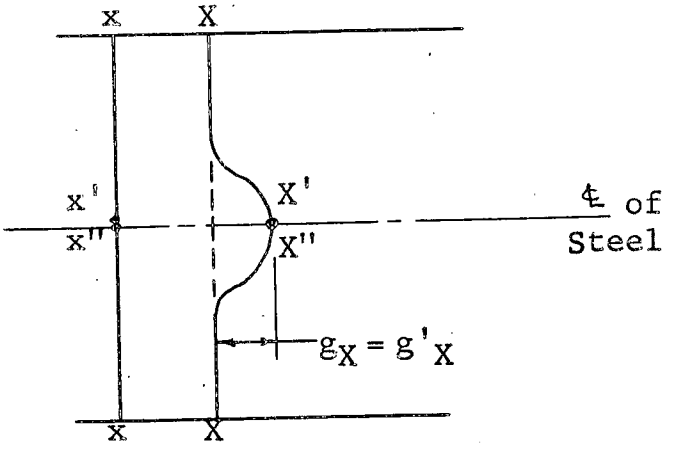

b.) elastic zone

Figure 2 - Local "Dishing" Effect Due to Released Prestress

A mathematical treatment of frictional and elastic transfer bond is given in Appendix A. The expressions obtained agree in form with experimental data, but have not been successfully applied to practical problems.

B. Bonding Action of Strands

The familiar seven-wire strand is inherently favorable to effective bonding. Because strand cross-section is not a true circle, there are "ridges" of concrete which fill the "valleys" between the exterior wires. And since the strand is wound in a helical pattern, these ridges will also follow the exact helical pattern of the wires in their displaced position due to initial prestress. Upon release, there is relative displacement between steel and concrete. But, while a single smooth wire slips straight in without any rotation, a strand must rotate, or screw-in, as a threaded bolt, following the predetermined grooves in the concrete. Also, as the stress in the steel is decreased from its initial pre-release value, the strand not only expands radically, due to Poission's ratio, but alwo decreases in length, longitudinally. This decrease in length is represented by a decrease in pitch of the original helical pattern of the strand. Since, in the friction zone, the decrease in steel strain is greater than the increase in concrete strain, $g'_x > g_x$, at the interface, the amount that the steel pitch decreases will be limited by the amount that the pitch of the concrete ridges decreases. This effect results in a mechanical bonding as shear stresses are developed along the concrete ridges.

This shear resistance adds to the pure friction resistance to make the force transferred in the friction zone of a strand greater than that of a straight cable having the same cross-sectional perimeter. The total length of the friction zone for strand will therefore be less than that of the similar straight cable (wires touching). The bond capacity of either a strand or similar cable is greater than that of a single smooth wire of equal area simply because of their greater cross-sectional perimeters. The means of bond development in the friction zone for a strand, therefore, is not friction alone, but is a combination of friction and the resistance of the concrete ridges to mechanical shearing. Evans and Williams (1) point out this fact to explain why the transfer lengths

for strand and deformed wires do not increase significantly with time as do those for plain wires. The increased length is the result of radial creep which lessens the radial force necessary to develop the frictional forces. Mechanical bonding forces developed by shear can be only slightly affected by creep in the concrete.

III CONSIDERATION OF FLEXURAL BOND STRESSES

There has been much confusion as to the available means of evaluating flexural bond stresses and in particular, great abuse of the familiar expression $u = V/\Sigma_o\, a$ in which V is total shear, Σ_o is total perimeter and "a" is the distance from the centroid of the steel to the resultant of the resisting forces developed in the concrete.

All expressions for bond stress are basically founded on the equilibrium of a segment of reinforcing

(Figure 3) From which:

$$T_R - T_L = \Delta T \qquad T = u \Sigma_o \Delta X$$

$$u_{avg} = \frac{\Delta T}{\Delta X \Sigma_o} \tag{III-1}$$

or

$$u = \frac{1}{\Sigma_o} \frac{dT}{dX} \tag{III-1a}$$

Various forms are derived by appropriate substitutions for ΔT. Derivations for both prestressed and conventionally reinforced beams will be considered for the following conditions: precrack, postcrack and ultimate.

A. Before Cracking

(1) Non-Prestressed

The forces acting on a segment of a conventionally reinforced uncracked beam inflexure are shown in Figure 4. Elastic strains in the concrete produce forces T_c and C_c in the concrete. The resultant of these, C, is at an elevation "a" above the steel centroid. The steel forces, Ts, are given by:

$$T_{SL} = M_L \frac{en\, A_s}{I_c} \qquad T_{SR} = M_R \frac{en\, A_s}{I_c}$$

Substituting into (III-1)

$$u = \frac{(M_R - M_L)}{\Delta X} \frac{en\, A_s}{\Sigma_o I_c} = \frac{V}{\Sigma_o} \frac{en\, A_s}{I_c} \tag{III-2}$$

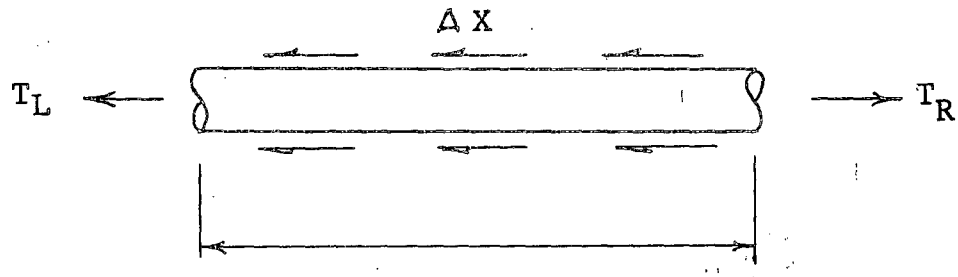

Figure 3 - Free-Body Diagram of an Element of Reinforcement

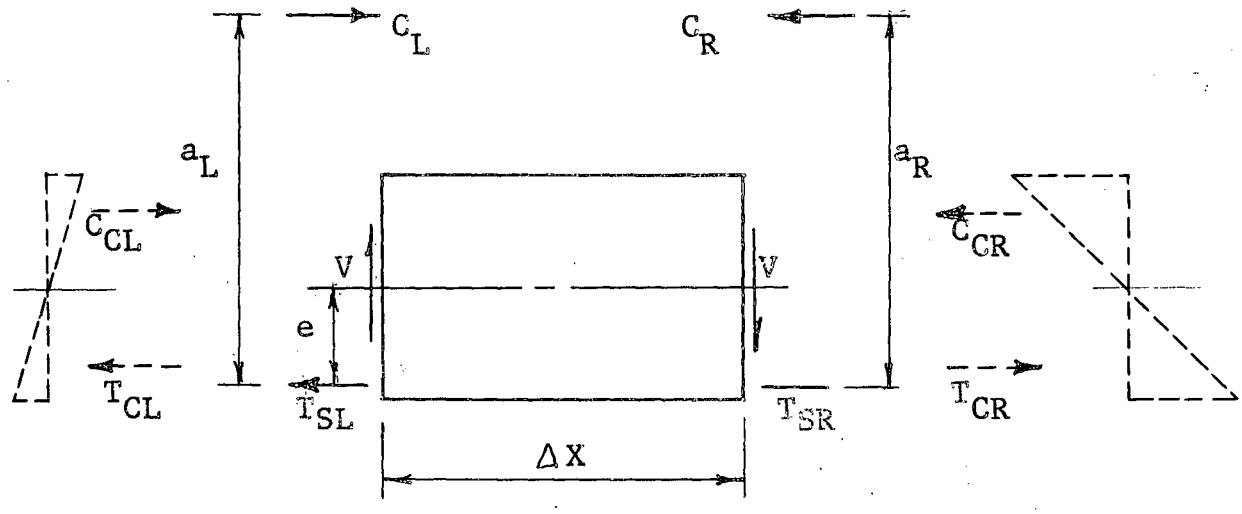

Figure 4 - Forces Acting on an Element of a Non-Prestressed Beam

This expression may be written in the form $u = V/\Sigma_o a$ as follows:

$$a_L = \frac{M_L}{T_{SL}} = \frac{I_c}{en\ A_s} \qquad a_R = \frac{M_R}{T_{SR}} = \frac{I_c}{en\ A_s}$$

Therefore "a" is a constant and III-2 becomes $u = \frac{V}{\Sigma_o a}$

Values of "a" are extremely large in usual cases and bond stresses trivial.

(2) Prestressed

A segment of the member remote from the transfer zone is shown in Figure 5. Upon release of prestress the concrete strains shown in Figure 5a produce a total resisting force, C_e in the concrete equal and opposite to the effective prestress, T_e, acting in the steel. Flexure due to dead and live load sets up the additional internal forces shown in Figure 5b. The resultant of the tensile and compressive forces in the concrete, Tc and Cc, is C, located a distance b above the centroid of the steel. This figure is similar to the non-prestressed case, and by the same arguement:

$$b_R = b_L = \frac{I_c}{en\ A_s}$$

The combined internal forces are given in Figure 5c. The change in the steel tension across the segment is

$$\Delta T = T_{SR} - T_{SL}$$

where

$$T_{SL} = M_L \frac{en\ A_s}{I_c} \qquad T_{SR} = M_R \frac{en\ A_s}{I_c}$$

Substituting into (III-1)

$$u = \left(\frac{M_R - M_L}{x}\right)\left(\frac{en\ A_s}{I_c}\right) = \frac{V}{\Sigma_o}\left(\frac{en\ A_s}{I_c}\right) \qquad \text{(III-4)}$$

an expression identical to equation (II).

This expression can be written as:

$$u = \frac{V}{\Sigma_o b} \qquad \text{(III-5)}$$

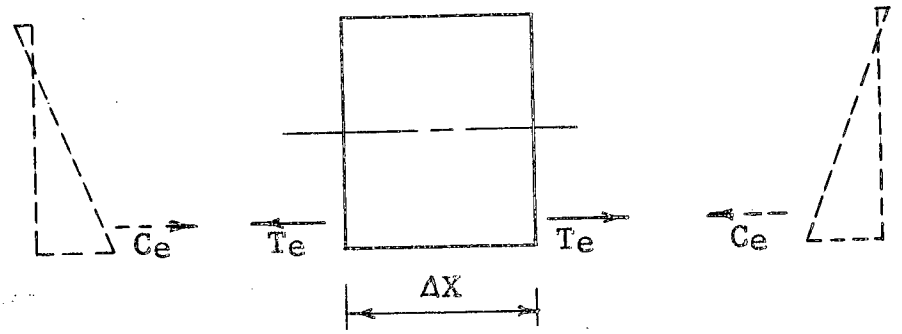

(a)

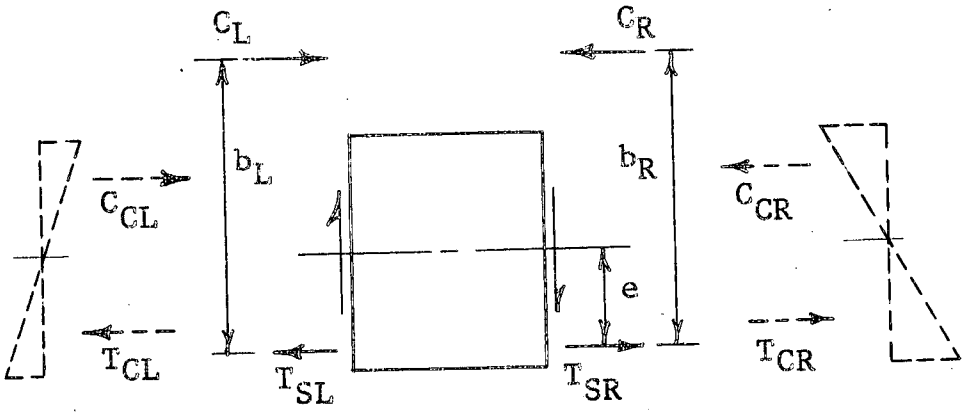

(b)

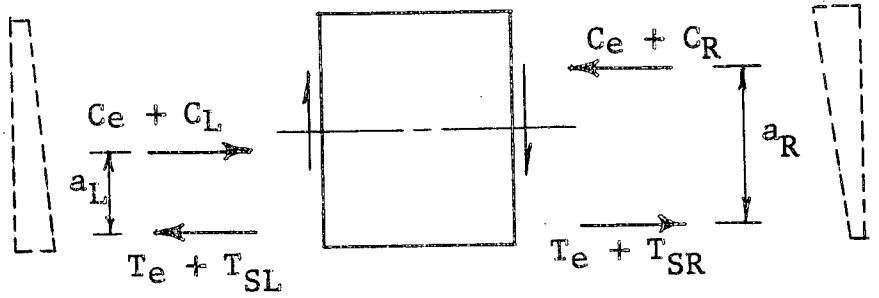

(c)

Figure 5 - Forces Acting on an Element of a Prestressed Beam

which is obviously quite different from the widely used form $u = V/\Sigma_o a$.

The total moment arm, a, is given by:

$$a_L = \frac{M_L}{T_e + T_{SL}} = \frac{M_L}{T_e + M_L\left(\frac{en\ A_s}{I_c}\right)}$$

$$a_R = \frac{M_R}{T_e + T_{SR}} = \frac{M_R}{T_e + M_R\left(\frac{enA_s}{I_c}\right)}$$

It is thus demonstrated that "a" is a variable, a function of both prestressing and applied moment. Near the end of a member, as M approaches zero, "a" also approaches zero. If the expression $u = V/\Sigma_o a$ were correct, flexural bond stress would be a minimum under the load and infinite at the support.

From Equations III-3 and III-4 it should be noted that bond stresses before cracking are very small for prestressed members and are independent of the degree of prestress except insofar as the prestressing determines the cracking load.

B. After Cracking

(1) Non-Prestressed

In the design of conventionally reinforced members bond stresses are computed for the cracked section at design load by $u = V/\Sigma_o jd$, where jd has the same meaning as "a", and is compared with an allowable value. The derivation follows from a figure similar to Figure 4 except that the tensile concrete is inoperative, its load being transferred to the steel. Thus both T_S and C increase sharply at cracking and "a" assumes a value which is constant so long as both steel and concrete are elastic and is less than the effective depth. Hence, either Equation III-2 or III-3 may be used in the evaluation of the bond stress so long as I_c of the cracked section is used.

Of course bond stresses computed by these formulae are ficticious quantities. The very opening of a crack requires the destruction of adhesive bond in the immediate vicinity. The adrupt change in the direction of the reinforcing as the crack widens, gives rise to high normal forces

and consequent highly effective frictional bonding, (Evans and Robinson) (2). Throughout the cracked zone the neutral axis must undulate between cracks. This alone would cause wide variations in bond stress. The design formulas and allowable stresses merely serve to correlate beam design with test results to assure satisfactory overall behavior.

(2) Prestressed

In the case of prestressed members after cracking, the theoretical moment of inertia and position of the neutral axis vary along the length of the beam as a rather complicated function of the applied moment, ruling out the use of Equation III-4. Average bond stresses can be found only by the computation of steel force at successive sections and the application of these values to Equation III-1. The evaluation of the steel forces can be performed with reasonable ease by the method presented by Warner (3).

Bond stresses between cracking and ultimate loads are of little practical interest. The most severe bond stresses must be present at ultimate and it is only these values which are significant in design since the bond capacity of the member is required to exceed the ultimate capacity of the member.

C. At Ultimate Load

Conditions in both conventionally reinforced and prestressed beams are essentially the same at ultimate load.

In under-reinforced beams the maximum bond stresses at ultimate do not occur at the section of maximum moment and shear because of the plasticity of the steel at high stress levels. The free-body diagram of Figure 6 illustrates the point. The applied loading is such that the externally applied moment is a maximum at the right face. As ultimate load is approached the steel yields plasticly. The crack widens and the neutral axis progresses upward. At the left face, where the moment is somewhat less, the same effect occurs but lags behind the action at the right. After the steel has yielded at both faces, then, there is no differential of steel force and bond stress is zero. The difference in moment is accomodated by the difference in the moment arms a_R and a_L.

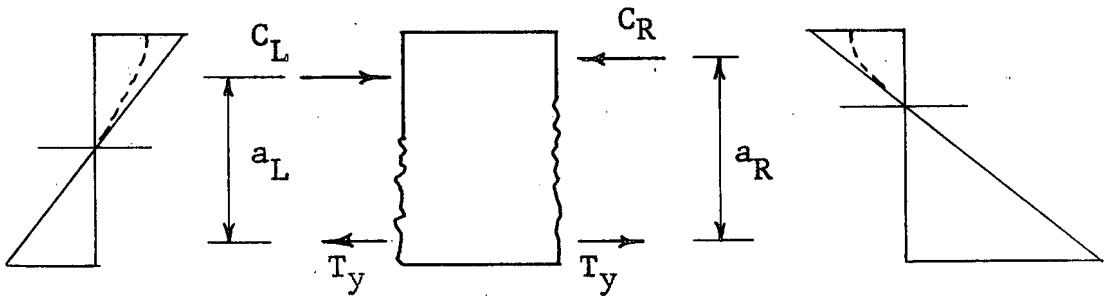

Figure 6 - Equilibrium of Element of Beam at Ultimate

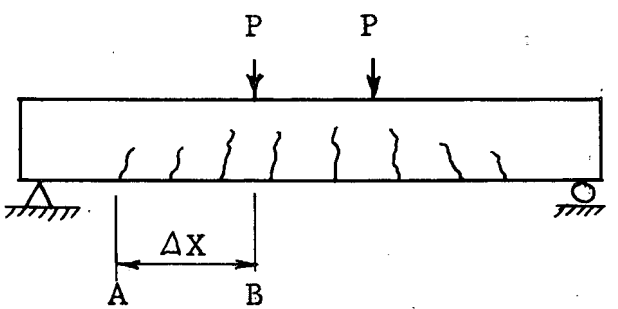

Figure 7 - Sketch of Cracked Beam

Since the maximum bond stresses do not occur close to the section under maximum moment and certainly not in the uncracked portion where they have been shown to be negligible, the greatest flexural bond stresses must develop at a section somewhere between the two.

It is most unlikely that a practical procedure for evaluating the maximum stress can be found because of the uncertainties of crack spacing and local effects. It would be quite reasonable, however, to apply Equation III-1 to the entire region between the section of maximum moment and the outermost crack to obtain a value of average bond stress which could be used in the comparison of experimental results.

Consider the under-reinforced pretensioned beam of Figure 7 for example. As ultimate load is approached the strand force at B approaches T while just to the left of A it may be considered essentially T_e, the effective prestress.

Then $$u_{avg.} = \frac{T_{ult} - T_e}{\Sigma_o \Delta X}$$

Values given by this equation for measured lengths Δx would be somewhat higher than actual because the strand force actually approaches Te same distance beyond the outermost crack, but nevertheless would offer a sound basis for comparison.

It is again emphasized that $u = V/\Sigma_o a$ is not valid at ultimate load for either conventional or prestressed members.

IV. The Problem of Anchorage Bond

The anchorage developed in a pretensioned member is in large measure dependent upon both the transfer of prestress and flexural action. The transfer length provides full anchorage for the strand at effective prestress. When flexure causes an increase in strand tension, additional embedment length is required to transfer the additional force.

It has been previously shown that the increase in strand tension due to flexure is quite small in the uncracked portions. If, however, the outermost crack were to occur close

to the transfer zone, the relatively large increase in strand tension could not be transferred in the short distance between the crack and the end of the transfer zone. The pull-out action would penetrate into the elastic portion of the transmission length, with the result that bond would become entirely frictional and mechanical over the entire length from the end of the member to the crack. The slightest additional increase in strand tension would then result in slip of the strand.

Consider a pretensioned beam as ultimate load is approached. The steel at the section of maximum moment is first to yield plasticly. At adjacent cracks steel strain is considerably less, but stress is essentially the same. While it is conservative to do so, it is not unrealistic to assume, then, that at ultimate load the strand force in an under-reinforced beam is the ultimate strength of the strand over the entire cracked portion. In this context the beam may be thought of as a post-tensioned member whose end anchorage is developed by bond over the embedment length L_e where L_e is the distance from the end of the member to the outermost flexural crack.

Such a condition is simulated by a beam as shown in Figure 8. Bond in the central portion is destroyed by encasing the strand in a tube or by some similar device. When the prestress is released to this member, the prestressing force in the strand builds up to its effective level over the transfer length L_t. Should the required transfer length be greater than the available embedment length, L_e, bond failure must occur at release of prestress. But, if the embedment length is great enough so that the beam withstands the transfer of prestress and the beam is subsequently loaded, increasing the strand force at the unbonded interior of the beam, the tendency for the strand to slip and screw inward is likewise increased. If at a given load the embedment length is not sufficient to develop a total bond force equal to the strand tension, the strand must slip.

For any particular type and size of prestressing steel there must theoretically exist a certain length of embedment which will provide just sufficient anchorage bond to develop its full tensile capacity. This embedment is the "ultimate anchorage length". Therefore, the ultimate anchorage length is that length of embedment which will permit the development of the ultimate strength of the steel just prior to bond failure or slip. It seems evident, therefore, that an

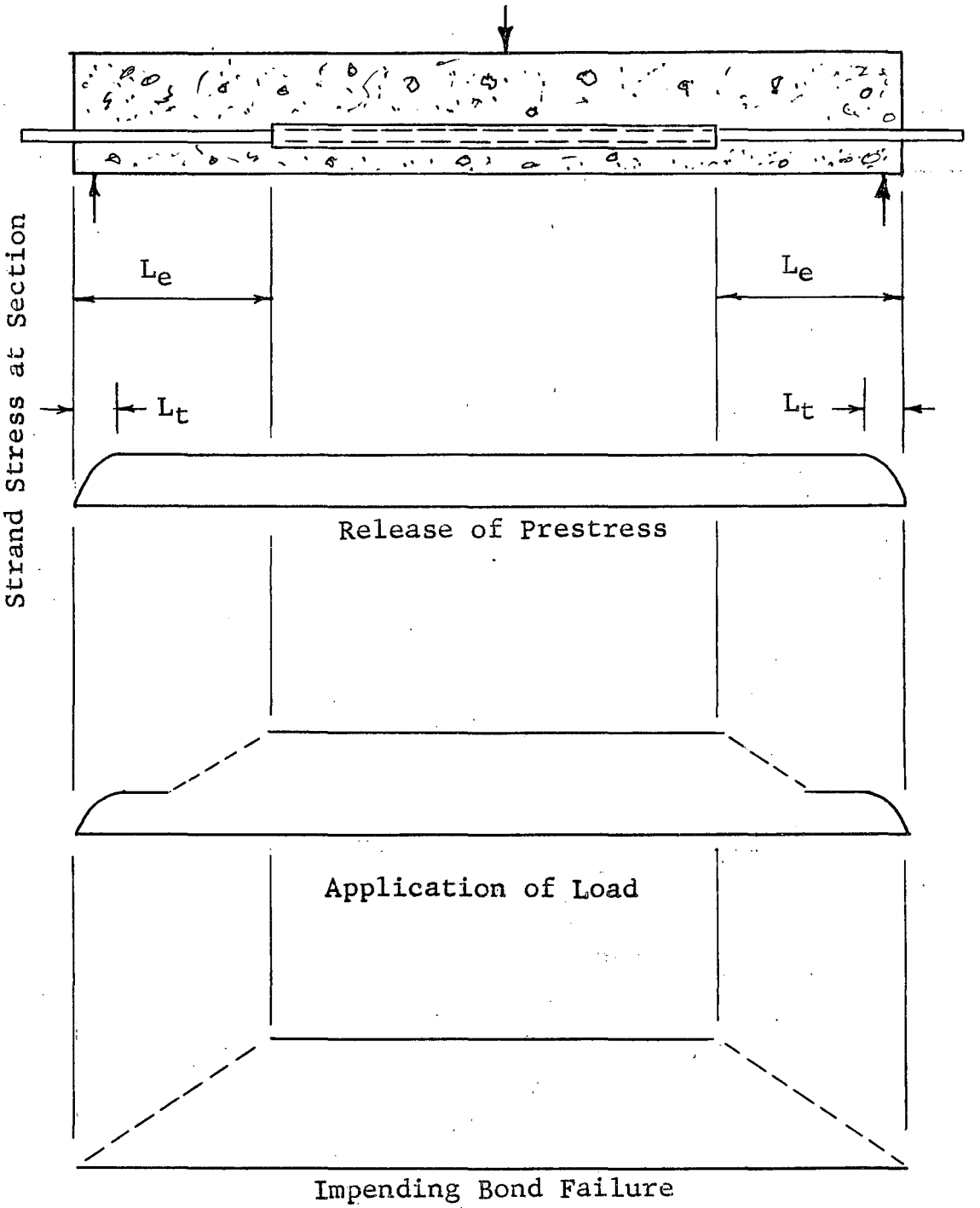

Figure 8 - End Anchorage Concept

embedment length less than the ultimate anchorage length will develop some level of strand tension less than its ultimate strength. Consequently, a "Slip-Limit Envelope", shown in Figure 9, which defines the bond capacities of various embedment lengths, may be postulated.

The solid curve indicates the steel stress distribution after release and all losses. The prestress is fully transferred over the length designated as the transfer length. The dashed curve indicates the various steel tensions which can be developed at various embedment lengths without slip. Any combination of steel tension and embedment length falling outside the slip limit envelope, i.e., falling in Area 1, should produce a bond failure. A combination giving a point within the envelope, i.e., in Area 2, would be expected to perform safely.

The basic idea of bond characteristics as defined by a slip limit envelope was initiated by Thorsen (4). He also proposed various methods for its determination, one of which, the pull-out test, was used in this investigation.

V. Available Anchorage Length in a Beam at Ultimate Load

To assure adequate anchorage, the embedment length available to provide anchorage must exceed the ultimate anchorage length. The available embedment is the distance from the outermost flexural crack crossing the reinforcement to the point of initial contact between the concrete and steel. Obviously a procedure is required by which the location of the outermost crack may be predicted with reasonable accuracy.

A simple approach can be made by an assumption of overall elastic behavior. The moment diagram at ultimate load is plotted as in the sketch below.

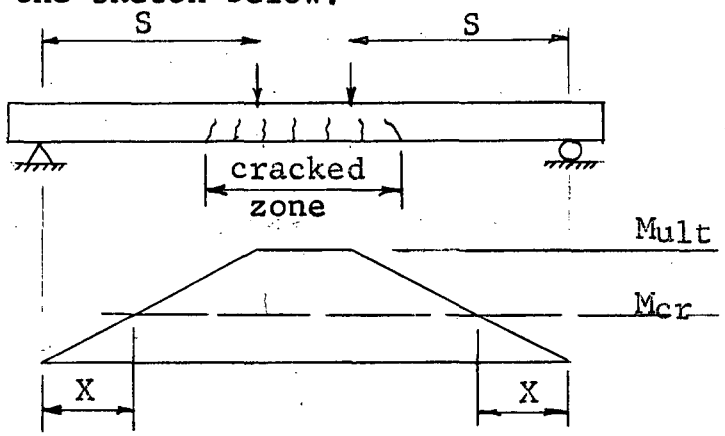

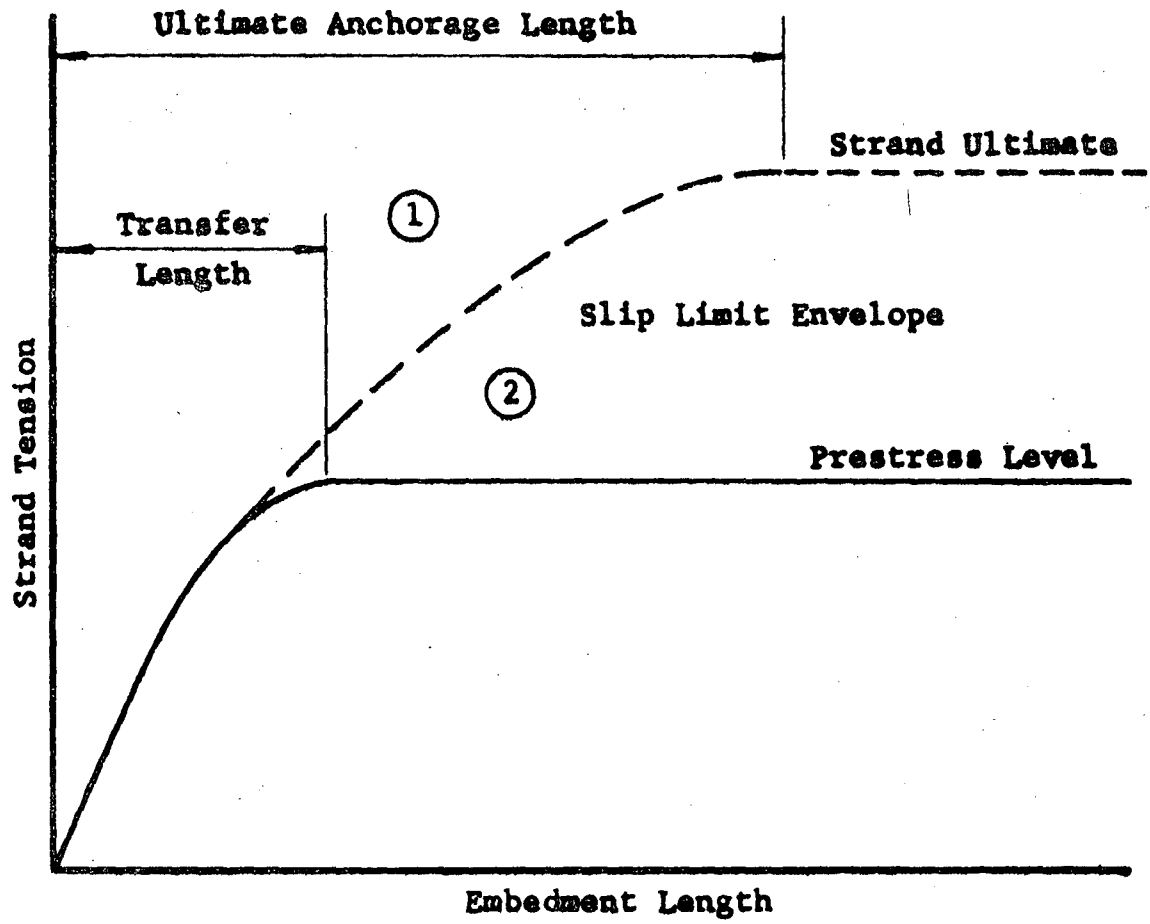

Figure 9. The Slip-Limit Envelope

The cracking moment is calculated from a suitable value of rupture modulus* and superimposed on the diagram. The intersections should locate the outermost cracks. For the simple loading given (and neglecting dead loads),

$$X = \frac{S}{M_{ult}/M_{cr}}$$

where X is the distance from the support to the outermost crack originating at the bottom fiber, and S is the shear span.

The values of X given by this relation are unrealistically small. If the approach were valid, new cracks would continue to develop under increasing load extending the cracked zone to a maximum length at ultimate. In laboratory tests, however, it is observed that the zone of flexural cracking is fully established at a load usually much less than the ultimate. Additional cracking under increased loads is confined to the existing cracked zone. This suggests that the simplicity of the approach might be retained with satisfactory results if a reduced value of the ratio M_{ult}/M_{cr} were used. Designating the reduced ratio by C, for beams loaded as above,

$$C = \frac{S}{X}$$

Data from 44 static tests of the rectangular beams listed in Table I were examined. In several of the tests strand slip and/or shear failure occurred, but only after the flexural cracking region had been fully defined. The distance X was scaled from photographs of the ruptured specimens and C calculated for each end. The 88 values lay between 1.0, for specimens with a single crack, to 1.72 for one whose outermost crack did not progress to the height of the reinforcing. The average was 1.33.

---

* Analysis of 212 rupture modulus specimens reported in the literature resulted in the lower bound expression:

$$MR = \frac{8}{9} (f'_c)^{-3/4}$$

TABLE I - CRACKING CHARACTERISTICS OF PRESTRESSED BEAMS IN LABORATORY TESTS

Beam No.	Source (Ref. No.)	f'_c at Test psi	P/P_b	% of Allowable Prestress	L ft.	S ft.	X Measured ft.		X** Computed ft.
1	20(RSI)	4200	6.69	100	11.5	5.00	3.8	3.8	3.1
2	21(A)	8850	1.09	100	18.0	6.25	4.1	4.4	3.9
3	21(D)	7730	1.24	100	18.0	6.25	4.0	4.1	3.9
4	21(F)	5750	1.68	100	18.0	6.25	4.0	4.4	3.9
5	22(3AI)	4780	1.09	100	11.5	5.75	4.0	3.2	3.6
6	22(3AII)	6150	0.84	100	11.5	5.75	4.2	3.8*	3.6
7	22(3BI)	4780	1.09	100	11.5	3.84	2.9	3.0	3.4
8	22(3BII)	6150	0.84	100	11.5	3.84	3.0	2.7	2.4
9	23(2B)	6200	0.22	100	10.0	3.75	5.0	5.0	2.3
10	23(2B)	6200	0.22	100	10.0	3.75	5.0	5.0	2.3
11	24(AI)	4020	1.52	100	11.5	3.84	3.2	3.2	2.4
12	24(AII)	7040	0.88	100	11.5	3.84	3.1	3.0	2.4
13	24(AIII)	8270	0.74	100	11.5	3.84	3.8	3.2	2.4
14	24(BI)	4020	1.52	100	11.5	3.84	3.1	3.5	2.4
15	24(BII)	7000	0.88	100	11.5	3.84	2.0	3.1	2.4
16	24(BIII)	6880	0.90	100	11.5	3.84	2.2	2.6	2.4
17	25	6810	1.93	76	11.0	3.67	2.9	2.8	2.3
18	26(B5)	6140	0.62	100	11.5	5.75	4.3	3.8	3.6
19	26(B5)	6140	0.62	100	11.5	3.84	2.8	3.2	2.4
20	27(2AI)	5530	1.11	100	11.5	5.75	4.6	3.8	3.6
21	27(2BI)	5540	1.11	100	11.5	5.75	4.0	4.3	3.6
22	27(2AII)	7430	0.83	100	11.5	5.75	3.2*	3.5*	3.6
23	27(aBII)	7590	0.81	100	11.5	5.75	3.3*	3.9	3.6
24	27(2AIII)	7800	0.81	100	11.5	5.75	3.6*	3.8	3.6
25	27(2BIII)	6870	0.89	100	11.5	5.75	3.3*	4.2	3.6
26	28(A3)	6460	1.32	31	9.0	3.00	1.9	2.5	1.9
27	28(A4)	6150	1.39	31	9.0	3.00	2.2	2.1	1.9
28	28(A5)	6410	1.33	58	9.0	3.0	2.3	2.2	1.9
29	28(A6)	6260	1.36	58	9.0	3.00	2.0	2.9	1.9
30	28(A7)	6140	1.39	85	9.0	3.00	2.7	2.4	1.9

Table I (Concld.)

Beam No.	Source (Ref. No.)	f'_c at Test psi	P/P_b	% of Allowable Prestress	L ft.	S ft.	X Measured ft.		X** Computed ft.
31	28(A8)	6260	1.36	85	9.0	3.00	2.9	2.7	1.9
32	28(A9)	6320	1.35	90	9.0	3.00	2.8	3.0	1.9
33	28(A10)	6320	1.35	90	9.0	3.00	2.8	2.8	1.9
34	28(B1)	6000	1.15	81	9.0	3.00	2.1	2.3	1.9
35	29(B2)	6150	1.15	81	9.0	3.00	2.3	2.3	1.9
36	28(B3)	7430	1.11	80	9.0	3.00	2.0	8.8	1.9
37	29(B4)	7430	1.11	80	9.0	3.00	2.6	2.3	1.9
38	28(B5)	6610	1.13	81	9.0	3.00	2.4	2.7	1.9
39	28(B6)	6610	1.13	81		3.00	2.3	2.2	1.9
40	29(G3)	5390	2.16	100	12.0	3.50	4.6	4.1	2.2
41	29(G6)	5600	1.85	100	12.0	5.25	3.5	3.2	3.3
42	29(P1)	6400	1.74	100	12.0	5.25	4.3	4.1	3.3
43	29(P2)	6400	1.74	100	12.0	5.25	4.3	4.2	3.3
44	29(P3)	6780	1.64	100	12.0	5.25	4.1	3.6	3.3

* Outermost crack did not progress above reinforcing. If this crack be neglected, x measured x computed.

** $X = \frac{S}{1.6}$

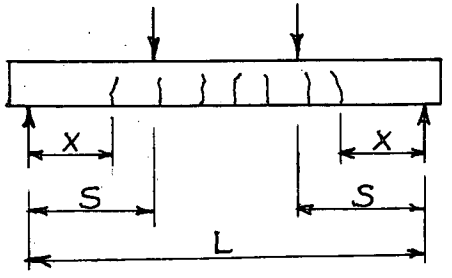

The data covers a broad range of steel ratios, concrete strengths, degrees of prestress, and strand sizes, but no emperical expression could be found for C as a function of these variables to give more consistant and safe values of X than are obtained by taking C a constant

$$C = 1.60$$

Values of X as computed, using this constant are compared with the observed lengths in Table I. In six cases the outermost observed crack did not attain the elevation of the steel. Had those cracks been neglected in the measurement the computed length would have been conservative in each instance. The computed length is unsafe in three additional cases, but only slightly so.

A number of full scale pretensioned beams have been tested in Fritz Laboratory. In some cased the members were subjected to dynamic as well as static loading, but this did not appear to materially influence the overall crack patterns. Observed and calculated values of X for these specimens are listed in Table II. The comparisons are again favorable. Computed values of X are in all cases less than those observed, but sufficiently close for practical purposes.

For any pretensioned beam, then, the distance X from the support to the outermost crack is found by plotting the live load moment diagram, or the curve of maximum moments, with a maximum ordinate of 1.6. The intercepts of the moment curve with a level line of unity locates the outermost cracks. The available embedment length L_a is the sum of X and the overhang except in instances where bond of some strands has been prevented at the ends of the beam to improve stress conditions in that region. In these circumstances L_a is the distance from outermost crack to the point of initial contact between steel and concrete.

The above discussion has been restricted to flexural cracks commencing at the bottom fiber. Diagonal tension cracks formed in the web may progress downward crossing the reinforcing. In beams with sufficient web reinforcing to assure flexural rather than shear failure it is unlikely that such cracks will develop sufficiently to cause strand slip, but the possibility cannot be fully excluded.

T A B L E II

CRACKING CHARACTERISTICS OF FULL SCALE BEAMS

Beam	Span Ft.	Shear Span Ft.	Section	X Measured		X Computed
1	67.3	23.0	36" x 33" Box Rectangular Void	16.0	14.8	14.4
2	54.0	23.0	do	15.0	16.0	14.4
3	67.6	33.8	48" x 33" Box, Rect. Void 4" Composite Deck Slab	27.5	26.5	21.1
4	36.0	12.0	36" x 21" Rect. 2 Voids 12-1/2" Dia.	9.2	9.6	7.5
5	39	13.0	Dbl Tee 48" x 14" Lightweight Concrete	8.8	?	8.2
6	39	13.0	Dbl Tee 48" x 14"	9.3	8.9	8.2

VI. DESCRIPTION OF PULL-OUT TESTS

A. Test Approach

The method selected for the determination of the slip limit envelope was the simple pull-out test. The tests can actually be thought of as "pull-in" tests since they simulate the pulling phenomenon of the strand in the available anchorage length of beams due to beam action. They are assumed to reproduce, with sufficient accuracy, the conditions existent in the uncracked end regions of fully bonded members with fully developed crack patterns until the instant of first slip.

The results of pull-out tests are conservative with respect to actual beam behavior. Pull-out tests indicate bond behavior with the concrete in compression, while in beams the stress is tensile. The diameter of the interface of the concrete and steel will expand due to compression of the concrete, and conversely, it will decrease if the concrete is in tension. Therefore, pull-out tests are conservative in this respect. Four beam tests were performed to demonstrate that the effect of the state of stress in the concrete is of minor importance.

Another reason why these reported pull-out tests are conservative is that strand intended for commercial use is generally exposed to the atmosphere with the result that a light coating of rust develops. The bonding properties of rusted strands have been shown to be better than those of clean strand. Also, a thoroughly clean strand exhibits the poorest bonding properties with the exception of strands whose surfaces have been artifically lubricated. Since accidental strand impregnation with oil is generally not a problem in commercial practice the tests are conservative in this respect also.

The degree of conservatism of pull-out tests is even more pronounced after first slip has occurred. Any slip of a strand, must be accompanied by strand rotation. In a simple pull-out test the extent to which the strand may pull in and rotate after initial slip is unlimited. In a beam, however, if the strand rotates as it slips in, the strand beyond the region of bond failure, say at the other side of the crack, must rotate also. But this strand cannot rotate freely. It is still effectively embedded in concrete. Even if this strand has slipped from the other direction also, it must rotate in a direction opposite to that accompanying the first slip to

allow the second slip to take place. Therefore, the amount of subsequent slip after first slip in a beam will be governed by the resistance of the strand itself to torsion, plus the shearing resistance of the concrete ridges, and friction. The pull-out tests are thus seen to represent actual beam behavior only up to the instant of first slip. Since the determination of the load causing slip for various lengths of embedment was the main purpose of the tests, the test approach is fully valid.

Though beam tests would provide an exact indication of the actual bond phenomena, the pull-out method has many unique advantages. Pull-out tests

(1) are economical.

(2) provide a clearer picture of longitudinal strain distribution. In beam tests it would be necessary to separate flexural strains from the total longitudinal strains at the end of the member to gain a clear picture of the effect of bond distribution.

(3) do not require elaborate testing machines.

(4) decrease the minimum amount of instrumentation required.

(5) allow more specimens to be tested in any given length of time.

The primary purpose of the tests was to determine the slip-limit envelope. The secondary purpose, although equally important, was to investigate and analyze bond distribution. To facilitate the interpretation of results, only one size of strand, 7/16 inch nominal diameter, was used, and only one concrete strength, 6,000 psi, was designated. The cross-sections of the specimens were the same except for those of Series IX and X.

B. Description of the Test Specimens

Forty-two pullout specimens were tested. All were prismatic and approximately square in cross-section. The specimens of the first eight series of tests were of various lengths (See Table X) and all 4" x 4" in nominal cross section. The cross-sections of Series IX and X were nominally 2-1/2" x

2-1/2" and 6" x 6". Their lengths are reported in Table XI. The specimens were all reinforced by a single, centrally located 7/16 inch pretensioned strand, with the exception of Series VII in which the strand was untensioned. The actual cross-sectional dimensions appear in Table III.

TABLE III TEST SPECIMEN DIMENSIONS

Series	Spec. No.	Cross-Section width x depth
I to III	all	4" x 4"
IV to VIII	all	4-1/8" x 4"
IX	1,3	6-1/2" x 6"
	2,4	2-1/2" x 2-1/2"
X	1,3	2-1/2" x 2-1/2"
	2	6-1/4" x 6"
	4	6-1/4" x 6-1/8"

Except for the first two series of pilot tests, the strand used was clean, without a trace of rust. Oil and dirt were removed by a thorough cleansing with acetone. The strand was stored in a dry atmosphere so that the rusting of strands was not a problem and the test variables to be analyzed were kept to a minimum.

C. Testing Sequence

The testing setup and the sequence of operations is outlined in Figure 10. The prestressing bed is seen to be essentially a rigid steel frame. Mechanical jacks bearing against the frame push against a movable beam. The strand is tensioned between the floating beam and the far end of the frame as the jacks are loaded. The specimen is then poured around the tensioned strand with one end bearing firmly against the jacking end of the frame. After the specimen is cured, the strand at the free end is burned and the specimen is then equivalent to the end portion of a cracked prestressed beam. The pull-in test is accomplished by additional jacking at the bearing end which produces increased strand forces simulating those arising from applied moment in a beam. The jacking is continued until the strand slips or ruptures.

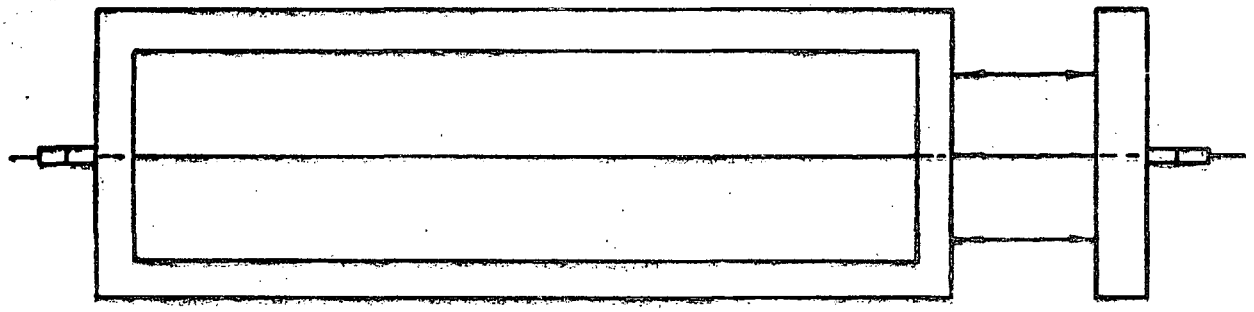

7/16" Strand Tensioned to 18,900 Lbs.

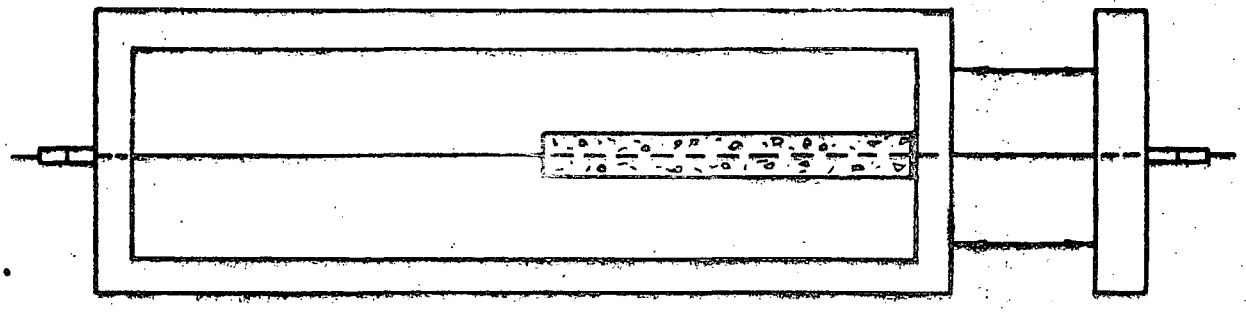

Beam Cast With One End Cast
Against Bulkhead

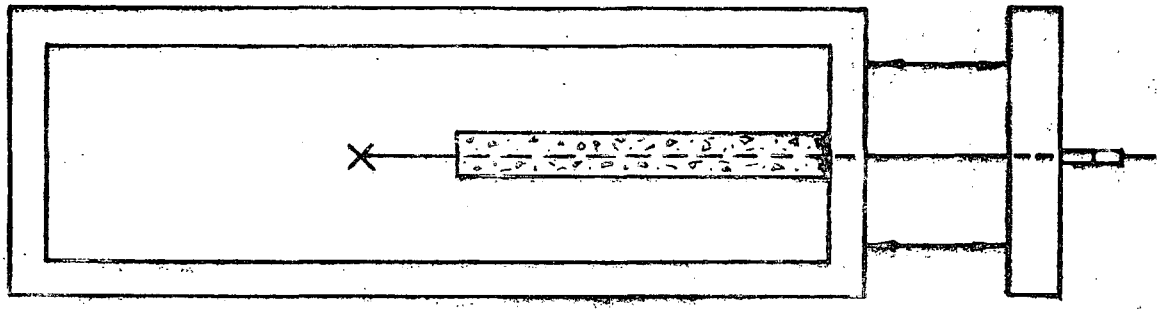

Strand Burned at Point X,
Then Jack Forces Increased
To Ultimate Load.

Figure 10 Diagrams Showing Sequence of Operations

The prestressing bed was modified in the course of the test program by the addition of a second floating beam and set of jacks. Jacking could then be performed at either end of the bed. This permitted the placing of specimens at both ends of the bed doubling the capacity. In this case prestress was released by burning the strand between the specimens. The actual testing was performed at each end independently.

The modification of the bed also made it possible to release specimens gradually. In this case they were cast at one end of the bed only. Gradual release was then accomplished by unloading the jacks at the far end in stages.

D. Procedures and Instrumentation

Although a basic procedure and method of instrumentation for preparing, pouring and testing the test specimens was adhered to, a certain amount of revision was found to be necessary as the program developed. Constant improvements were made and new apparatus was designed to insure obtaining the best data possible.

The basic procedure, method of instrumentation and refinements are best described with the help of photographs. Figure 11 shows the end of the prestressing bed with four strands under tension. The strands are gripped by patented chucks called "Strandvises".* These generally proved capable of withstanding the ultimate for the strand. However, the new strandvises and strandvise chucks ordered for the last phase of the tests proved to be totally incapable of sustaining the guaranteed ultimate of the strand. The strand of all seven of the specimens tested in Series IX and X failed in the grips at loads of from 79 to 93 percent of guaranteed ultimate. Three of these premature failures are shown in Figure 12.

Between the strandvises and the floating beam, in Figure 11, are the pipe dynamometers used in the measurement of strand tension. They consist of four SR-4 electrical resistance strain gages mounted on an extra heavy mild steel

---

* Manufactured by Reliable Electric Co., Chicago, Ill.

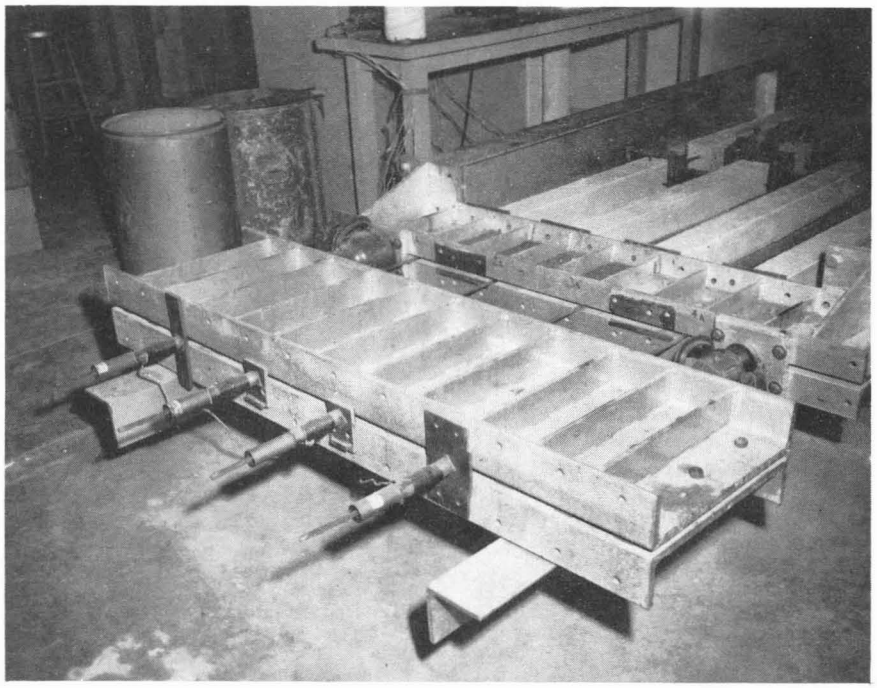

Figure 11 Tensioning Arrangement

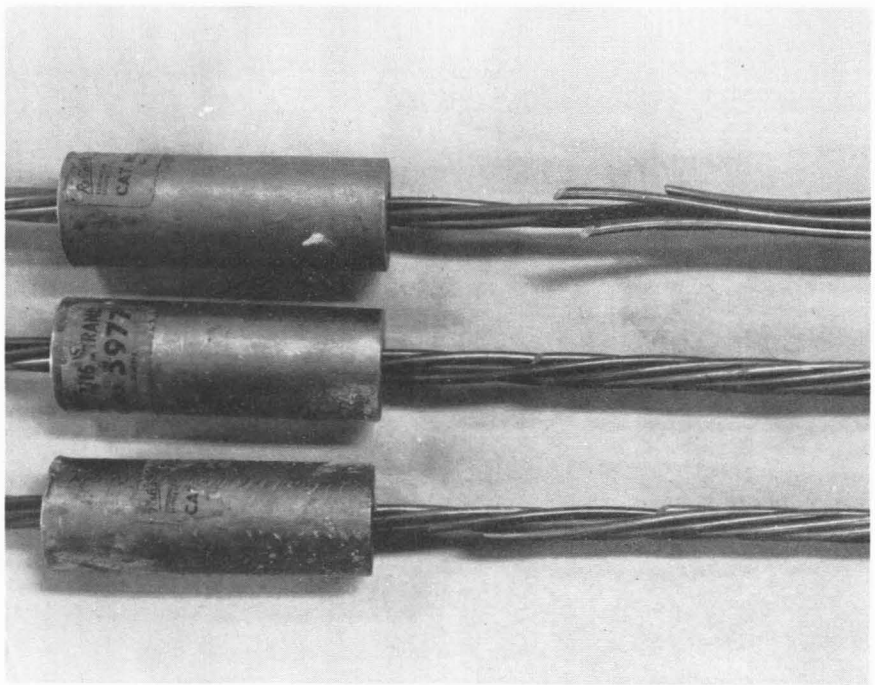

Figure 12 Strand Slip Instrumentation

pipe section so as to provide maximum strain magnification and temperature self-compensation. The calibration of the dynamometers was checked regularly to assure maximum accuracy. Their minimum accuracy was assumed to be $\pm$ 5 micro inches per inch, which is equivalent to approximately $\pm$ 62.5 pounds.

The specimens were cast in oiled, steel forms after the strand had been thoroughly cleaned with acetone. At the bearing end of the specimen the strand was passed through a bearing plate which also served as the end of the form. After the first three series of tests, 3/8 inch spacers were introduced between the bearing plate and the frame for all subsequent tests except those of Series VIII in which the specimens were uninstrumented. When these spacers were removed after the specimen was cured, the bearing plate was firmly clamped to the frame and a Carbo-Vitrobond* cap was poured between the end of the specimen and the bearing plate. This was done to assure positive bearing and to eliminate any prestress loss due to curing shrinkage. During curing, shrinkage caused the specimen to draw away from the bearing surface by a small amount. Upon release of prestress, the shortening of the strand allowed by this small opening resulted in an undesired prestress loss. In Figure 13, the caps are shown as poured in place at the bearing ends of the specimens.

The curing method was also modified after the third series of tests to minimize curing shrinkage. After wet burlap had been set on the initially hardened specimens, plastic sheeting was placed over the burlap and anchored down so the minimum of curing water was lost to evaporation. This modification proved to be sufficiently effective so that even after seven days of curing the burlap was still moist and no shrinkage was apparent at the bearing plate. Figure 14 shows typical specimens in the steel forms being cured under plastic (note the test control cylinders also under plastic beside the bed.)

An unbonded length was provided at the bearing end of the test specimens. This was done to avoid the local stress concentration existing at all bearing surfaces which, it was felt, would make the results of the pull-out test less applicable to actual beam behavior. In analyzing the longitudinal concrete

---

* A carbon-sulfur cylinder capping compound manufactured by the Atlas Mineral Products Company of Mertztown, Penna.

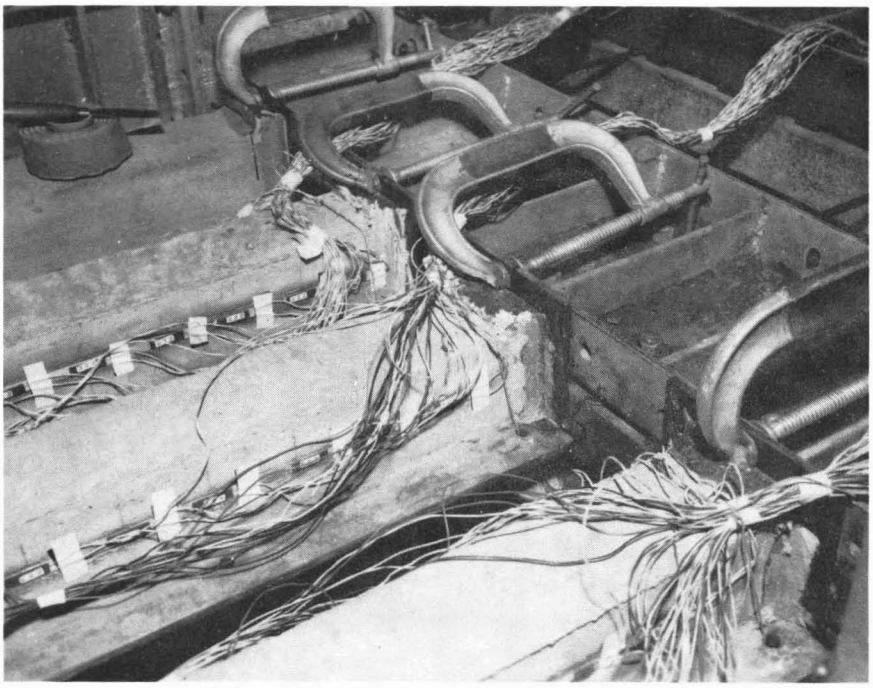

Figure 13 Bearing End of Specimen

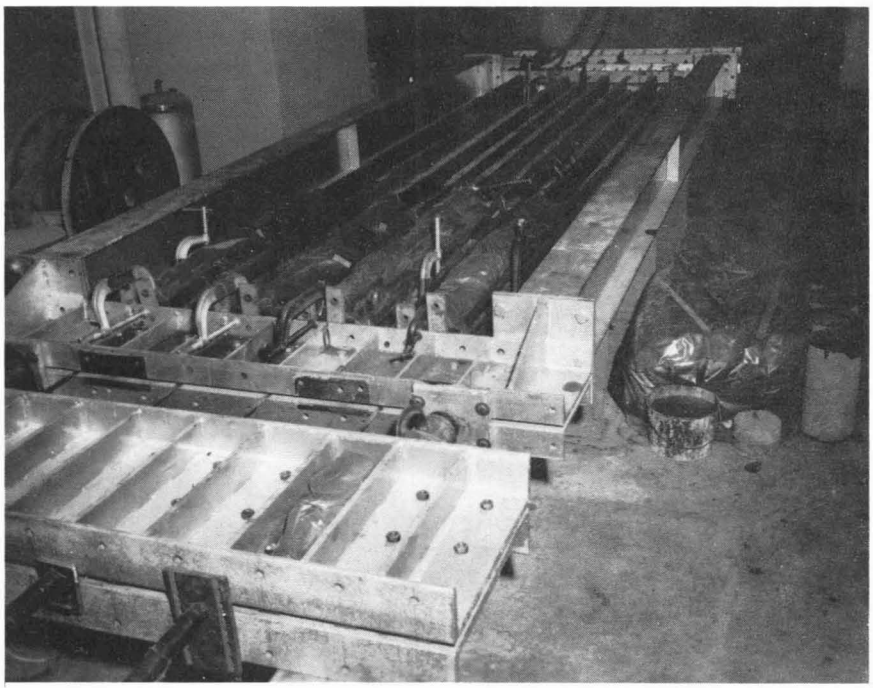

Figure 14 Curing Specimens

strain data of Series III and V, it was concluded that the original unbonded length prescribed was not sufficient to entirely avoid the super position of bearing strains on those describing bond distribution. The magnitude of unbonded length was therefore increased in the later series of tests.

In those test series in which stain data was to be taken, a greater unbonded length was provided so that a constant value of strain could be observed in the unbonded portion. It was assumed that this leveling of strain would provide an indication that the complete picture of bond distribution as represented by surface strains had been obtained without any inclusion of bearing strains.

The length of specimens discussed are the bonded lengths in all cases. In the unbonded portion, bond was effectively destroyed by wrapping the strand with waxed paper smeared with heavy grease. The resulting hole was cylindrical and no restraint was imposed on the strand within the length. The unbonded lengths provided in each series of tests and the particular types of strain instrumentation used are reported in Table IV.

TABLE IV UNBONDED LENGTHS AND STRAIN INSTRUMENTATION

Series	Specimen Number	Unbonded Length Feet	Instrumentation
I and II	all	.5	None
III	1	.5	SR-4 A-1
III	2	.5	None
IV	all	.5	None
V	1,2 & 3	.5	SR-4 A-1
V	4	.5	Huggenberger
VI	all	2.0	Huggenberger
VII	1	2.0	Huggenberger
VII	2,3 & 4	2.0	None
VIII	all	1.0	None
IX	1,2 & 3	1.5	SR-4 A-1
IX	4	1.5	None
X	all	1.5	SR-4 A-1

At the release or transfer of prestress, the strand shortens and, at the release end, is drawn into the specimen by a small amount. This is called "release slip" as distinguished from "strand slip", the term which will be used to describe bond failure. To record these movements, 0.001 inch Ames dials were used. As more was learned about the basic behavior of stranded wires, the arrangement of the dials in the limited space available to each specimen was modified to improve the accuracy of the data. The set-up used in the early tests to record release slip is shown in Figure 15 and that used to record strand slip in Figure 16.

Since any shock or vibration, such as that due to sudden release or strand rupture was liable to affect the dial readings, the arrangement shown in Figure 17 was devised. Here, two dials supported from a bracket firmly anchored in the specimen bear against a smooth steel plate mounted on the strand. This arrangement compensates for any movement of the strand. The average of two readings taken from dials whose centers lie in a line with the center of the strand gives a valid measurement of release slip. This set-up was used to measure slip at release and at test.

For the small specimens (cross-section 2-1/2 x 2-1/2 inches) of the last series of tests, the bracket arrangement of Figure 17 could not be used. This set-up was therefore modified as appears in Figure 18, in which the set-up is shown in various stages of assembly.

Bond distribution was analyzed by means of strain data taken along the entire length of several of the specimens at the level of the strand. Two different techniques were used. One involved the use of SR-4 gages, clearly visible in Figures 13 and 15. In Series III and V, A-1 gages mounted on the surface of small aluminum channels, whose flanges had been deformed as shown in Figure 19, were used. The aluminum strips were screwed to the steel forms before the concrete was poured. The deformed flanges provided complete bonding with the concrete and the aluminum offered a smooth, dry surface on which the gages could be mounted without fear of moisture contamination. The aluminum's load carrying capacity was negligible. This technique is believed to be quite novel and proved to be entirely practical.

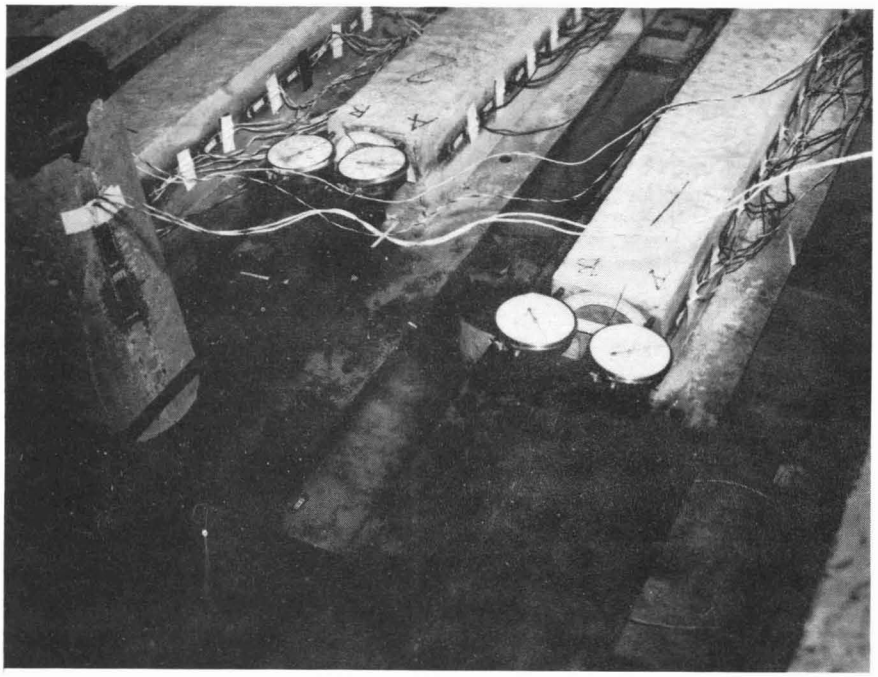

Figure 15 Release Slip Instrumentation

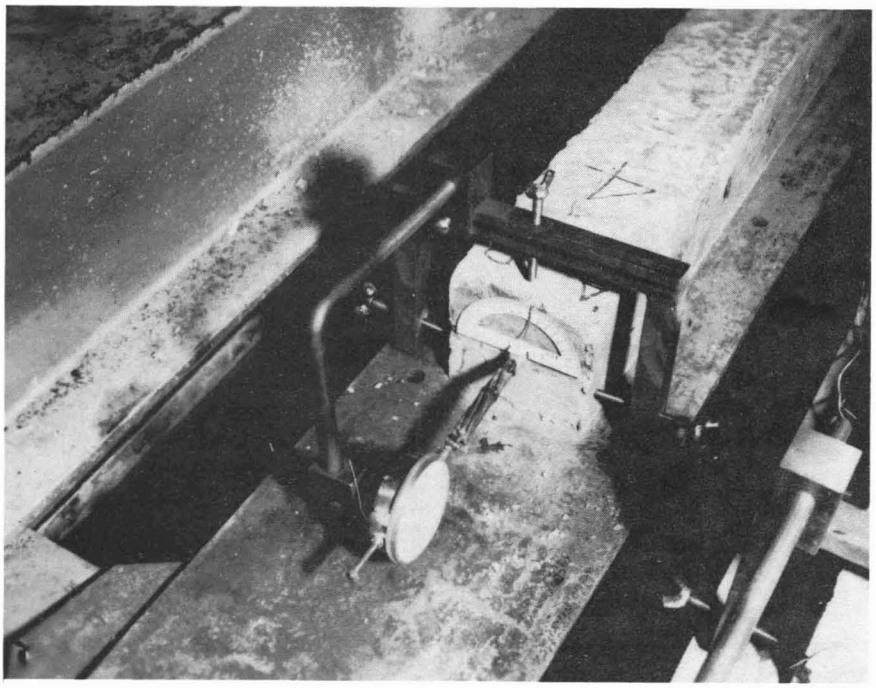

Figure 16 Strand Slip Instrumentation

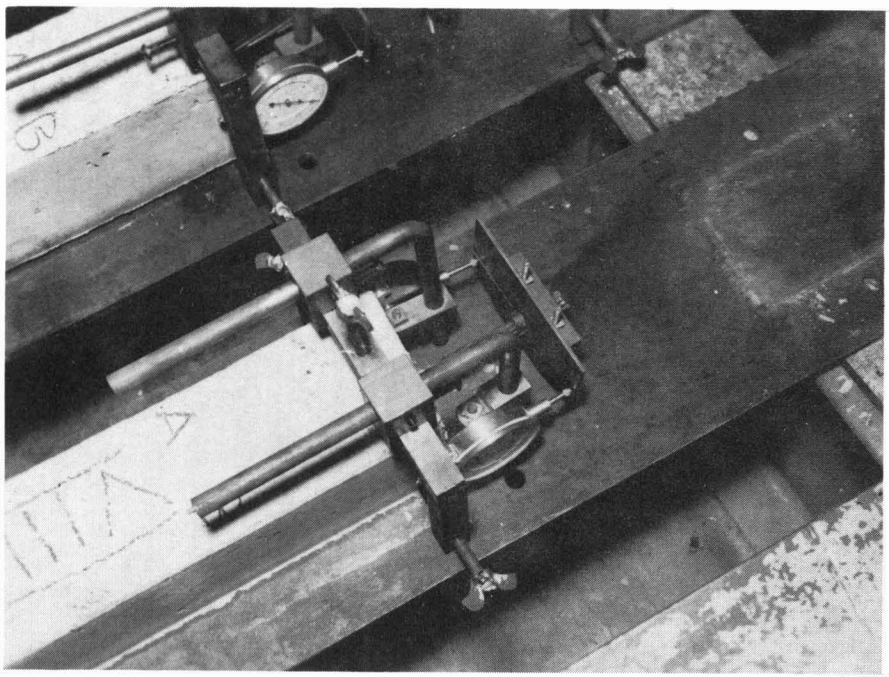

Figure 17 Slip Gages for Sudden Release

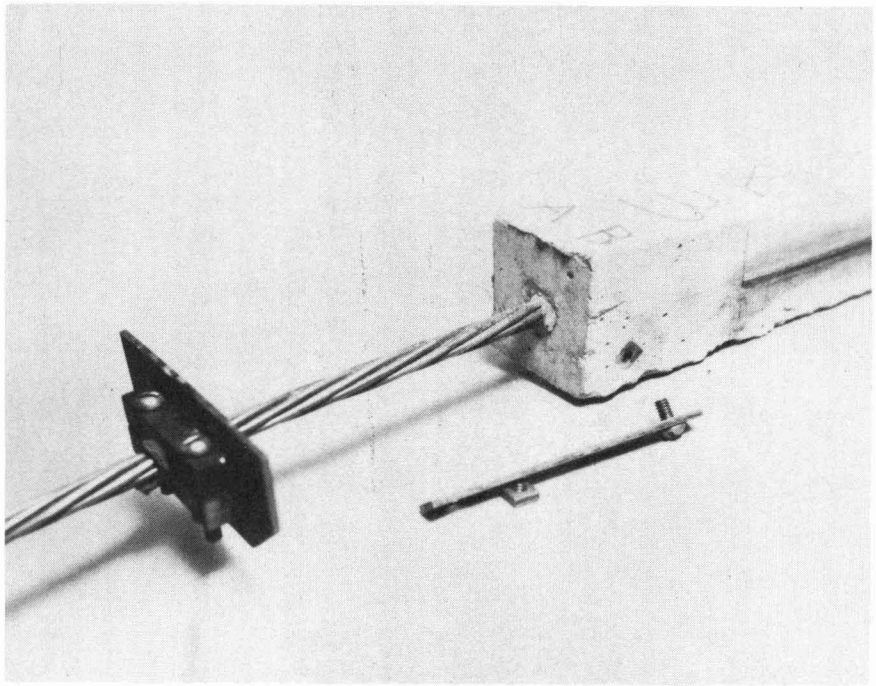

a.)

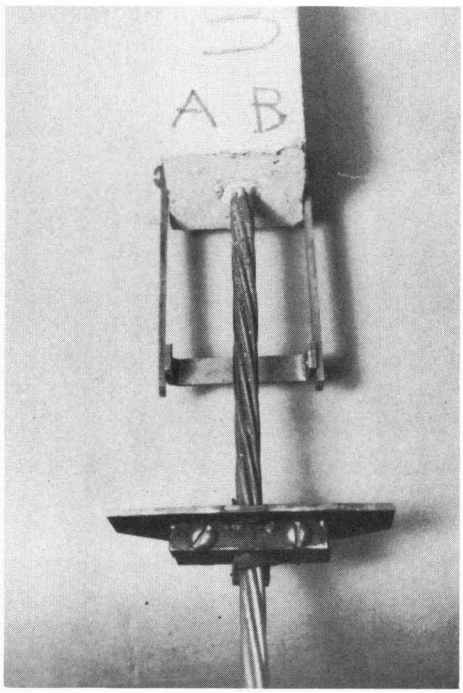

b.)

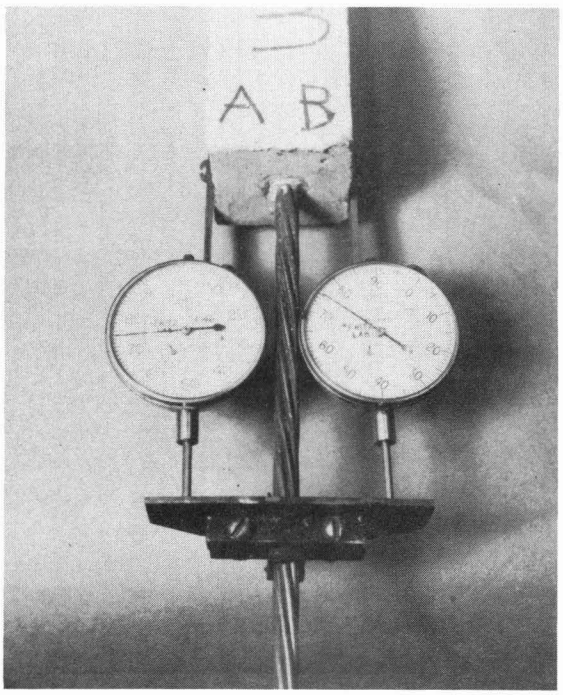

c.) assembly complete

Figure 18 Slip Gage Assembly for 2 1/2" x 2 1/2" Specimens

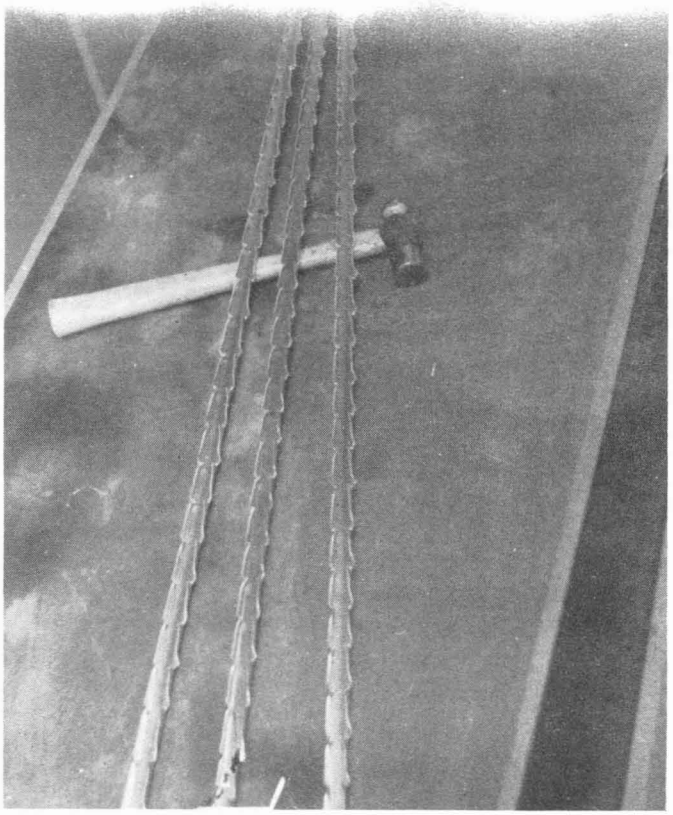

Figure 19
Aluminum Channels for mounting SR-4 Gages

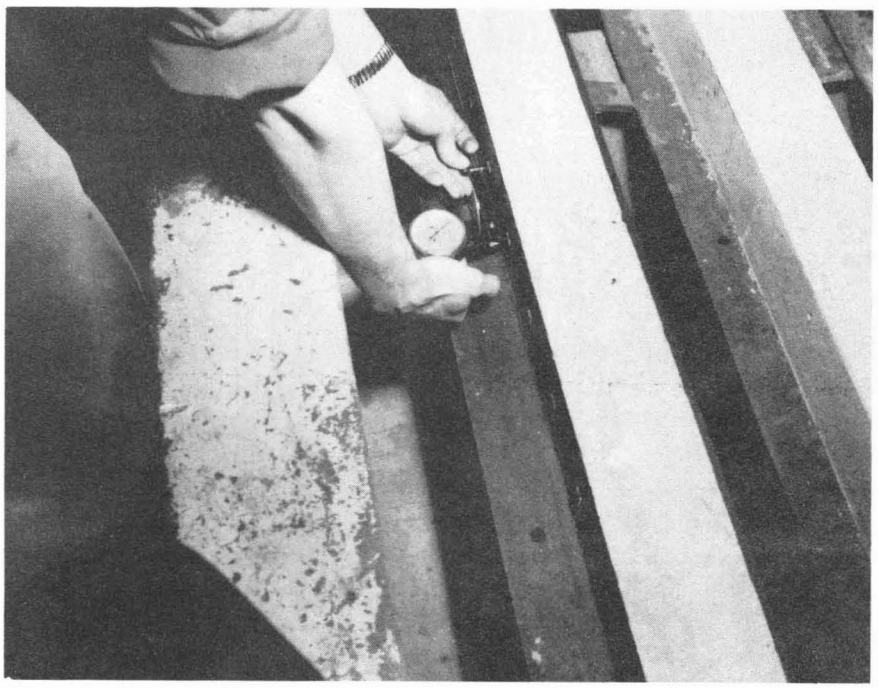

Figure 20
Huggenberger Tensometer Measuring Concrete Strains

In Series IX and X, the use of aluminum channel was omitted since the modification of the steel forms necessary for these sections prohibited its use. The A-9 gages used in these tests were mounted on a concrete surface which had been allowed to dry thoroughly and which was carefully smoothed with fine emery paper and a thin coating of Duco cement. Both the A-1 and A-9 SR-4 gages were read to an accuracy of $\pm$ 5 micro inches per inch.

The second procedure is illustrated in Figure 20. Instead of electrical gages a mechanical instrument, the Huggenberger Tensometer, was used over a gage length of ten centimeters. Small holes in the probes of the gage slip over minute steel spheres set into small aluminum plates which are, in turn, cemented to the sides of the specimen. The technique is slow and laborous but readings can be duplicated consistently. Corrections must be applied to the data for temperature changes in both the specimen and the instrument. The final results appeared to be in good agreement with those obtained with electrical gages. For control cylinders on which both techniques were used, the agreement was almost perfect. The tensometer was read to an accuracy of $\pm$ 5 microinches per inch. Accuracy was maintained by taking the average of three separate readings which were accepted only if the maximum and minimum readings were not more than ten micros apart. Zero references were taken as the average of five such readings.

To give an approximate indication of strand rotation, protractors were included in one series of tests, as can be seen in Figure 16.

Figure 21 gives an overall view of a typical test set-up for gradual release. The specimens shown ar those of Series V in which three of the four were fully instrumented with SR-4 gages. Temperature compensating gages were mounted on aluminum channels encased in the cylinder shown in the foreground of the picture.

The twelve specimens of Series VIII are shown in Figure 22, which is a typical test set-up for sudden release. The four specimens at the center of the frame are short "beams" cast around well-oiled strands. These and one similar specimen in Series VI were included in the test program in an attempt to facilitate the interpretation of the strain data and to investigate the greater resistance to slip existant in beams discussed earlier. These specimens are discussed in detail in Chapter VIII.

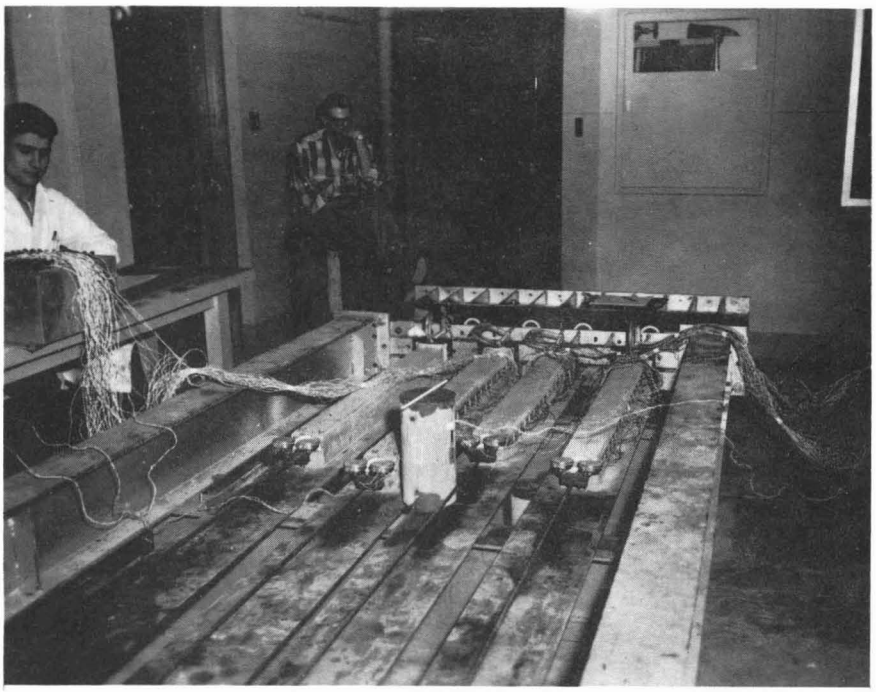

Figure 21 Series V During Gradual Release

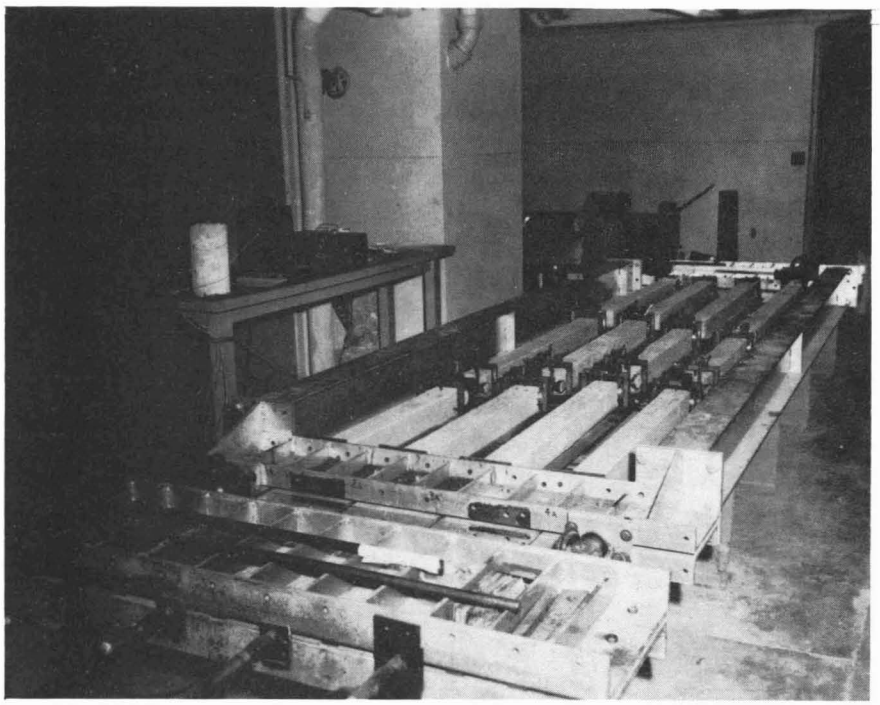

Figure 22 Overview of Set-Up for Series VIII

VII. MATERIALS

A. Concrete Physical Properties

The sand and coarse aggregate used in this investigation were specially ordered so maximum control and minimum variation of quality of materials could be maintained.

The concrete mixes were designed for strength of 6,000 psi at 7 days and 28 days, for Type III and Type I cements respectively, in accordance with Pennsylvania standard commercial practice. Air entraining, by admixture* or by specific type of cement, was used in all the tests, also in accordance with Pennsylvania standard practice.

It was originally decided to use Type III cement to reduce the curing time, but some difficulty was encountered in obtaining the desired strength with a mix or workable consistency. After four trial batches and the first two sereis of tests (pilot tests) in which Type III cement with an air-entraining admixture were used, Type I A cement was finally decided upon for the remainder of the tests. The mix was designed by the method described in the Concrete Manual of the Bureau of Reclamation, U.S. Department of the Interior (5). The basic proportions for one cubic yard so determined appear in Table V.

TABLE V NOMINAL CONCRETE MIX PROPORTIONS PER CUBIC YARD

Water	274.5	lbs.
Cement	776	lbs.
Coarse Aggregate (3/4")	1840	lbs.
Sand	1201	lbs.

Air content (Assumed) = 6%
Cement factor = 8.26 sacks/cu. yd.
W/C Ratio = 4 gallons/sack = 0.354 (by weight)
Slump = 2 to 3 inches

One trial batch of the aforementioned mix indicated an air content of only 3%. The mix would theoretically have to be redesigned for an additional 25.5 pounds of water to compensate for the decreased air content. The desired strength was obtained, however by simply adding sufficient water to obtain the desired consistency, i.e., 2 to 3 inches of slump. Therefore, the proportions of the dry constituents were left unchanged.

The coarse aggregate used was a washed and well graded crushed limestone of 3/4" maximum size indigenous to Eastern Pennsylvania. The sand used was also washed, well-graded and of local source. The cement used was obtained from local manufacturers and in all but the first few series of tests was from the same source.

The actual mix proportions used in each series of tests and their properties are given in Table VI. They differ from the basic mix because the sand was not saturated, surface dry in each case.

All the concrete excepting that in Series IX was mixed in a Type SW12 mixer, manufactured by the Posey Iron Works Co., Inc., Lancaster, Pa. The concrete of Series IX was mixed in a Type EB-4 mixer manufactured by the same company. Some difficulty was experienced in mixing the concrete of Series IX, as can be seen by the zero slump reported in Table VI and the relatively low strength and modulus of elasticity reported in Table VII. This was due basically to unfamiliarity with the then new mixer, and a misunderstanding as to its practical capacity.

Vibration was used for all concrete placing, for both the specimens themselves and the control cylinders. The slump data was obtained according to standard procedure. Two vibrators were used throughout the tests, a Model L type manufactured by the Vibro Co. of Los Angeles, Calif., and a Type ESV 35 manufactured by the Vibro-plus Products of Stanhope, New Jersey.

B. Concrete Mechanical Properties

The concrete strengths at time of release, at test, and at 28 and 7 days, for Types I and III cements respectively are reported in Table VII. These strengths were obtained by

TABLE VI MIX PROPORTIONS AND PROPERTIES

Series	Mix Quantities in lb/cu yd.				Cement Factor sacks/ cu yd.	W/C Ratio gal. sack	Slump inches	Air Content % *
	Water	Cement	Sand	Stone				
I	284	695	1418	1623	7.4	4.6	1-1/4 to 1-1/2	3.3
II	300	685	1400	1602	7.3	5.0	ND	ND
III	275	776	1201	1840	8.3	4.0	1 to 1-1/2	3.0
IV	320	755	1170	1790	8.0	4.8	1 to 1-3/4	2.7
V	290	770	1190	1830	8.2	4.2	1-1/2 to 2-1/4	2.8
VI	336	755	1125	1790	8.0	5.0	1-1/2 to 3	2.5
VII	300	757	1195	1795	8.1	4.5	1 to 2-1/2	3.0
VIII	320	750	1160	1780	8.0	4.5	1 to 3-1/2	3.0
IX	334	760	1180	1800	8.1	5.0	0	ND
X	320	757	1140	1790	8.1	4.8	2-1/4 to 3	ND

ND: Not Determined

* The amount of entrained air was measured on a PRESS-UR-METER, Type B, manufactured by the Concrete Specialties Co. of Spokane, Washington

TABLE VII CONCRETE STRENGTHS AND MODULI OF ELASTICITY

Series	Age in Days		Concrete Strength in psi			Tang. Modulus in psi x 10^6		Cylinder Instrumentation
	At Release	At Test	At Release	At Test	At 28 days	At Test Flexure	At Test Cylinder	
I	4	7	4600	5250	a	ND	ND	---
II	6	7	4700	4500	a	ND	ND	---
III	25	26	6500	6500	6500	5.3	ND	---
IV	7	7	4250	4250	5600	ND	ND	---
V	19	37	5800	b	b	4.8	ND	---
VI	34	40	6100	6530	6100	ND	5.3	Huggenberger
VII	c	17	c	5650	5860	ND	5.2	Huggenberger
VIII	39	39	6150	6150	5950	5.0	6.0	Huggenberger
IX	18	22	4300	4400	4630	3.0	4.0	SR-4, Type A-1
X	9	9	4700	4700	5500	4.0	4.7	SR-4, Type A-9

ND: Not Determined

a - No 28-day strength for high early strength cement

b - Cylinders were tested when loading machine was poised in middle of beam test. The low strengths obtained, average 4950 psi, are believed to be due to the resulting load eccentricity introduced

c - These specimens were not prestressed

The stress-strain and load deflection curves from which the above values were derived are shown in Appendix B

testing standard 6 inch by 12 inch cylinders at a load rate of from 7 to 10 seconds per 10,000 lbs. The control cylinders were cured in the same atmospheric conditions as the test specimens.

Modulus of Elasticity, E, values were determined for those series in which strain data was taken. This was done by two methods:

(1) cylinder test, where E was obtained directly from the observed strains.

(2) flexure test of a specimen, where E was obtained from the expression for elastic deflection.

In each case where an E was determined from a flexure test, the exact deflection expression for that particular loading was used.

Two types of instrumentation were used to determine E from cylinder tests. One was by means of SR-4 electrical resistance strain gages. Two types of SR-4 gages were used; Type A-1 with a gage length of one inch and Type A-9 with a gage length of six inches. The other type of instrumentation was by means of a mechanical gage, the Huggenberger Extensometer. The gage length used was ten centimeters. In all cases strain readings were taken on diametrically opposed sides of the cylinder with the gage length centered at mid-height of the cylinder.

The values of E, and the particular type of instrumentation used on each cylinder appear in Table VII.

C. Steel Properties

The type of steel used exclusively in the tests herein reported is stress releived, uncoated, seven-wire strand of 7/16 inch nominal diameter.

The manufacturer* gives the following properties:

Area = 0.1089 square inches

---

* John A. Roebling's Son's Corporation, Trenton, New Jersey

Ultimate strength = 27,000 pounds = 247,930 psi

$E = 27 \times 10^6$ psi

Recommended Tensioning Load = 18,900 pounds
= 173,550 psi

Recommended Design Load (assuming 20% total losses)
= 15,120 pounds = 138,850 psi

A number of tests conducted on this strand during this investigation and in the past by the authors and colleagues at Lehigh University indicate that the ultimate strength of the strand, if not failed at a weld, varies with few exceptions between 28 and 30 kips. The modulus of elasticity has similarly been found to be approximately 28×10^6 psi. This value of E has been used in all the calculations in which it enters. A typical load-elongation curve for the strand used is shown in Figure 23.

In the initial tensioning of strands, the 18.9 kip recommended load was approached as nearly as possible. With as many as four strands involved at a time, all could not be brought exactly to this figure.

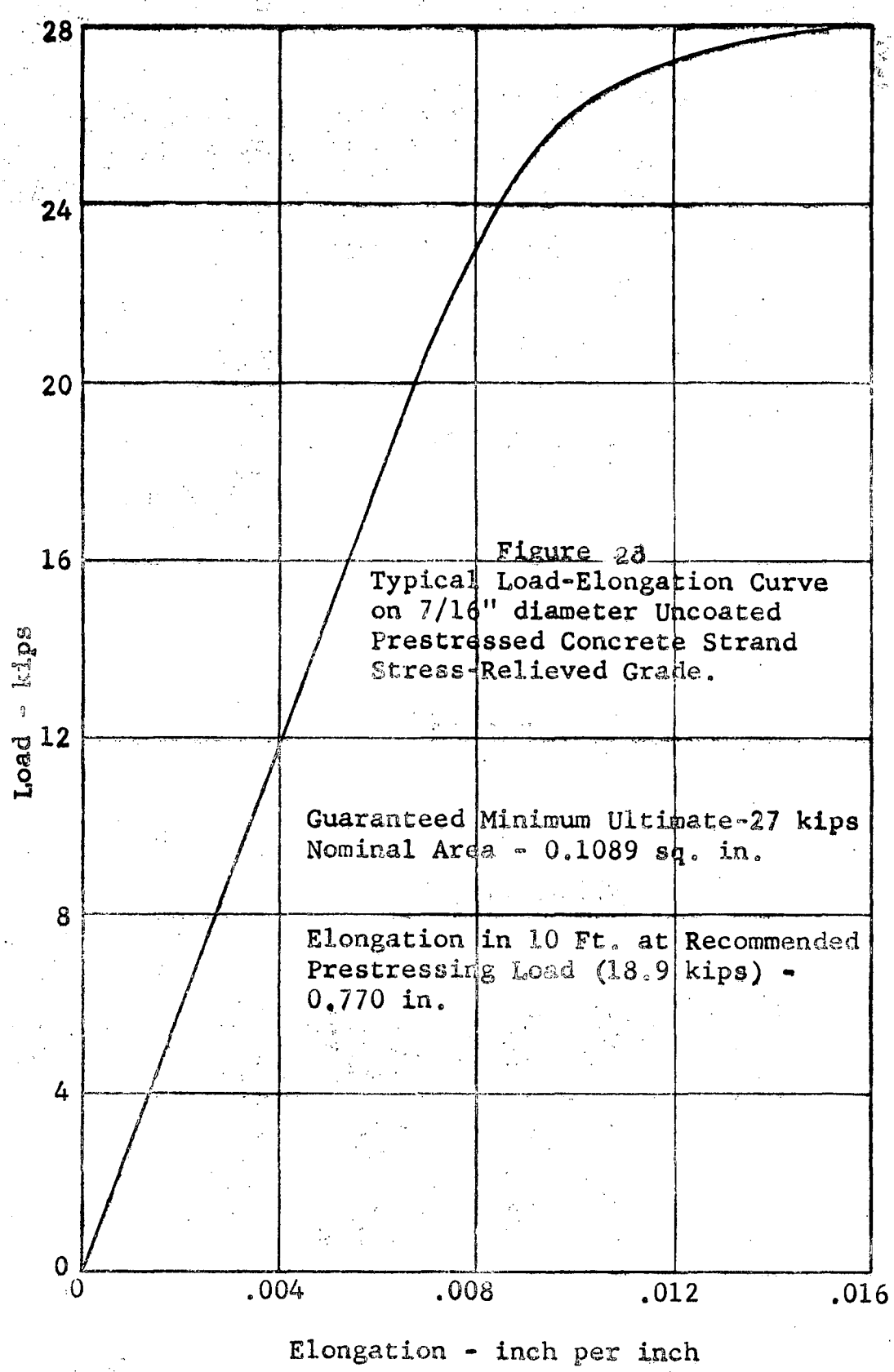

Figure 28
Typical Load-Elongation Curve on 7/16" diameter Uncoated Prestressed Concrete Strand Stress-Relieved Grade.

VIII EVALUATION OF TEST RESULTS

A. Ultimate Anchorage and Slip-Limit Envelope

The pertinent date required for the determination of the ultimate anchorage and the establishment of the slip limit envelope are presented in Table VIII arranged in order of length of specimens, and plotted in Figure 24. Only those specimens of Series I to VIII are included since the strand ultimate was obtained in Series IX and X. The results of these latter series will be discussed fully in the next section.

The 34 specimens tested in Series I to VIII ranged in length from one to twelve feet. (All Lengths referred to are fully bonded lengths). No specimens of more than four feet in length slipped either at prestress or under applied load. Two of the four specimens four feet long slipped (Specimens IV-8 and V-3), but none of the six specimens between four and six feet did.

An examination of Figure 24 will show that the performance of specimens of four feet and less in length was highly erratic. No definite slip limit envelope has been established. The scatter of data points was even more pronounced than would normally be expected from concrete test results. This does not preclude the existence of an envelope with maximum and minimum limits but many more specimens would have to be tested to establish those limits. However, these would have limited applicability to a problem as critical as premature bond failure.

Besides the variables indigenous to concrete manufacture, a logical reason why the results are so inconsistent is that bond is basically a local phenomenon. Bond strength is dependent upon the behavior of a relatively small concrete area, namely the circumferential perimeter along the embedded length of the steel. Test results which are dependent upon the behavior of a relatively large mass of concrete are generally more consistent.

The three data points which confuse the picture of Figure 24 are the three, three and one-half, and four foot specimens of Series V which slipped at release. It is felt that these data are quite extraordinary and are not representative of normal bond behavior. The reasons for this statement will be presented later in the discussion of each individual test series.

TABLE VIII TABULATED RESULTS OF TEST SERIES I TO VIII, BY LENGTH

Spec. No.	Bonded Length Feet	Type Release	Strand Ult. Kips	Strand Slip	Slip Load Kips	Prestress Kips Init.	Prestress Kips Effec.	Release Slip** Inches	f'c at Test Psi
I-2	12	Sudden	29.8	None	----	19.4	17.9	.033	5250
I-1	10	Sudden	29.6	None	----	19.6	18.0	.014	5250
II-2	8	Sudden	29.5	None	----	16.9	15.8	.028	4500
VI-3	8	Sudden	26.8*	None	----	18.3	16.7	ND	6530
III-2	7	Sudden	28.4*	None	----	16.9	15.1	.047	6500
VII-4	7	------	26.5*	None	----	0	0	---	5650
II-1	6	Sudden	28.8	None	----	16.8	15.4	.042	4500
VII-1	5.5	------	27.1*	None	----	0	0	---	5650
III-1	5	Sudden	28.3	None	----	16.8	15.2	ND	6500
IV-4	4.5	Sudden	28.5*	None	----	17.7	16.7	ND	4250
VIII-8	4.5	Sudden	28.2*	None	----	18.9	16.9	.028	6150
VII-2	4.25	------	26.4*	None	----	0	0	---	5650
IV-8	4	Sudden	----	L	22.5	17.7	16.5	ND	4250
V-3	4	Gradual	----	R	11.8	17.3	7.6	.340	5800
VI-1	4	Gradual	24.6	None	----	18.2	17.5	.021	6530
VIII-7	4	Sudden	25.6	None	----	19.7	17.2	ND	6150

* Maximum Load Attained. Strand not broken.
** This reported value is the observed slip minus the elastic shortening of the gage length.
L At Load
R At Release
ND Not Determined

TABLE VIII (continued)

Spec. No.	Bonded Length Feet	Type Release	Strand Ult. Kips	Strand Slip	Slip Load Kips	Prestress Kips Init.	Prestress Kips Effec.	Release Slip** Inches	f'c at Test Psi
IV-2	3.5	Sudden	29.5	None	----	19.5	17.7	ND	4250
V-1	3.5	Gradual	---	R	7.1	18.3	4.2	.403	5800
V-4	3.5	Gradual	27.9	None	----	18.0	17.6	.030	5800
VI-2	3.5	Sudden	27.4*	None	----	18.4	16.3	.006	6530
VI-4	3.5	Gradual	28.6*	None	----	18.5	17.4	.027	6530
VIII-5	3.5	Sudden	28.8*	None	----	19.1	18.2	ND	6150
VIII-6	3.5	Sudden	26.8*	None	----	19.7	17.1	.023	6150
IV-3	3	Sudden	29.3	None	----	18.0	17.0	ND	4250
V-2	3	Gradual	---	R	6.5	17.9	4.1	.379	5800
VIII-3	3	Sudden	30.0	L	29.4	19.7	17.6	.037	6150
VIII-4	3	Sudden	27.4*	L	27.0	18.9	17.6	.030	6150
VII-3	2.75	------	---	L	19.8	0	0	--	5650
IV-7	2.5	Sudden	---	L	20.6	18.0	16.0	ND	4250
VIII-2	2.5	Sudden	---	L	23.7	19.7	17.9	.028	6150
IV-6	2	Sudden	---	R	ND	19.5	14.0	ND	4250
VIII-1	2	Sudden	---	L	16.7	19.1	16.7	.051	6150
IV-1	1.5	Sudden	---	L	18.0	18.5	16.8	ND	4250
IV-5	1	Sudden	---	R	ND	18.5	10.1	ND	4250

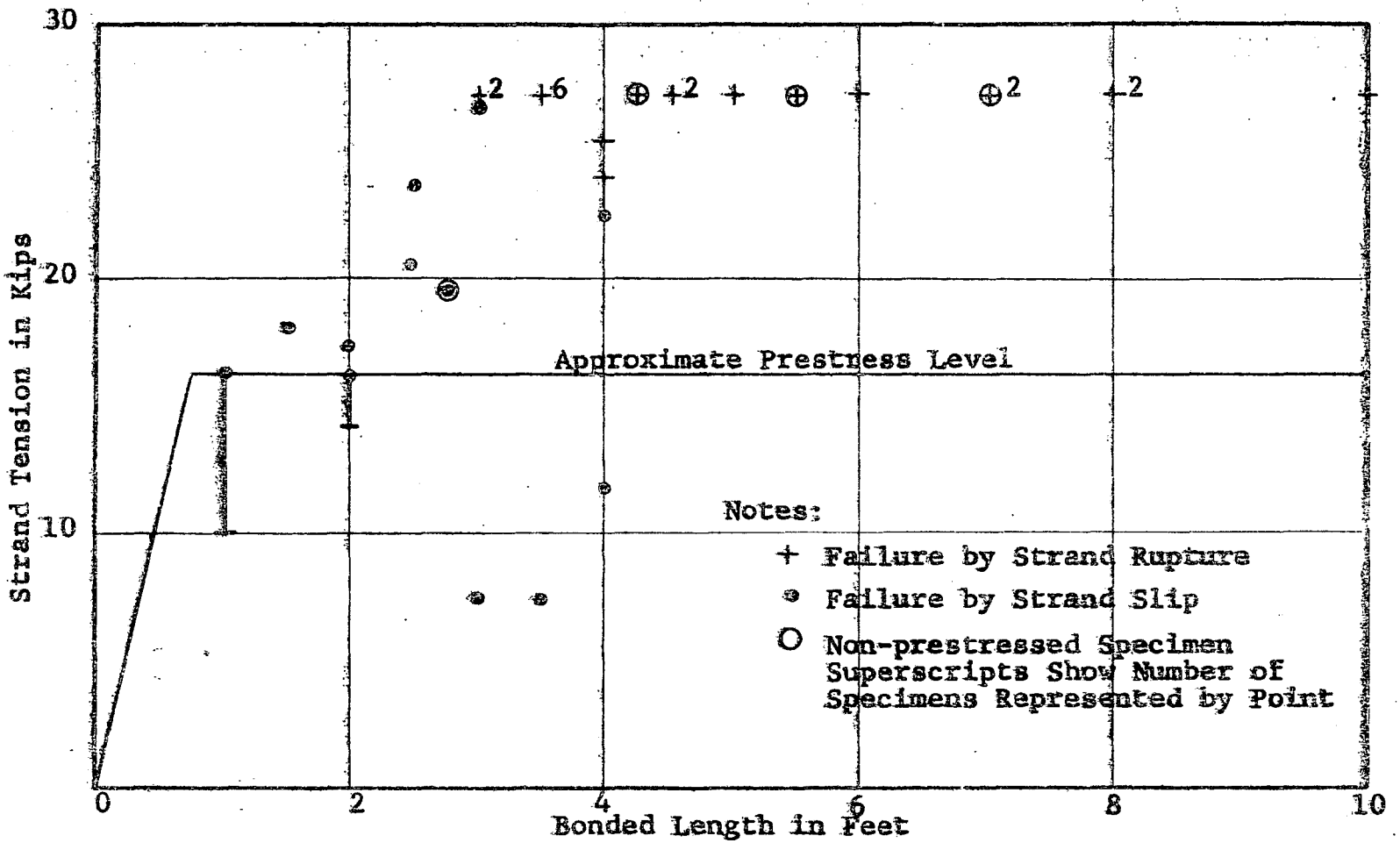

Figure 24 Strand Tension at Failure vs Embedment Length

No specimen in any of the tests reported in Table VIII showed any cracking, spalling or any other indication of distress in the concrete. Only in Series VIII were any sounds heard from the specimens. These were sharp reports, very similar to that of strand rupture, which accompanied abrupt slipping of the strand. This unique effect is discussed in detail later.

All of the specimens tested were later broken open and the grooves in the concrete surrounding the strands studied. In all cases in which slip occurred the grooves were highly polished, but not in any way destroyed. A polished groove indicated that relative movement between the strand and the concrete had taken place. All of the specimens which did not fail in slip showed the same polished appearance in the transfer region and also at the loading (bearing) end. In that portion of these specimens between the transfer zone and the region affected by applied loading, the grooves exhibited a dull, rather chalky appearance. This dull appearance indicated that adhesive bond had not been destroyed in this region and no relative movement of strand and concrete had taken place. The contrast between polished and dull groove appearance was not sufficiently pronounced to permit the measurement of the various lengths by these observations.

(1) Discussion of the Tests

The date presented in Table VIII is rearranged in order of series in Table IX to facilitate the following individual discussion of each series of tests.

Series I and II

These were preliminary tests to establish the order of magnitude of the ultimate anchorage length. The strand was drawn from old laboratory stack and was therefore somewhat rusted. The measurement of release slip was crude; a single dial was attached to the strand prior to the sudden release by burning of the strand. Slips of from .014 to .042 were observed by this method.

Series III

New, clean strand was used for this and all subsequent tests.

One of the two specimens of this set was instrumented with SR-4 gages placed longitudinally at the level of the

TABLE IX TABULATED RESULTS OF TEST SERIES I TO VIII, BY SERIES

Spec. No.	Bonded Length Feet	Type Release	Strand Ult. Kips	Strand Slip	Slip Load Kips	Prestress Kips Init.	Prestress Kips Effec.	Release Slip** Inches	f'c at Test Psi
I-1	10	Sudden	29.6	None	----	19.6	18.0	.014	5250
I-2	12	Sudden	29.8	None	----	19.4	17.9	.033	5250
II-1	6	Sudden	28.8	None	----	16.8	15.4	.042	4500
II-2	8	Sudden	29.5	None	----	16.9	15.8	.028	4500
III-1	5	Sudden	28.3	None	----	16.8	15.2	ND	6500
III-2	7	Sudden	28.4*	None	----	16.9	15.1	.047	6500
IV-1	1.5	Sudden	---	L	18.0	18.5	16.8	ND	4250
IV-2	3.5	Sudden	29.5	None	----	19.5	17.7	ND	4250
IV-3	3	Sudden	29.3	None	----	18.0	17.0	ND	4250
IV-4	4.5	Sudden	28.5*	None	----	17.7	16.7	ND	4250
IV-5	1	Sudden	---	R	ND	18.5	10.1	ND	4250
IV-6	2	Sudden	---	R	ND	19.5	14.0	ND	4250
IV-7	2.5	Sudden	---	L	20.6	18.0	16.0	ND	4250
IV-8	4	Sudden	---	L	22.5	17.7	16.5	ND	4250

* Maximum load attained. Strand not broken
** This reported value is the observed slip minus the elastic shortening of the gage length
L At Load
R At Release
ND Not Determined

TABLE IX (continued)

Spec. No.	Bonded Length Feet	Type Release	Strand Ult. Kips	Strand Slip	Slip Load Kips	Prestress Kips Init.	Prestress Kips Effec.	Release Slip** Inches	f'c at Test Psi
V-1	3.5	Gradual	----	R	7.1	18.3	4.2	.403	5800
V-2	3	Gradual	----	R	6.5	17.9	4.1	.379	5800
V-3	4	Gradual	----	R	11.8	17.3	7.6	.340	5800
V-4	3.5	Gradual	27.9	None	----	18.0	17.6	.030	5800
VI-1	4	Gradual	24.6	None	----	18.2	17.5	.021	6530
VI-2	3.5	Sudden	27.4*	None	----	18.4	16.3	.006	6530
VI-3	8	Sudden	26.8*	None	----	18.3	16.7	ND	6530
VI-4	3.5	Gradual	28.6*	None	----	18.5	17.4	.027	6530
VII-1	5.5	-----	27.1*	None	----	0	0	--	5650
VII-2	4.25	-----	26.4*	None	----	0	0	--	5650
VII-3	2.75	-----	----	L	19.8	0	0	--	5650
VII-4	7	-----	26.5*	None	----	0	0	--	5650
VIII-1	2	Sudden	----	L	16.7	19.1	16.7	.051	6150
VIII-2	2.5	Sudden	----	L	23.7	19.7	17.9	.028	6150
VIII-3	3	Sudden	30.0	L	29.4	19.7	17.6	.037	6150
VIII-4	3	Sudden	27.4*	L	27.0	18.9	17.6	.030	6150
VIII-5	3.5	Sudden	28.8*	None	----	19.1	18.2	ND	6150
VIII-6	3.5	Sudden	26.8*	None	----	19.7	17.1	.023	6150
VIII-7	4	Sudden	25.6	None	----	19.7	17.2	ND	6150
VIII-8	4.5	Sudden	28.2*	None	----	18.9	16.9	.028	6150

strand. This was done so that the approximate ultimate anchorage length might be determined from the strain distribution and to observe the bond distribution from the resultant strains. This value of ultimate anchorage length was required to guide the selection of lengths for the future tests.

Specimen III-1 was instrumented with A-1 and A-12 gages spaced three inches on center on both sides of the member. The plotted strains are the average of two strain values at each section. The strain history of the specimen is recorded in Figure B1*. Immediately after release an average strain of 180μ** was observed in the length beyond the transfer region. This strain when divided into the concrete stress after release determines a modulus of elasticity of 5.3×10^6 psi which agrees very well with the values listed in Table 6.

The zero readings prior to the actual testing were taken twenty-three hours after release. The effect of creep is readily seen in Figure B1 by the fairly uniform increase in strain of the zero pretest level above that at release. This strain increase due to creep is also readily apparent in the strain distribution curves of the subsequent specimens.

The date of Figure B1 is also shown in Figure B2 with the pretest strains taken as base. This was done to separate the release strains from those resulting from applied load to facilitate the interpretation of the data. Similar curves were drawn for all instrumented specimens.

The pronounced dip in the strain distribution curves at the bearing end of Specimen III-1 suggested the desirability of capping future specimens as was discussed in Chapter VI.

It should be noted from the strain distribution at loading or jacking end of Figure B2 that the load applied after re-

---

* Figures designated by the letter "B" have been assembled in Appendix B. This is done to preserve the continuity of the discussion since the figures are quite numerous.

** μ is a measure of strain equal to one micro inch per inch or μ = inch per inch x 10^{-6}.

lease has left the transfer portion of the original release curve completely unaffected. Presumably if the jacking action had produced strains encroaching on this portion of the curve, the strand would have slipped. It would be reasonable to conclude therefore that the ultimate anchorage length would be the sum of the transfer length, about ten inches, and the length affected by applied load, approximately two and one-half feet for this specimen. Both of these lengths will be seen to be variable in the later tests.

The type of slip instrumentation used in these tests is that shown in Figure 15. The slip phenomena will be discussed in a later section.

Series IV

The primary purpose of this series of tests was to obtain data points defining the slip limit envelope. Therefore longitudinal strain instrumentation was not provided on any of these specimens. The previous tests indicated that the ultimate anchorage length was approximately three and one-half feet. Consequently the lengths of this set of specimens were graduated from one to four and one-half feet in six inch increments.

The date of this series of tests gave ample evidence of the inconsistency of concrete test results which sould be expected from this type of test. The two foot specimen slipped at release but the one and one-half foot specimen did not. The four foot specimen slipped under applied load but the three and one-half foot specimens developed the strand ultimate. These tests indicated that a statistical approach would be required to determine an accurate average slip limit envelope.

Release slip data was not taken for these specimens since some doubt existed concerning the accuracy of the data obtained for sudden release by the previous method. Slip during loading was measured by the method of Figure 16.

Series V

The effect, if any, of gradual release of the prestress was the object of this series of tests. Three specimens, V-1, V-2, V-3, of the four in this series were instrumented with Type A-1 SR-4 gages over their entire lengths. The gages were spaced three inches apart and staggered evenly with respect to each other on opposite sides of each specimen. The bonded lengths were three, three and one-half, and four feet. The

fourth uninstrumented specimen was another with the three and one-half feet length indicated as being the ultimate anchorage length in Series III.

Release slip was measured by the method of Figure 15. The three instrumented specimens all showed abnormal slipping before the prestress was fully transferred. The strand dynamometer data indicated that Specimens 1 and 2 failed after not quite 55 percent of the prestress had been released and Specimen 3 after approximately 70 per cent. These specimens slipped from 0.34 to 0.40 inches. The fourth specimen however successfully transferred the prestress and exhibited a slip of only 0.030 inches.

The strain gages along the length of the specimens should have provided an excellent picture of the slip failure phenomena. However, the malfunction of several laboratory switch boxes resulted in the loss of the zero references making the interpretation of the data very difficult. The picture which finally emerged is indicated in Figure B3. Curve 1 represents the release of a small per cent of prestress, for example 10%. It shows a normal development of transfer length. The release of additional prestress somehow exceeds the capacity of the immediate transfer length and Curve 2 results. The curve develops a slope in the straight line portion indicating frictional bond. The member has apparently failed locally in the region of the first transfer length. A further build up in the form of a second transfer zone therefore develops at a region of better concrete further in the interior of the specimen. The release of additional prestress however exceeds its capacity as before and the strand slips through the full length of the specimen with the resultant collapse of the strains to the level of Curve 3. The bond is now entirely frictional.

These three remarkable specimens had shown that the transfer length could be greater than four feet if they were truly representative specimens. This was questioned however because the fourth specimen, similar in every way except instrumentation, not only declined to fail at release but developed the strand ultimate at 27.9 kips without slip when tested. Strand slip was measured by the method of Figure 16.

This grossly inconsistent behavior prompted the breaking open of these and all other specimens so that the interface grooves could be examined. The grooves of the three specimens of this series which failed at release exhibited a pitted, pock-

marked appearance. This pitting was so pronounced that only about a third to a half of the available bond surface was actually in contact with the strand. If the lengths of these specimens were reduced according to the effective contact surface, it is seen that these adjusted results would be in good agreement with the other test results.

This pitted appearance was present in some of the other specimens but not to the extent observed in this series. This fact plus the extraordinarily different behavior of the fourth specimen from the other three of this series led the authors to conclude that whatever caused this gross inconsistency was something which was done to each specimen individually. It was finally hypothesized that the pock-marks were most probably caused by some impropriety in the vibration technique used for compacting the wet concrete. The next series of tests were to investigate this possibility.

Before jacking forces were applied, Huggenberger tensometer gage points, see Figure 20, were applied along the length of the fourth specimen. The gage points were spaced ten centimeters apart and staggered on opposite sides of the specimen. This spacing was adhered to in all cases in which the tensometer was used to measure strains. The technique of staggering the gages proved to result in much clearer strain curves and was used in all subsequent instrumented tests.

Under load, the curves of Figure B 4 were obtained. They are quite similar to those obtained in Series III except that the influence of jacking penetrates a somewhat shorter distance, about a foot and one-half.

Series VI

The four specimens of this series were intended to clarify the unexpected results of Series V, and to reproduce them if possible. Two factors in particular were to be checked. It was felt that the gradual release of the prestress might have had an effect and secondly, that the interface pits were caused by over-vibration of the wet concrete. It was thought that a foam may have collected on the stranddue to the excessive vibration of the air-entrained concrete.

A four foot and a three and one-half foot specimen were released gradually. A three and one-half and an eight foot specimen were released suddenly. All specimens were thoroughly

vibrated and the eight foot specimen was severely over-vibrated. All the specimens were instrumented with tensometer gages over their entire lengths.

As indicated in Table IX, none of the specimens slipped either at release or under test. In each case either the strand ruptured or attained its guaranteed ultimate load.

The development of the concrete strains during the gradual release of Specimens VI-1 and VI-4 is shown in Figures B 5 and B 12 respectively. The transfer lengths are approximately fifteen and thirteen inches respectively. Figures B 6, B 13, and B 14 show the development of strains under test. A wire in the strand of the four feet Specimen VI-1, failed (probably at a weld) at 24.6 kips just before a set of strain data was to be taken. Therefore only one set of readings was obtained for this specimen after the start of the test. The data indicated that the effect of jacking was felt for only about eight inches into the bonded length. By direct proportion, this length would have been twelve to thirteen inches if the strand had attained a maximum load comparable to that of the other specimens. This length agrees with those obtained for the other specimens.

The curves for Specimen VI-4, three and one-half feet in length, show the effect of jacking to be penetrating only about sixteen inches into the specimen. The curve resulting after the maximum strand force, termed strand "failure" on the figures, had been attained and subsequent release of all strand force would show a "transfer length" of about sixteen inches at the jacking end. (After the strand force at the loading end has been decreased to zero, the specimens are, in effect, short axially prestressed beams.) This is quite in contrast to the similar curves of Specimens III-1 and V-4, but in each case the curve resulting after strand failure is a good mirror image of the jacking curve immediately preceeding the failure and release of all load.

The three and one-half foot specimen, Specimen VI-2, which was suddenly released, had a transfer length of about nine inches. The influence of the jacking force penetrated sixteen inches. The ultimate anchorage length indicated by this specimen therefore was about two feet. The strain development is shown in Figures B 7 and B 8.

The strain distribution curves for the eight foot specimen, VI-3, which was released suddenly are extremely irregular:

Figures B 9, B 10, and B 11. The data was taken simultaneously with that for the other specimens and must be accepted as reliable. The transfer length indicated is approximately eleven inches. The influence of the jacking forces penetrated only about thirteen inches.

There is no evidence that over-vibration of the mix had any adverse effect on the bonding. Quite to the contrary, it appears from comparing these data with that of Series V that the pitted contact surfaces and resultant adverse results of the latter were most probably due to insufficient rather than too much vibration. It would seem evident from these observations and the results of beam tests by Montemayor, presented in Chapter IX, that the degree of compaction of the plastic concrete is a parameter of paramount importance in determining bond strength. The well vibrated and compacted concrete exhibited better bond characteristics than the under-vibrated concrete. The fear of the possible detrimental effects of over-vibration was probably the ultimate cause of the poor results.

Release slip and slip under load, where measured by the method shown in Fig. 17.

Series VII

The four specimens of this series were made with unpretensioned strands to investigate the effect of level of steel prestressing. The specimens were seven, five and one-half, four and one-quarter, and two and three-quarters feet in length. The wide range of length was prescribed, because no previous bond investigations on untensioned strand had been discovered in the literature. The shortest specimen indicated slip failure, as measured by the method of Figure 16, at a load of about 19.8 kips. The others developed the ultimate strength of the strand.

Tensometer gage points were provided only on the five and one-half foot specimen, Specimen VII-1. The resulting strain curves are shown in Figure B 15. The influence of the applied jacking forces has in this case penetrated about thirty seven inches into the specimen. Observations and conclusions regarding the effect of level of prestressing will be reserved for a later section in this chapter.

Series VIII

The eight specimens of this series of tests ranged in bonded length from two to four and one-half feet. This group

of tests was intended primarily to provide additional data points for Figure 24 in the critical range of lengths. Therefore, none of the specimens was instrumented to provide strain information. Slip instrumentation both at release and under applied load was as shown in Figure 17.

The two foot specimen, Specimen VIII-1, sustained an effective prestress of 16.7 kips and slipped under the action of the first small increment of jacking load. Evidently the transfer length was almost two feet for this specimen. The two and one-half foot specimen, Specimen VIII-2, managed a load of 23.7 kips before slipping. The other two specimens at the same end of the testing frame, Specimens VIII-3 and VIII-4, were three feet long. Both indicated a slight slip at loads exceeding the guaranteed strand ultimate. The remaining four specimens, ranging in length from three and one-half to four and one-half feet, developed the ultimate strength of the strand and showed no slip.

Special Short Columns

Some of the extra space available in the forms for Series VI and VIII was utilized to pour five short column specimens. Two of these were three feet long. The others were three and one-half, four and one-half, and five feet in length. The columns were the same section as the pull-out specimens.

The purpose of these tests was to investigate the self-locking action developed in the absence of adhesive bond. All adhesive bond was destroyed by thoroughly impregnating the strand with oil prior to the pouring of the beams. Any transferred prestress would then be due solely to friction, shear resistance of the concrete ridges, and the self-locking action previously mentioned. The strain data derived from the tests would also provide an opportunity to observe strain distribution due mainly to friction and concrete ridge resistance since the self-locking action would be concentrated mainly in the center region of each specimen.

All of these columns were released suddenly. All were instrumented with Huggenberger Tensometer gage points. Slip data was not successfully obtained. Figures B 16 through B 20 show the strain distribution at the time of release and several days after. It is evident that some readjustment took place during this interval in several of the specimens since the indicated creep is obviously not proportional to the original strains.

Each of the curves, however, shows a more or less constant rate of increase in the strain at release. The maximum value at the interior of the beams is somewhat greater than what would be expected from a normal extension of the strain curves. It is believed that this inordinate peak strain is due primarily to the localization of the strand locking action.

The maximum strains attained in these specimens are an indication of the order of effective prestress. The strain is a function of the effective prestress and the modulus of elasticity of each specimen. The curves of Specimen VI-5, Figure B 16, indicate that a normal level of effective prestress had been achieved. The maximum strain of about 270 millionths agrees very well with the maximum strain of the regular pull-out specimens of Series VI.

The remaining four column specimens are all of Series VIII. No strain data was obtained for the pull-out specimens of this series so no direct comparison of maximum strains can be made. However the maximum value of 220 millionths of Specimen VIII-9 is approximately what would be expected for a normal level of effective prestress. This specimen is five feet long. The relative values of effective prestress of the remaining specimens, assuming a strain level of 220 millionths as the 100 per cent index, are, 66 per cent for Specimen VIII-10, length four and one-half feet, 75 per cent for Specimen VIII-11, length three and one-half feet, and 58 per cent for Specimen VIII-12, length three feet. As would be expected for frictional bond, the level of effective prestress is roughly proportional to the length.

B. Effect of Strand Cover on Surface Strains

This effect was explored in Series IX and X. The pertinent data is presented in Table X. The section sizes selected were 2-1/2 x 2-1/2 inches and 6 x 6 inches nominal. The actual specimen dimensions are reported in Table III. All specimens were axially prestressed with a single 7/16 inch strand pretensioned to approximately its allowable 18.9 kip load. Release of prestress was gradual.

The lengths prescribed were three and four feet. These were selected with the thought that the three foot specimens would slip under applied load and the four feet specimens would develop the strand ultimate. The actual results for each individual test series are presented in the following discussion.

TABLE X TABULATED RESULTS OF TEST SERIES IX AND X

Spec. No.	Bonded Length feet	Nominal Cross Section inches	Strand Ult.* kips	Strand Slip	Slip Load kips	Prestress kips		Release Slip**	f'_c at Test psi
						Init.	Effec.		
IX-1	3	6 x 6	22.3	None	--	19.2	17.9	0.031	4400
IX-2	4	2-1/2 x 2-1/2	23.0	None	--	18.9	15.0	.024	4400
IX-3	4	6 x 6	23.9	None	--	19.1	18.1	.081	4400
IX-4	3	2-1/2 x 2-1/2	a	None	--	18.4	16.2	.018	4400
X-1	3	2-1/2 x 2-1/2	21.6	None	--	18.6	16.4	.037	4700
X-2	4	6 x 6	21.3	None	--	18.4	17.5	.075	4700
X-3	4	2-1/2 x 2-1/2	25.2	None	--	19.1	17.0	.042	4700
X-4	3	6 x 6	--	R	16.2	18.7	14.8	.212	4700

* All loaded specimens failed prematurely in strandvise grips

** This reported value is the observed slip minus the elastic shortening of the gage length

a Specimen failed due to creep in the period between release and test

R At Release

Series IX

Four specimens, each of a different length and section, were cast. As was mentioned in Chapter V, some difficulty was experienced with the premature setting of the concrete. The mix was quite stiff when placed and was vibrated with difficulty. The tests were conducted anyway even though the concrete strength proved to be relatively low.

The first three specimens were instrumented along their total lengths with Type A-9 SR-4 gages spaced about seven and one-half inches apart and staggered on opposite sides. Slip instrumentation consisted of dial mountings similar to that shown in Figure 15 except that in these cases the dial pointers were in contact with a smooth aluminum or thin steel plate attached to the specimen ends with sealing wax. This method is not as accurate as those shown in Figures 16 and 17 but was necessary due to the unusual size of cross-sections.

The buildup of strains during gradual release is shown in Figures B 21, B 24, and B 27. None of the specimens slipped at release. The transfer lengths indicated are twenty-six inches for both 6" x 6" specimens, IX-1 and IX-3, and fifteen inches for the 2-1/2" x 2-1/2" specimen, IX-2.

It is evident that the curves are much more regular and smooth than for the previous test. The primary reason for this is the relatively long gage length, six inches, of the A-9 gages. A long gage length tends to minimize any discontinuity or stress concentration in the concrete due to air pockets or large pieces of aggregate close to the surface. The curves shown are the averages of the curves obtained for the two instrumented faces.

The time elapsed between release of prestress and actual testing was about ninety-four hours. In this interval, the fourth specimen, which was uninstrumented for strain, failed by concrete crushing due to excessive creep in the unbonded eighteen inch length at the bearing end.

There was no indication of change of transfer length with time for any of the specimens reported in this paper with the possible exception of Specimen IX-3, Figure B 27. In this case the inordinate increase of strain in the region past the transfer zone is most probably due to creep, which is proportional to the original strain, in a region where the concrete was not thoroughly vibrated. The initial strain

readings were unusually high immediately after full release indicating a low elastic modulus in this region. This specimen and the one which failed by crushing due to creep were the last two placed. Their somewhat abnormal behavior is undoubtedly due to incomplete compaction of the very stiff mix.

The strain distributions due to applied jacking loads are shown in Figures B 22, B 23, B 25, B 26, B 28 and B 29. Again the curves are relatively smooth, considering the measured level of strain, and show a gradual build-up and increase of length influenced by the jacking forces. As was mentioned before, the strand force for this sereis and for Series X did not reach ultimate load because the new strandvises obtained for these tests proved incapable of developing the strand ultimate. In all cases for these two series of tests, the strand failed prematurely in the strandvise, (Figure 12). The maximum loads attained are reported in Table X.

Series X

Test Series X was conducted to check the results of Series IX with respect to both the transfer lengths and the premature strand failures. The slump of the mix used for these specimens was relatively high to facilitate the placing of the concrete for the small, 2-1/2 x 2-1/2 inch crosssection, specimens. Release and strand slip were measured by the method of Figure 18 for the small specimens and Figure 17 except that the plates were one piece, for the large specimens. All four specimens were instrumented with A-9 SR-4 gages spaced approximately seven and one-eighth inches apart and staggered on opposite sides.

At release Specimen X-4, 6" x 6" crossection and three foot bonded length slipped when 87% of the initial prestress had been transferred. The other three specimens successfully transferred the prestress. Specimen X-2, the other 6" x 6" specimen exhibited a transfer length of twenty-nine inches. Specimens X-1 and X-3 had indicated transfer lengths of eighteen and twenty-nine inches respectively.

Strain curves for release are shown in Figures B 30, B 33, B 36 and B 39. The strain distributions of Specimen X-4, Figure 39, tend to support the concept of bond failure at release which was shown pictorially in Figure B 3.

At test the strands again ruptured prematurely in the strandvises even though the first few rows of teeth in the gripping chucks had been filed down. The strain curves for these specimens under applied load are given in Figures B 31, B 32, B 34, B 35, B 37, B 38, B 40 and B 41.

Two inter-related variables were present in these test series (IX and X). As the strand cover is increased the precompression of the concrete is sharply reduced. Since actual bonding occurs at the interface of the steel and concrete, the cover has no direct bearing on the actual transfer length. Obviously, however, it will be of great significance when bond effects are to be investigated by surface strain measurements. It was pointed out in Chapter II that the transfer length observed from surface strains is necessarily greater than the actual at the interface.

The equations developed in Appendix A show the effect of stress level in the concrete to be minor, in fact Janney (6) neglected it entirely. A decrease in precompression as results from increasing the crossection should result in a minor shortening of the transfer length. Since the larger specimens exhibited the greater transfer lengths, it is evident that the effect of strand cover is of greater importance than that of the state of stress. The results are not susceptible to quantitative interpretation, however.

C. Effect of Prestressing on Bond

Test Series VII, in which unpretensioned strands were prescribed was undertaken primarily to investigate this variable. The effect of the greater reduction in strand diameter according to Poisson's ratio due to applied tensile loads up to strand ultimate for unpretensioned strands was the phenomenon to be analyzed.

The results show that the two and three-quarter foot specimen failed in bond at about 19.8 kips. This combination of embedment length and total strand force falls in the scatter of data points plotted in Figure 24. The instrumented specimen, Specimen 1, indicated that the influence of a strand force of 27 kips penetrated about thirty-seven inches into the specimen. The strain curves of Figure B15 indicate a leveling of

strain taking place about seven inches into the unbonded length. If this distance be added to the observed penetration, the total indicated anchorage length is forty-four inches, which agrees with the results of prestressed specimens. Specimen 2, which was four and one-quarter feet long, developed 97.8 per cent of the guaranteed strand ultimate when the test was stopped. Similar tests on unpretensioned 7/16 inch strand reported by Walther and Warner (7) indicate bond failure in twelve inches of embedment at from 8 to 9 kips of load.

The results of these latter tests and those of Series VII indicate that the degree of steel prestress is relatively unimportant in the determination of the bond capacity of strand. The ultimate anchorage length for untensioned specimens appears to be essentially the same as for those tensioned to recommend values. This is to be expected since in both cases the bond is entirely mechanical and frictional at slip. It further suggests that the contribution of Poisson's effect is relatively minor.

D. Slip

Slip is the general term used to define a relative movement of the steel with respect to the concrete. Two general types of slip are possible. The first is that which takes place at the release of prestress, called "release slip". This is simply the pulling in or shortening of the steel with respect to the release end as prestress is transferred from steel to concrete. The second type of slip is that which denotes bond failure and is called "strand slip" or simply "slip". The specimen has failed in bond, or has slipped, when the steel has moved relative to the total length of concrete in which it was initially embedded. The load or strand force at which bond failure takes place is defined as the "slip load".

The values of release slip for those specimens which did not fail at release reported in this paper are directly comparable to those measured for beams. It is doubtful, however, that bond failures at release as observed in these tests are possible in beams. The reasons, foremost of which is the self-loacking action of strand, for this observation are stated in the beginning of the previous chapter. Also the five simulated beam specimens, which were cast to investigate this phenomenon and reported earlier, indicate that this observation is valid. The values of strand slip are only of practical interest inso-

far as their initial values indicate bond failure. The subsequent development of strand slip for pull-out specimens is only of academic interest since, as has been previously pointed out, this "free" slip observed in these specimens is not possible in a beam.

Bond failure at release was indicated when an inordinate amount of release slip was observed, viz., for most cases, a slip exceeding 0.10 inches. Actual failure, however, was recognized when the strand dynamometers at the bearing ends of the specimens, indicated a decrease in strand force in excess of that to be normally expected for the amount of prestress released. All specimens which failed at release also exhibited immediate strand slip at the inception of applied load.

Bond failure at test was reported when a value of strand slip of 0.0020 inches was observed which increased with each succeeding increase in applied strand force. This method of observing bond failure was necessary due to the minimum assumed accuracy of the dials and the slip measuring apparatus in total which was sensitive to any external shock or disturbance. This amount of strand slip in the lengths of specimens herein reported would result in decrease of strand force less than the assumed minimum accuracy of the strand dynamometers.

The technique of releasing the prestress gradually permitted the development of release slip to be observed. Release slip is plotted against per cent of prestress released for the specimens of Series V in Figure B 42. These curves show that once slipping has fully developed, i.e., the specimen has completely failed in bond, it becomes directly proportional to the prestress released. In Figure B 43, the per cent of prestress lost at the load or bearing end is plotted with the slip and again the three curves are parallel and reasonably straight once slip has developed throughout the length of the specimens. The same phenomenon is observed in the release slip curve of Specimen 4, Figure B 49. Again it should be noted that in an actual beam the physical restraints imposed by the concrete place definite limits on the loss of prestress which can occur.

The curve for the fourth specimen, which successfully transferred the prestress, is compared in Figure B 45 with those for the specimens of Series VI which also transferred the prestress. If these curves are compared to those for the successful specimens of Series IX and X, it is observed that they are basically similar.

The progression of strand slip with applied jacking forces for the applicable specimens of Series IV and V is shown in Figure B 44. Similar curves for Specimens VII-3 (unpretensioned) and X-4 are shown in Figure B 46 and B 50, respectively. It is seen that mechanical as well as frictional bond is indicated since the load carrying capacities of these specimens continue to increase as the slip progresses at an almost constant rate after slip has sufficiently developed. Also, it appears that the rate of increase, or slope, of the curves is greatest for specimens slipping at high loads and a minimum for specimens slipping (failing) at release.

The strands of the Series IV specimens had been burned off close to the specimens. After bond failure, continued jacking resulted in the "button" on the strand formed by this burning eventually being drawn into the specimen. It is striking therefore that slopes of load-strand slip curves for these specimens which failed at release are the same as those for the specimens of series X which also failed at release and which were burned several inches from the ends of the specimens so no buttons were present to influence the results.

The load-strand slip relation for the specimens of Series VIII, shown in Figures B 46 and B 47, indicate that another type strand slip, different from the one previously discussed, exists. The slip curves are quite unusual. The curves for specimens one and two, Figure B 46, do not seem to follow any definite pattern of regular behavior. At the first slip, a sharp decrease in strand force was observed. The applied load was then increased without any additional slip until the process was eventually repeated. Each sudden slip was accompanied by a sharp report very similar to that made by a strand rupturing. The only possible explanation would be that a sudden redistribution of bond force was taking place. This hypothesis is unsubstantiated however because no strain date was obtained for these specimens. The jacking was discontinued for almost two days. No slip occurred during this time, but upon resumption of jacking the performance was repeated.

The slip curves of Figure B 47, Specimens VIII-3 and VIII-4, only slightly resembled those depicting normal behavior. Both indicated a very slight slippage at loads less than what has been reported as the slip load. This observed slippage did not progress with increased applied strand force. Therefore no bond failure was reported for these specimens until this con-

dition had been attained. When bond failure did take place however during the two day interval previously mentioned, a sudden decrease in strand force was observed. After a small amount of additional load with no accompanying increase in slip, the specimens commenced to behave in normal fashion, exhibiting an almost constant rate of load-slip increase. Eventually the strand of specimen three ruptured at about 30 kips and the strand force of specimen four decreased with additional slip.

The general shape of the release slip curves, Figures B 42, B 45, B 48, B 49, provides information concerning the transfer phenomenon. Release slip is a measure of the elastic shortening of the strand in the transfer zone. Transfer is accomplished basically by friction and mechanical bond, or elastic bond or a combination of the two. For relatively small amounts of transferred strand tension, it is entirely possible that the bond is solely elastic. Strand shortening, in this case, would be controlled by the contact interface concrete deformation. Therefore the transfer length is short and the slip small. As more initial strand tension is released the bond eventually becomes a combination of friction and elastic bond, the transfer length increases and the slip increases at a greater rate, i.e., the slope of the release slip curve decreases. If the bond were entirely frictional, slip would be directly proportional to the transfer length and slope should become constant, as it does for those specimens which failed at release, (Figures B 42 and B 49). If the release slip curves of those specimens which successfully transferred the prestress are observed, it will be noted that they approach a constant slope in the final stages of the release of pretension. This is taken as an indication that the transfer of the level of pretension prescribed in these tests, 18.9 kips for 7/16 inch strand, is accomplished mainly by friction and the mechanical effect of changing pitch of the strand helix.

It would naturally follow from this hypothesis that the order of magnitude of release slip should provide an indication of the magnitude of the transfer length. A large amount of release slip should accompany a long transfer length and vice-versa. Such a relationship is indicated from the data but it is not sufficiently consistent to permit the derivation of any formal design expression. Ratz, et al ([8]) have recently presented a thorough analysis of this relationship.

E. Bond Stress Values and Distribution

(1) Stresses

To evaluate bond stresses from strains measured at the surface it is necessary to assume a uniform distribution over the entire cross-section of the concrete. The limitations of this assumption have been previously discussed. It was concluded that bond stresses so obtained are comparable only for specimens having the same strand cover.

Repeating Equation III-1, bond stress is

$$u = \frac{A_s}{\Sigma o} \frac{df_s}{dx} \qquad \text{(VIII-1)}$$

The steel stress may be expressed as

$$f_s = \epsilon_s E_s \qquad \text{(VIII-2)}$$

The total tension in the steel at any section will equal the total compression in the concrete. Assuming ϵ_c constant over the cross-section of concrete,

$$\epsilon_s E_s A_s = \epsilon_c E_c A_c$$

$$\epsilon_s = \frac{E_c A_c}{E_s A_s} \epsilon_c \qquad \text{(VIII-3)}$$

Combining equations VIII-1, VIII-2, and VIII-3, the bond stress is

$$u = \frac{A_c E_c}{\Sigma o} \frac{d\epsilon_c}{dx} \qquad \text{(VIII-4)}$$

Since $\frac{d\epsilon_c}{dx}$ is the slope of the longitudinal concrete strain distribution curve at any section, bond stresses may be determined from surface strains in this manner.

In Table XI are listed the release bond stresses for all the instrumented test specimens determined according to Equation VI-4. The slopes used were the average maximum slopes in the transfer zone of each specimen. The transfer lengths indicated from surface strains are listed in Table XI in the column headed by "L_t". These were determined by measuring distance from the release end at which the strains assumed a maximum, constant value. For the short column specimens, L_t is the distance to the peak strain. Their bond stress values provide

TABLE XI MAXIMUM BOND STRESSES AT RELEASE

Specimen Number	Type of Gages	$\frac{d\epsilon_c}{dx}$ max. in/in^2 x 10^{-6}	$\frac{A_c}{o}$ in.	E_c psi x 10^6	Bond Stress psi	L_t in.	Slipped at Release
III-1	A-1	23.3	9.26	5.3	1145	10	No
VI-1	Hugg.	27.3	9.26	5.3	1340	15	No
VI-2	Hugg.	35.5	9.26	5.3	1740	9	No
VI-3	Hugg.	28.4	9.26	5.3	1390	11	No
VI-4	Hugg.	29.5	9.26	5.3	1450	13	No
IX-1	A-9	9.46	22	4.0	830	26	No
IX-2	A-9	89.7	3.44	4.0	1230	15	No
IX-3	A-9	7.66	22	4.0	675	26	No
X-1	A-9	61.0	3.44	4.7	990	18	No
X-2	A-9	4.72	21.2	4.7	470	29	No
X-3	A-9	54.5	3.44	4.7	885	21	No
X-4	A-9	5.66	21.6	4.7	574	>36	Yes
VI-5 L*	Hugg.	27.5	9.26	5.3	1350	15	--
VI-5 R*	Hugg.	15.3	9.26	5.3	750	21	--
VIII-9 L	Hugg.	ND	9.26	6.0	---	33	--
R	Hugg.	10.6	9.26	6.0	590	27	--
VIII-10 L	Hugg.	5.6	9.26	6.0	311	39	--
R	Hugg.	14.7	9.26	6.0	816	15	--
VIII-11 L	Hugg.	ND	9.26	6.0	---	23	--
R	Hugg.	13.1	9.26	6.0	728	19	--
VIII-12 L	Hugg.	ND	9.26	6.0	---	19	--
R	Hugg.	ND	9.26	6.0	---	17	--

* L Left end of specimen as shown on appropriate figures.
R Right end of specimen as shown on appropriate figures.

an excellent basis of comparison with the normal pull out specimens since the strands in these specimens were oiled.

The value of circumferential perimeter, Σo, for the seven wire strand used in these tests was obtained from the relationship shown in Figure B 51. It was chosen in preference to the expression recommended by ACI-ASCE Joint Committee 323 (9), viz. $\Sigma o = \frac{4}{3} D$, as being more exact.

Similar bond stresses for the strain instrumented beams in the literature are shown in Table XII. The bond stresses, determined from the slope of the strain curves due to applied jacking loads for the instrumented pull-out specimens are listed in Table XIII. The distance L_D is the indicated bonded length utilized to develop the jacking force by bond.

The bond stresses listed in Tables XI, XII and XIII show a wide scatter. No consistent relationships appear to exist other than that transfer stresses are several times greater than those developed by jacking. It would seem unwise to recommend any design criteria based on bond stress.

Values of average bond stress over the entire effective anchorage length L_e are listed in Table XIV. These are computed from

$$u = \frac{T}{\Sigma o L_e} = \frac{T}{\Sigma o (L_t + L_D)} \qquad \text{(VIII-5)}$$

in which T is the strand tension at slip for specimens that failed and the maximum strand force attained for those which did not. L_t is the transfer length and L_D the length affected by jacking force.

Eight of these specimens slipped. Bond stresses at slip ranged from 266 to 569 psi with an average of 413. The highest and lowest values were given by specimens of the same series--and had the same cylinder strength. Evidently the difference must reflect non-uniformity of compaction. No correlation with f'c is indicated by the data.

Five specimens developed the ultimate strengths of the strand. In these cases values ranged from 402 to 635 with an average of 527.

TABLE XII BEAM MAXIMUM BOND STRESSES AT RELEASE

Beam No.	Source (Ref. No.)	Pretensioned Reinforcement	Ac (in^2)	ϕ_o (in.)	$\frac{d\epsilon_c}{dx}$ (1/in.)	E_c psi x 10^6	Bond Stress (psi)	L_t (in.)
I	20	6-3/8" strands	60	9.05	21.7	2.1	305	32
II	20	6-3/8" strands	60	9.05	29.5	2.35	460	20
III	Ch IX-A	1-7/16" strand	40	1.76	13.9	4.8	1510	21
III	do	1-7/16" strand	40	1.76	14.5	4.8	1570	21
IV	do	1-7/16" strand	40	1.76	33.8	4.75	3630	13
IV	do	1-7/16" strand	40	1.76	29.2	4.75	3140	13
V	22	2-7/16" strands	72	3.52	15.7	3.9	1250	24
VI	22	2-7/16" strands	72	3.52	17.9	3.9	1350	32

TABLE XIII MAXIMUM BOND STRESSES AT TEST, JACKING END

Spec. No.	Type of Gages	A_c / o (in.)	$d\epsilon_c/d_x$ * (1/in.)	E_c psi x 10^6	Bond Stress psi	L_D (in.)	Slip at Test
III-1	A-1	9.26	4.41	5.3	216	30	No
V-4	Hugg.	9.26	7.16	4.8	318	18	No
VI-2	Hugg.	9.26	9.83	5.3	482	16	No
VI-3	Hugg.	9.26	14.68	5.3	720	13	No
VI-4	Hugg.	9.26	16.32	5.3	800	16	No
VII-1	Hugg.	9.26	6.50	5.2	313	37	No
IX-1	A-9	22	1.35	4.0	119	12	No
IX-2	A-9	3.44	26.1	4.0	359	16	No
IX-3	A-9	22	2.34	4.0	206	12	No
X-1	A-9	3.44	13.67	4.7	221	15	No
X-2	A-9	21.2	0.65	4.7	65	16	No
X-3	A-9	3.44	26.25	4.7	425	19	No

* These maximum slopes were taken from the strain curves for the highest load at which strains were recorded.

TABLE XIV - CRITICAL AVERAGE BOND STRESSES

Spec. No.	Length (in.)	Maximum Load (kips)	$u = \frac{T_s}{\Sigma_o L_e}$ (psi)	Release Age (days)	Release f'c (psi)	Test Age (days)	Test f'c (psi)	% of Avg. f'c
III-1	40*	28.3	402	25	6500	26	6500	6.20
IV-1	18	18.0 S	569	7	4250	7	4250	13.38
IV-7	30	20.6 S	390	7	4250	7	4250	9.18
IV-8	48	22.5 S	266	7	4250	7	4250	6.26
VI-1	23*	24.6	608	34	6100	40	6530	9.62
VI-2	25*	27.4	625	34	6100	40	6530	9.89
VI-3	24*	26.8	635	34	6100	40	6530	10.03
VI-4	29*	28.6	560	34	6100	40	6530	8.85
VII-1	37*	27.0	415	--	----	17	5650	7.35
VII-3	33	19.8 S	341	--	----	17	5650	6.04
VIII-1	24	16.7 S	396	39	6150	39	6150	6.44
VIII-2	30	23.7 S	450	39	6150	39	6150	7.32
VIII-3	36	29.4 S	465	39	6150	39	6150	7.56
VIII-4	36	27.0 S	426	39	6150	39	6150	6.93

* Length=transfer plus length affected by jacking determined from measured strains, $L_t + L_D$.

S Slip Load

TABLE XIV (continued)

Spec. No.	Length (in.)	Maximum Load (kips)	$u=\frac{T_s}{\Sigma_o L_e}$ (psi)	Release Age (days)	Release f'c (psi)	Test Age (days)	Test f'c (psi)	% of Avg. f'c
IX-1	36*	22.3	352	18	4300	22	4400	8.00
IX-2	31*	23.0	422	18	4300	22	4400	9.60
IX-3	38*	23.9	358	18	4300	22	4400	8.14
X-1	33*	21.6	373	9	4700	9	4700	7.94
X-2	45*	21.3	269	9	4700	9	4700	5.72
X-3	40*	25.2	358	9	4700	9	4700	7.62
X-4	36	16.2 S	256	9	4700	9	4700	5.45

* Length=transfer plus length affected by jacking determined from measured strains, $L_t + L_D$.

S Slip Load

All of these values being fairly consistent, it might appear reasonable to establish a lower limit as a design specification. However, this would hardly be practicable since no practical way has been found to predict the lengths L_t and L_D and, indeed, no consistent relationship is indicated between these quantities themselves.

(2) Prestress Transfer Distribution

The steel stress as well as the bond stress distribution may be observed from concrete surface strains. By combining Equations VIII-2 and VIII-3, as follows,

$$f_s = \frac{A_c}{A_s} E_c \epsilon_c \qquad \text{(VIII-6)}$$

It is seen that the concrete strain is directly proportional to the steel stress within the limitation of the assumption of uniform stress distribution over the concrete cross-section.

If the assumption is made that frictional bond denotes a constant bond stress, the slope of the steel stress distribution curve will be constant, i.e., the curve will be a straight line, in the friction zone, according to Equation VIII-1. Guyon (10) makes such an assumption. The shape of the stress distribution curve, according to both Guyon and the authors' derived expression for elastic bond, Equation III-22, will be a curve of gradually decreasing slope. The transfer stress distribution according to these theories should be similar to Curve A in Figure 25.

Janney's (6) and the authors expressions for friction bond distribution do not result in a straight line distribution. The transfer stress distribution according to these theories would be a curve of gradually decreasing slope similar to Curve B of Figure 25.

It would seem that more than one type of transfer stress distribution is possible. Guyon (10) in fact, takes exception to the simplifying friction straight line assumption by saying, "It appears that the curve for f (f_s in present notation) has in some cases a variable slope over its entire length, whereas in other cases its slope remains constant over a certain distance s from the origin."

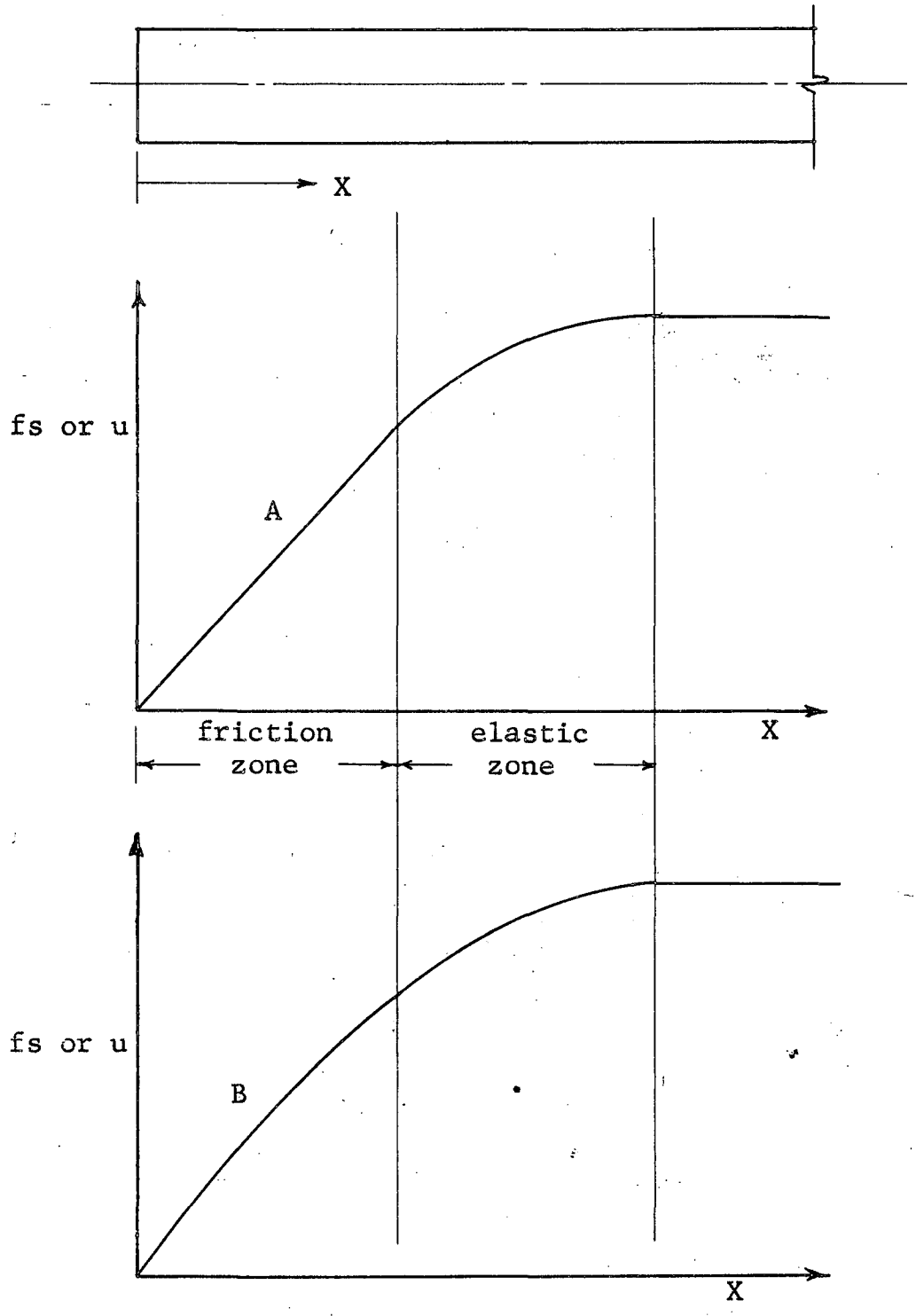

Figure 25 - Theoretical Transfer Stress Distribution Curves

(3). Distribution Due to Applied Load

The strain curves showing the effect of applied jacking forces all reveal a somewhat similar shape. Figure B 25 shows the phenomenon most clearly. It is seen that the strain distribution is basically an S-curve rotated to the right or the jacking end. The middle portion of the S-curve assumes a straight line shape indicating friction bond. The strains of the top portion, that closest to the jacking end, are seen to increase at a decreasing slope. This would appear to indicate a loss of friction bond as the higher strand force in this region results in a more pronounced separation of steel and concrete at their contact surface.

The strains at the lower portion of the S-curve are seen to increase from a constant pretest level at an increasing slope until the straight line configuration is attained. The strand force in this region of increasing slope is assumed to be developed by elastic bond.

The strain distributions analyzed and discussed in this report indicate that the bond development is mostly due to friction bond. The same observation was made for transfer bond. It would seem that this is the case since both Janney (6) and Peattie and Pope (11) make similar statements. The latter, in fact, say, "The ultimate bond resistance, expressed as an 'average' bond stress, is dependent predominantly on the frictional effect."

IX COMPARATIVE BEAM TESTS

A. Tests by Montemayor

(1) Description of Specimens

Four beams were tested by Montemayor in Fritz Laboratory as a part of the present investigation. The beams were 4 x 10 inches in cross-section. Reinforcement consisted of a single 7/16 inch strand, pretensioned to 0.70 f's and located two inches above the bottom fiber resulting in a prestress at strand level comparable to that of the first eight series of pull-out tests and an identical cover. All of the beams were 10'-6" in length and tested on a 10'-0" span.

The beams were cast and tested in pairs. The first pair were designated as Beams B1, B2, and the second as B3 and B4. After considering the results for the first pair, Beam B1 was selected as the prototype for the second.

In Beams B1, B3 and B4 the bond between strand and concrete was destroyed in the center portion of the specimens. For this purpose, the strand was wrapped with two layers of oiled wax paper. By this arrangement a symmetrical "available embedment length" or "bonded length" was provided at each end of the beams. The bonded length was 3'6", 4'0", and 2'6" for Beams B1, B3, and B4. At the center of the beams, SR-4 electrical strain gages were mounted on the strands.

Beam B2 differed from the others in that the available anchorage length was limited by a simulated vertical crack formed by an oiled plastic sheet 1/8 inch thick placed 3'-3" from the end of the beam. The crack went from the bottom of the beam up to a height of 8 inches, the theoretical level of the neutral axis at ultimate. The bonded length was later reduced during testing by a new crack that developed at 2'8" from the end of the beam, measured at the level of the steel.

The loading condition for the four beams are shown in Figure 26.

(2) Materials and Concrete Properties

The mixes were designed to yield a 6000 psi concrete at twenty-eight days, in all cases. Type 1A cement was used. The air entrained in the mixes was about three percent. The mix contained 8.3 sacks of cement per cubic yard and 4 gallons of

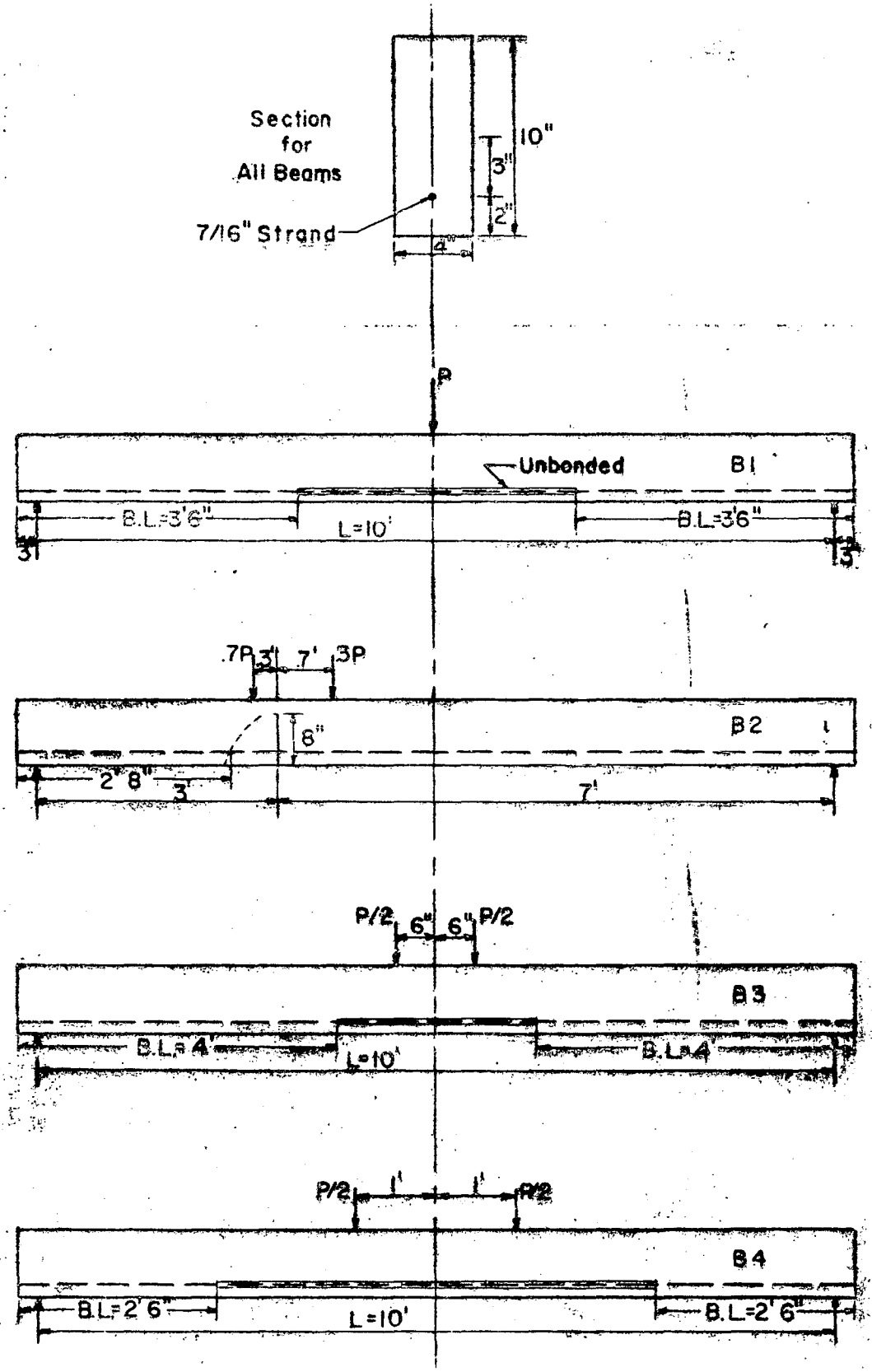

Figure 26 Dimensions and Load Conditions of the Beams.

water per sack with adjustments for the free moisture content of the aggregates. 1201 pounds of surface dry sand per cubic yard was used as the fine aggregate. Crushed limestone of a 3/4 maximum size was used as coarse aggregate, 1840 pounds per cubic yard in quantity.

Concrete properties are given in Table XV.

The strand used in the four beams was the same used in the pullout tests.

The percentage of steel "p" was 0.34%. The balanced steel percentage according to the B.P.R. formula is P_{bal} = 0.368% for f'c = 5000 psi and for 6000 psi concrete P_{bal} = 0.441%.

(3) Manufacture

Tensioning was performed in the frame used for the pull-out tests. The strand was tensioned in increments to 90% of ultimate to permit calibration of the SR-4 strain gages attached to the wires and then relaxed to the initial prestress level of 70%.

Beams B1 and B2 were cast on their sides. B3 and B4 in the normal vertical position. The beams were cured under burlap and plastic tarpaulins. Cylinders were given like treatment. The release operation is shown in Figures 27 and 28.

(4) Instrumentation and Testing Procedure

(a) Release

The instrumentation in the two pairs of beams was slightly different, but the data obtained was essentially of the same nature.

The set-up for slip readings was the same for all beams. It consisted of two 0.001" Ames dial gages at each end of the beam. These gages were attached to the strand. To provide a smooth surface to the arm of the gage, small steel plates were attached to the concrete surface. (Figure 29).

The camber set-up for Beams B1 and B2 consisted of five 0.001" Ames dial gages per beam (Figure 28). The two dial gages at the ends provided a base line. The other three were located at the center line and the quarter points respectively.

TABLE XV CONCRETE PROPERTIES OF TEST BEAMS

Beam	Age in Days At Release	Age in Days At Test	Concrete Strength in psi At Release	Concrete Strength in psi At Test	Concrete Strength in psi At 28 days	Tangent Modulus psi x 10^6 At Release	Tangent Modulus psi x 10^6 At Test
B1	8	12	4710	5170	6130	---	5.25 (c)
						4.49 (f)	5.20 (f)
B2	8	14	5560	5830	6630	--	4.75 (c)
						4.66 (f)	4.55 (f)
B3	12	23	6040	6640	6600	4.84 (c)	4.17 (c)
						4.82 (f)	5.15 (f)
B4	12	30	5900	6940	6620	4.75 (c)	4.25 (c)
							5.38 (f)

(c) Obtained by cylinder test

(f) Release values computed from camber data
Test values from deflection data

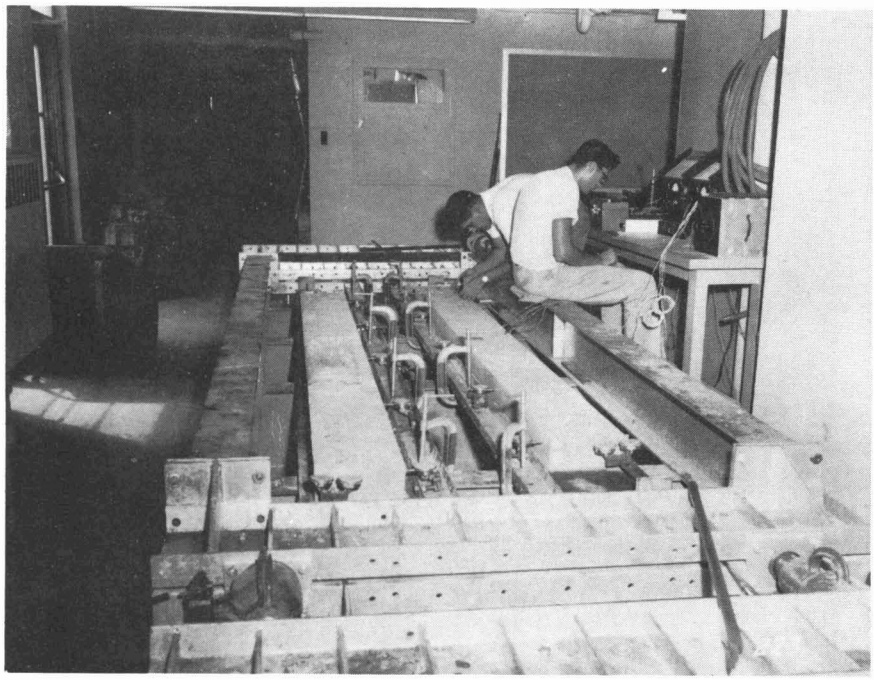

Figure 27. Release of Beams B1 and B2

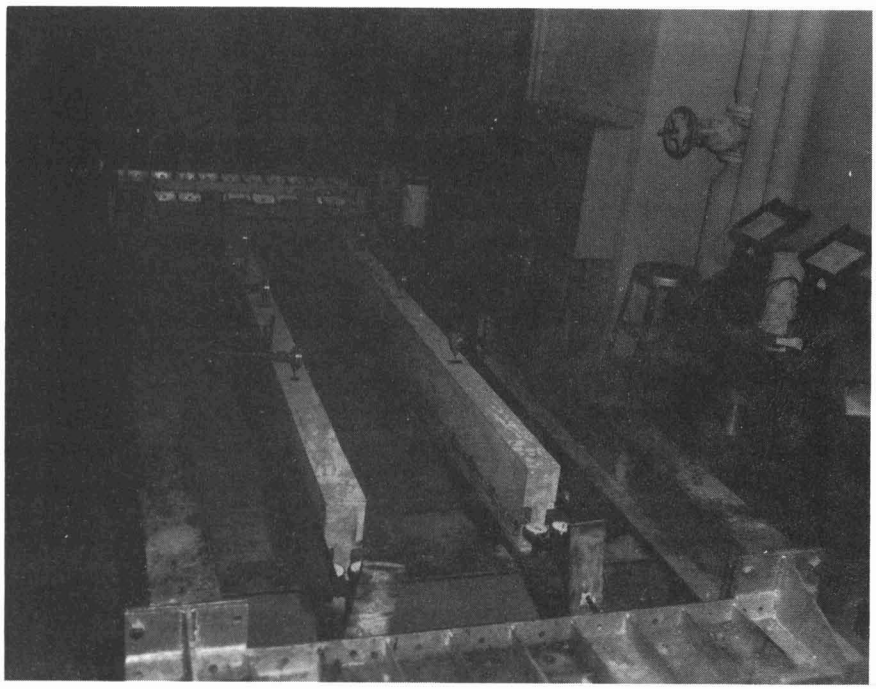

Figure 28. Release Set-Up for Beams B3 and B4

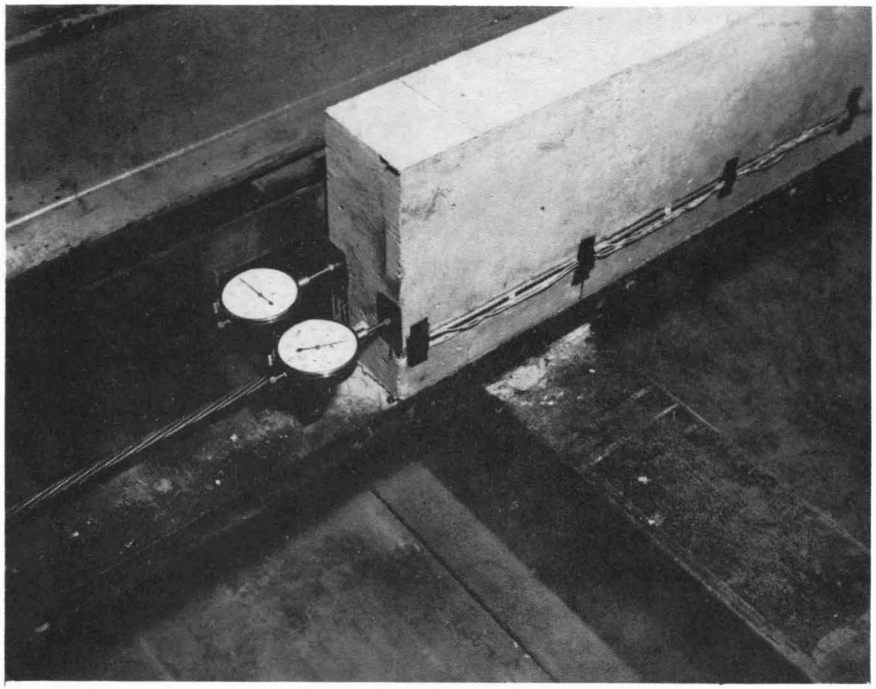

Figure 29. Slip Gages at Release - Beam B4

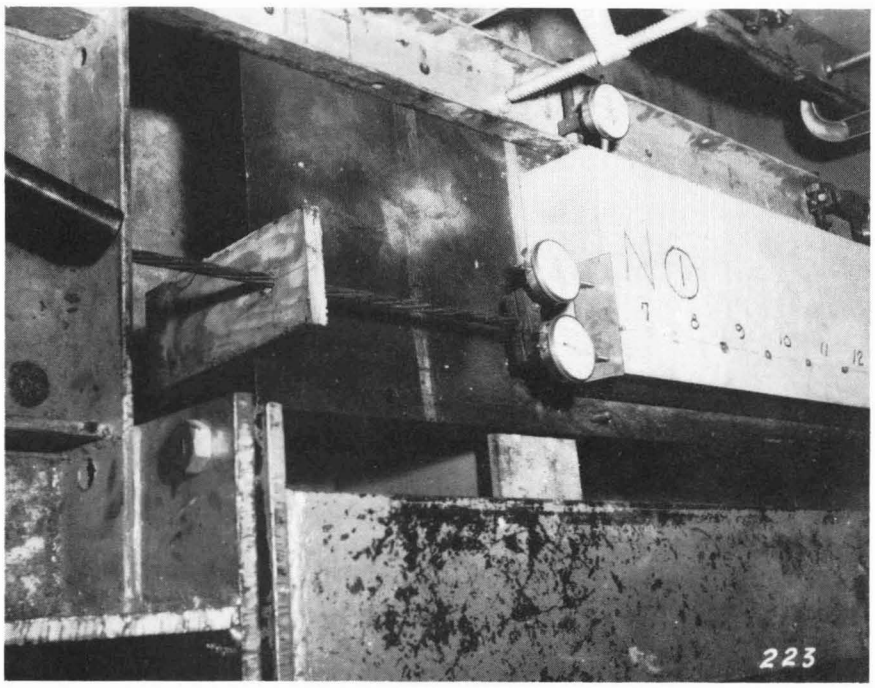

Figure 30. Points for Huggenberger Tensometer

For Beams B3 and B4 the set-up consisted of 3 gages per beam, for reading at the center and quarter points. The base line was provided by an angle on which the dial gages were supported. The angle rested on pivots that were embedded in the concrete at the ends of the beams.

Concrete strains were measured in the anchorage zones of B1 and B2 with a Huggenberger tensometer with gage length of 10 centimeters. (Figure 30). Because of the position in which these beams were cast, measurements could be made on one side of the beams only. Type A-9 SR-4 electrical strain gages were used on the second pair of beams. These were mounted on small aluminum channels with deformed flanges cast into the concrete at strand level (Figure 19).

The release operation was completed in the first pair of beams in four steps and 12 steps in Beams B3 and B4. All readings were taken at each increment.

Strain gages on the strand

SR-4 electrical strain gages of the A-12 type were mounted on the strands the middle of Beams B1, B3, and B4. It is relatively difficult to place them following the helicoidal axis of one of the stranded wires and to keep the gage in that position until the cement dries. The gages and the surrounding area must be effectively waterproofed to avoid damage during pouring and curing.

The following procedures were developed for application of the gages. All seven gages applied in this manner gave excellent performance. The gages were mounted and waterproofed before tensioning.

1. The portion of the strand, where the gages were to be placed, was preheated with a propane torch.
2. A very thin layer of petroelastic asphalt was applied and the surface brushed with the flame of the torch. Care was taken to make sure that the asphalt had penetrated the strand.
3. The excess asphalt was wiped off while it was still warm.
4. The exact location of each gage was cleaned with liquid solvent and sand paper.

5. The excess of paper was cut off the gage. Cement was applied to the wire and to the paper of the gage. The gage was placed and molded to the shape of the wire. Gentle pressure was applied to the gage by wrapping the strand with thin strips of rubber sheeting. After several hours in this position the strips were taken off and the gage allowed to dry for a day.

6. The leads were soldered to waterproofed leads which were bent in a zig-zag manner, and taped to the strand to protect the gage against pulling. Over the gage a piece of folded tape was placed so to protect the gage from the heat of the asphalt that was to be placed afterwards.

7. Several layers of asphalt were applied and brushed with the flame until a good coverage was attained.

The gages were checked at each stage of the operation. Compensating gages were mounted on a short length of strand, waterproofed and embedded in a concrete cylinder.

During testing readings of strand slip and centerline deflection were taken for all beams (Figure 34). In addition steel stress was obtained from gages on the strand for B1, B3 and B4. Huggenberger readings at the simulated crack of B2 (Figure 32) were taken to locate the neutral axis at the section permitting an accurate calculation of the steel tension. Data from the strain gages at strand level mounted on the aluminum channels visible in Figures 33 and 34 were recorded but were not successfully interpreted and have been omitted from the results.

Loadings were shown previously in Figure 26. The results of the beam tests are summarized in Table XVI. Two of the beams, B1 and B2 had strand slip failures. These had bonded lengths of 42 and 32 inches respectively. Beams B3 and B4 with lengths of 48 and 30 inches showed no slip of strand whatever.

The test results show satisfactory agreement with the pullout specimens and substantiate their validity.

Release data for all of the beams are collected in Appendix C.

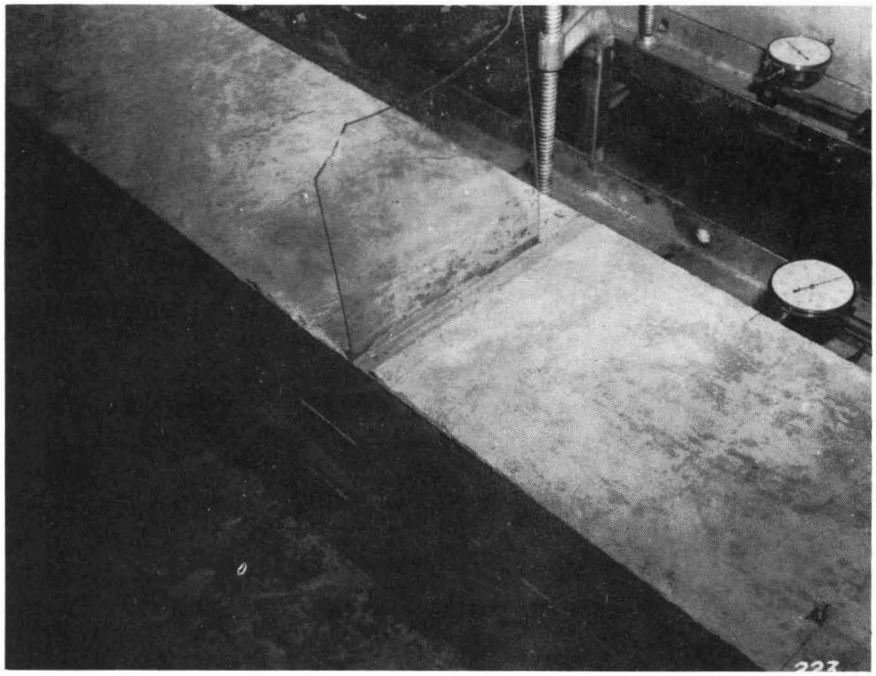

Figure 31. Simulated Crack - Beam B2

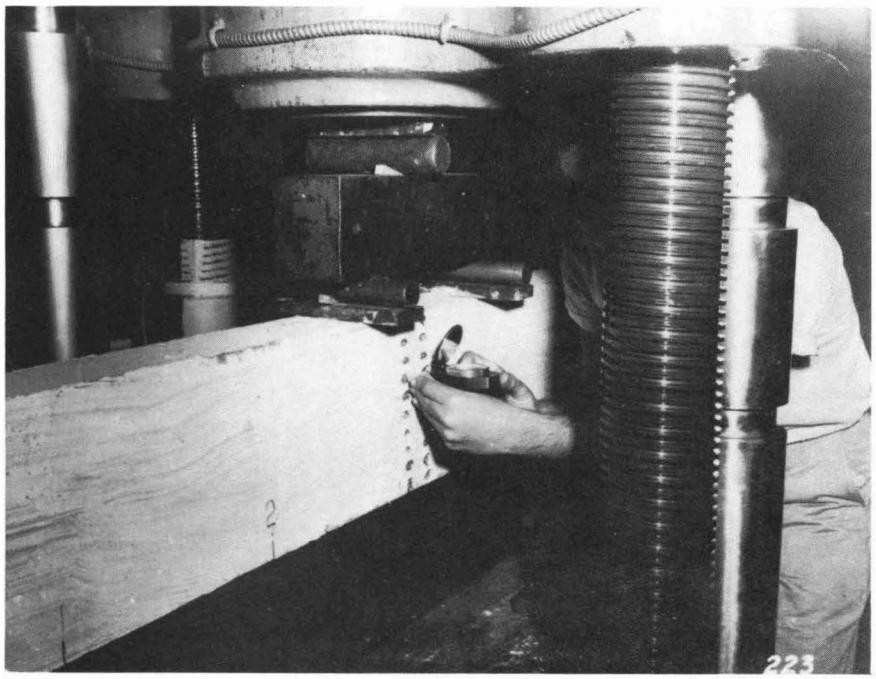

Figure 32. Measuring Simulated Crack with Tensometer

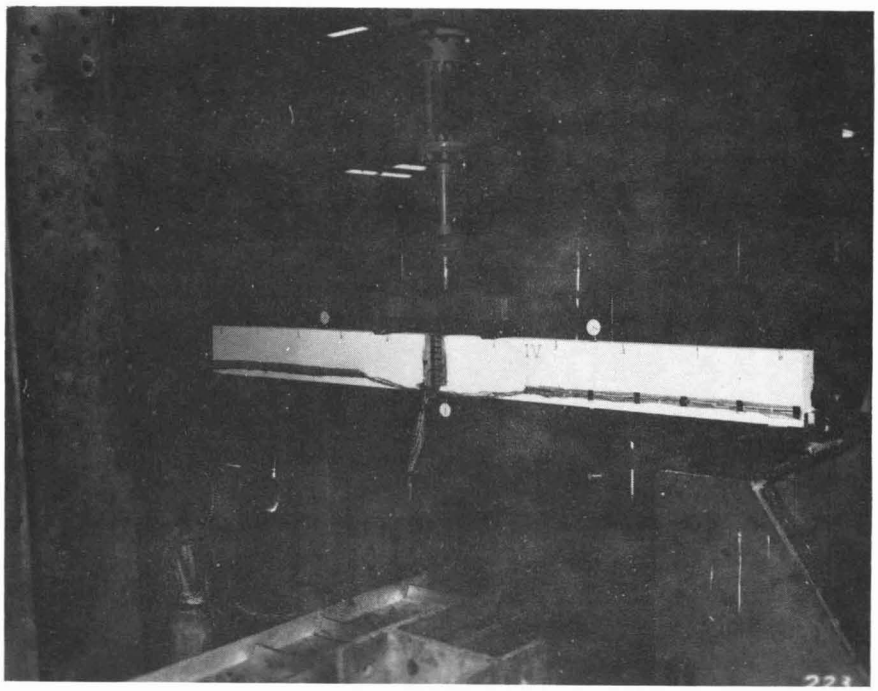

Figure 33. Test Set-Up - Beam B4

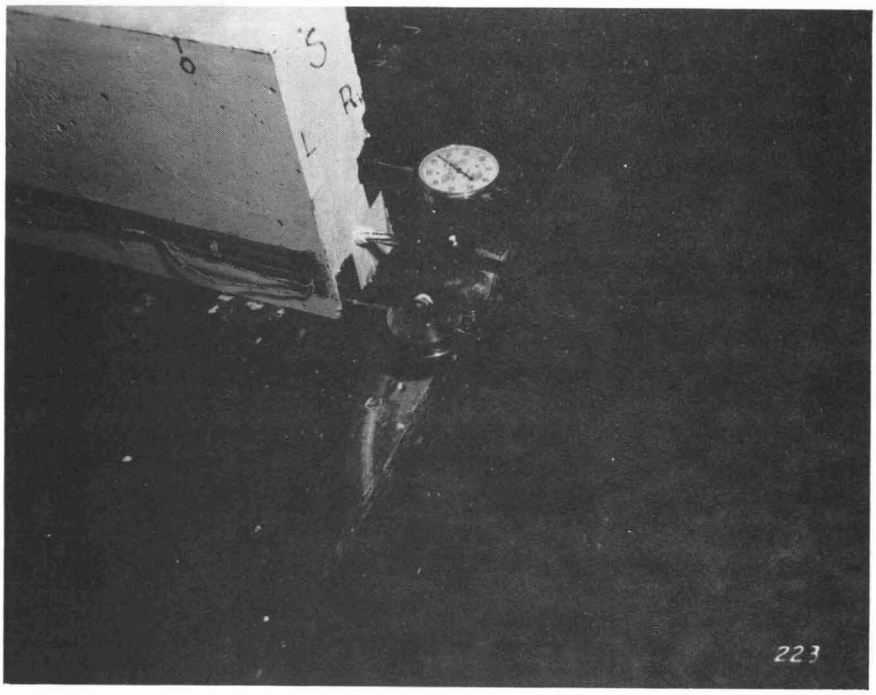

Figure 34. Slip Gages at Test

Table XVI - SUMMARY OF RESULTS OF BEAM TESTS BY MONTEMAYOR

Datum	Units	Beam B1	Beam B2*	Beam B3	Beam B4
cyl. f'c	psi	5170	5830	6640	6940
Bonded length	in	42	32**	48	30
Transfer length	in	16, 20	20, >24	21	13
Effective Prestress	kips	17.5	17	17.5	17.5
P crack (computed)	lbs	4000	3260	4350	4950
P crack (observed)	lbs	4400	4500	4200	4500
Pult (computed)	lbs	6300	8500	7170	8090
Pult (observed)	lbs	6800	9330	7140	7800
Measured Strand force at ultimate	kips	28.6	28.1	27	25.15
Failure mode		Bond	Bond	Flexure	Flexure
Load at slip	lbs	6600	8000	No slip	No slip
Slip load	% Pult	97.1	85.8	No slip	No slip
Measured Strand force at slip	kips	27.4	25.8	No slip	No slip

* Beam with the pre-cracked section.

** Determined by the distance from the end to the outermost crack.

(5) Test Results

(a) Performance of Beam B1

The computed cracking load was 4000 lbs. The first crack was observed at 4400 lbs. and had already progressed to at mid-depth of the beam. However, from the load-deflection diagram, Figure 35, it can be seen that cracking must have occurred at about 60% of the ultimate load or 4,080 lbs. The beam had only one crack which was divided into two and later three branches.

The ultimate load computed by Whitney's method was 6,300 pounds. The observed ultimate was 6,800 lbs.

The South end portion of the strand in B1 slipped when the load was 6,600 lbs. Then the ultimate load, 6,800 lbs. was reached for the first time. The load dropped to 6,560 lbs. presumably by slippage of the strand. At this point the beam started to take load again. At 6,600 lbs. the concrete started crushing. When 6,800 lbs. was reached for the second time, the beam failed. The load-slip diagram Figure 36 shows very clearly that part of the test. From the beginning of the test to 73.5% of Pult (5000 lbs.) the slip, as reported by the slip dials, was almost imperceptible. It amounted to 0.0003 inches. From 88.2% of Pult (6 kips) the slip started to increase, but still in a very small amount until 97.1% of Pult (6.6 kips). From here on the slip was definite and uniform.

The strand force was computed from strain measurements from one SR-4 electrical strain gage on the strand.

(b) Performance of Beam B2

Because of the simulated crack in this beam, it was difficult to detect the cracking load. The figure given for P cracking in Table XVI is the load at which the simulated crack was open to the naked eye. Theoretically the cracking load was at the point when the compressive stress at the bottom fiber reached zero value. The load deflection diagram for Beam B2, Figure 35, shows that at about 40% of ultimate there is the transition from the straight line to the curve. The load corresponding to that point is 3,730 lbs. which is a closer figure to the theoretical cracking load of 3,260 lbs. The load-deflection diagram presents a smooth curve with a very gradual change in slope. This is a consequence of the

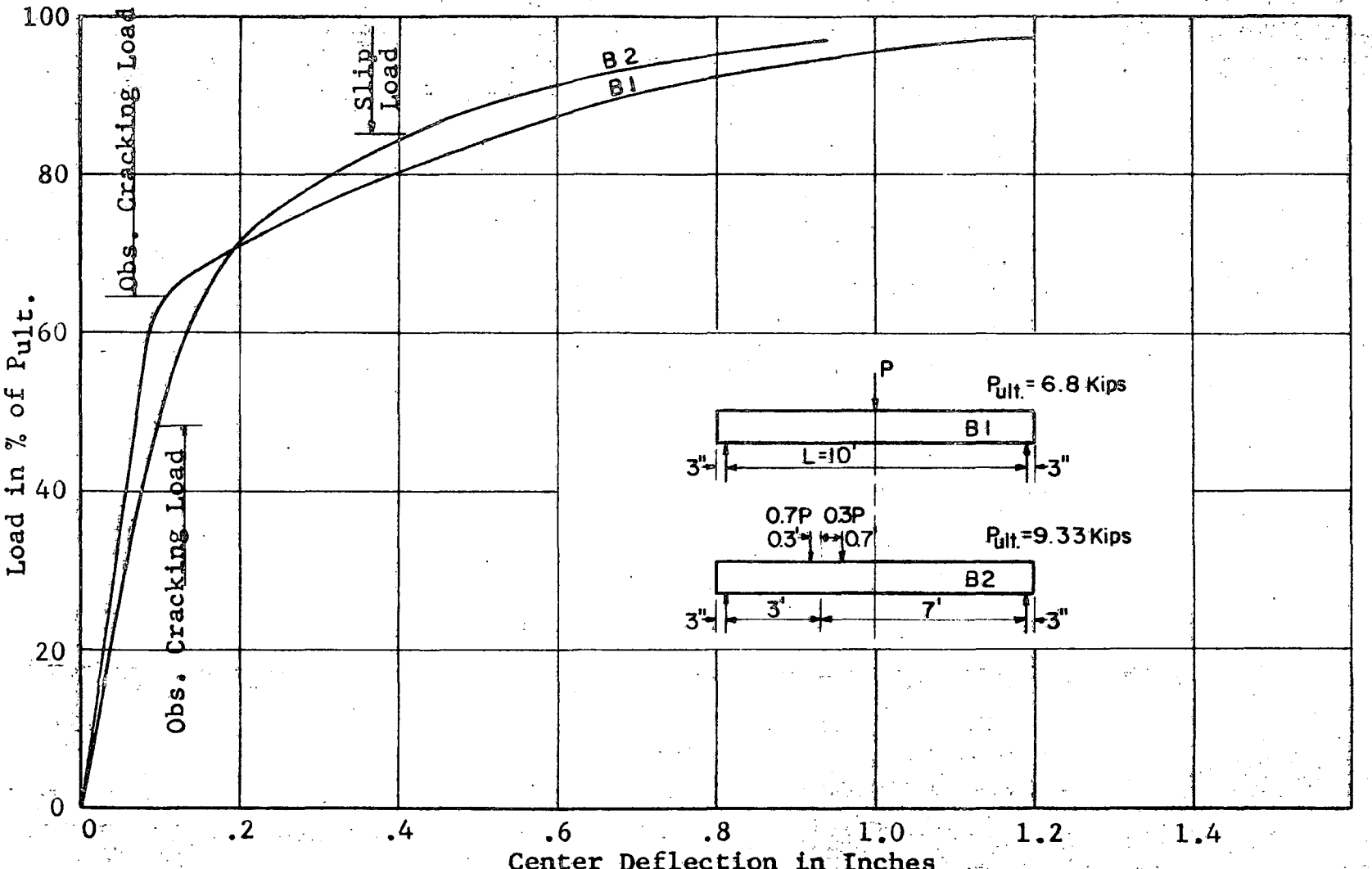

Figure 35. Load-Deflection Diagrams of Beams B1 and B2.

cracked section in the specimen. The N-end of Beam B2 suffered slip at 85.8% of the actual ultimate carrying capacity of the specimen. The progression of slip during the test can be seen in Figure 36. The N-end dial gages record very little slip up to 5,500 lbs. of load. No slip occurred between 59% of Pult. (5.5 kips) and 69.7% of Pult. (6.5 kips). Again from 69.7% of Pult. (6.5 kips) to 85.8% of Pult. (8 kips), the slip was very slight and occurred slowly. At 85.8% of Pult. the slip failure started. The highest load taken by the member was 9,330 lbs.

It must be noted that in the range from 6.5 kips to 7 kips a real crack started forming within the bonded length. The formation of that crack coincided with the resumption of slipping. The crack reduced the bonded length, defined by the simulated crack, by nearly 7 inches. Figure 37 shows that crack between the 7 foot and 8 foot marks. It is possible that without any crack the specimen would have had a flexural failure. Presumably before the bond failure, of the specimen, the bond was entirely lost in the seven inches between that crack and the simulated crack. This actual crack was also the failure crack. The depth of the neutral axis at ultimate measured from the top of the beam was 1-3/8 inches.

The strain readings taken across the simulated crack were corrected for temperature. Figure 38 shows the results of this data in the diagram Position Along Depth of the Beam vs. Strain. Since the measured strains are based on zero at pre-test, they do not directly give the true position of the neutral axis because of the existing state of stress at that section at pre-test. In order to locate the position of the neutral axis, the measured strains were reduced by the pre-test strains.

The proximity of the load (3.6 inches) had a marked effect for the readings near the top of the beam. However, the purpose of this data was the determination of the depth of the neutral axis, and this is well defined. The depth of the neutral axis values found in this way were used to compute the strand force assuming a parabolic distribution of concrete stresses. Figures 39 and 40 show a comparison between these computations and theoretical calculations.

Reasonable agreement is obtained between the measured and calculated values for strand force of Beam B1, shown in Figure 39. The measured strand force was made from only one gage in this instance, moreover, and this gage was calibrated

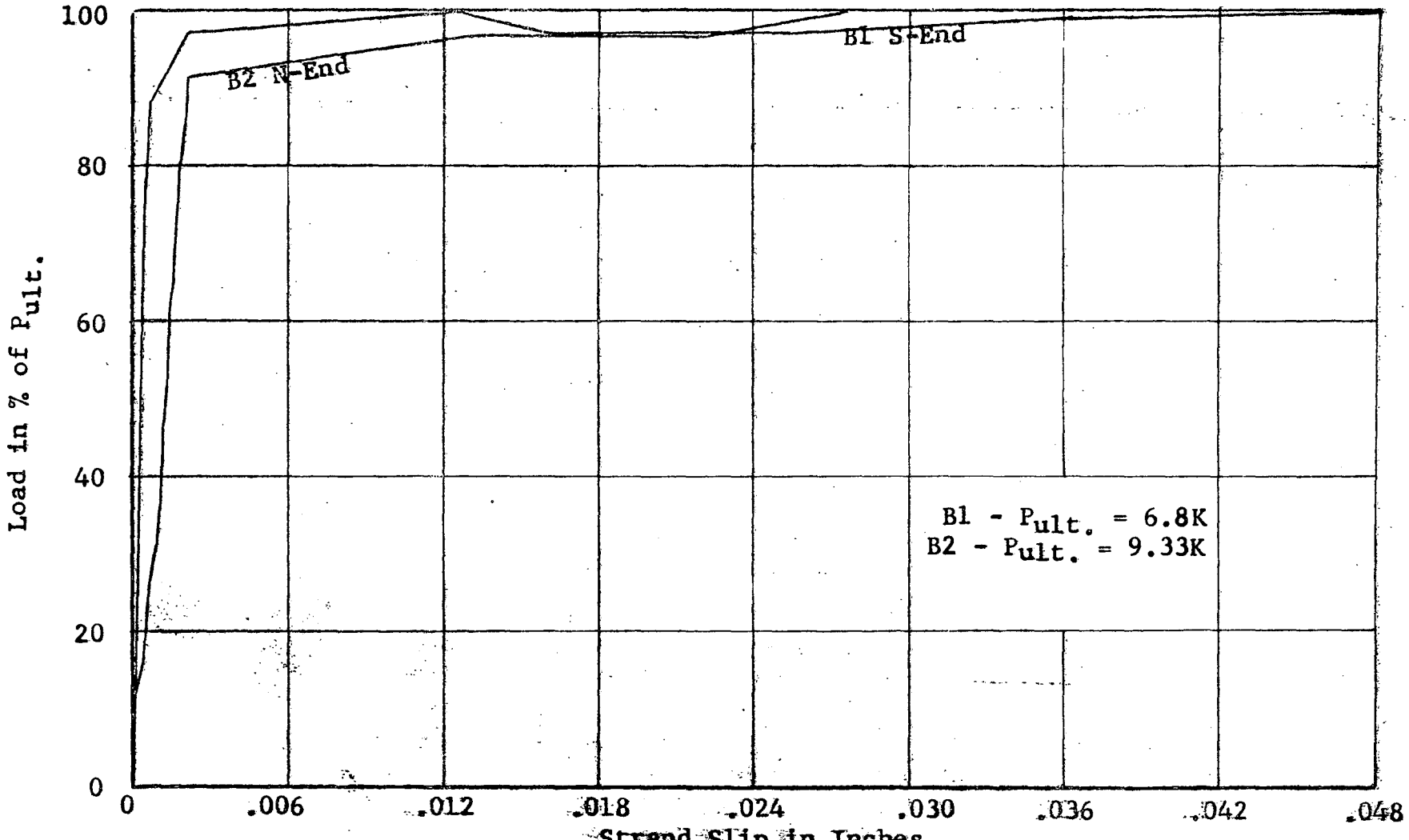

Figure 36 Progression of Strand Slip During Test of Beams B1 and B2.

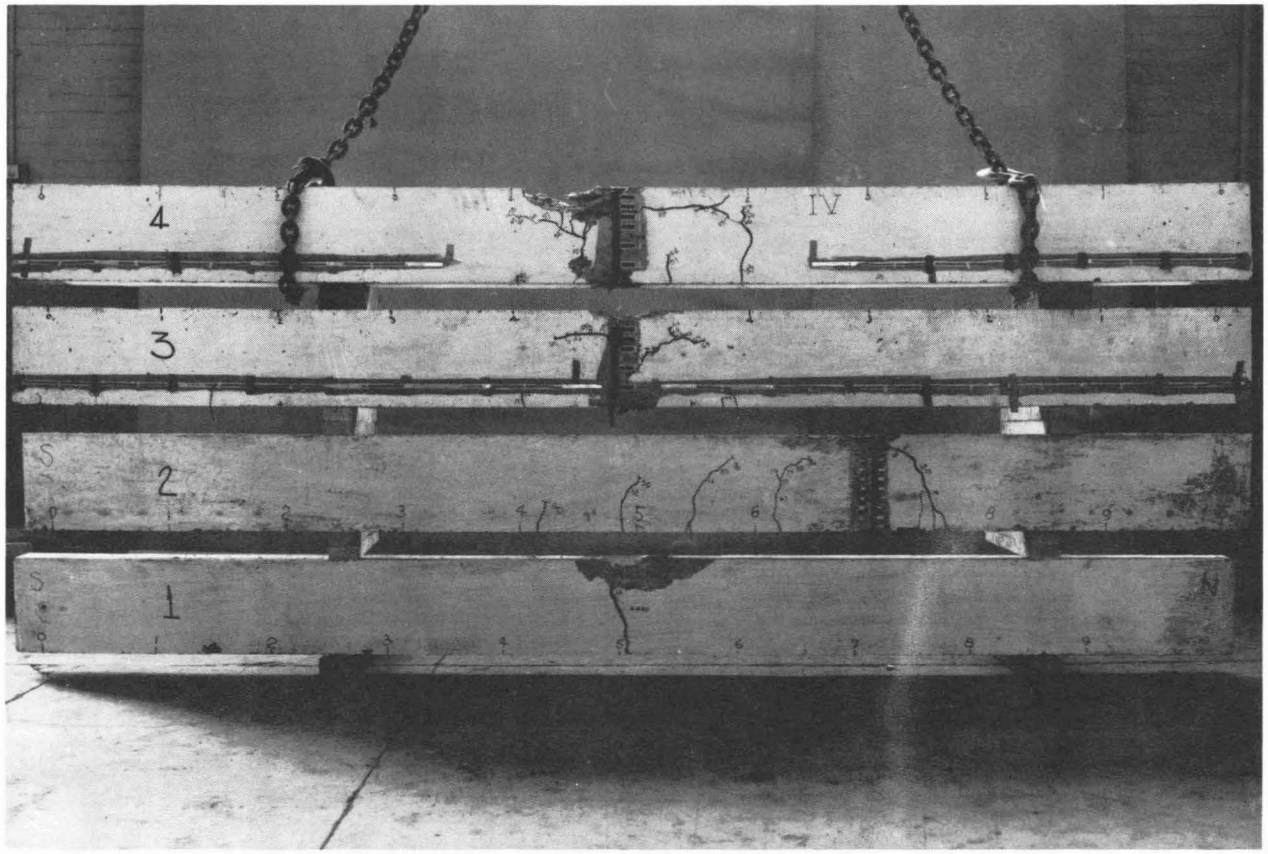

Figure 37. Beams After Test

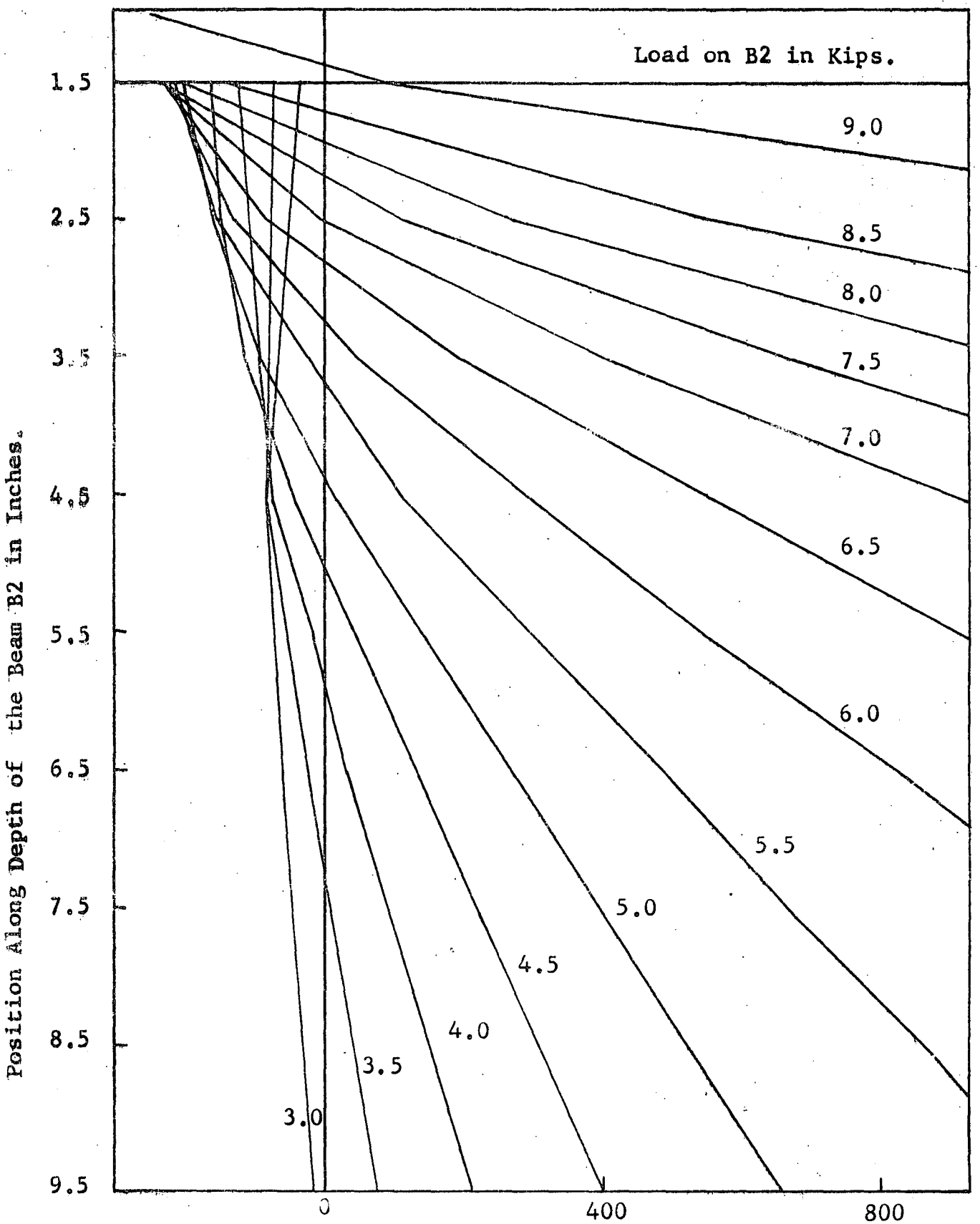

Figure 38.. Variations of Neutral Axis of Beam B2 During Test

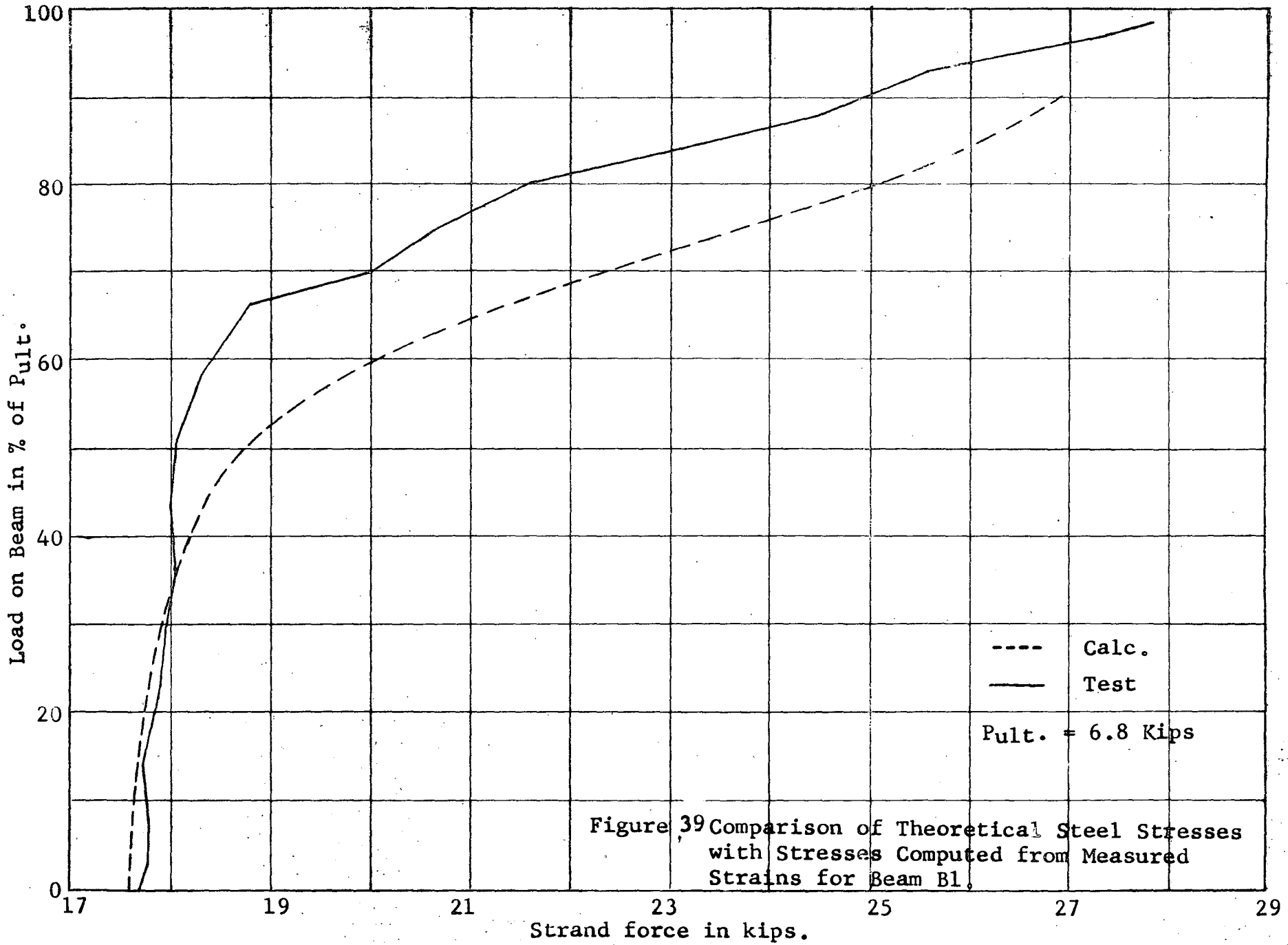

Figure 39 Comparison of Theoretical Steel Stresses with Stresses Computed from Measured Strains for Beam B1.

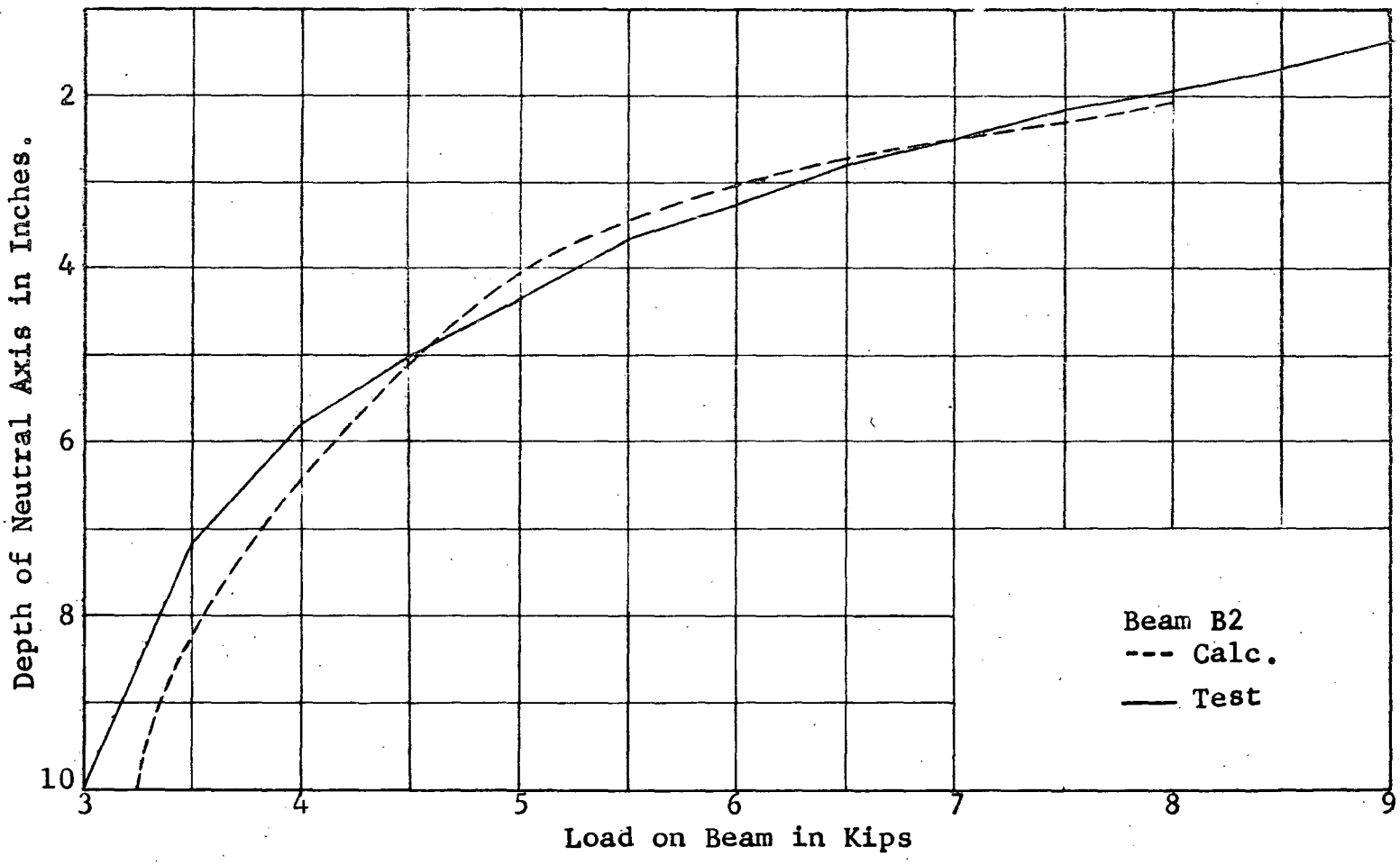

Comparison of Theoretical and Test Depth of Neutral Axis for Beam B2

Figure 40.

only up to 19,000 lbs. Higher values were extrapolated. Figure 40 shows a comparison between the calculated theoretical depth of the neutral axis of beam B2 and the depth computed from test data. A very good agreement is obtained for the higher loads.

(c) Performance of Beams B3 and B4

For both beams the cracking and ultimate loads were slightly lower than the calculated values. The observed values of the cracking load are consistent with the load-deflection diagram, Figure 41.

Figure 42 shows the strand force values for these beams. Each value was the average of three gages on each strand. The gages were calibrated up to 24 kips when the strands were tensioned before pouring. After reaching 24 kips the load was released to the initial prestressing force. The calibration curve was extrapolated for higher tensions.

SR-4 gages were placed on the concrete at midspan to obtain incidental data to check strand stresses. The gages are shown in Figures 33 and 37. They failed to produce reliable results.

The slip dials at the two ends of B4 did not report any slip at all in the whole test. One end of B3 had a negligible slip, about 0.0003 inches. B3 had a bonded length of 4 feet whereas B4, despite a 2'-6" bonded length, showed outstanding bonding characteristics.

B. Discussion of Beam Tests by Others

The other beams in the literature reinforced with 7/16 inch pretensioned strands have exhibited similar performance. Altogether twenty beams, including the four already discussed, representing forty data items or "specimens", were studied. All were loaded on spans of 11.5 feet or less and were 12 feet or less in total length. Only ten specimens, all of three and one-half feet anchorage length or less as determined from the location of the outermost crack, failed in bond. Of four with available anchorage lengths of two and one-half or less, only two slipped. One slipped at a strand force of 74 percent of guaranteed strand ultimate, the other at 99 per cent. One of two specimens with bonded lengths greater than two and one-half but equal to or less than three feet slipped at a strand force

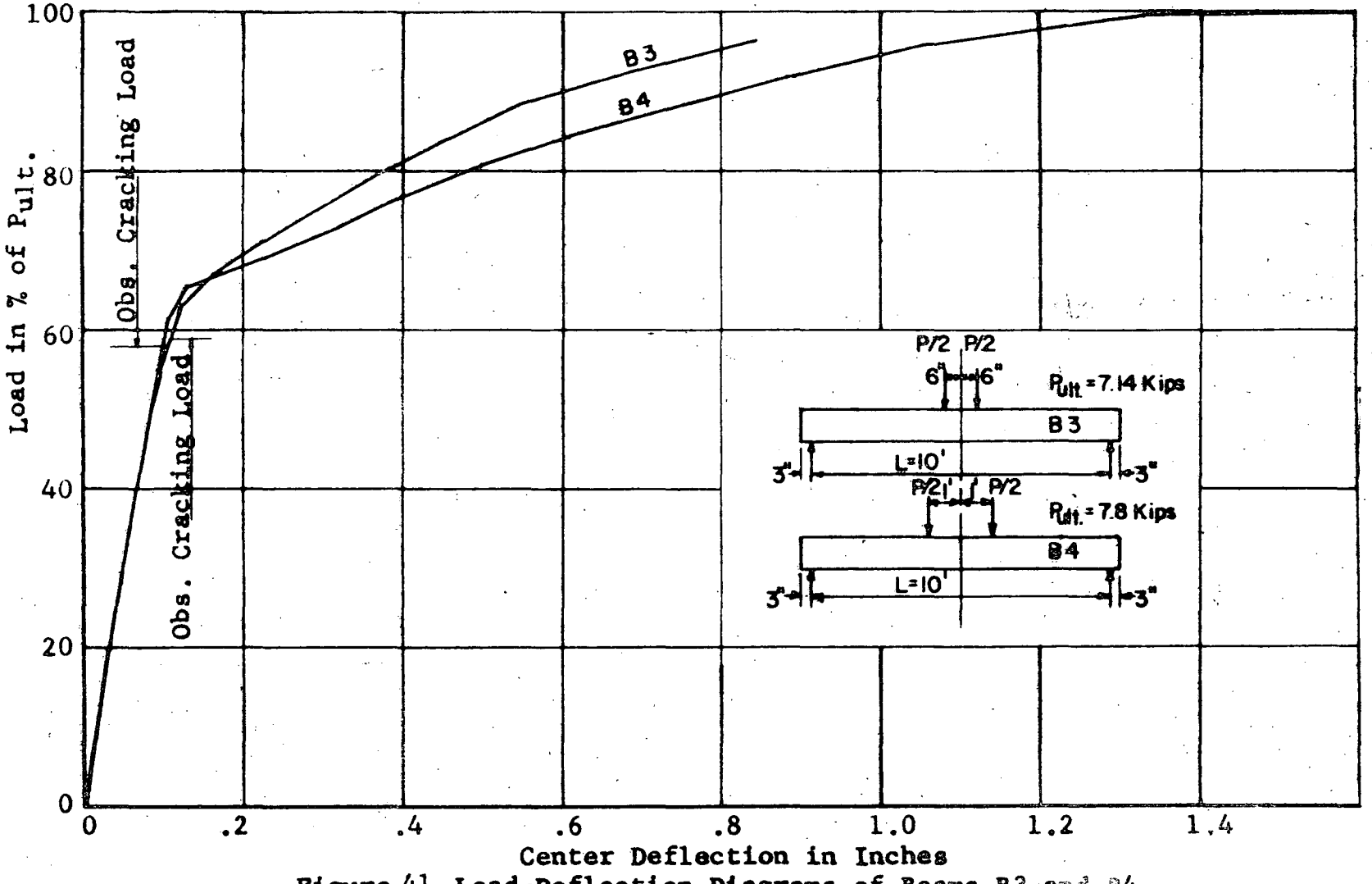

Figure 41 Load-Deflection Diagrams of Beams B3 and B4.

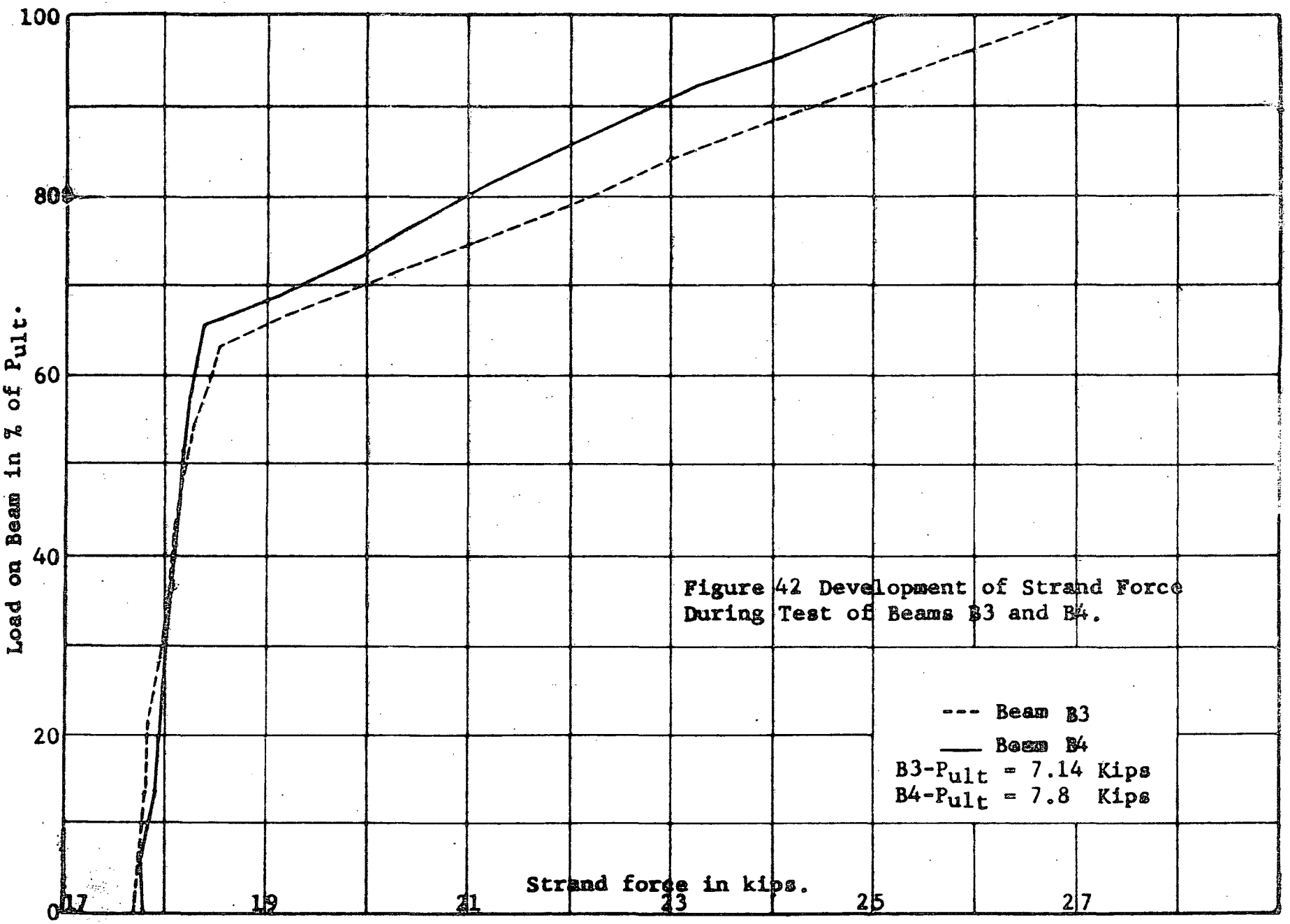

Figure 42 Development of Strand Force During Test of Beams B3 and B4.

of 92 per cent of strand ultimate. Seven of thirteen specimens greater than three but equal to or less than three and one-half feet in anchorage length failed in bond at strand forces of from 73 to 101 per cent of strand ultimate. All eleven specimens with bonded length greater than three and one-half but equal to or less than four and one-half feet indicated no bond failure. The remaining two specimens had anchorage lengths less than five feet and also exhibited no slip.

Five beams representing ten specimens reinforced with 3/8 inch strand were also analyzed. The available anchorage length ranged from three to six feet. Only one instance of bond failure was reported. This occurred in one end of a beam with six feet of bonded length at a strand force in excess of the strand ultimate. However, this beam was very highly underreinforced and the transfer length (more than three feet) was much greater than those measured for the companion beams. These data indicate that probably the concrete was not sufficiently vibrated when the beam was poured.

One beam reinforced with 5/16 inch strand having an available anchorage length of about two and one-half feet failed in bond at a strand force of approximately two-thirds of strand ultimate.

One beam using 1/4 inch strand with available anchorage lengths of between three and three and one-half feet at each end was failed without any observed bond deficiency.

Strand of 1/2 inch nominal diameter was successfully bonded at both ends of three beams which provided anchorage lengths of from four and one-half to five feet.

C. Conclusions from Beam Tests

Similar to the pull-out test results, the 7/16 inch strand beam test results also do not define a consistent strand-force embedment-length relationship. Since no practical slip limit envelope has been established for either pull-out specimens or beams, it would seem logical to propose a lower-bond type of bond criteria which would be conservative with respect to all the representative observed test results. It would seem reasonable, therefore, that any design using 7/16 strand or smaller which prohibits the formation of a crack at a distance of less than four feet from the end of a member will be secure against bond failure.

This recommendation is conservative. As the beam tests indicate, even though a beam may fail in bond, the small amounts of slip which accompany such failure generally do not prohibit the beam from acting normally and achieving its anticipated ultimate flexural strength. Also the value of four feet has been indicated from the test results to be a safe value for ultimate anchorage length.

In a beam which is bonded over its entire length before cracking, the strand force at a cracked section four feet from the end at ultimate load will, in the great majority of cases, not be maximum. It will have some values less than that at the maximum stressed section and greater than that indicated by elastic theory. Therefore, the strand force at the critical section for bond will seldom if ever reach the value of strand ultimate. A minimum value of four feet of bonded length, which includes the overhang at the supports, should in all cases guarantee no bond failure for well compacted beams reinforced with 7/16 inch strands.

Pull-out tests should be conducted to determine similar safe anchorage lengths for the other strand sizes. Insufficient data is contained in the literature to enable the authors to recommend any definite minimum anchorage lengths for strand sizes other than the 7/16 inch size investigated in these tests. It is obvious, however, that smaller strands will require less embedment length and larger strands more embedment length.

X CONCLUSIONS AND RECOMMENDATIONS

1. The test results indicate that no practical slip limit envelope exists.

2. The recommended criteria to assure safety against anchorage failure is as follows:

   (1) The location of the outermost crack is first established. The moment diagram, or the curve of maximum moments is plotted with a maximum ordinate of 1.6. The intersections of this curve with a level line of ordinate 1.0 locate the outermost cracks.

   (2) The available embedment length is the distance from the point of initial contact between the concrete and strand to the outermost crack.

   (3) If the available embedment length determined in Section 2 is four feet or greater (for 7/16" strand or smaller) the member is satisfactory in bond.

   (4) If the available embedment length determined in section 4 is less than four feet, the beam is unsafe with respect to bond. This condition may be remedied as follows:

   a.) use a post-tensioned, grouted beam.

   b.) provide positive anchorage by means of a mechanical device.

   c.) increase the overhang at the beam supports to provide the minimum embedment length.

   d.) use a smaller strand the ultimate anchorage length of which is equal to or less than the available anchorage length.

3. Friction appears to be the major component determining ultimate bond strength.

4. The ages and strengths of concrete investigated in this research, four to forty days and 4,250 to 6,940 psi respectively, do not appear to be the principal variables affecting bond strength.

5. The degree of vibration and resultant compaction of the wet concrete appear to be the most significant variables affecting the bond strength of high strength, low slump concrete. Thorough vibration gave consistently better results whereas insufficient vibration was the most probable cause of the exceptional, poor results. The authors recommend the establishment of a standard practice for vibration and compaction of low slump concrete to prevent the excessively low bond strengths shown by some of the test specimens.

6. The bond resistance of strand was not seen to be affected by either gradual or sudden release.

7. Transfer length was not observed to increase in the time interval investigated maximum of which was 136 hours.

8. The bond strength of strand does not appear to be significantly affected by the degree of initial steel pretension.

XI BIBLIOGRAPHY

General References*

1. Evans, R.H.; Williams, A., "The Use of X-Rays in Measuring Bond Stresses in Prestressed Concrete", Proceedings of the World Conference on Prestressed Concrete, University of California, July, 1957.

2. Evans, R.H.; Robinson, G. W., "Bond Stresses in Prestressed Concrete from X-Ray Photographs", Proceedings of the Institution of Civil Engineers, London, Part 1, 1955.

3. Warner, R.F., "The Calculation of Flexural Stresses in a Prestressed Concrete Member", Lehigh University, Fritz Laboratory Report 223.20, November, 1958.

4. Thorsen, N., "Use of Large Tendons in Pre-Tensioned Concrete", Journal of the American Concrete Institute, No. 6, Vol. 27, February, 1956.

5. Bureau of Reclamation, United States Department of the Interior, Concrete Manual, United States Government Printing Office, Washington, 1955.

6. Janney, J. R., "Nature of Bond in Pre-Tensioned Prestressed Concrete", Proceedings of the American Concrete Institute, Vol. L, 1954.

7. Walther, R. E.; Warner, R. F., "Ultimate Strength Tests of Prestressed and Conventionally Reinforced Concrete Beams in Combined Bending and Shear", Lehigh University, Fritz Laboratory Report 223.18, September, 1958.

8. Ratz, E. H.; Holmjanski, M.M.; Kolner, V.M., "The Transmission of Prestress to Concrete by Bond", Third Congress of the Federation Internationale De La Precontrainte, Berlin 1958, Session III, Paper No. 10.

9. ACI-ASCE Joint Committee 323, "Tentative Recommendations for Prestressed Concrete", Journal of the American Concrete Institute, January, 1958.

* References are listed in the order cited.

BIBLIOGRAPHY (Continued)

10. Guyon, Y., Prestressed Concrete, John Wiley and Sons, Inc., New York, 1955.

11. Peattie, K.R.; Pope, J.A., "Effect of Age of Concrete on Bond Resistance", Journal of the American Concrete Institute, No. 6, Vol. 27, February, 1956.

Sources of Beam Test Data

20. Nuwaysir, F.S., Fatigue Study of Prestressed Concrete Beams and Their Components, Lehigh University, Fritz Engineering Laboratory, (unpublished), June, 1958.

21. Slutter, R.G.; Ekberg, C.E., Jr., Static and Fatigue Tests on Prestressed Concrete Railway Slabs, Lehigh University, Fritz Laboratory Report 240.01, November, 1957.

22. Debly, L.J., Static Tests on Prestressed Concrete Beams Using 7/16" Strands, Lehigh University, Fritz Laboratory Report 223.12, June 1956.

23. Brown, D.H., Bond of Prestressed Strands, Lehigh University, Fritz Lab. Report 223.7, 232.2, September, 1953.

24. Smislova, A., Static Tests on Prestressed Concrete Beams using 7/16" Strands, Lehigh University, Fritz Laboratory Report 223.11, June 1955.

25. Mayo, R.; Fore, F.; Loewer, A.C., Jr.; Eney, W.J., A Comparison Between Ordinary Reinforced and Prestressed Reinforced Concrete Beams, Lehigh University, Fritz Laboratory Report 223.1, February, 1952.

26. Debly, L. J., Special Report on 3/8 Inch Galvanized Strands, Lehigh University, Fritz Laboratory Report, (unpublished), June, 1956.

BIBLIOGRAPHY (Continued)

27. Debly, L.J., Static Tests on Prestressed Concrete Beams Using 7/16 Inch Strands, Lehigh University, Fritz Laboratory Report 223.12, September, 1955.

28. Walther, R.E.; Warner, R.F., "Ultimate Strength Tests of Prestressed and Conventionally Reinforced Concrete Beams in Combined Bending and Shear", Lehigh University, Fritz Laboratory Report 223.18, September, 1958.

29. Nordby, G.M., A Study of Steel Strand for Prestressing Concrete Beams of Expanded Shale and Conventional Aggregate, University of Colorado, 1956.

APPENDIX A

THEORETICAL ANALYSIS OF TRANSFER BOND

The previous discussions have dealt with the transfer bond phenomenon in more or less a general manner. The more basic approaches to the various types and ranges of bond stress have been expressed mathematically by Guyon (10), Janney (6) and others. The material that follows will not be radically different from what has already been developed. An attempt will be made, however, to expand the previous work and make it more exact.

To facilitate the mathematical derivations, we will again analyze the transfer zone of a prismatic unit prestressed with a single, centrally located prestressing element.

(1) Friction Bond

The mechanism of pure frictional bond resistance has been ably developed principally by Janney (22). The method of analysis consists essentially of the treatment of the friction part of the transfer zone as a hollow, concentric, thick-walled cylinder. See Figure A1. The inner radius, r, is assumed as one-half the nominal diameter of the prestressing element. The outer radius, R, is assumed much larger than the inner radius so that the ratio $\frac{R}{r}$ is much greater than unity.

When a wire is under tension and the tension is decreased, the wire shortens according to $\frac{PL}{AE}$. But, due to Poisson's ratio, the wire also expands radially. The expression for this radical expansion is obtained from the general theory of elasticity. The expanding wire and the concrete section enclosing it are solids of revolution which are symmetric about the longitudinal axis, i.e., with respect to θ, (Figure A2). The general problem is one of three dimensional stress and strain. The coordinate axes are established in Figure A2.

According to the theory of elasticity, the expression which determines the radial expansion is

$$\epsilon_\theta = \frac{\partial u_\theta}{r\,\partial\theta} + \frac{\Delta r}{r}$$

For this special case, the problem being axially symmetric, . Therefore, the problem is now one of plane stress and strain and the general expression for radial strain is,

$$\epsilon_\theta = \frac{\Delta r}{r} = \frac{f_c - \gamma(f_z + f_r)}{E} \qquad (A\text{-}1)$$

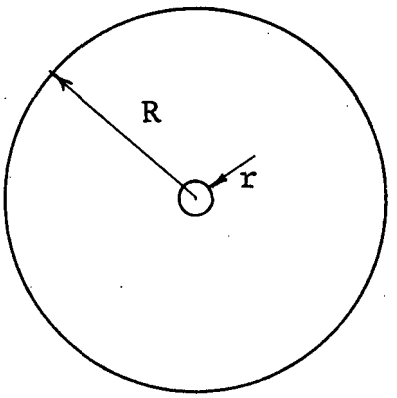

Figure A1 - Friction Transfer Zone as a Hollow, Concentric, Thick-walled Cylinder

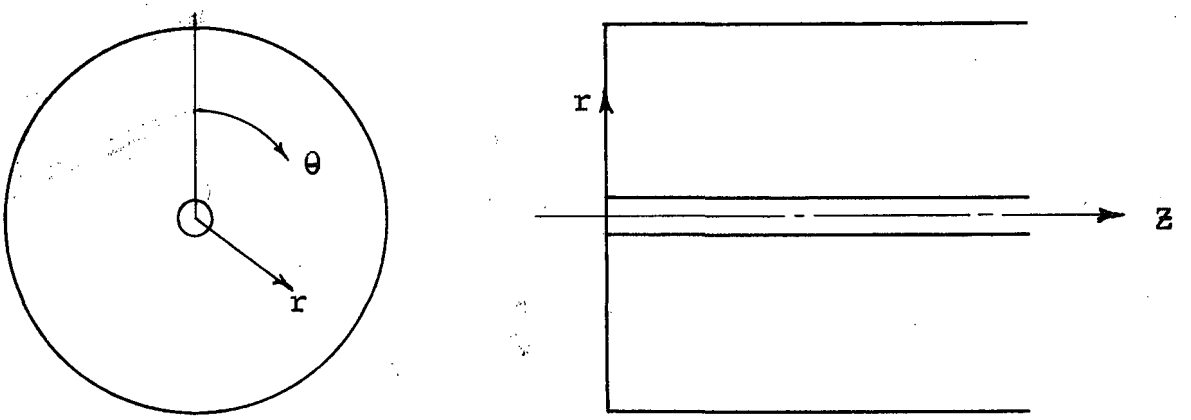

Figure A2 - Coordinate Axes of Friction Transfer Zone

In the above expression, positive stresses, f, are tensions, and r is the radius of wire in its initially stressed condition.

Now, if the tension in the wire is released, and the wire is free to expand, f_r and f_θ are zero. Therefore, Equation A1 becomes:

$$\frac{\Delta r}{r} = \frac{r \gamma_s \Delta f_z}{E_s}$$

where Δf_z is the decrease in tension and therefore a negative quantity. If this wire is a prestressing element, the decrease in tension is actually the difference between initial pretensioning steel stress and the steel stress at any section after release. Therefore,

$$\Delta r = \frac{r \gamma_s (f_{si} - f_s)}{E_s} \qquad \text{(A-2)}$$

But the wire is not free to expand. Its expansion is resisted by the concrete in which it is embedded. The problem now becomes one of a hollow, concentric, thick-walled cylinder under internal pressure and axial compression. The internal pressure is the radial stress due to the expansion of the wire as prestress is released. The axial compression is due to amount of prestress effective at a given section. In Janney's (22) derivation the effect of axial compression was neglected, but will be included here.

Equation A1 may be used to express the radial deformation. In this situation, however, Δr is the change in radius of inner hole and will be called Δr_i to differentiate it from the of a freely expanding wire. Therefore,

$$\frac{\Delta r_i}{r} = \frac{f_\theta - \gamma (f_z + f_r)}{E} \qquad \text{(A-3)}$$

The radial and tangential stresses at the face of the inner hole, f_r, and f_θ respectively, due to an internal pressure, P_i, are given in any advanced text on strength of materials. These stresses are

$$f_r = \frac{-P_i r^2}{R^2 - r^2}\left(\frac{r^2 - R^2}{r^2}\right)$$

$$f_\theta = \frac{P_i r^2}{R^2 - r^2}\left(\frac{r^2 + R^2}{r^2}\right)$$

For a hollow, concentric, thick-walled cylinder whose outer radius is much greater than its inner radius, it can be said, with negligible error, that

$$R^2 \pm r^2 \cong R^2$$

Therefore,

$$f_r = -P_i$$

$$f_\theta = P_i$$

But the internal pressure, P_i, is the radial pressure exerted by the swelling steel on the concrete. Therefore, if it is recognized that this internal pressure is the radial steel stress, f_{sr}, then $P_i = f_{sr}$ (compression).

Now, f_z is the concrete axial compression stress due to transferred prestress. If the assumption is made that this stress is distributed over the entire cross-section, it follows that,

$$f_z = \frac{fsAs}{A_c} = pfs$$

Substituting these values in Equation A3 with their proper signs,

$$\frac{\Delta r_i}{r} = \frac{f_{sr}(1+\gamma_c) + p f_s \gamma_c}{E_c} \qquad \text{(A-4)}$$

where Δr_i, is a positive value which means the inner radius is increasing.

The radial stress in the steel can now be found from strain compatibility as follows:

$$\frac{f_{sr}}{E_s} = \frac{\Delta r}{r} - \frac{\Delta r_i}{r}$$

or

$$f_{sr} = \frac{\Delta r - \Delta r_i}{r} E_s \qquad \text{(A-5)}$$

By the substitution of Equations A2 and A4 into A5, the complete expression for f_{sr} is,

$$f_{sr} = \frac{(f_{si} - f_s)\gamma_s - p f_s \gamma_c n}{1 + (1+\gamma_c) n} \tag{A-6}$$

Now, if the bond is purely frictional, the bond stress may be expressed as,

$$u = \phi f_{sr} \tag{A-7}$$

where ϕ is the coefficient of friction. It can be easily shown that the bond stress, u, at any section in the transfer zone is equal to the differential change in strand force divided by the differential area on which it acts. Therefore,

$$u = \frac{A_s \, df_s}{\Sigma_o \, dz} \tag{A-8}$$

Equating A7 and A8 and substituting A6 for f_{sr},

$$\frac{(f_{si} - f_s)\gamma_s - p f_s \gamma_c n}{1 + (1+\gamma_c) n} = \frac{A_s \, df_s}{\phi \Sigma_o \, dz} \tag{A-9}$$

By assigning the constants

$$\alpha = \frac{\phi \Sigma_o \gamma_c p n}{A_s [1 + (1+\gamma_c) n]}$$

and

$$\beta = \frac{\phi \Sigma_o \gamma_s}{A_s [1 + (1+\gamma_c) n]}$$

Equation A9, rewritten in solvable form is,

$$\frac{df_s}{dz} + (\alpha + \beta) f_s = \beta f_{si} \tag{A-10}$$

Equation A 10 is a simple, first order, non-homogeneous differential equation with constant coefficients, the solution of which is,

$$f_s = A e^{-(\alpha+\beta)z} + \left(\frac{\beta}{\alpha+\beta}\right) f_{si} \tag{A-11}$$

The bondary condition necessary to determine A is

$$z = 0, \quad f_s = 0$$

Therefore,

$$A = -\left(\frac{\beta}{\alpha+\beta}\right) f_{si}$$

and

$$f_s = \left(\frac{\beta}{\alpha+\beta}\right) f_{si} \left[1 - e^{-(\alpha+\beta)z}\right] \tag{A-12}$$

Replacing β and α with their actual values,

$$f_s = \left(\frac{\gamma_s}{\gamma_s + \gamma_c np}\right) f_{si} \left[1 - e^{-\frac{\phi \Sigma_o (\gamma_s + \gamma_c np}{A_s [1+(1+\gamma_c)n]} Z}\right] \qquad \text{(A-12a)}$$

Utilizing Equation A8 and the first derivative of A 12a with respect to Z, the expression for bond stress obtained is,

$$u = \frac{\phi \gamma_s}{1+(1+\gamma_c)\, n} f_{si}\, e^{-\frac{\phi \Sigma_o (\gamma_s + \gamma_c np)}{A_s [1+(1+\gamma_c)n]} Z} \qquad \text{(A-13)}$$

To obtain a direct expression for Z, the equation to be solved is

$$d Z = \frac{d f_s}{\beta f_{si} - (\alpha + \beta) f_s} \qquad \text{(A-14)}$$

A 14 may be solved by straight integration, yielding

$$Z = - \frac{\ln [\beta f_{si} - (\alpha + \beta) f_s}{\alpha + \beta} + C$$

Utilizing the boundary condition that $f_s = 0$ when $Z = 0$,

$$C = \frac{\ln \beta f_{si}}{\alpha + \beta}$$

Therefore,

$$Z = \frac{\ln \left[\frac{\beta f_{si}}{\beta f_{si} - (\alpha+\beta) f_s}\right]}{\alpha + \beta} \qquad \text{(A-15)}$$

Replacing β and α with their actual values,

$$Z = \frac{A_s [1+(1+\gamma_c)\, n\,]}{\phi \Sigma_o (\gamma_s + \gamma_c np)} \ln \frac{f_{si}}{f_{si} - (1 + \frac{\gamma_c}{\gamma_s} np) f_s} \qquad \text{(A-15a)}$$

In examining Equation A 15a, it is seen that Z is a function of f_{si}, f_s, section and material properties. The only unknown is f_s. If the f_s that determines the end of the friction zone, (or the beginning of the elastic zone, since they are the same thing), is known or can be determined, a solution for the length of the friction zone can be obtained.

The preceding equations may be easily rewritten for any type of prestressed unit by simply using the appropriate value

of f_z instead of that on page 114.

For example, for eccentrically prestressed beams,

$$f_z = n\left(p f_s + \frac{f_s A_s \bar{r}^2}{I_c}\right)$$

If the effect of axial compression is neglected in the foregoing expressions, equations (A-12a), (A-13) and (A-15a) become,

$$f_s = f_{si}\left(1 - e^{-\frac{\phi \Sigma_o \gamma_s Z}{A_s[1+(1+\gamma_c)n]}}\right) \qquad \text{(A-16a)}$$

$$u = \frac{\phi \gamma_s}{1+(1+\gamma_c)n} f_{si}\, e^{-\frac{\phi \Sigma_o \gamma_s Z}{A_s[1+(1+\gamma_c)n]}} \qquad \text{(A-16b)}$$

$$Z = \frac{A_s[1+(1+\gamma_c)n]}{\phi \Sigma_o \gamma_s} \ln\left(\frac{f_{si}}{f_{si} - f_s}\right) \qquad \text{(A-16c)}$$

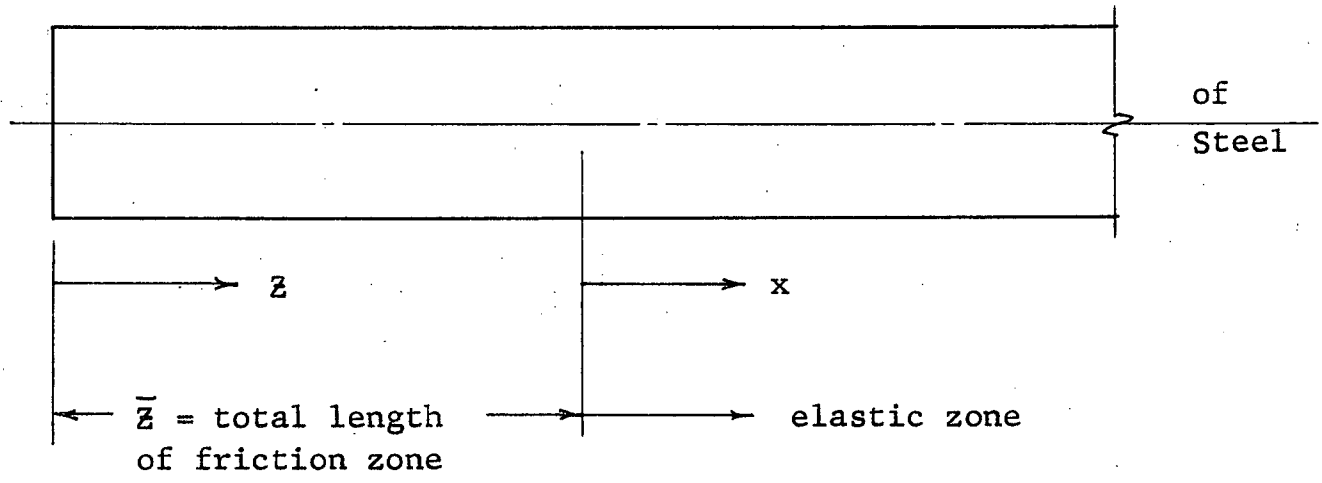

Figure A3 - Notation for Elastic Zone

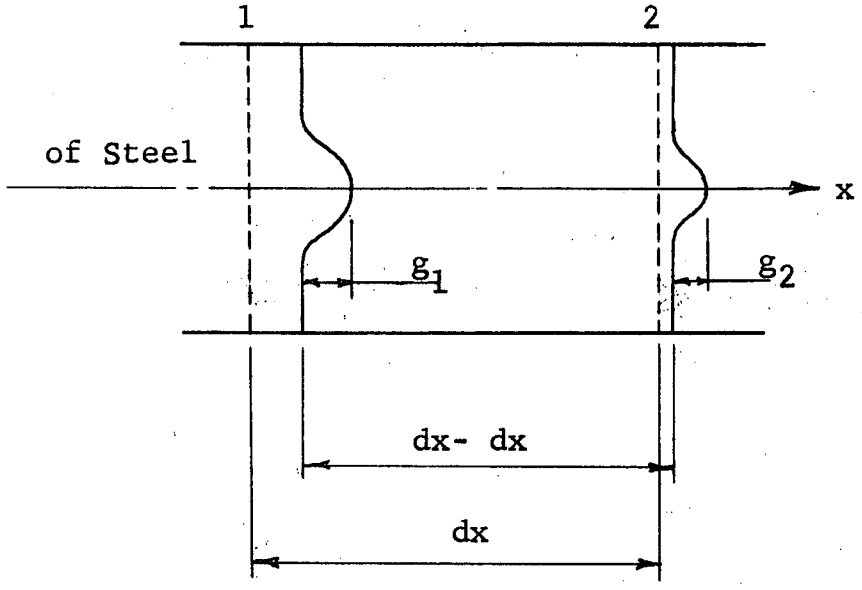

Figure A4 - Deformation of Differential Segment of Elastic Zone

(2) Elastic Bond

As mentioned before, the elastic zone is that part of the transfer zone in which there is no relative displacement at the interface of the concrete and steel. The adhesion between steel and concrete has not been destroyed and therefore the type of bond in this zone is elastic.

To facilitate the subsequent derivations, the longitudinal coordinate axis in the elastic zone will be designated by the letter x. The friction zone ends at some finite value of z. The origin of x will therefore be taken at this value of z. This is shown pictorially in Figure A3.

To derive the expressions for the parameters f_s, u, and x, a differential segment in the elastic zone of Figure 1 (page 4) is analyzed and is shown in Figure A4. In Figure A4, before release the segment is dx long. After the prestress is released, there will be two types of relative displacement.

The first is the relative displacement due to axial compression. The other is that due to the localized concentration of the steel force. This effect is represented by g.

If it is assumed that prestress force at any section is uniformly distributed over the entire concrete section, the average compression stress in the concrete at any section is,

$$f_c = \frac{f_s A_s}{A_c} = p f_s$$

The strain due to uniform compression for any differential segment is then

$$\varepsilon = \frac{f_c}{E_c} = \frac{p f_s}{E_c}$$

and the shortening of the segment is ε dx.

But, $$\varepsilon dx = \Delta dx = \frac{p f_s}{E_c} dx$$

The shortening of the segment due to the local dishing effect is $g_1 - g_2 = \Delta g$.

But Δ g for a differential segment is dg.

The total shortening which occurs at the interface is the combination of the two effects, Δdx and Δg.

Therefore

$$\Delta dx + \Delta g = \frac{p f_s}{E_c} dx + dg$$

However, there is no relative displacement of steel and concrete at their interface in the elastic zone. The strain that the steel undergoes as a result of the decrease in tension from its initial value, f_{si}, to its value at any section, f_s, must equal the concrete strain due to the transferred prestress at any section at the interface.

Therefore $\varepsilon_s = \varepsilon_c$.

$$\frac{f_{si} - f_s}{E_s} = \frac{dg + \frac{p f_s}{E_c} dx}{dx} \qquad \text{(A-17)}$$

For elastic bond, it may be assumed that the bond stress is a function of the total strain. This assumption may then be expressed as

$$u = K \varepsilon_c \qquad \text{(A-18)}$$

K may therefore be thought of as the "Bond Modulus of Elasticity". It may be considered constant, as is Young's Modulus, E, or variable, as E actually is.

If K is considered constant, the basic differential equation may be formulated as follows:

Substituting the value for ε_c of Equation A-17 into A-18,

$$u = K \left(\frac{dg}{dx} + \frac{p f_s}{E_c} \right) \qquad \text{(A-19)}$$

It has been shown that

$$u = \frac{A_s \, df_s}{\Sigma_o \, dx} \qquad \text{(A-8)}$$

Combining A-8 and A-19,

$$\frac{dg}{dx} = \frac{A_s}{K \Sigma_o} \frac{df_s}{dx} - \frac{p f_s}{E_c} \qquad \text{(A-20)}$$

Substituting A-20 into A-17 and rearranging,

$$\frac{df_s}{dx} + \lambda f_s = \lambda f_{si} \qquad \text{(A-21)}$$

where $$\lambda = \frac{K \Sigma_o}{E_s A_s}$$

The solution of this first order, non-homogeneous differential equation with constant coefficients is,

$$f_s = A e^{-\lambda x} + f_{si} \qquad \text{(A-21a)}$$

The constant, A, may be determined from the boundary condition, when $x = \bar{x}$, $f_s = f_{se}$.

In the above expression, $\bar{x}$ is that length of the elastic zone which determines the end of the transfer length.

$$A = (f_{se} - f_{si})\, e^{\lambda \bar{x}}$$

Substituting this value back into A-21

$$f_s = f_{si} - (f_{si} - f_{se})\, e^{\frac{K \Sigma_o}{E_s A_s}(\bar{x} - x)} \qquad \text{(A-22)}$$

To determine the bond stress, u, Equations A-8 and 111-22 give,

$$u = (f_{si} - f_{se}) \frac{K}{E_s} e^{\frac{K \Sigma_o}{E_s A_s}(\bar{x} - x)} \qquad \text{(A-23)}$$

To determine the expression in which x is the dependent variable, Equation A-21 is rewritten to give

$$dx = \frac{df_s}{\lambda (f_{si} - f_s)}$$

The solution is

$$x = -\frac{\ln (f_{si} - f_s)}{\lambda} + C \qquad \text{(A-24)}$$

The constant, C, is determined from the boundary condition that when $x = \bar{x}$, $f_s = f_{se}$

$$\therefore \quad C = \bar{x} + \frac{\ln (f_{si} - f_{se})}{\lambda}$$

The complete solution is,

$$X = \bar{X} + \frac{E_s A_s}{K \Sigma_o} \ln\left(\frac{f_{si} - f_{se}}{f_{si} - f_s}\right) \qquad \text{(A-25)}$$

The only unknowns in Equations A-22, A-23 and A-25 are X and K. These might conceivably be determined experimentally and a representative value used in the above equations.

The term, λ, examined dimensionally, is observed to have a value of $\frac{1}{\text{length.}}$ It may therefore be said that $1/\lambda$ is the "characteristic length" of the elastic zone. The "characteristic length" is that length of the elastic zone required to completely transfer that amount of prestress not transferred in the friction zone if the bond stress, u_o, at x = 0 were to remain constant. This is shown pictorially is Figure 9.

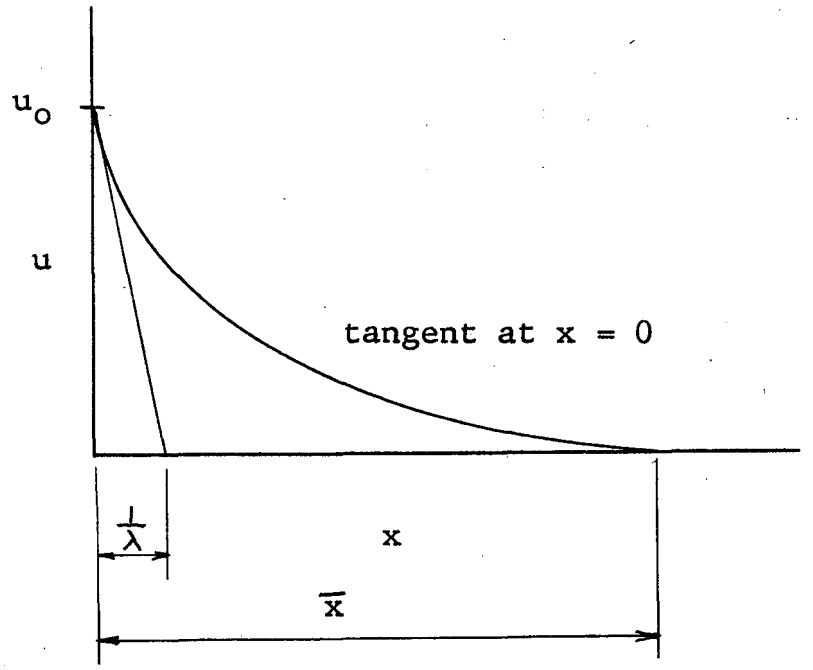

Figure 9 - Characteristic Length at the Elastic Zone

(3) Discussion

Unfortunately the equations obtained in the preceeding analyses are principally of academic interest since they have not been applied quantitatively with success.

The final expressions for frictional bond include the modular ratio, n. At the concrete--steel interface radial stresses are of such magnitude that the concrete must be in a plastic state and one is at a loss to evaluate the term. Also, the coefficient of friction, $\emptyset$, is taken as constant whereas in actuality it must be highly sensitive to local variations in concrete quality and particularly to the effectiveness of compaction. Furthermore, the mechanical bonding action produced by surface deformations on the reinforcement, or, in the case of strands, the change of pitch of the helix is neglected entirely.

It should also be noted that in the derivation of the expressions for elastic bond the factor K, Bond Modulus of Elasticity, was introduced and taken as a constant without justification. Its actual nature is unknown. Guyon's (10) attempts to evaluate the characteristic length and the maximum bond stress u, for smooth wires were inconclusive.

APPENDIX B

FIGURES RELATING TO PULL-OUT TESTS

In the order mentioned in the text

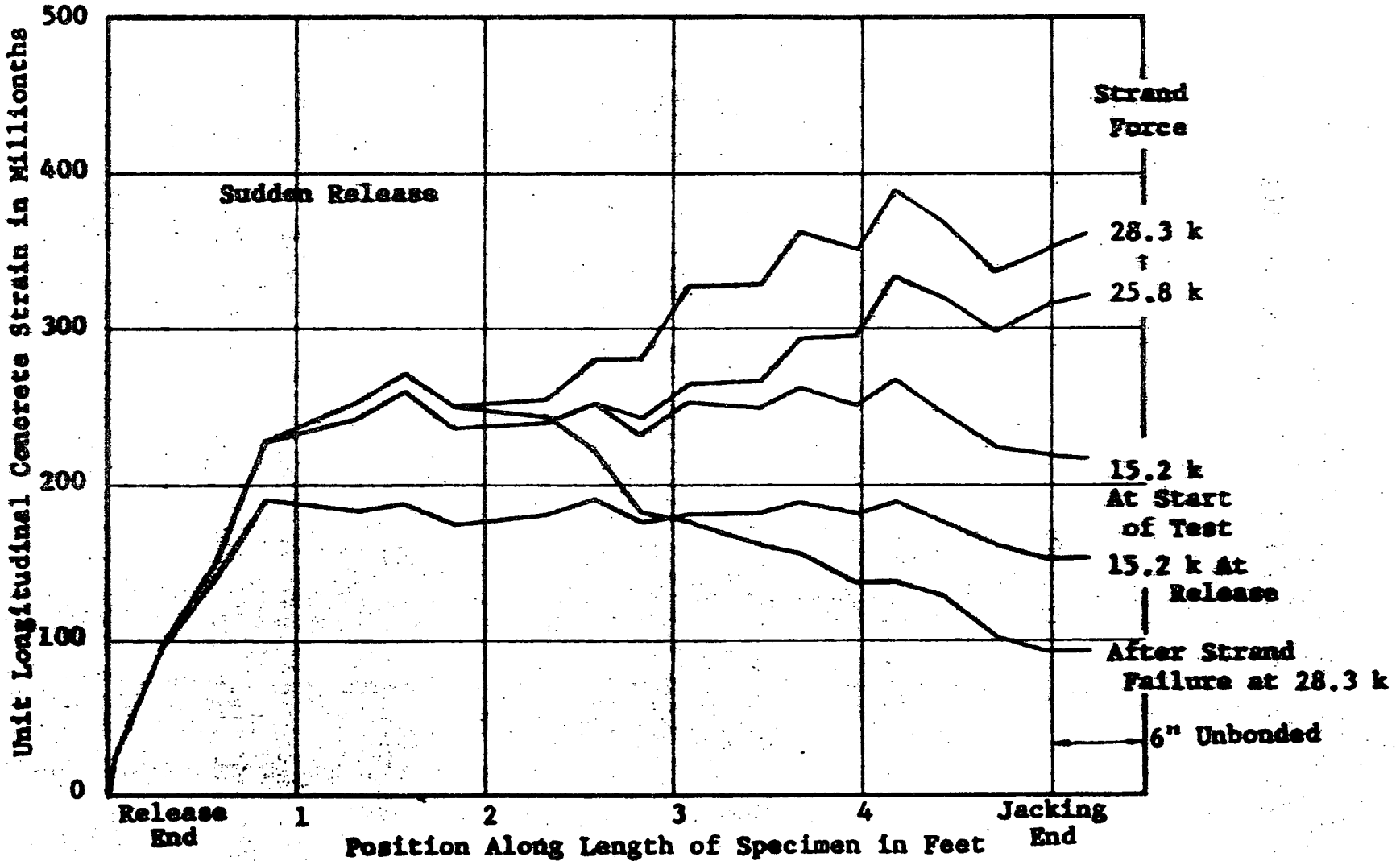

Figure 22 Development of Concrete Strain Over Length of Specimen III-1

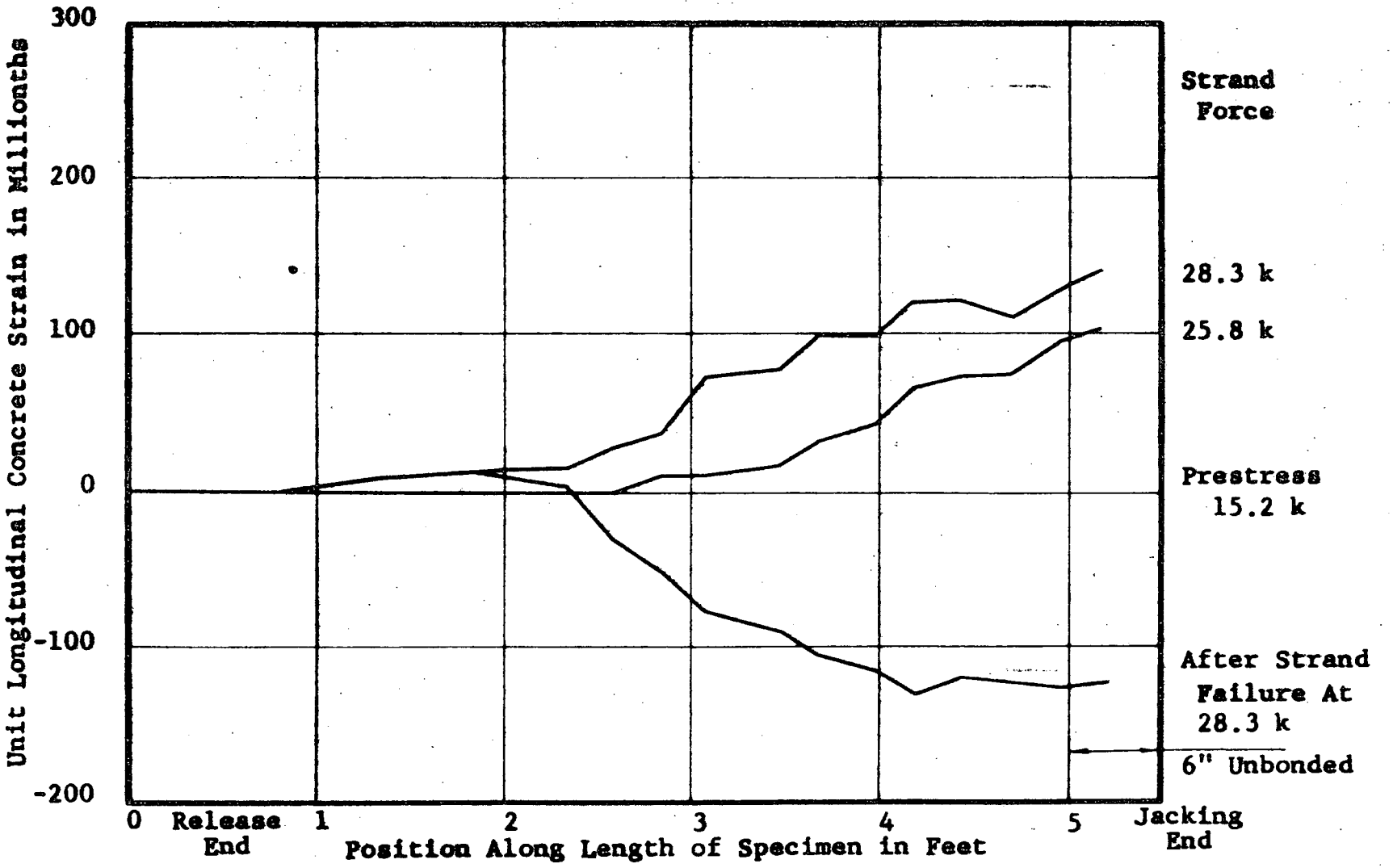

Figure B2 Development of Concrete Strain Over Length of Specimen III-1

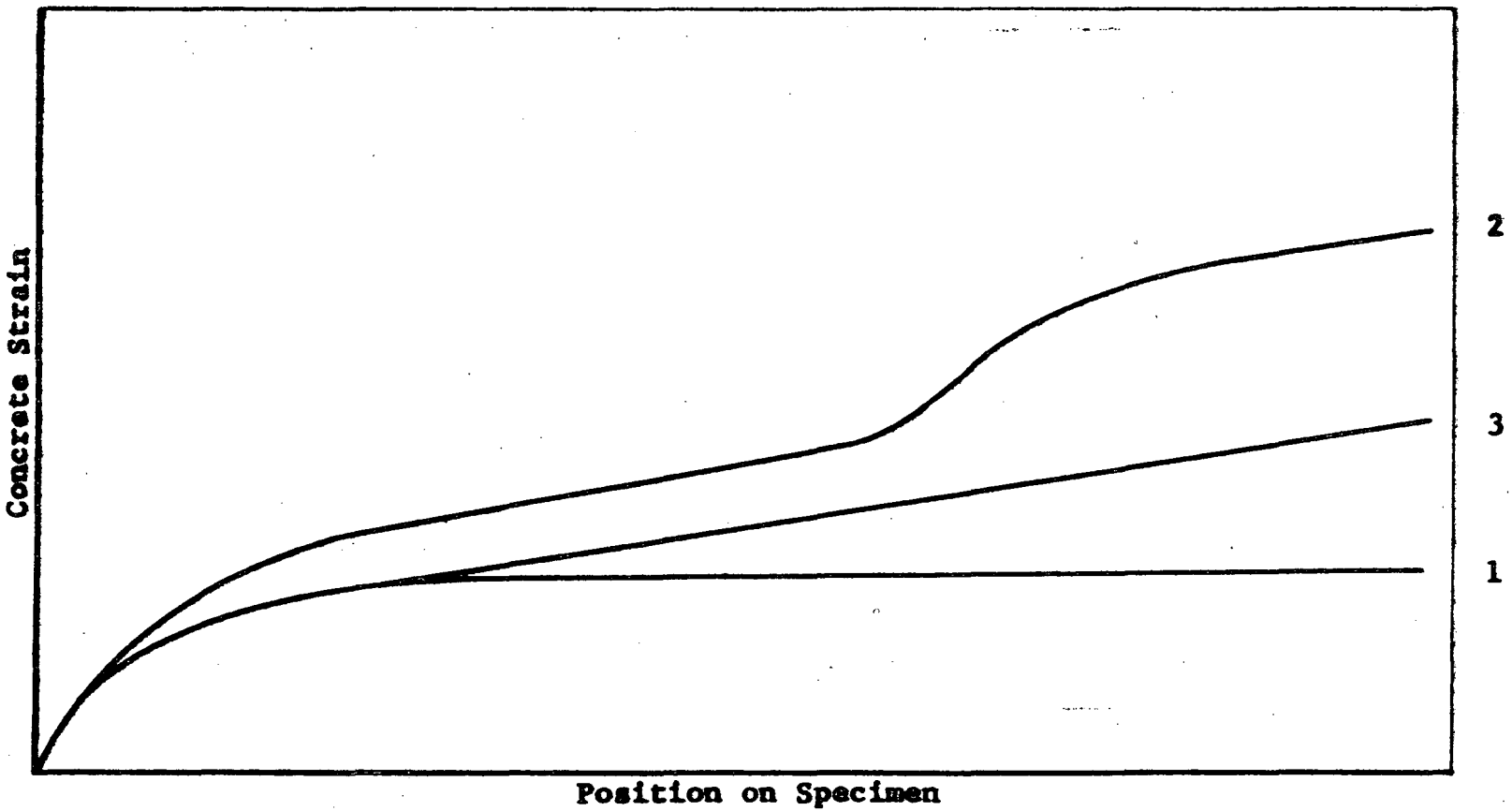

Figure B3 - Slip Failure at Release - Series V

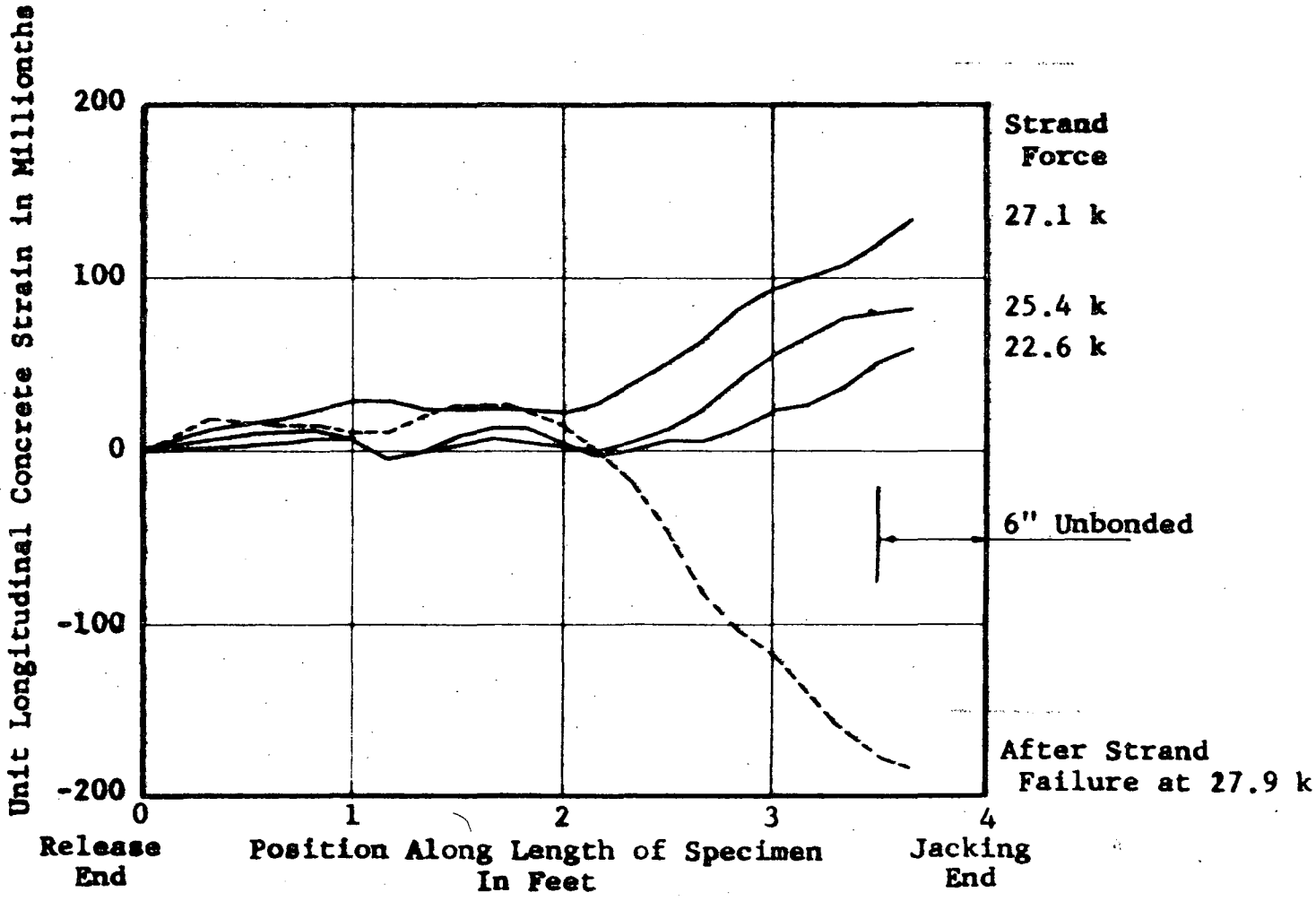

Figure 84 Development of Concrete Strain Over Length of Specimen V-4 During Test

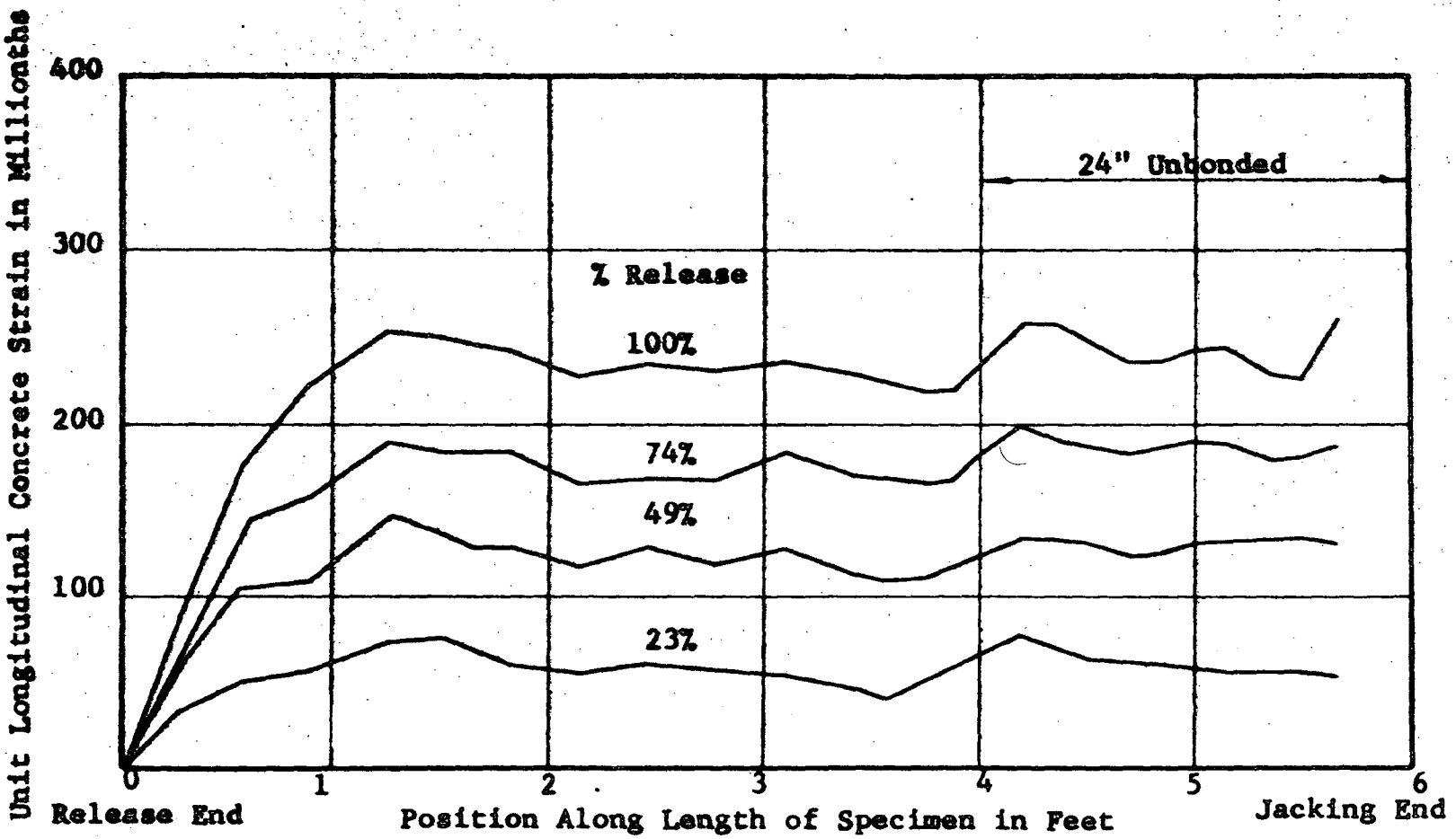

Figure 25 Development of Concrete Strain Over Length of Specimen VI-1 During Gradual Release

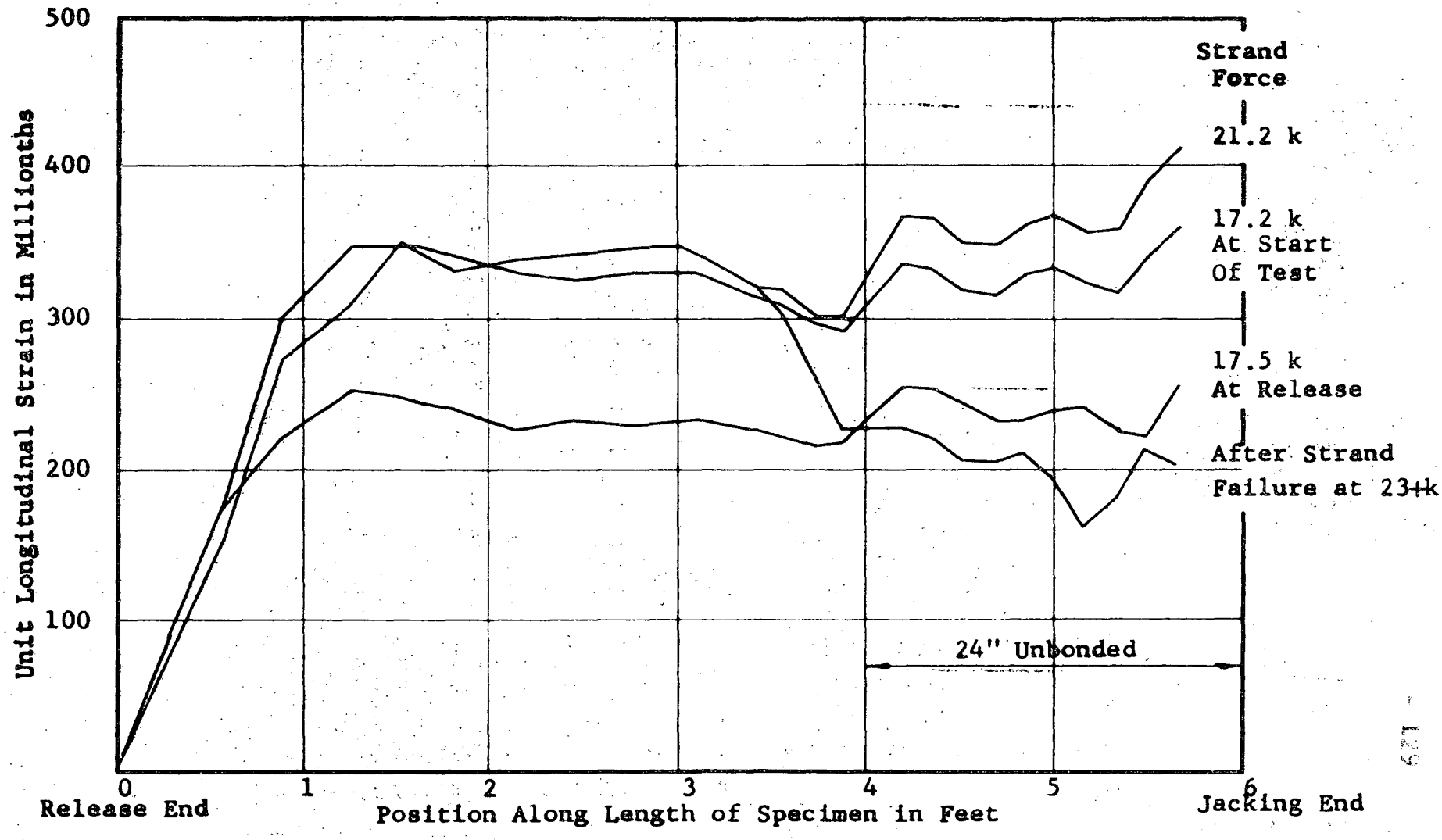

Figure B6 Development of Concrete Strains Over Length of Specimen VI-1 During Test

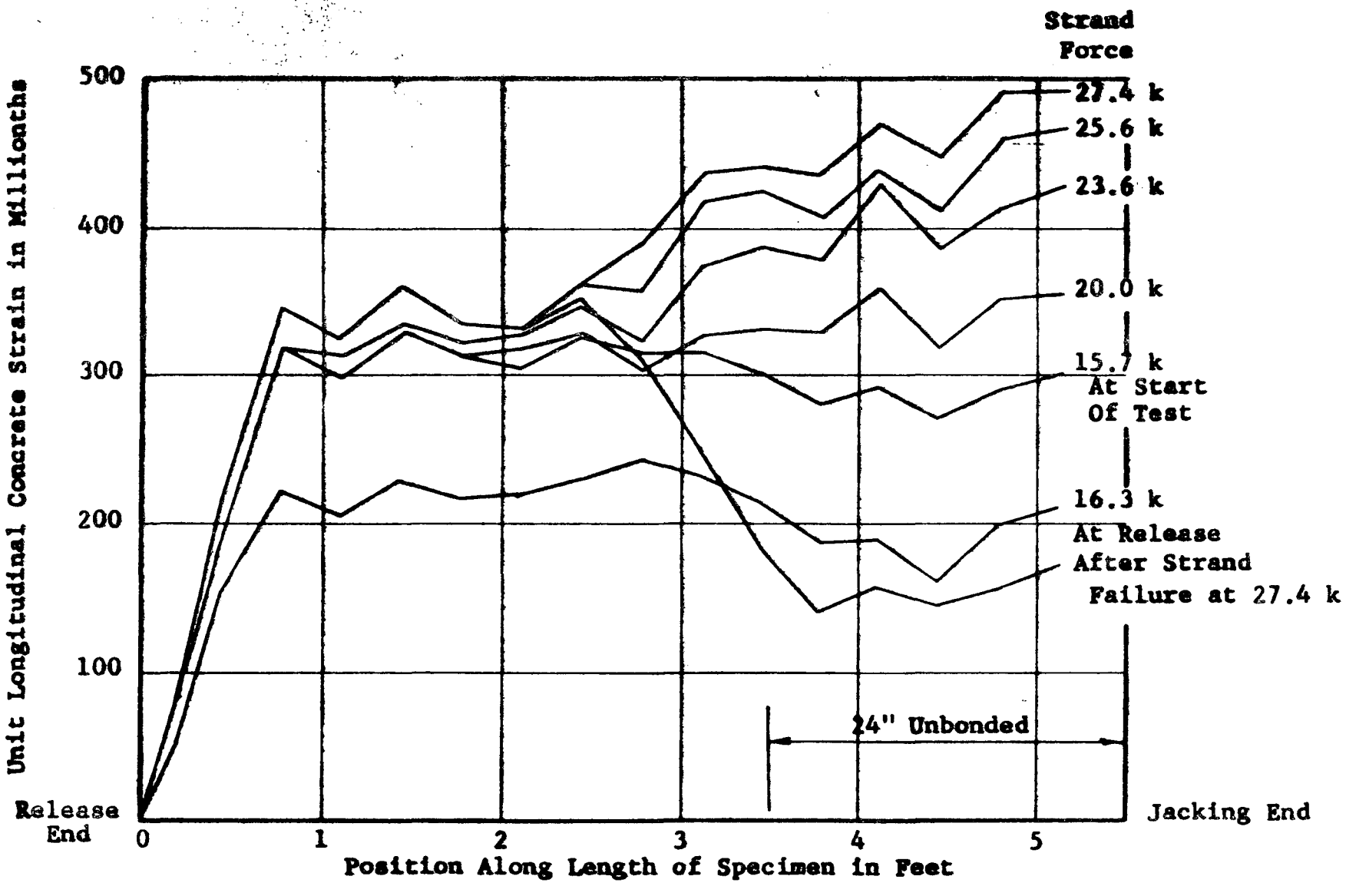

Figure 27 Development of Concrete Strain Over Length of Specimen VI-2

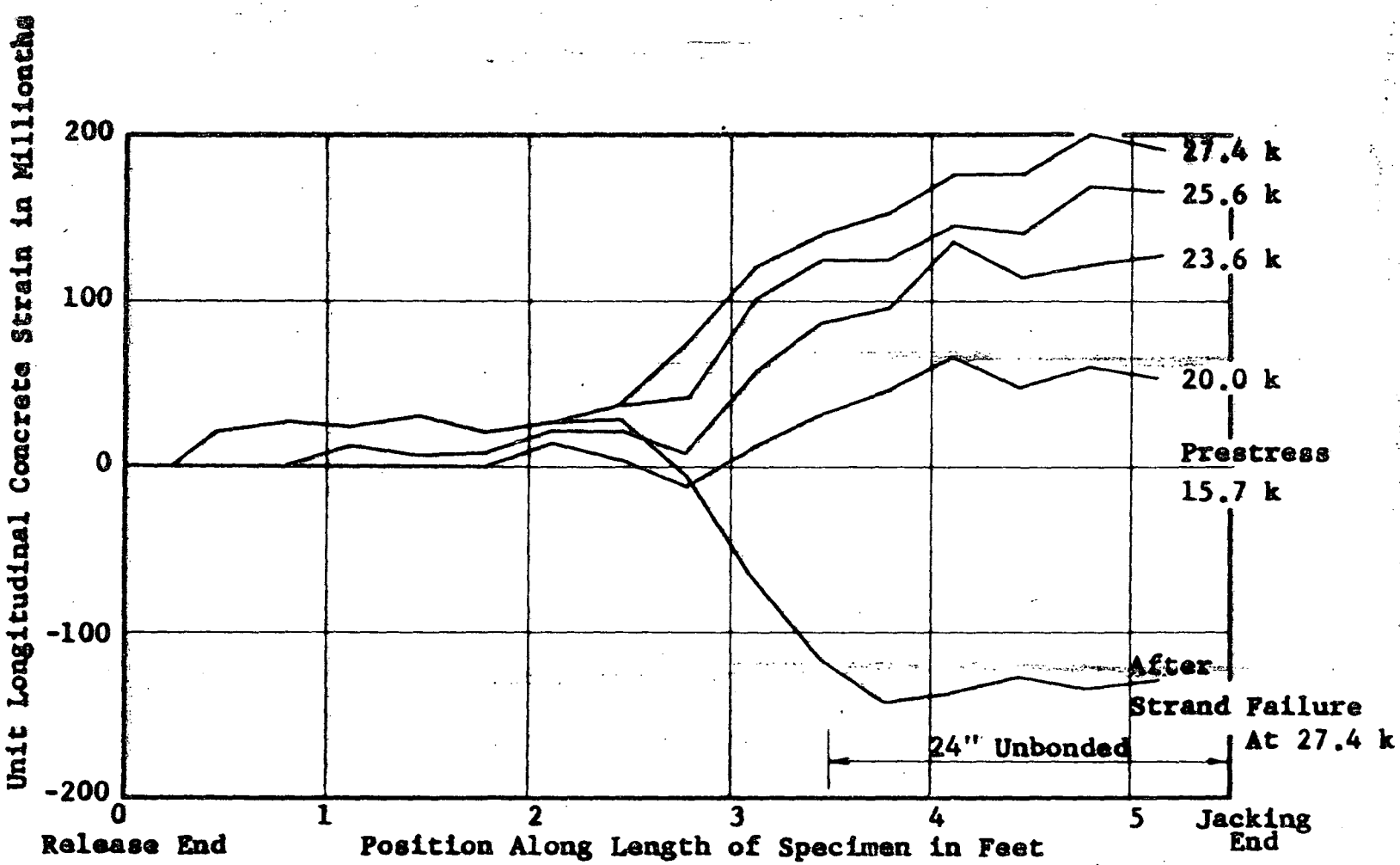

Figure 38 Development of Concrete Strain Over Length of Specimen VI-2 at Test

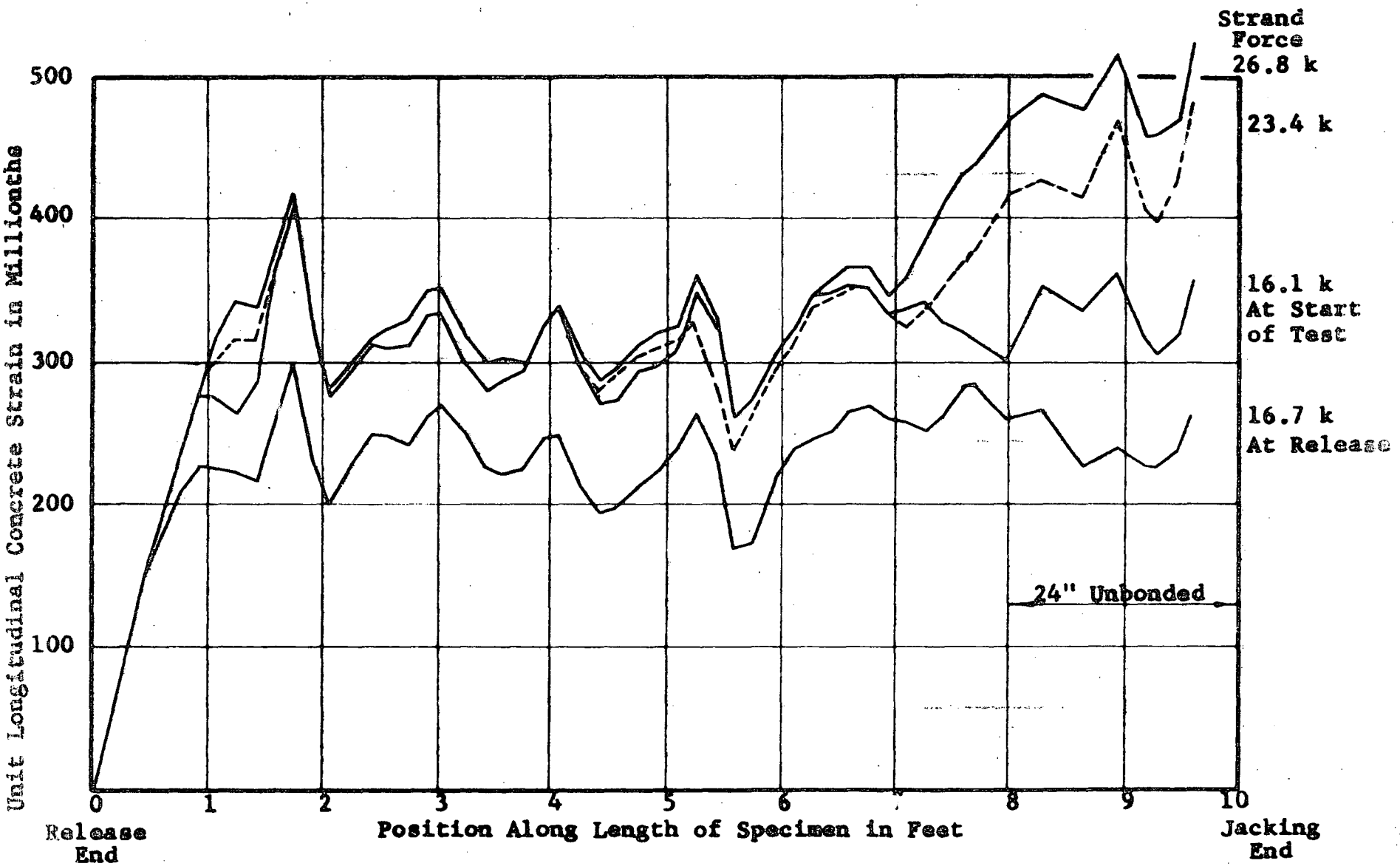

Figure 89 Development of Concrete Strain Over Length of Specimen VI-3

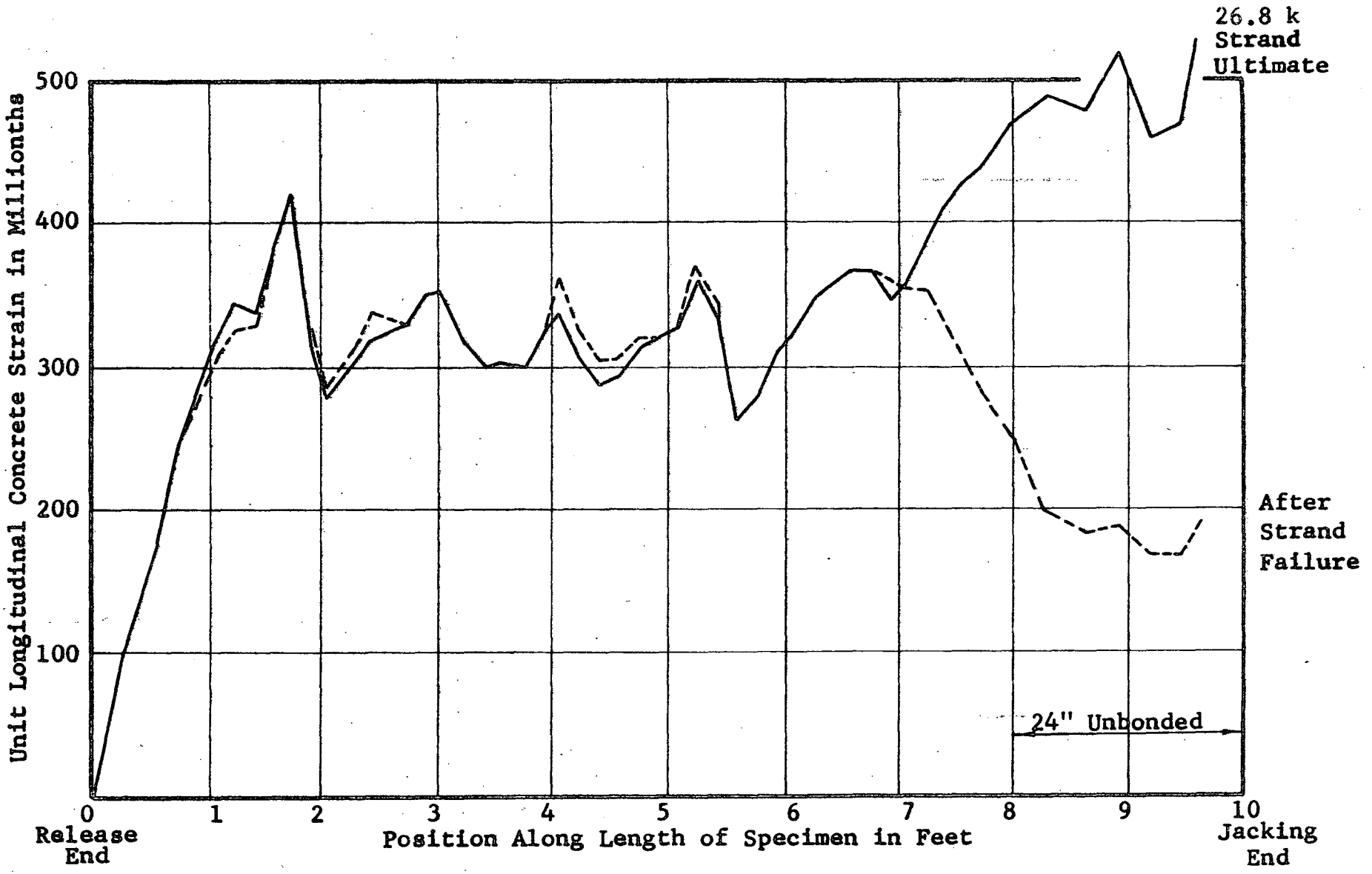

Figure B10 Change in Concrete Strains at Strand Failure for Specimen VI-3

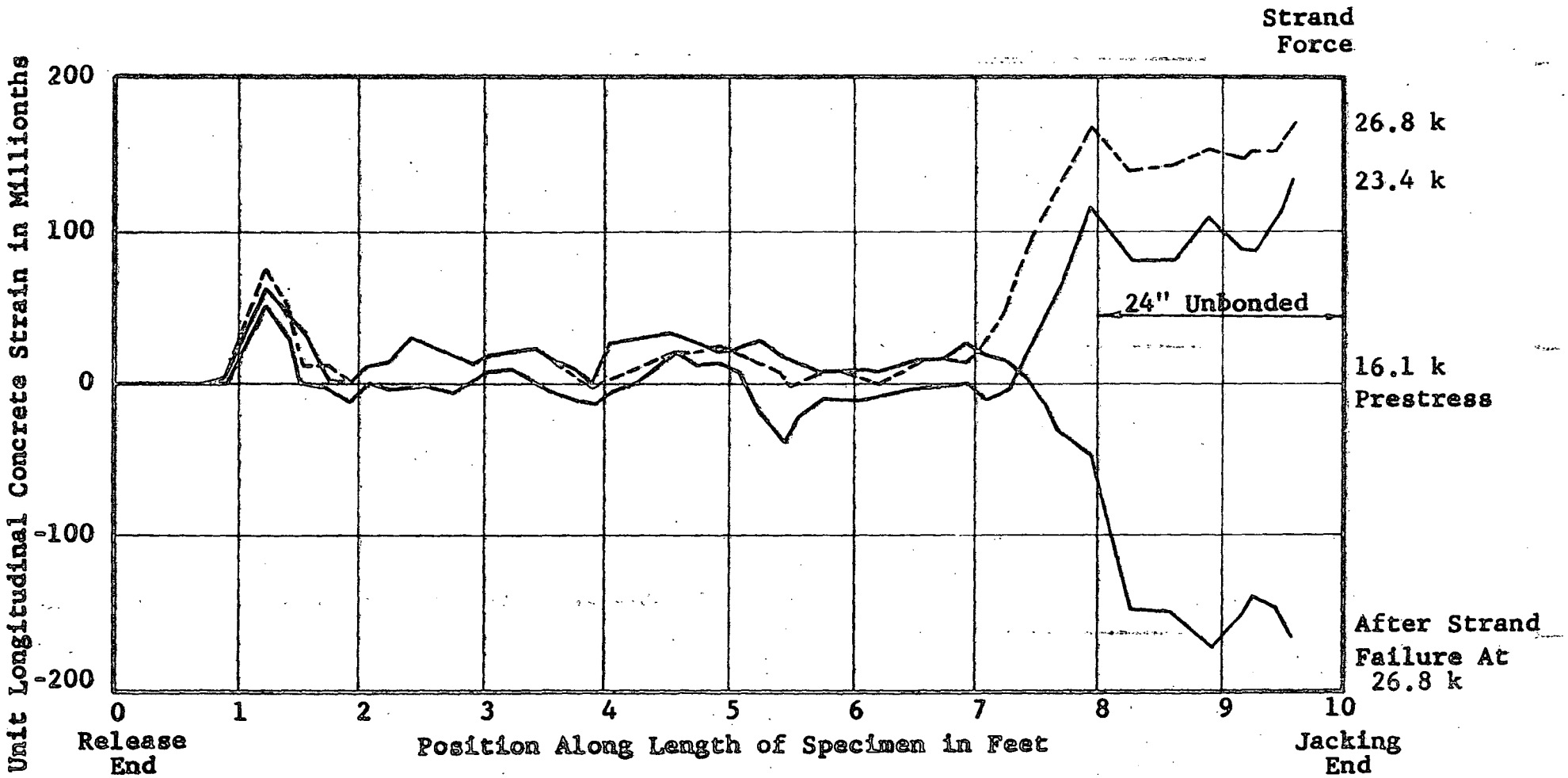

Figure B11 Development of Concrete Strains Over Length of Specimen VI-3 During Test

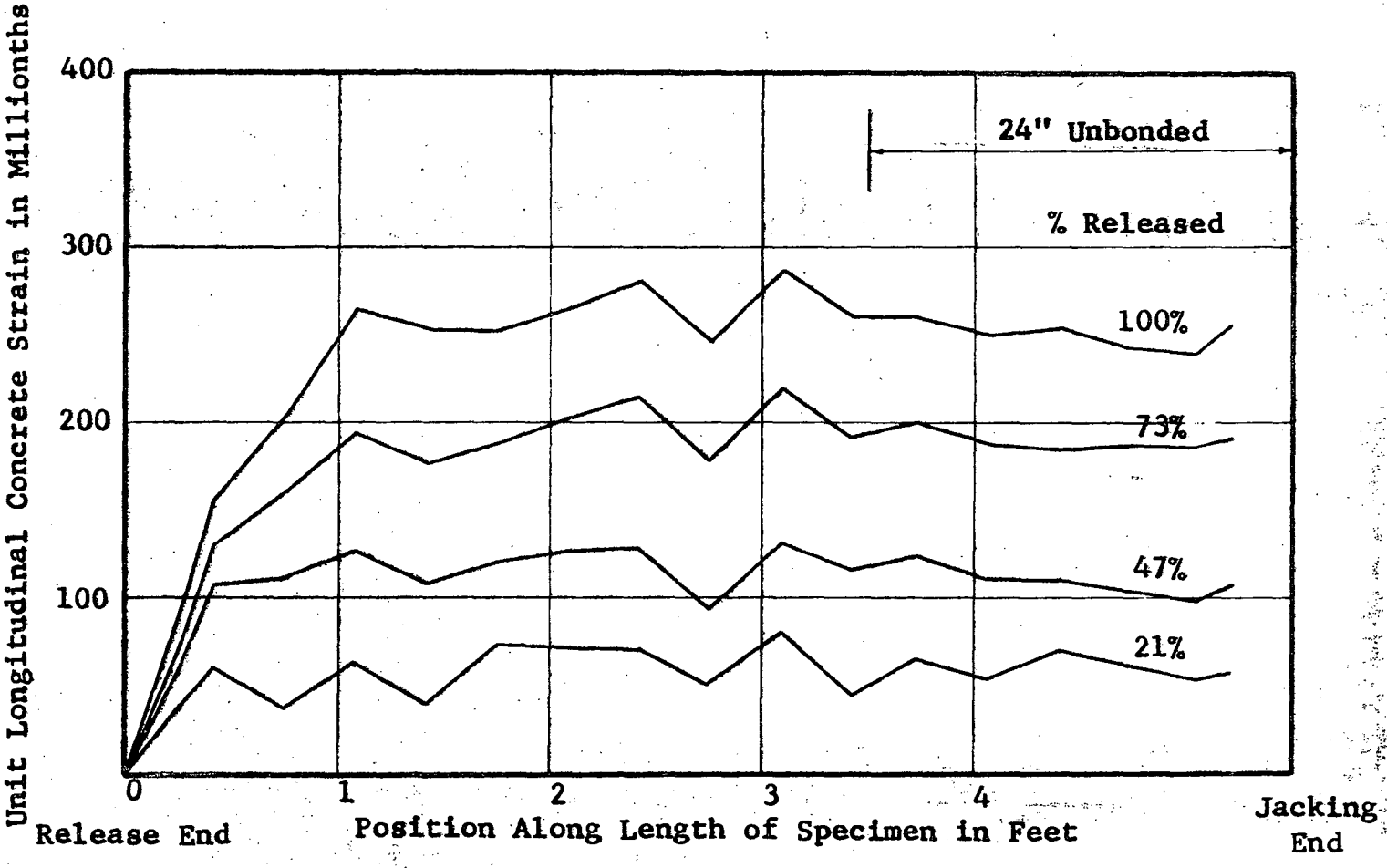

Figure B12 Development of Concrete Strain Over Length of Specimen VI-4 During Gradual Release

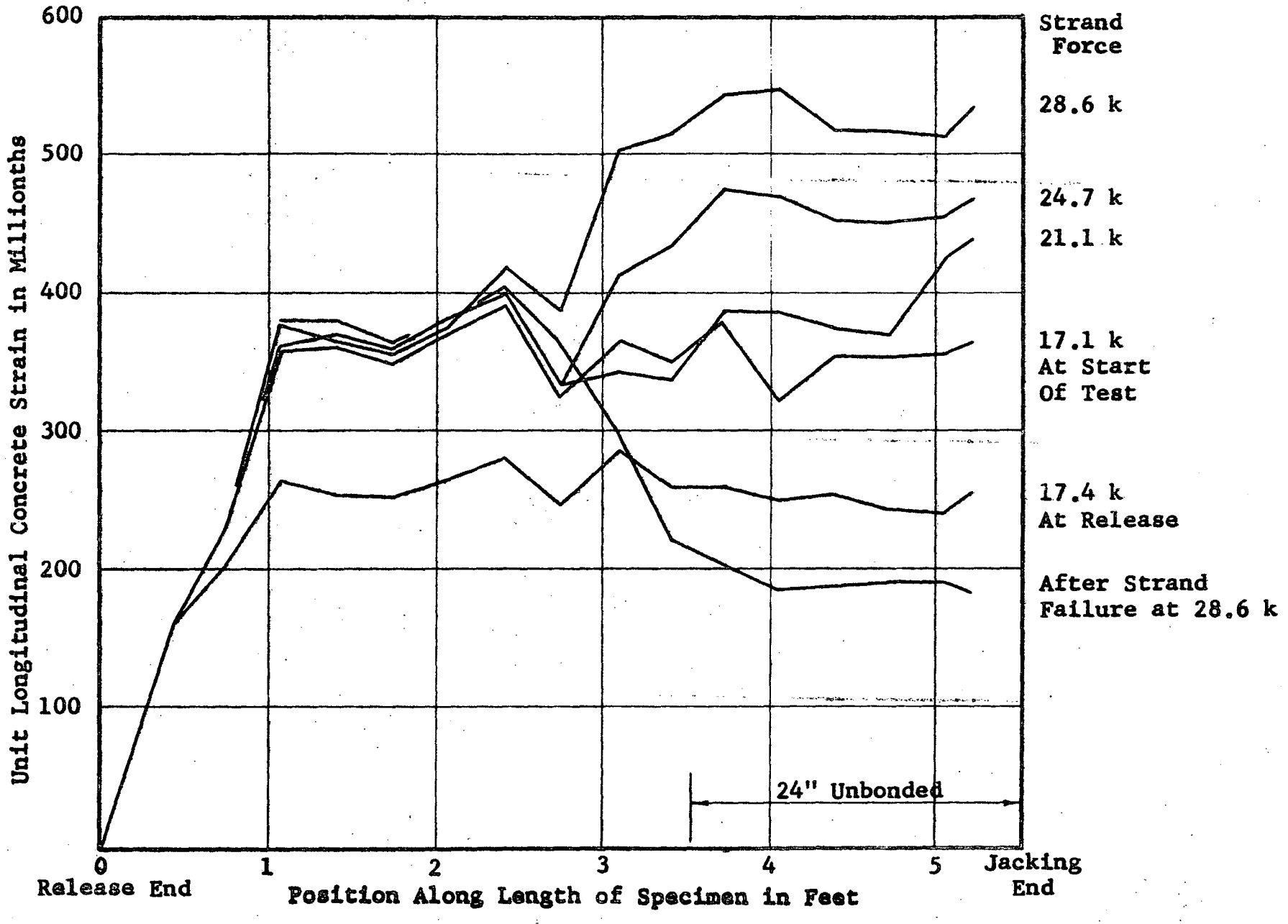

Figure B13 Development of Concrete Strain Over Length of Specimen VI-4 During Test

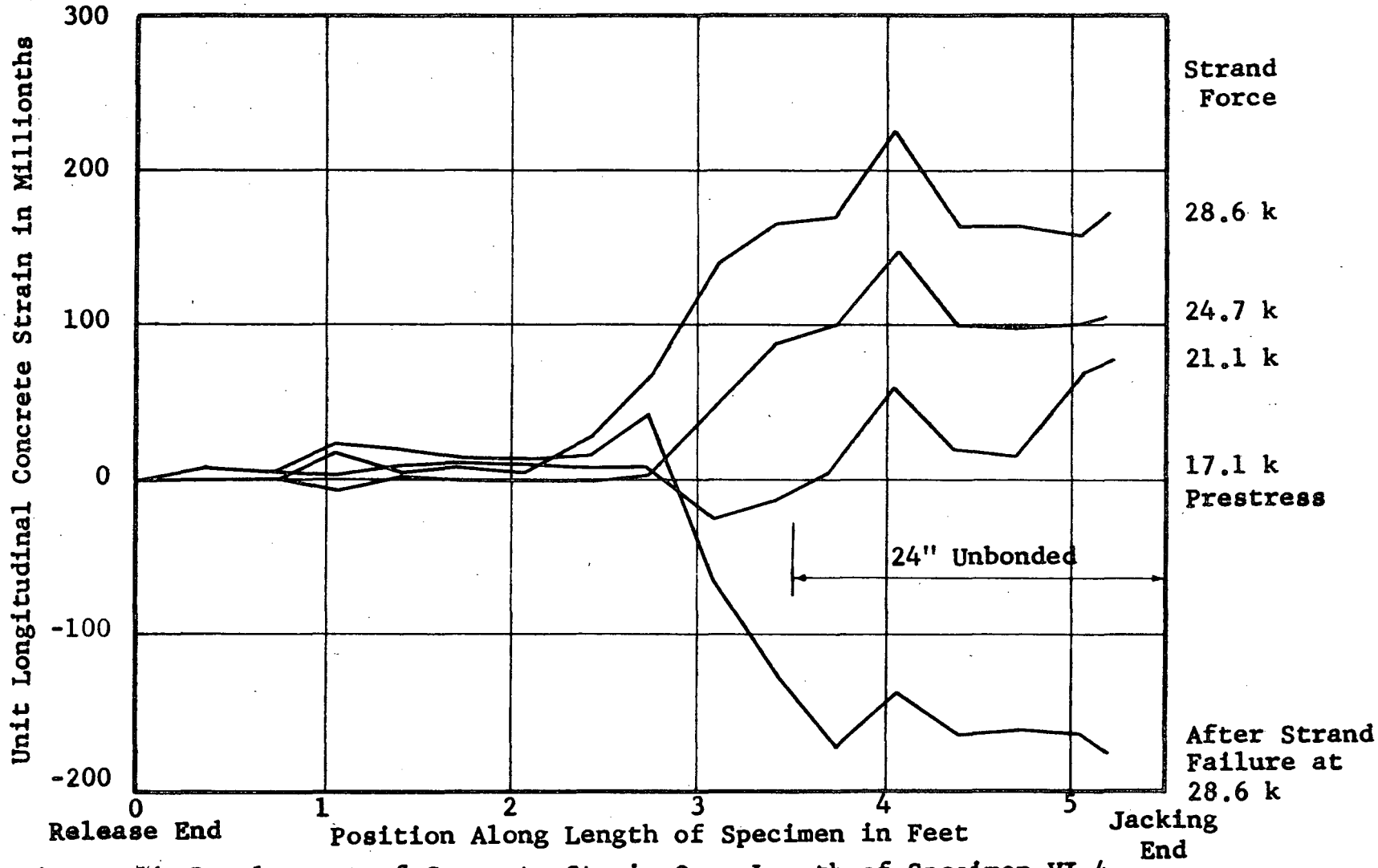

Figure B14 Development of Concrete Strain Over Length of Specimen VI-4 During Test

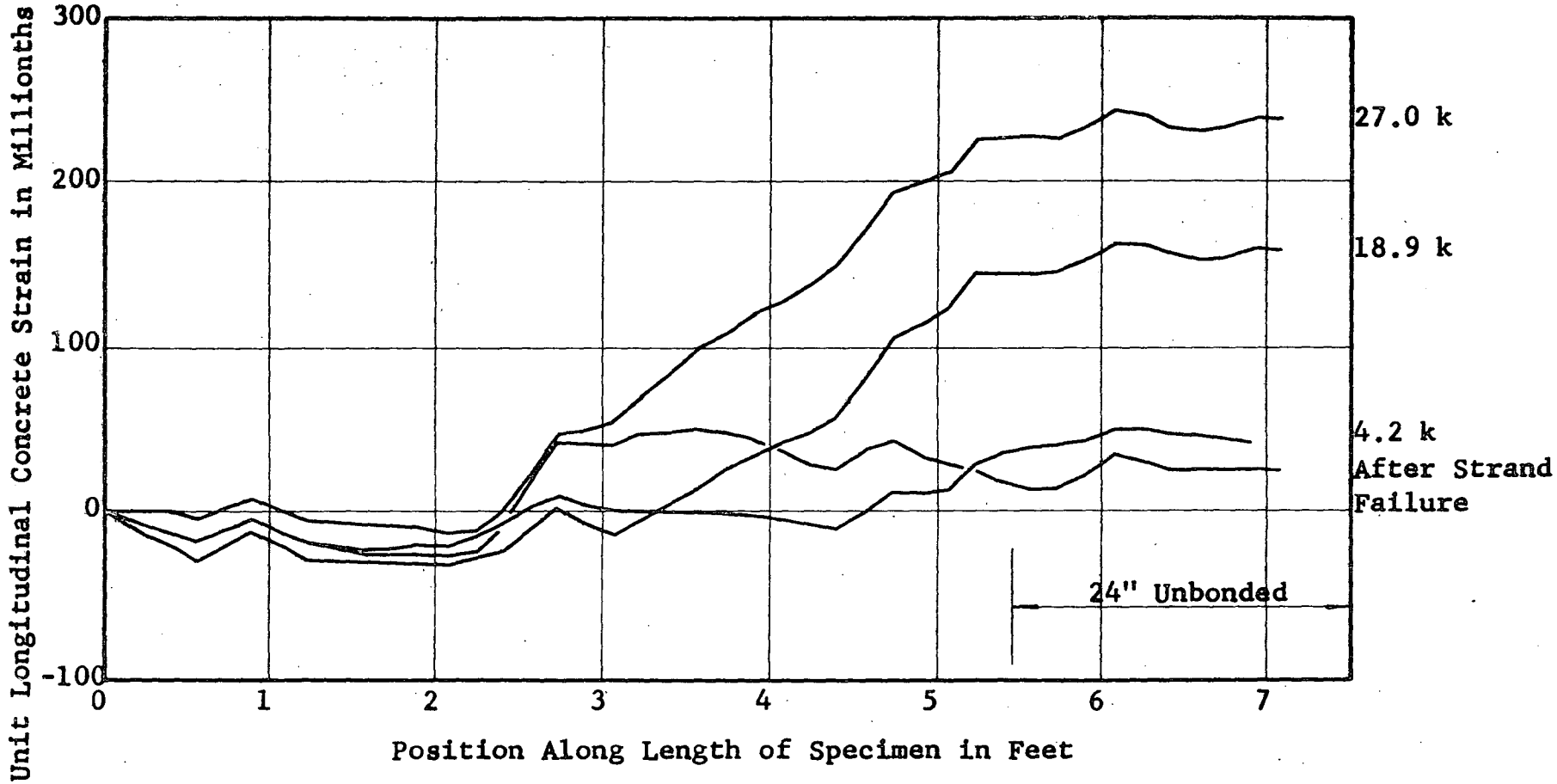

Figure B15 Development of Concrete Strain Over Length of Specimen VII-1 At Test

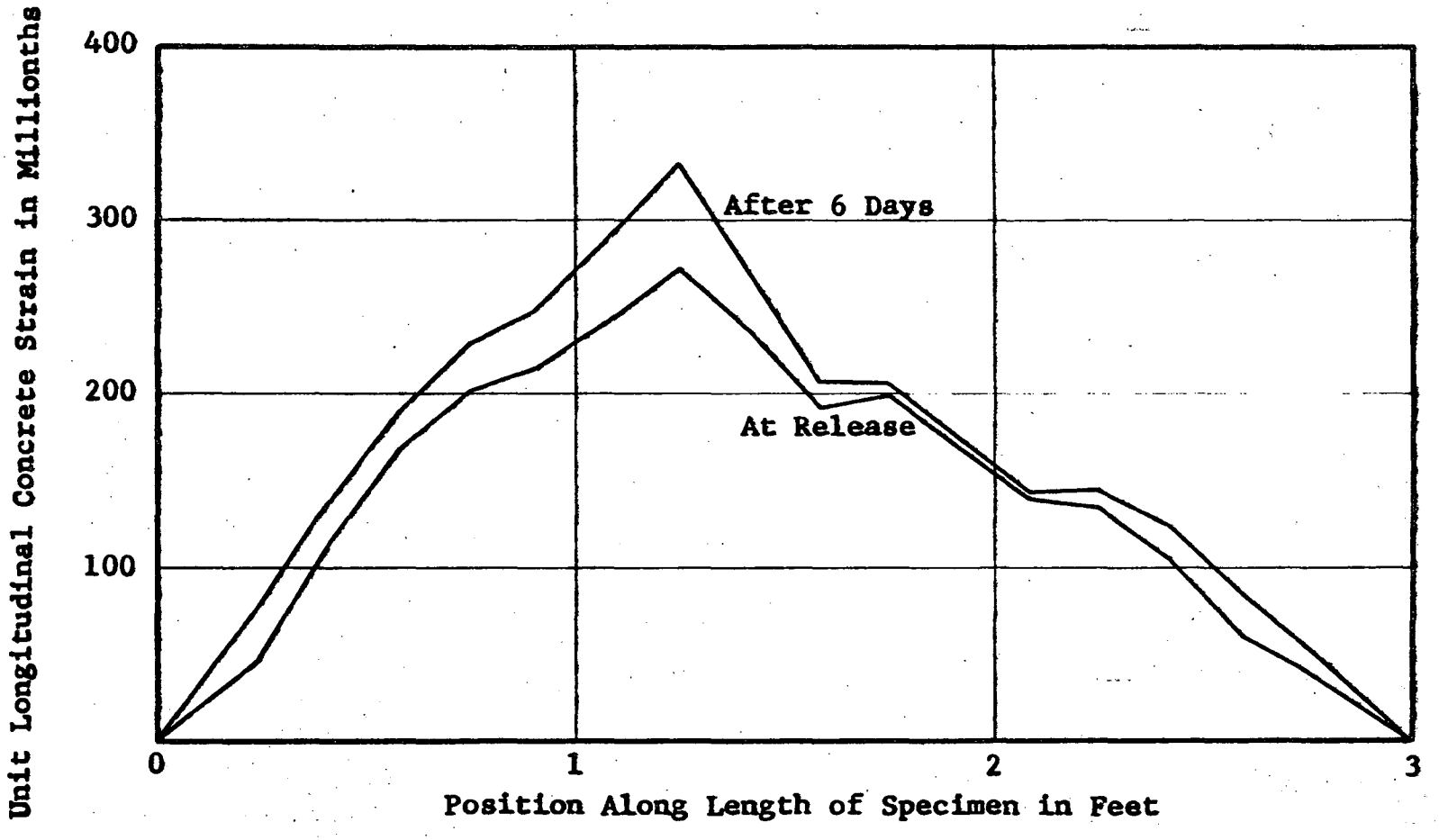

Figure 16 Development of Concrete Strain Over Length of Specimen VI-5, Col. With Oiled Strand

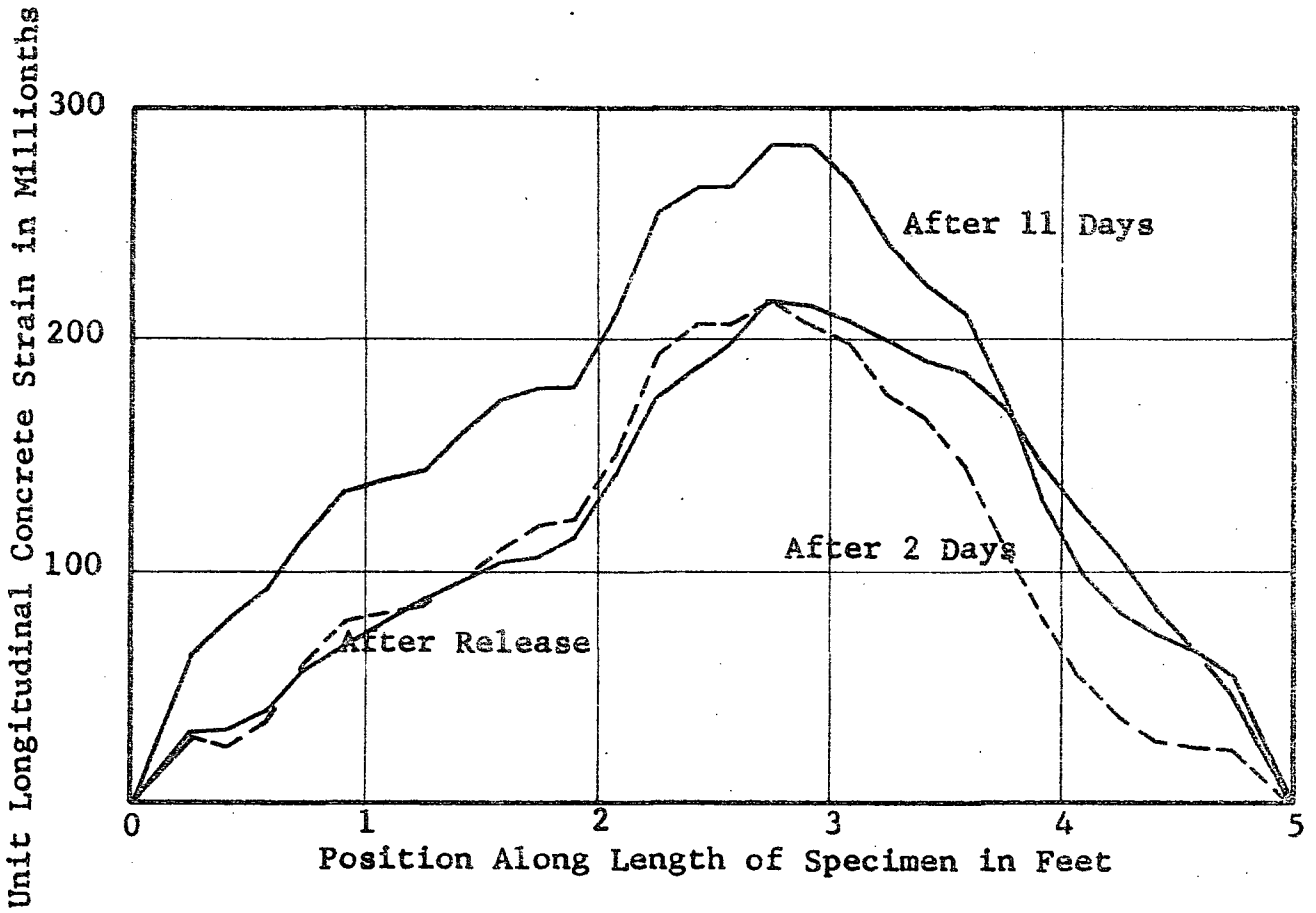

Figure B-17 Concrete Strain Distribution Over Length of Col. VIII - 9

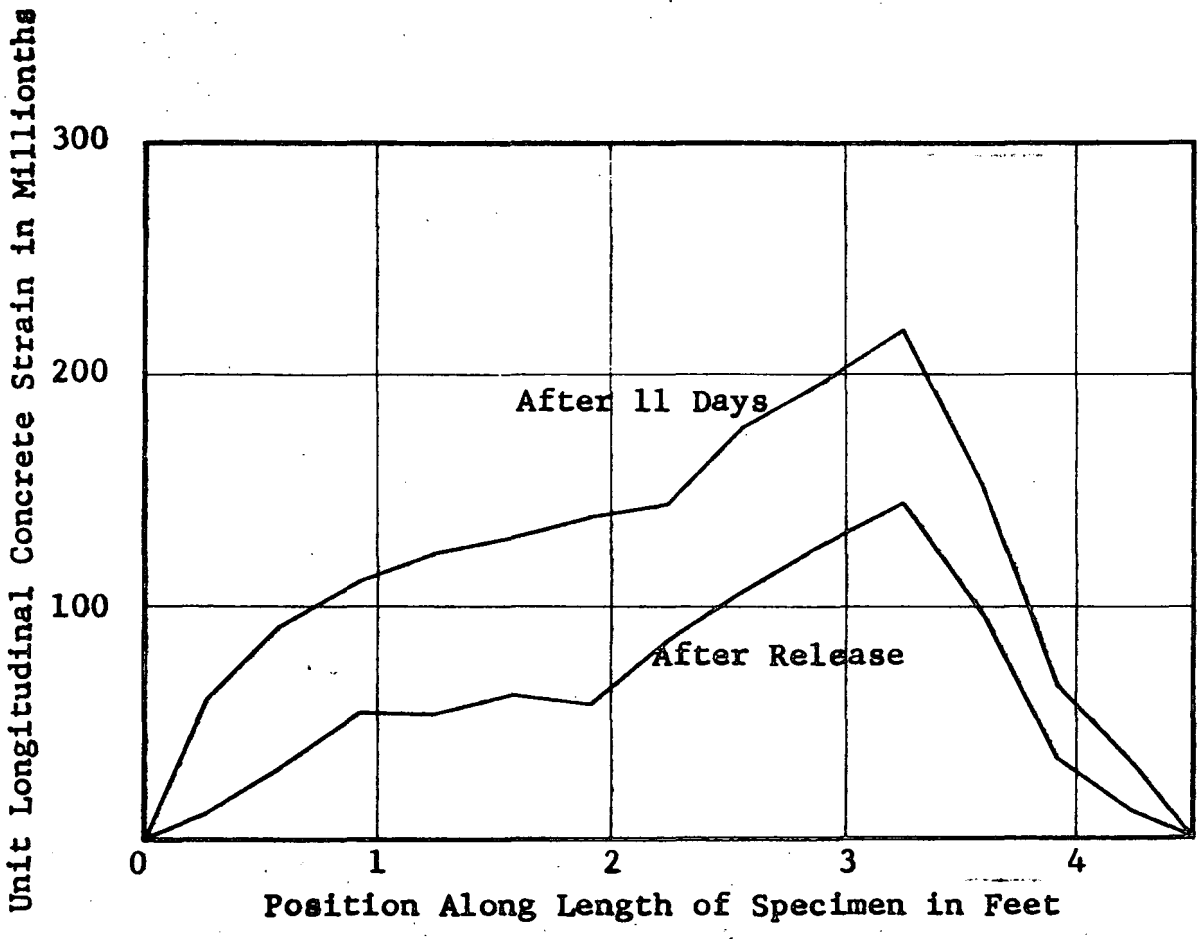

Figure B18 Concrete Strain Distribution Over Length of Col. VIII - 10

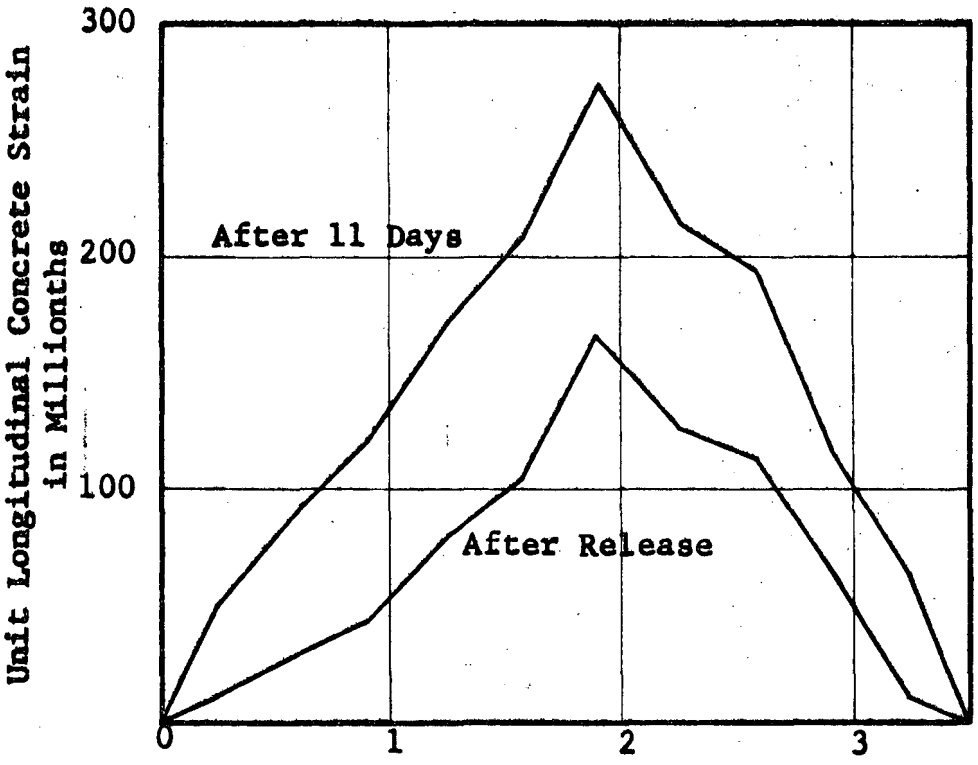

Figure B19 Concrete Strain Distribution Over Length of Column VIII - 11.

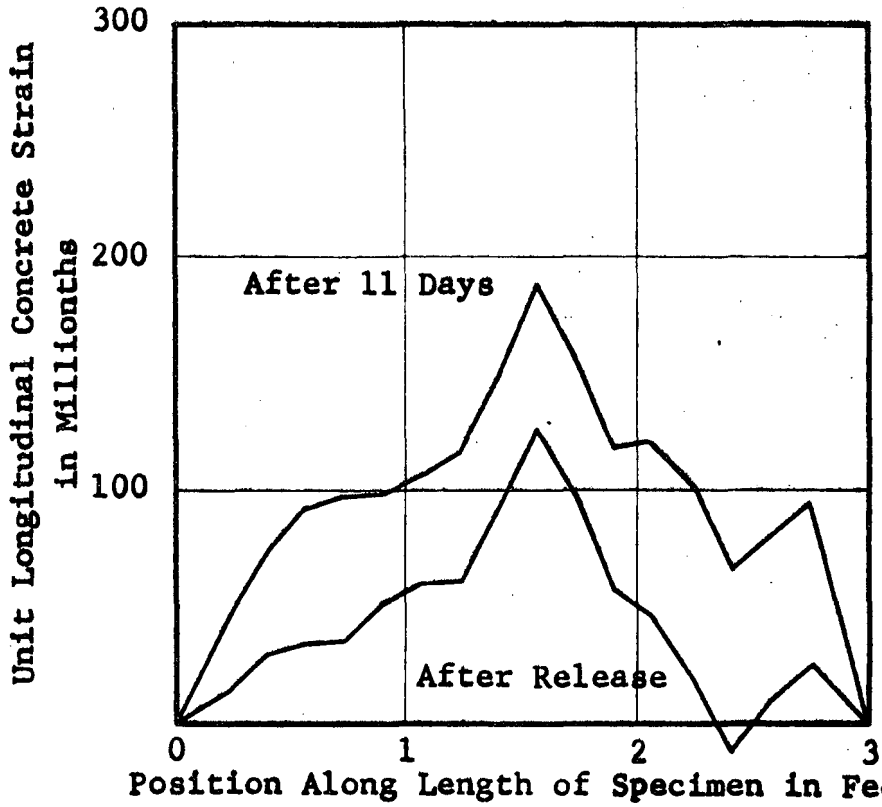

Figure B20 Concrete Strain Distribution Over Length of Col. VIII - 12.

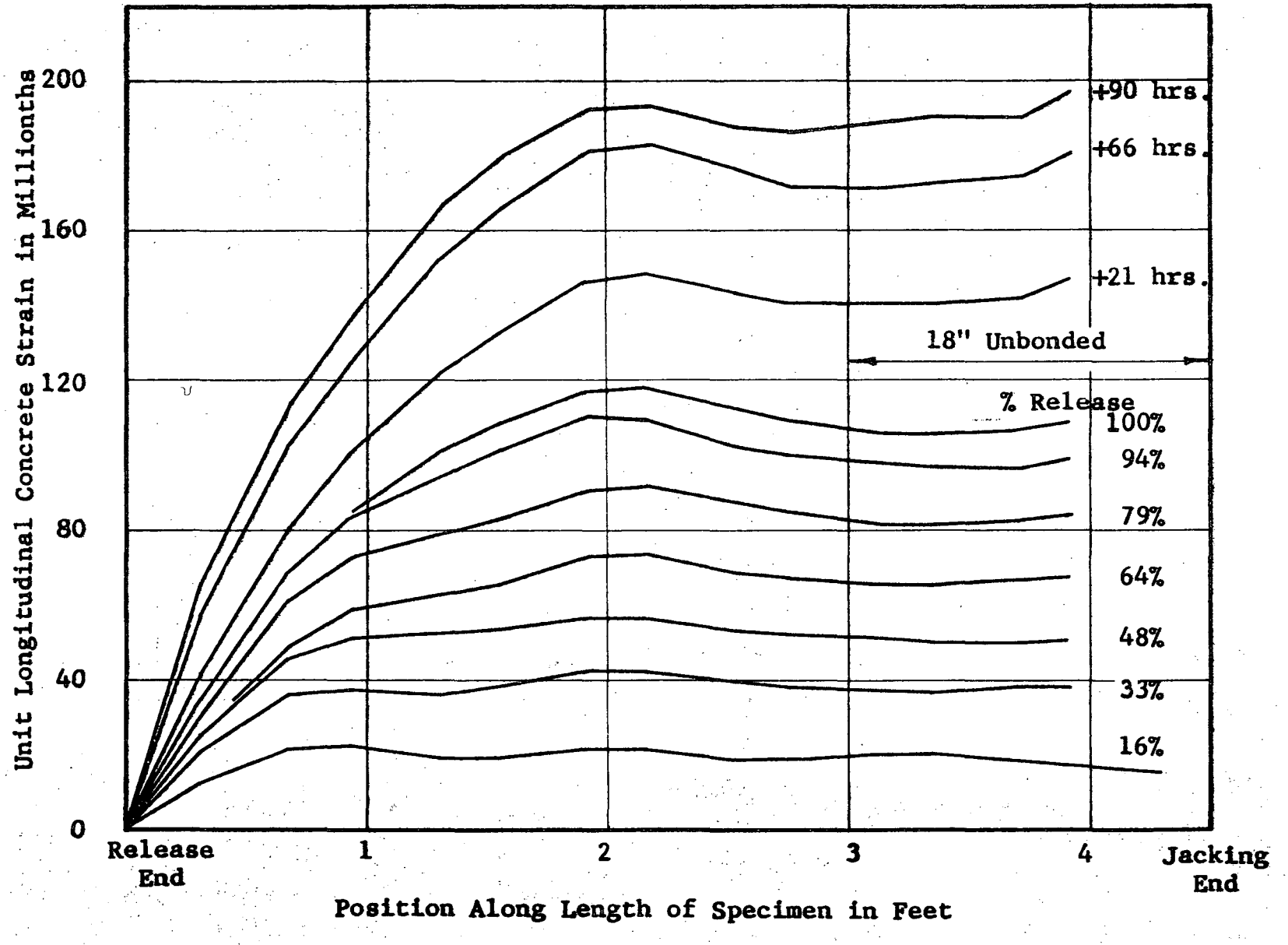

Figure B21. Development of Concrete Strain Over Length of Specimen IX-1 During Gradual Release

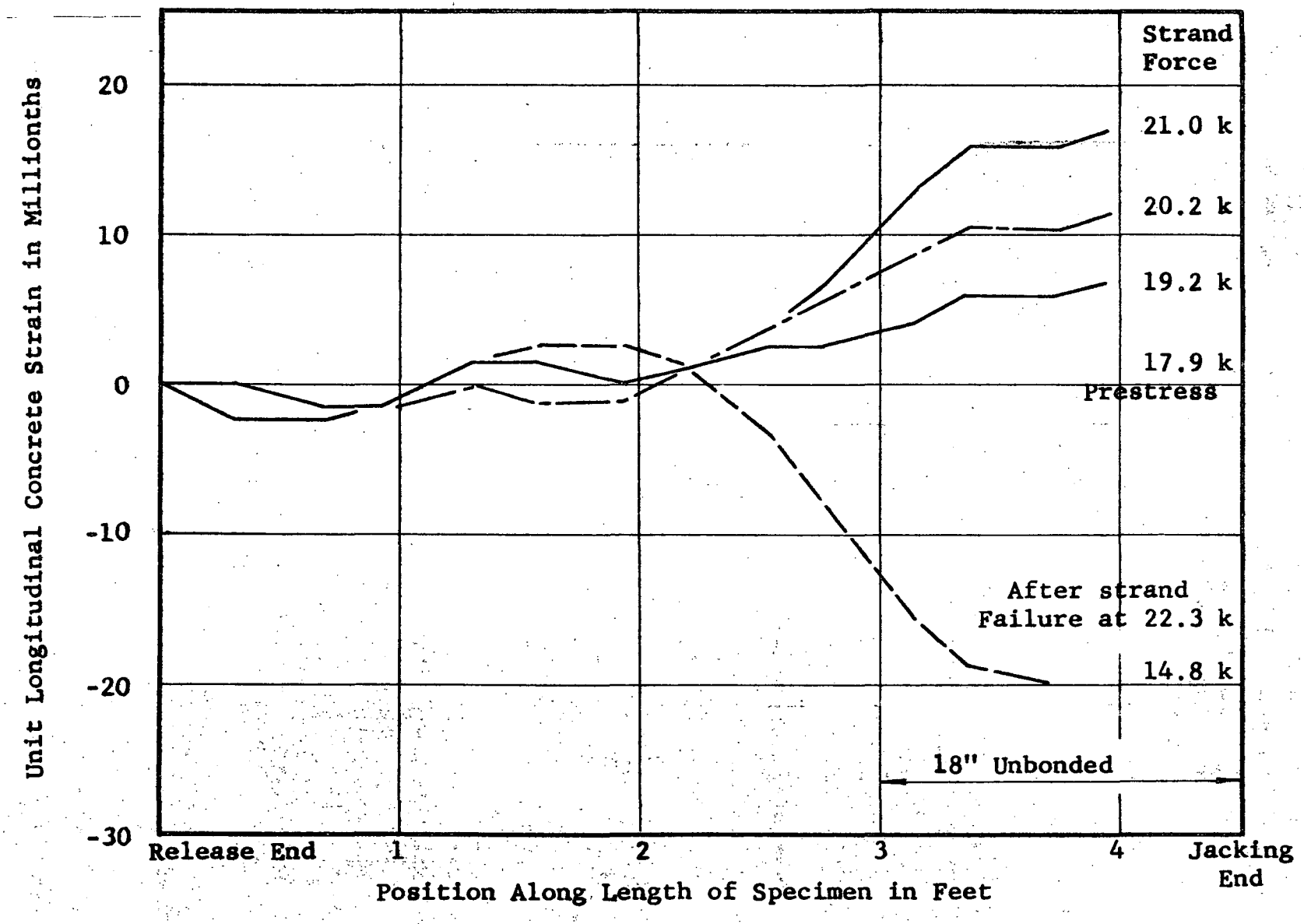

Figure B22. Development of Concrete Strain Over Length of Specimen IX-1 During Test

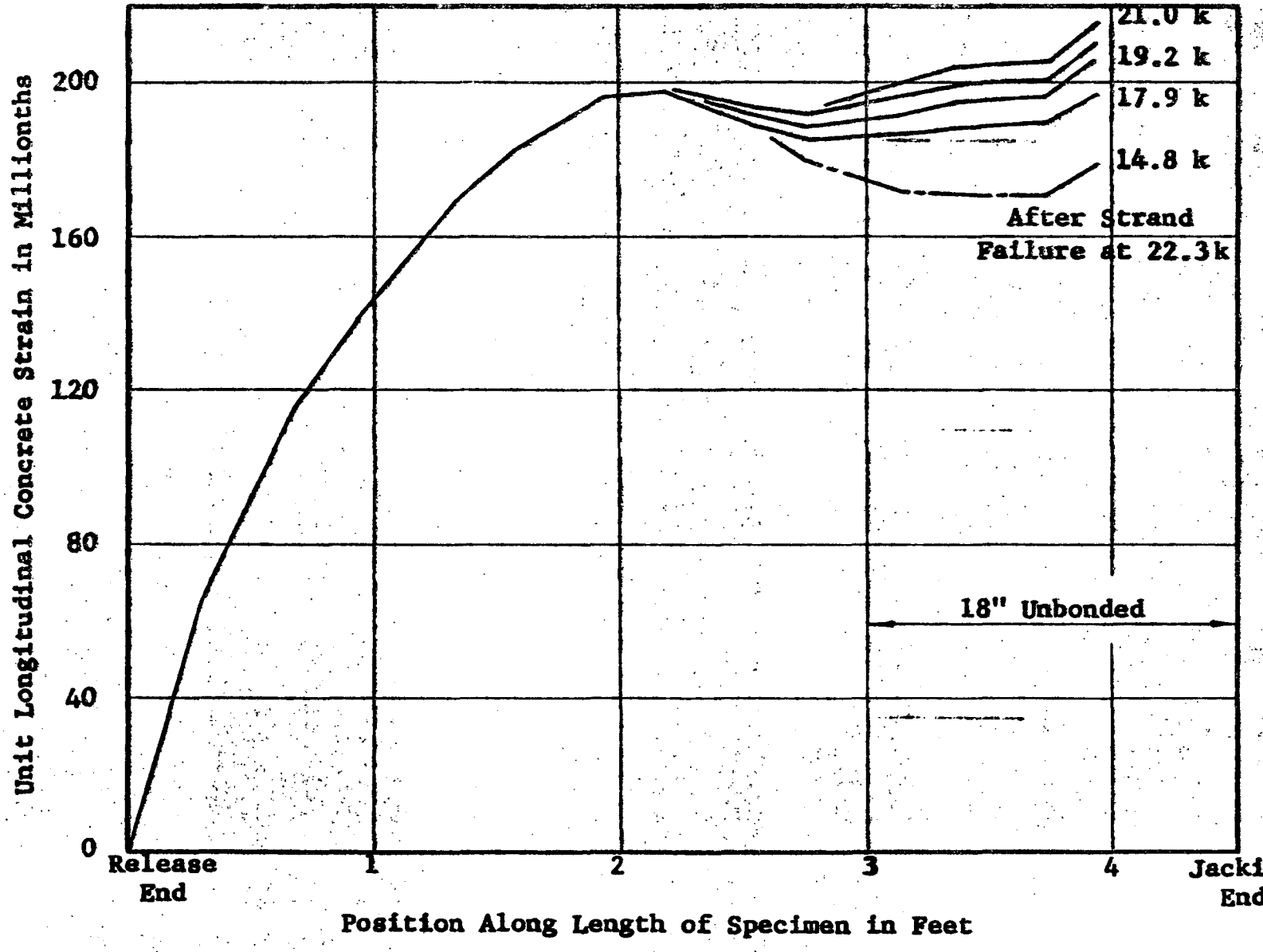

Figure 823 Development of Concrete Strain Over Length of Specimen IX-1 During Test

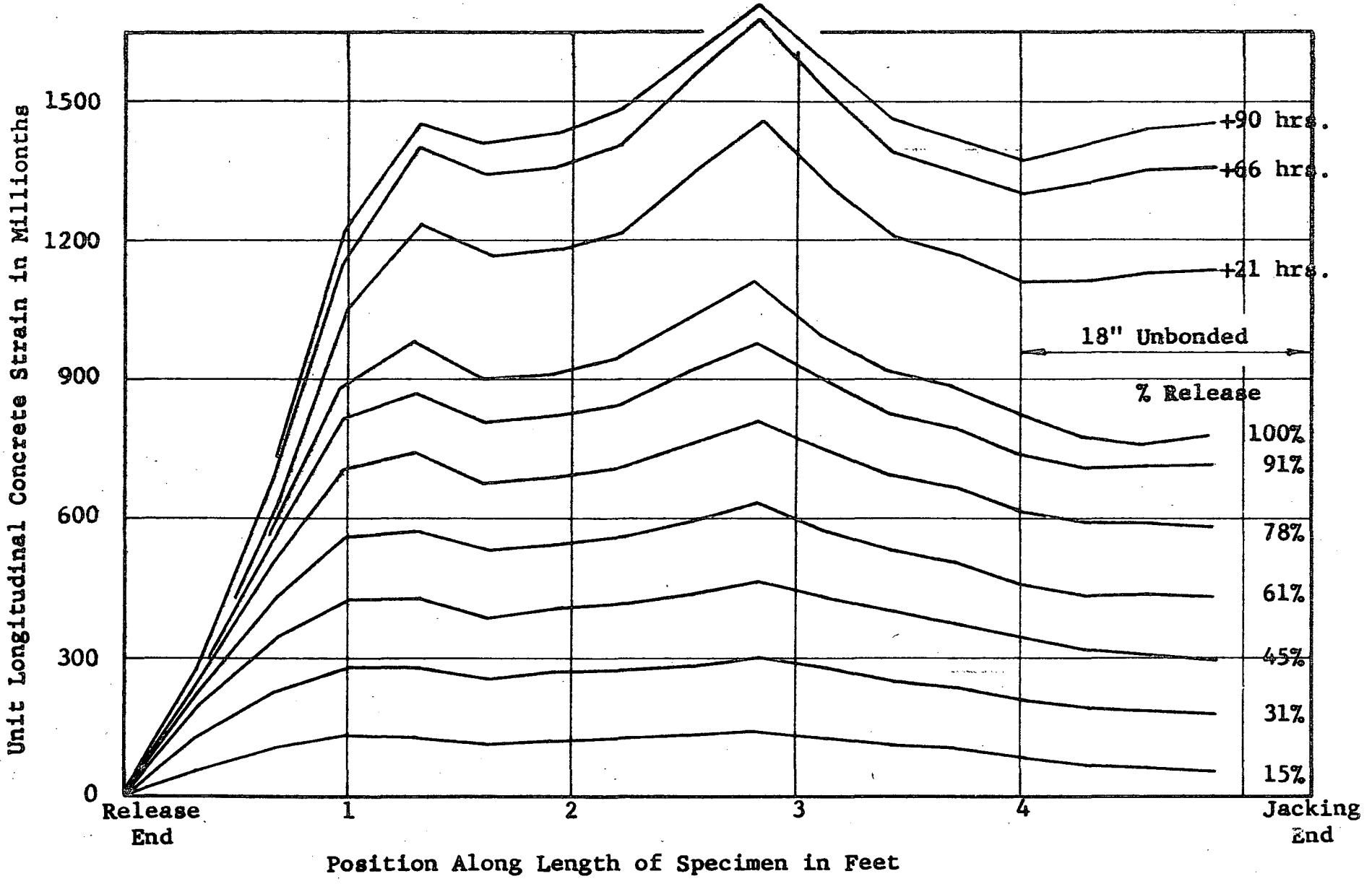

Figure B24 Development of Concrete Strain Over Length of Specimen IX-2 During Gradual Release

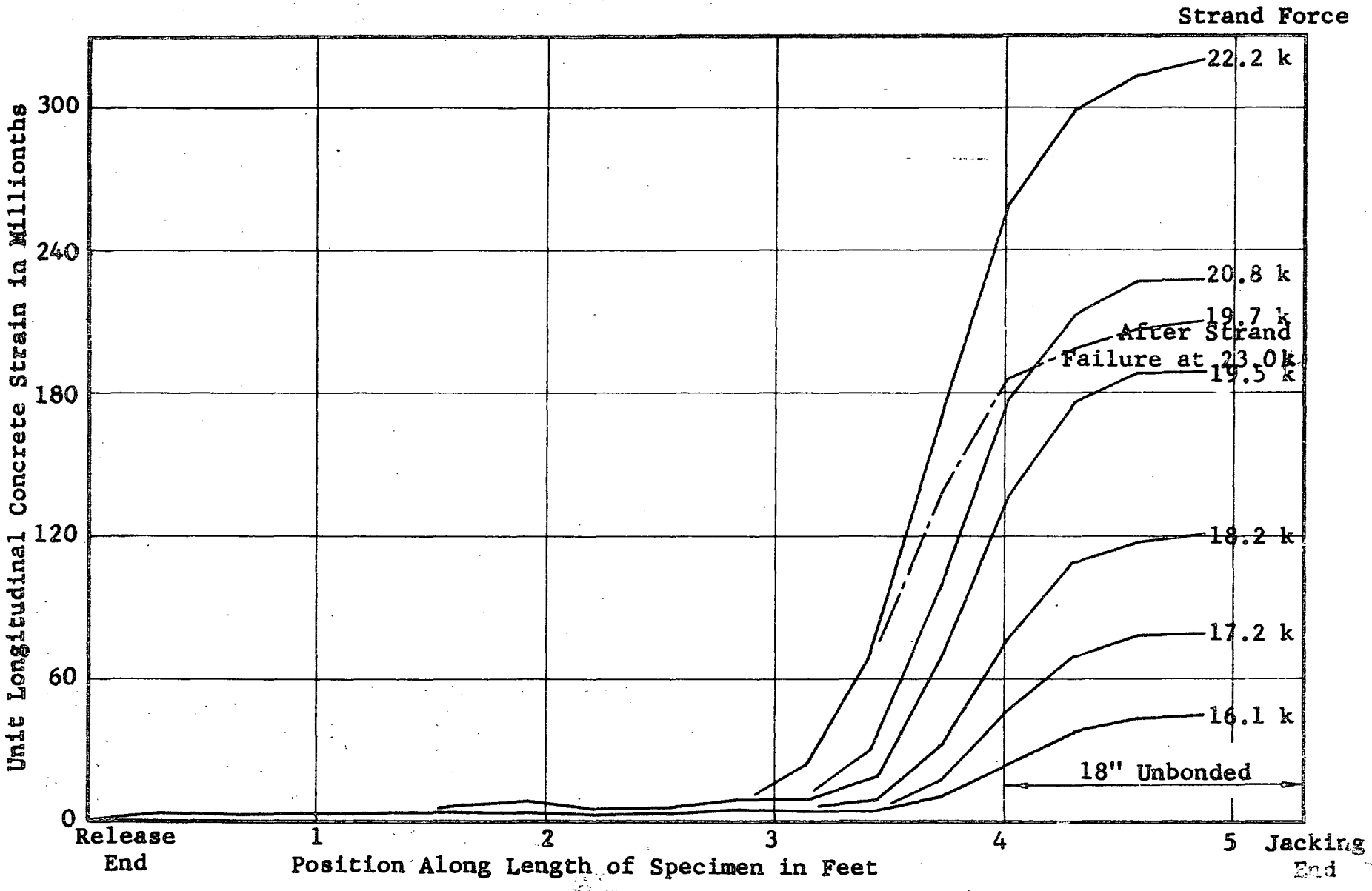

Figure B25 Development of Concrete Strain Over Length of Specimen IX-2 During Test

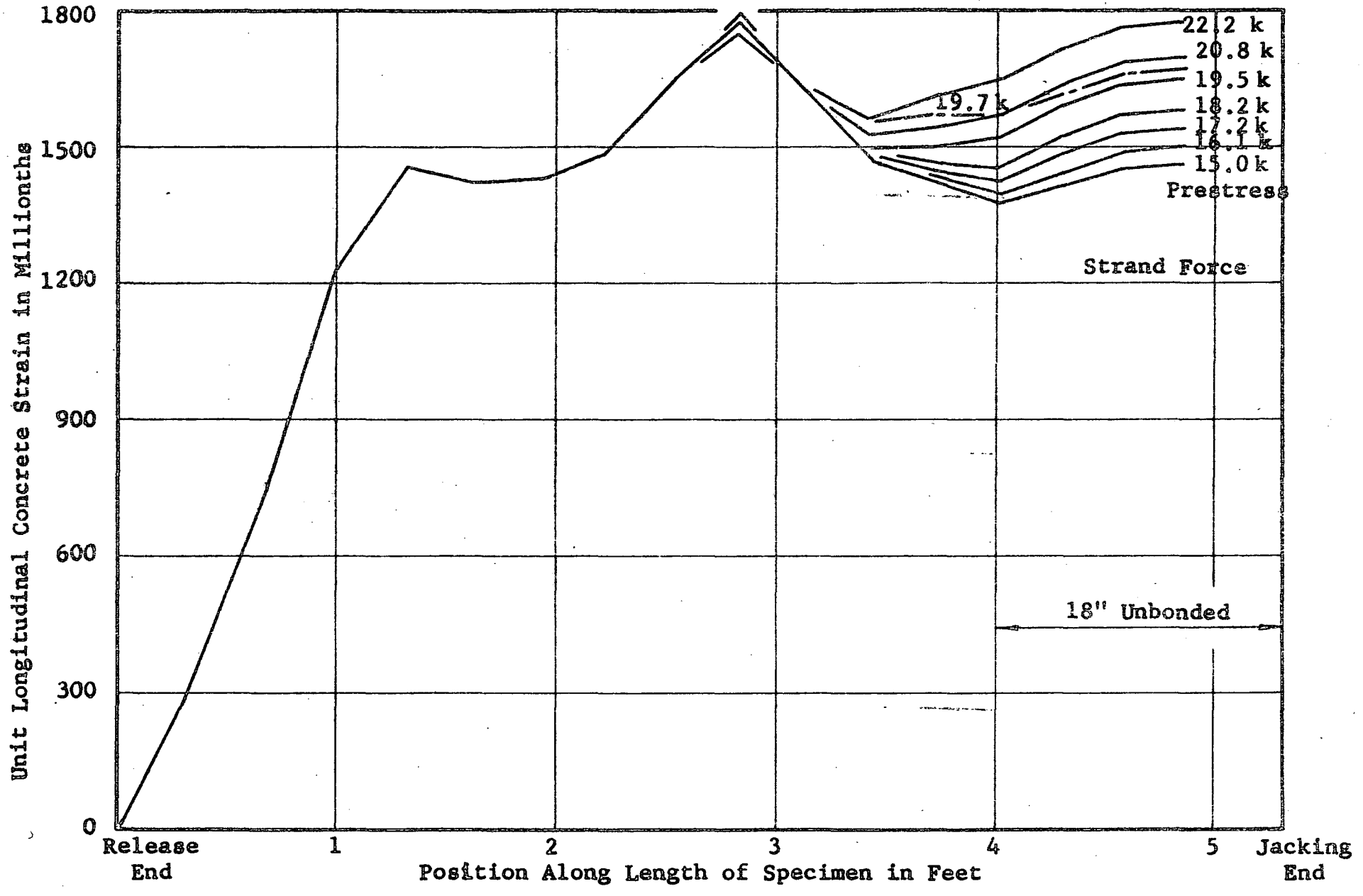

Figure B26 Development of Concrete Strain Over Length of Specimen IH-2 During Test

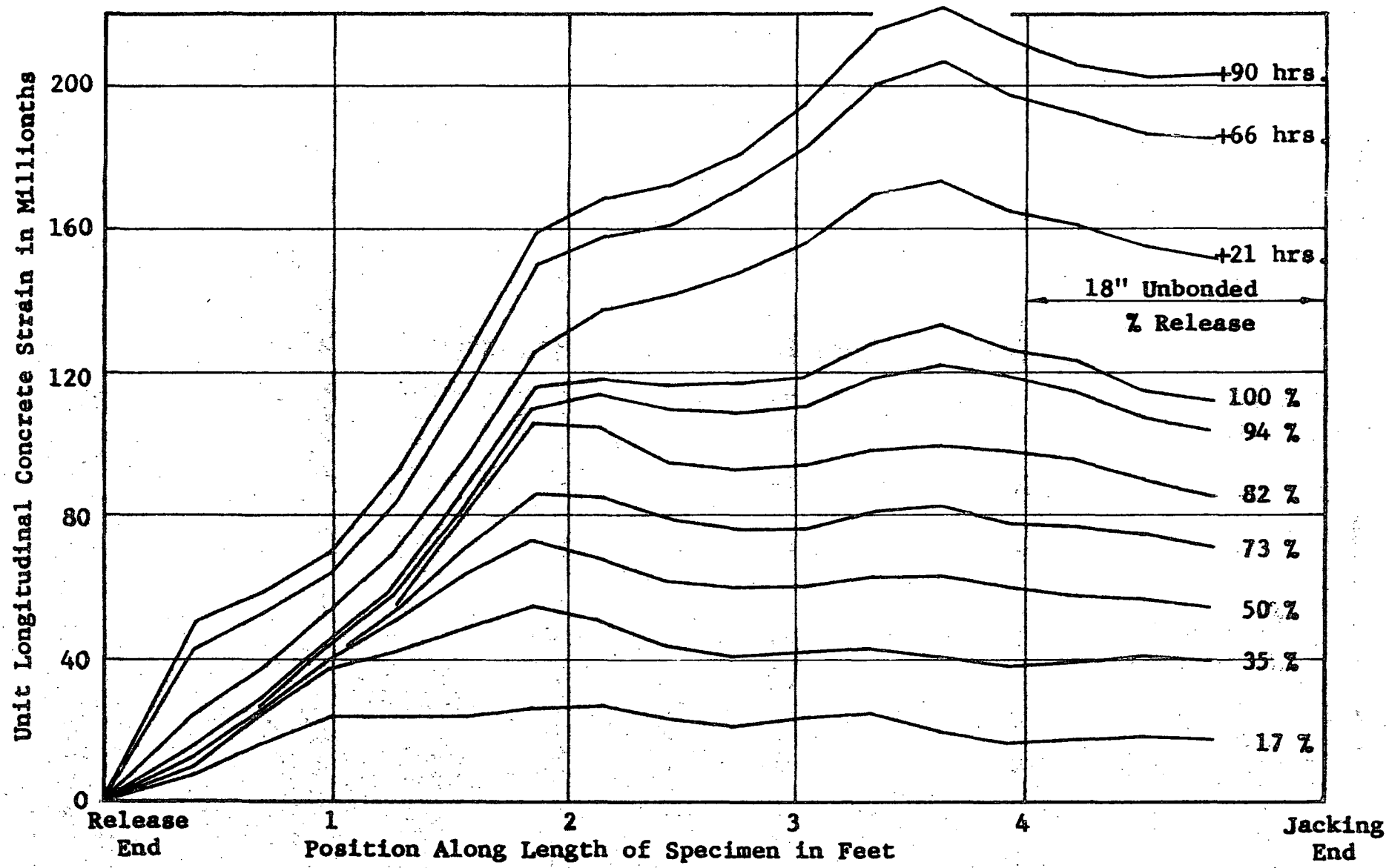

Figure B27. Development of Concrete Strain Over Length of Specimen IX-3 During Gradual Release

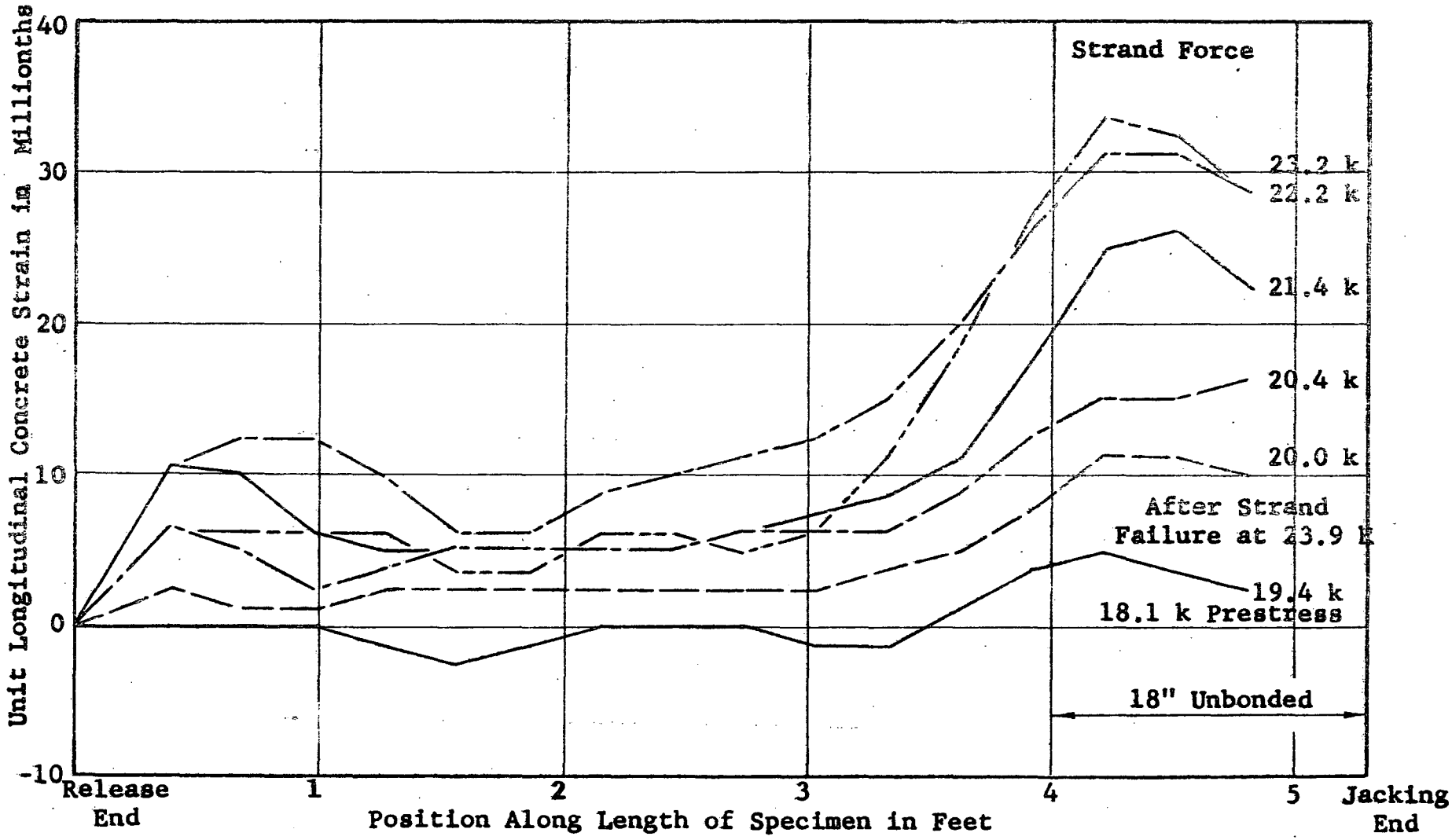

Figure B28 Development of Concrete Strain Over Length of Specimen IX-3 During Test

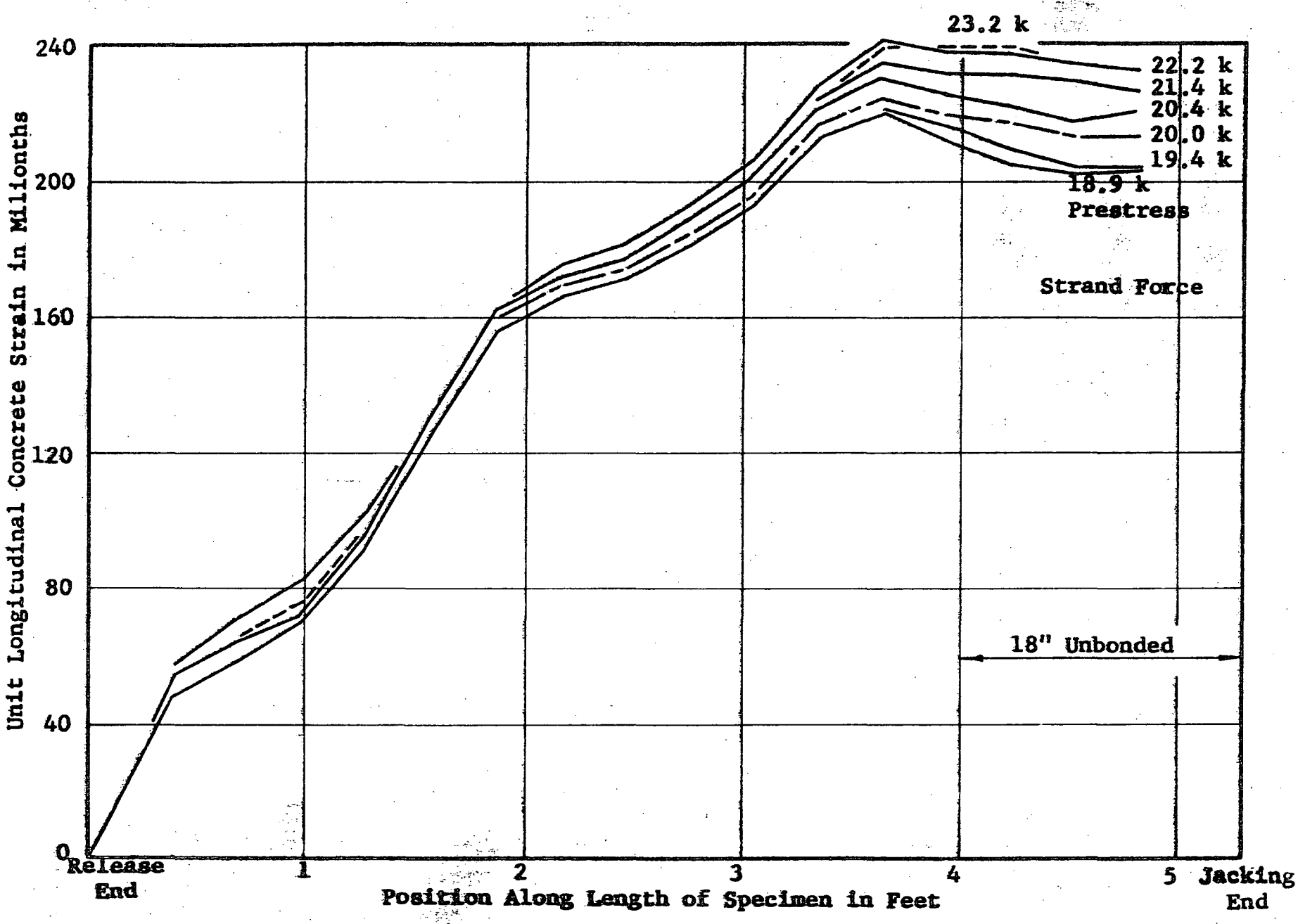

Figure B29 Development of Concrete Strain Over Length of Specimen IX-3 During Test

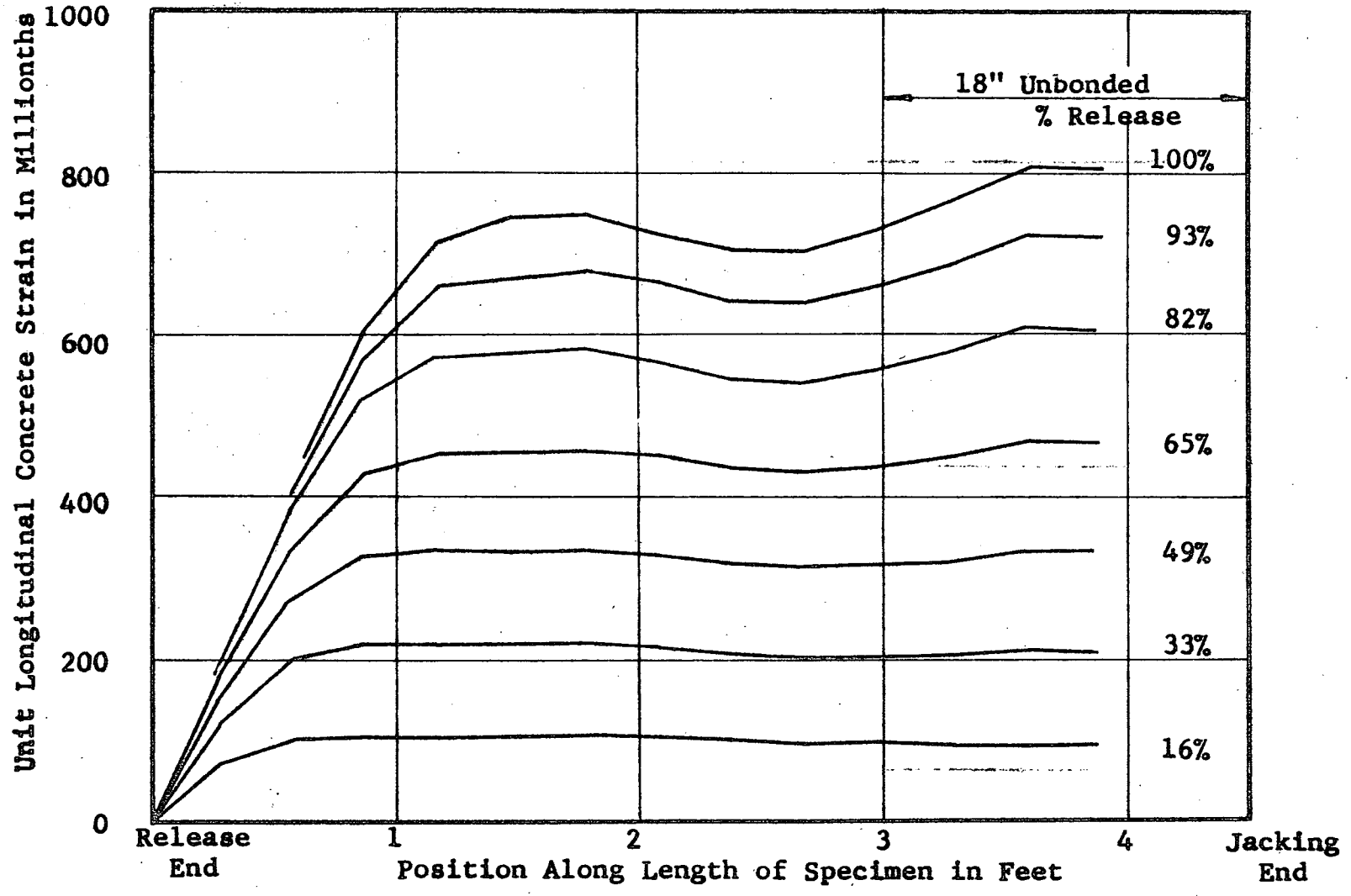

Figure B30 Development of Concrete Strain Over Length of Specimen X-1 During Gradual Release

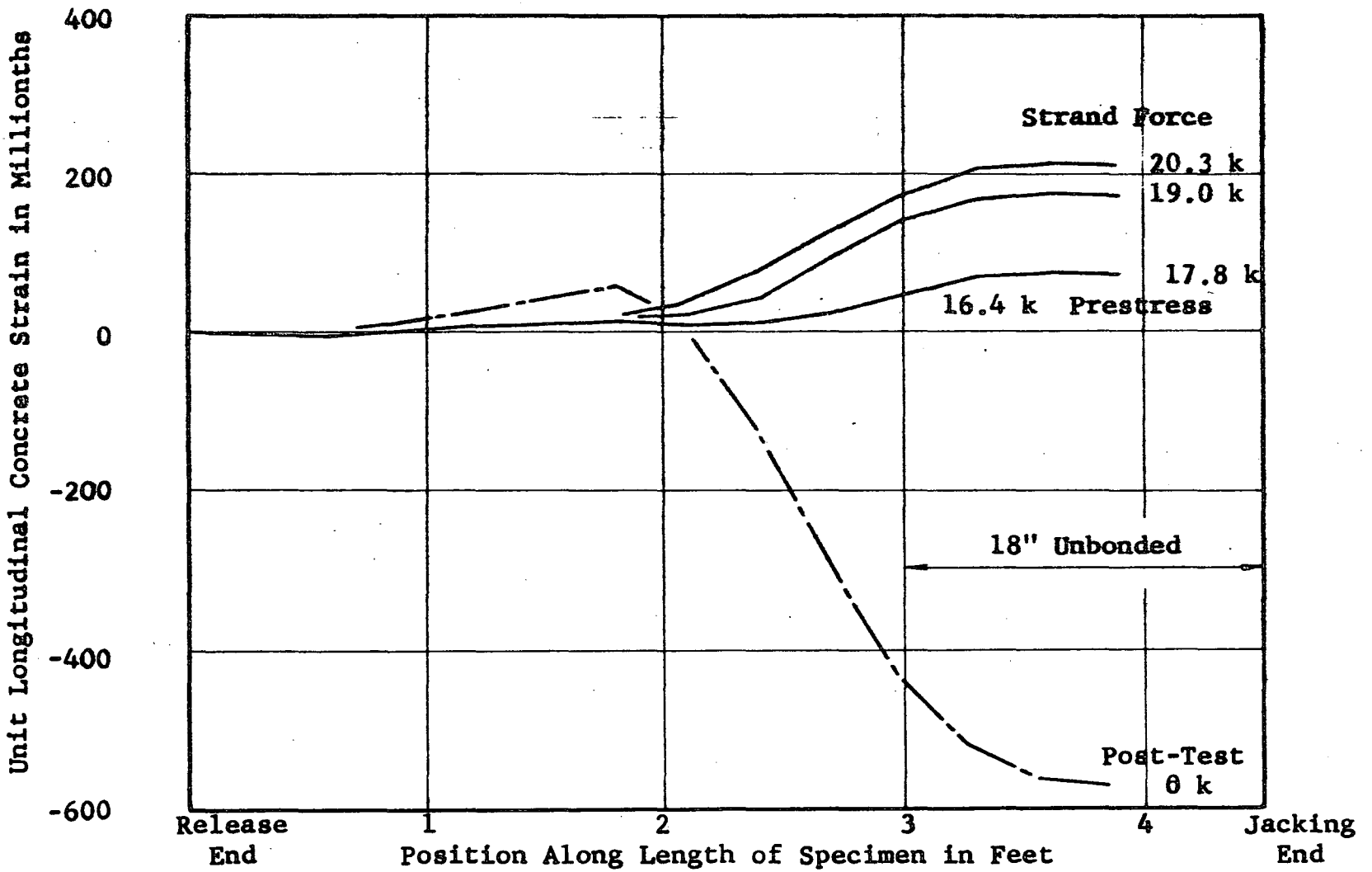

Figure B31 Development of Concrete Strain Over Length of Specimen X-1 During Test

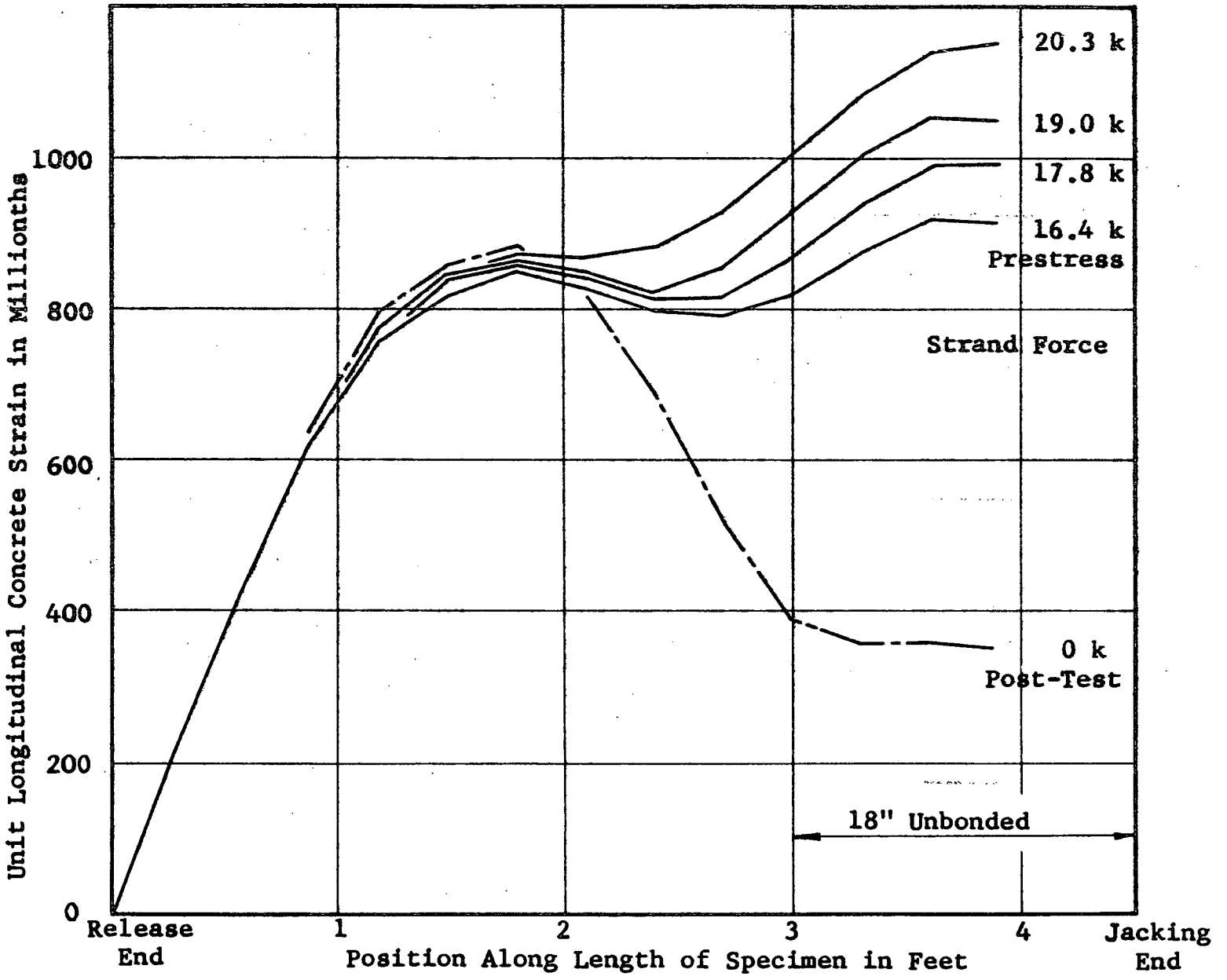

Figure B32. Development of Concrete Strain Over Length of Specimen X-1 During Test

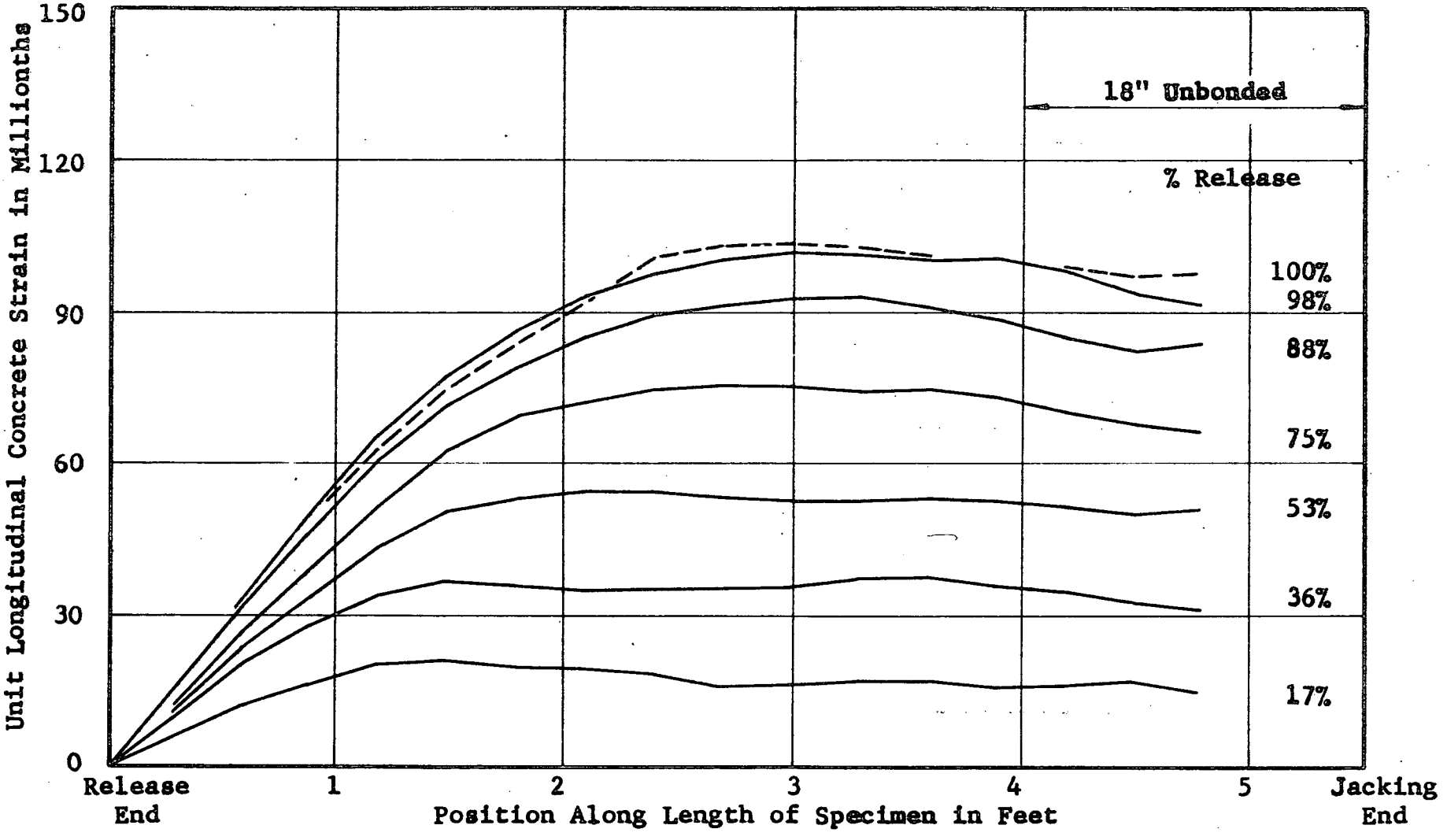

Figure B33. Development of Concrete Strain Over Length of Specimen X-2 During Gradual Release

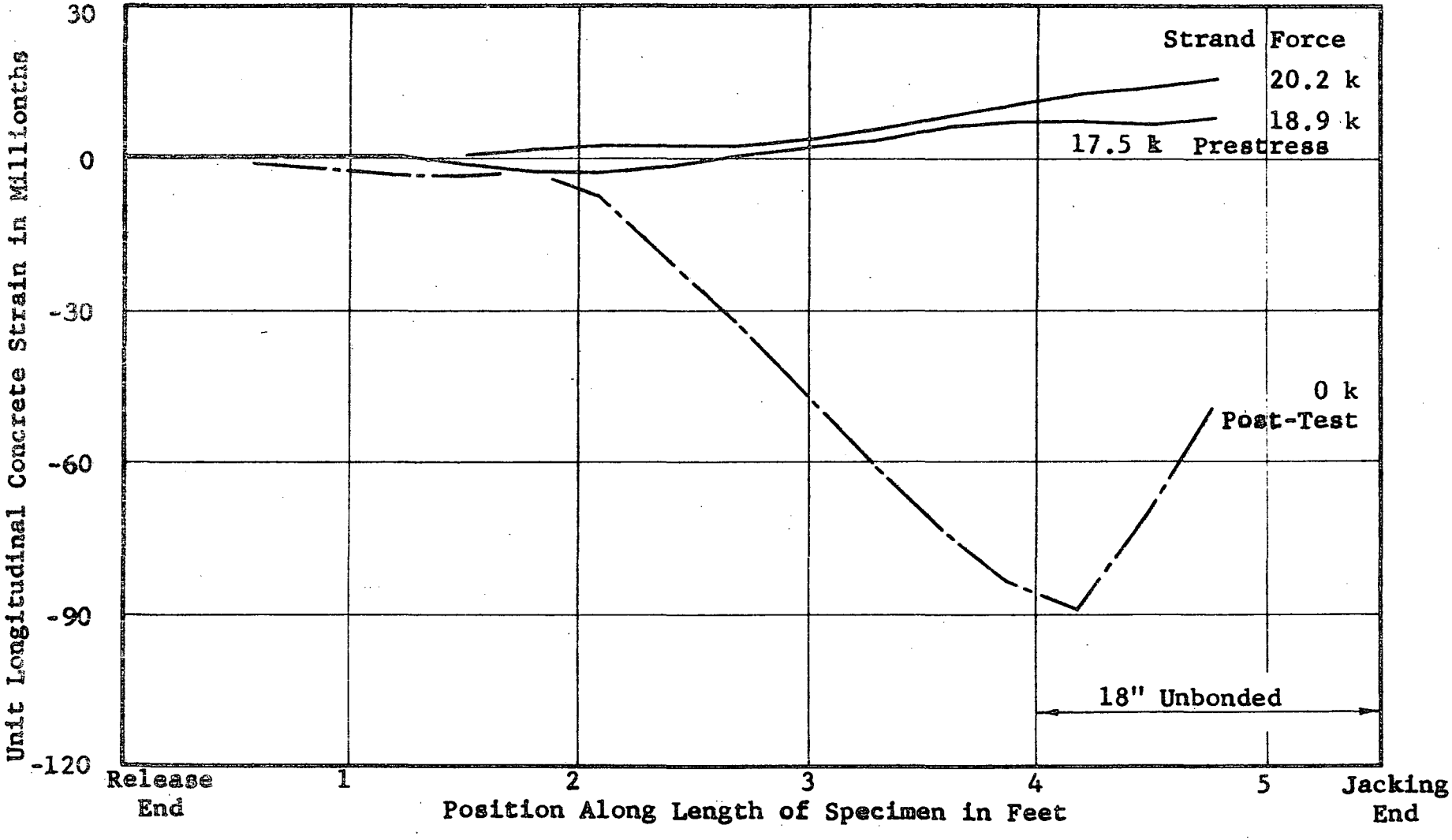

Figure B34 Development of Concrete Strain Over Length of Specimen X-2 During Test

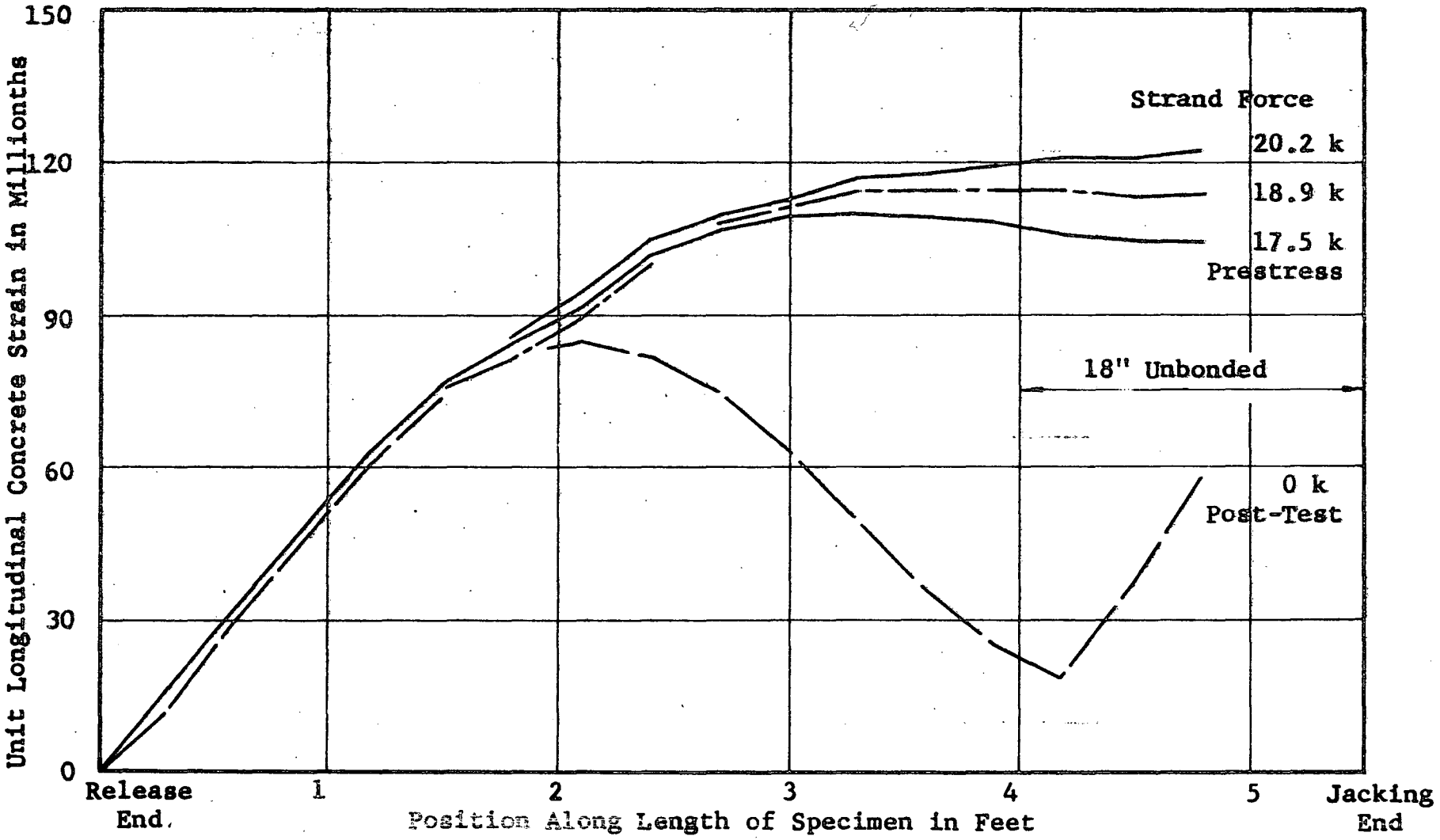

Figure B35. Development of Concrete Strain Over Length of Specimen X-2 During Test

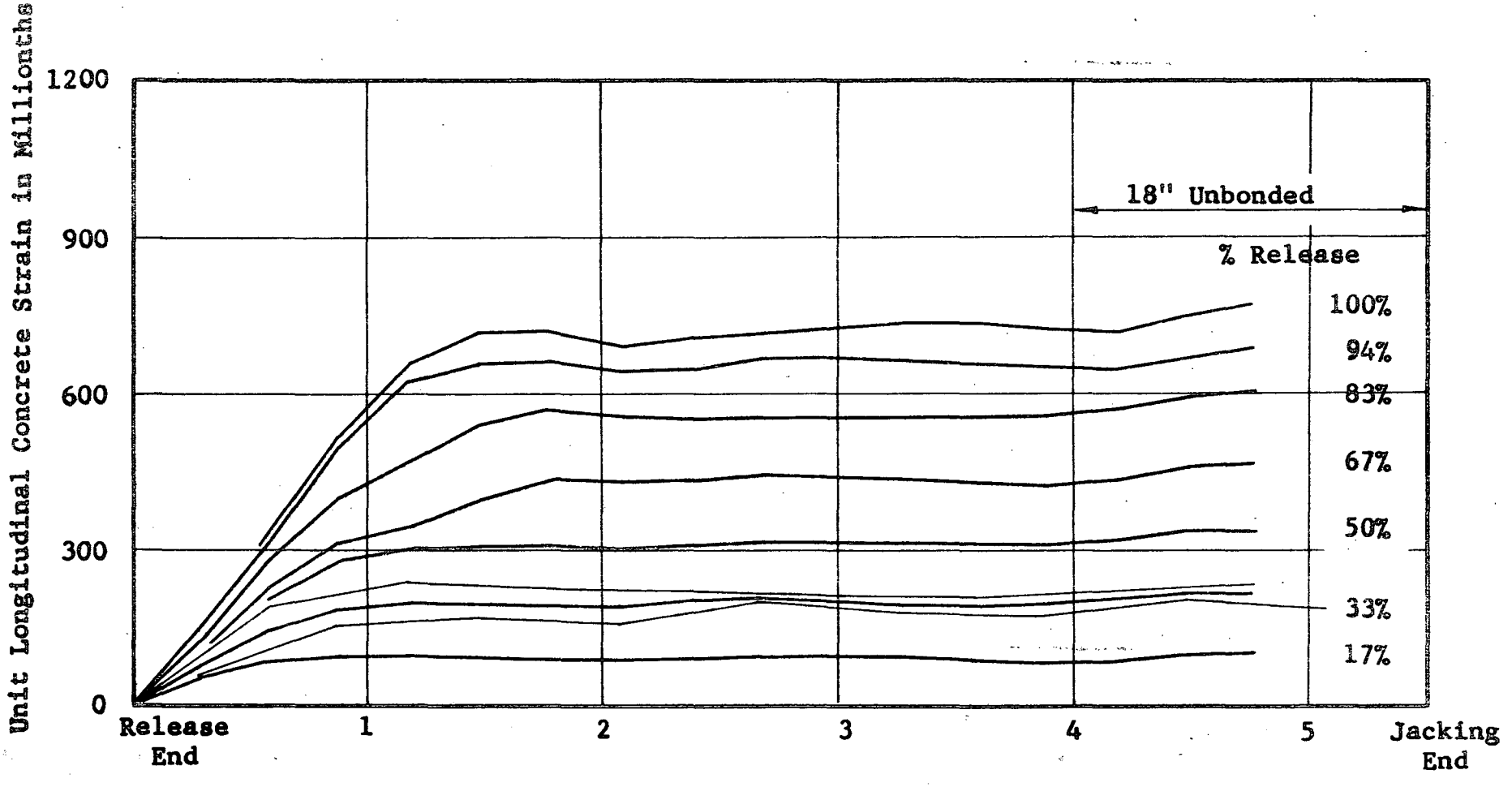

Figure B16 Development of Concrete Strain Over Length of Specimen X-3 During Gradual Release

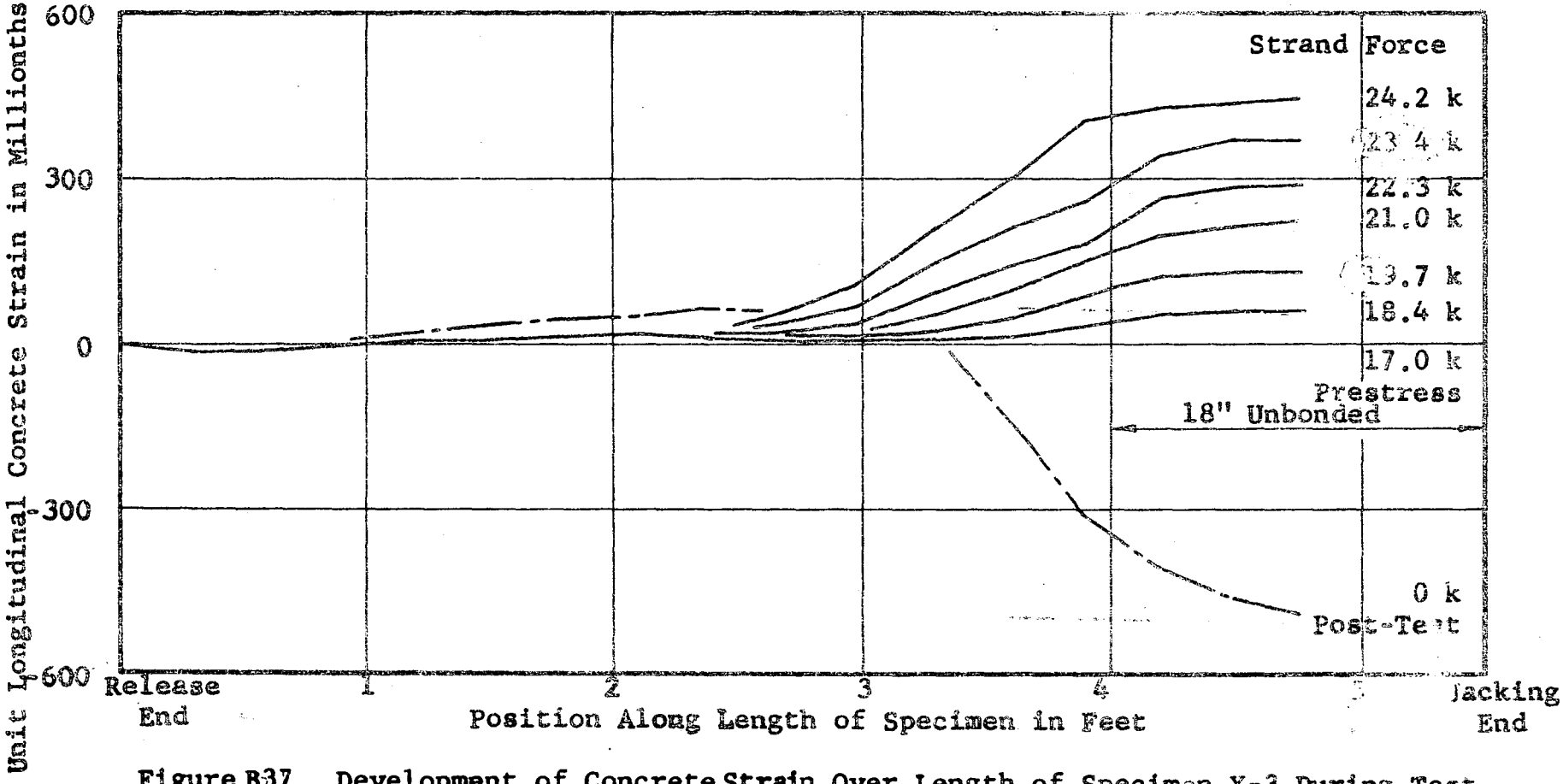

Figure B37. Development of Concrete Strain Over Length of Specimen X-3 During Test

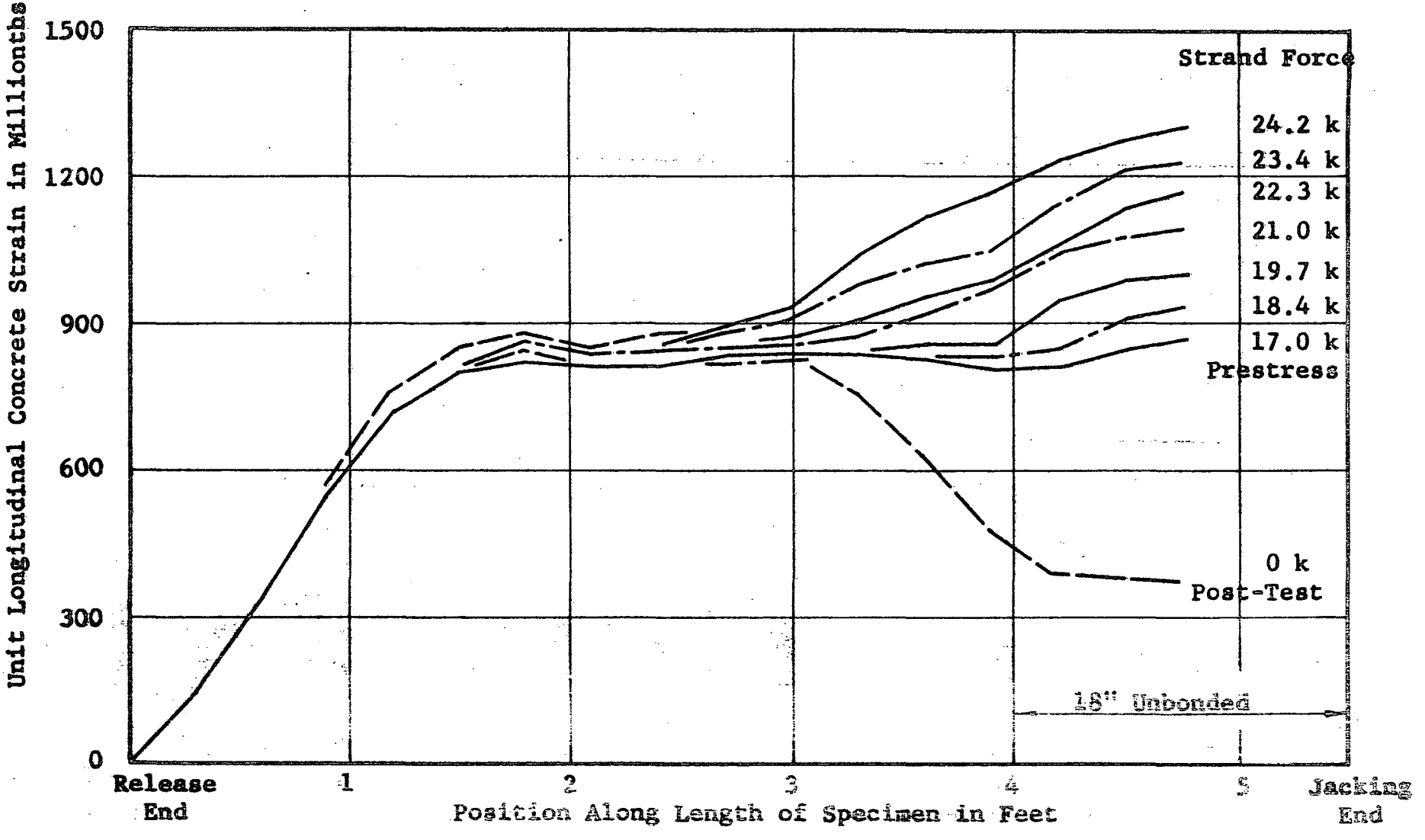

Figure B38 Development of Concrete Strain Over Length of Specimen X-3 During Test

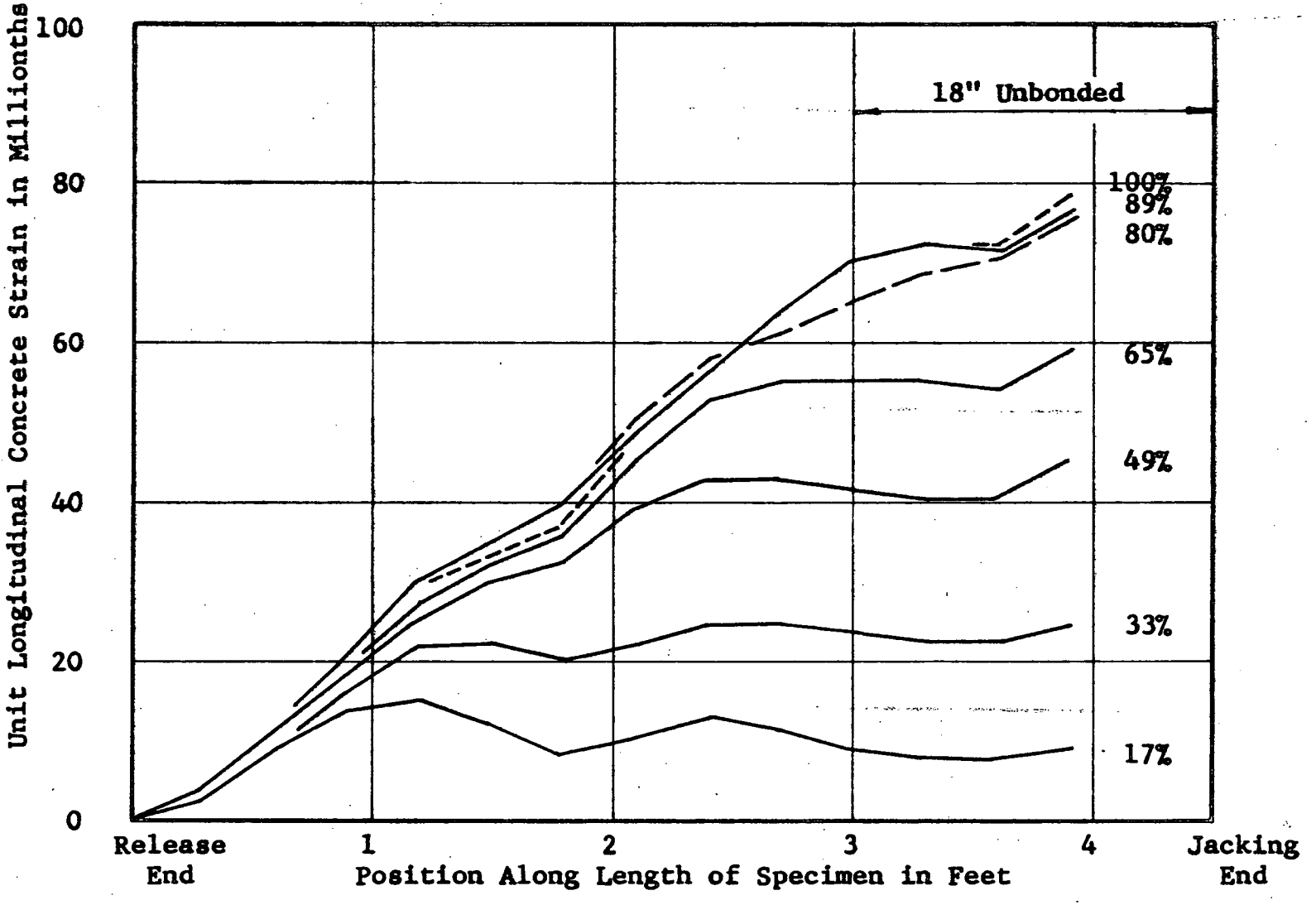

Figure B39 Development of Concrete Strain Over Length of Specimen X-4 During Gradual Release

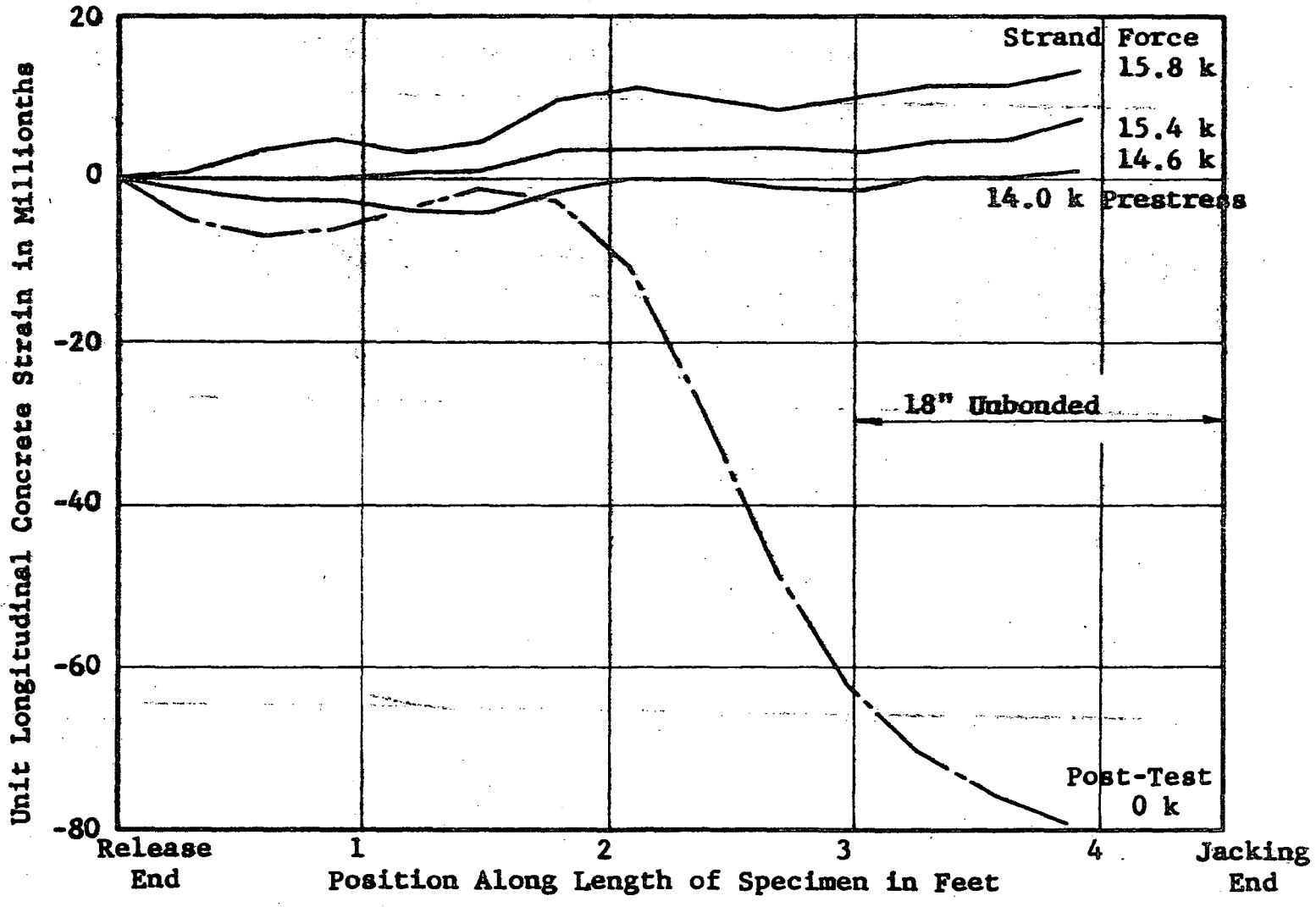

Figure 40 Development of Concrete Strain Over Length of Specimen X-4 During Test

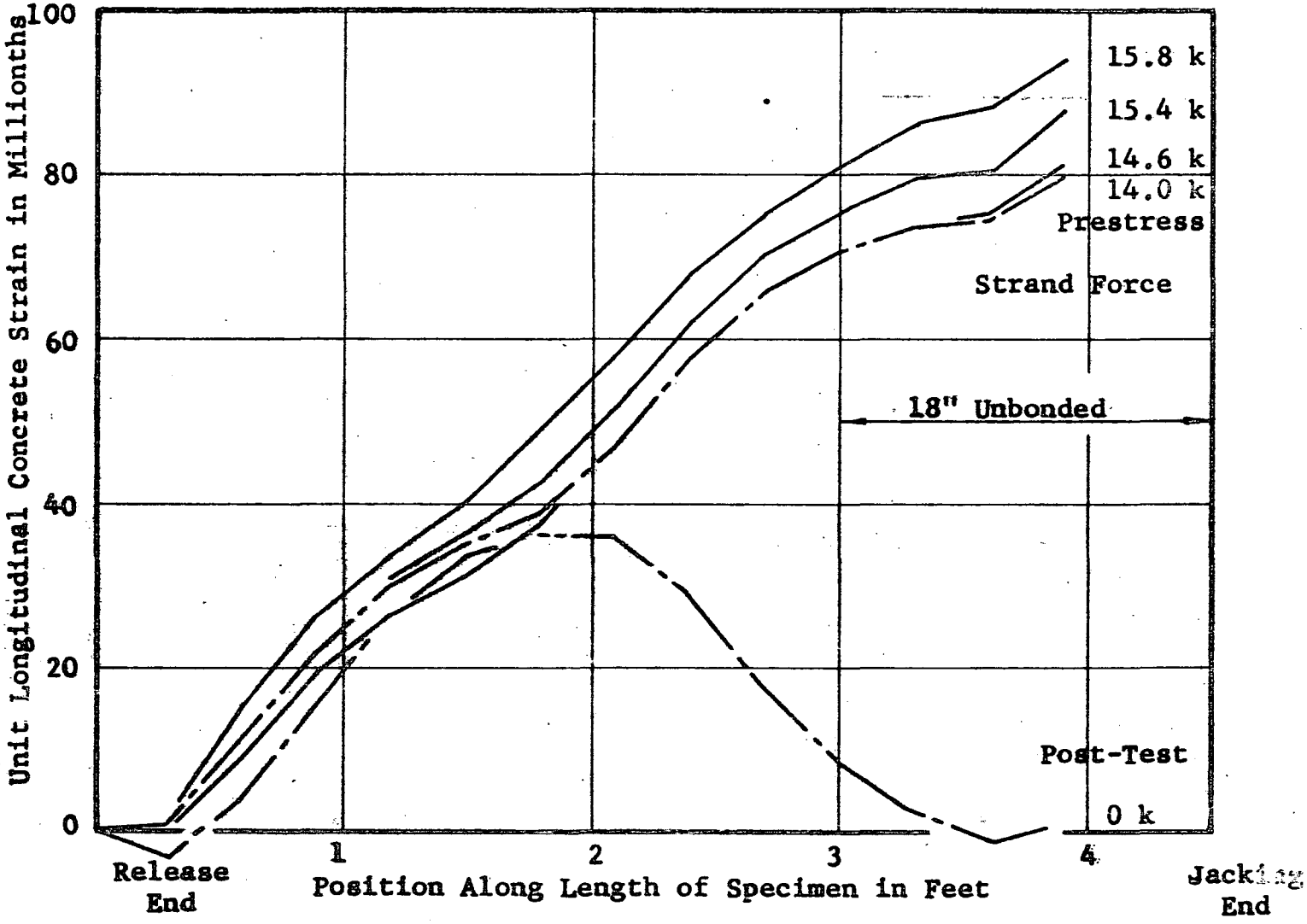

Figure B41. Development of Concrete Strain Over Length of Specimen X-4 During Test

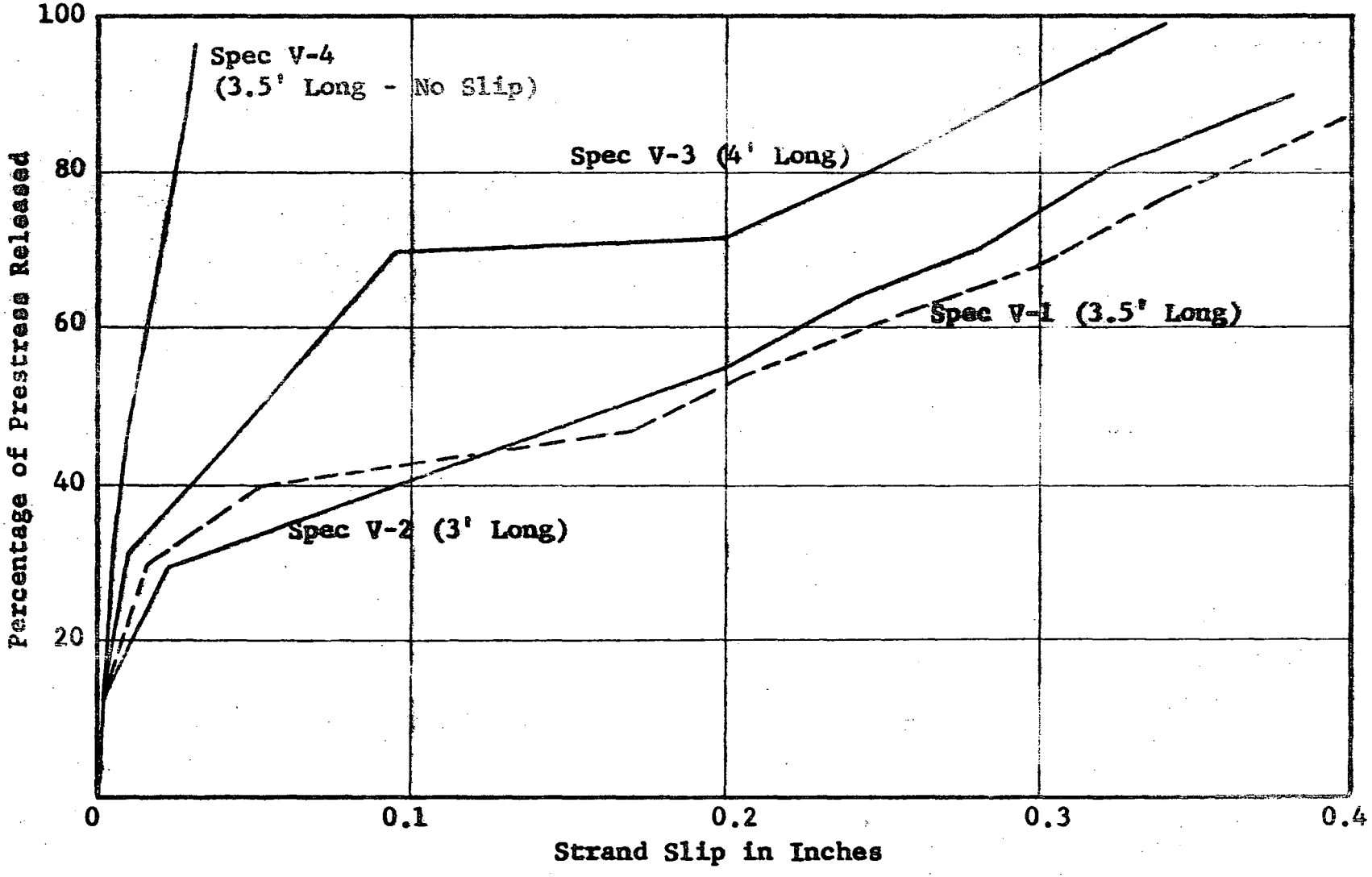

Figure 42 Strand Slip vs Prestress Released for Series V Specimens Failing During Gradual Release

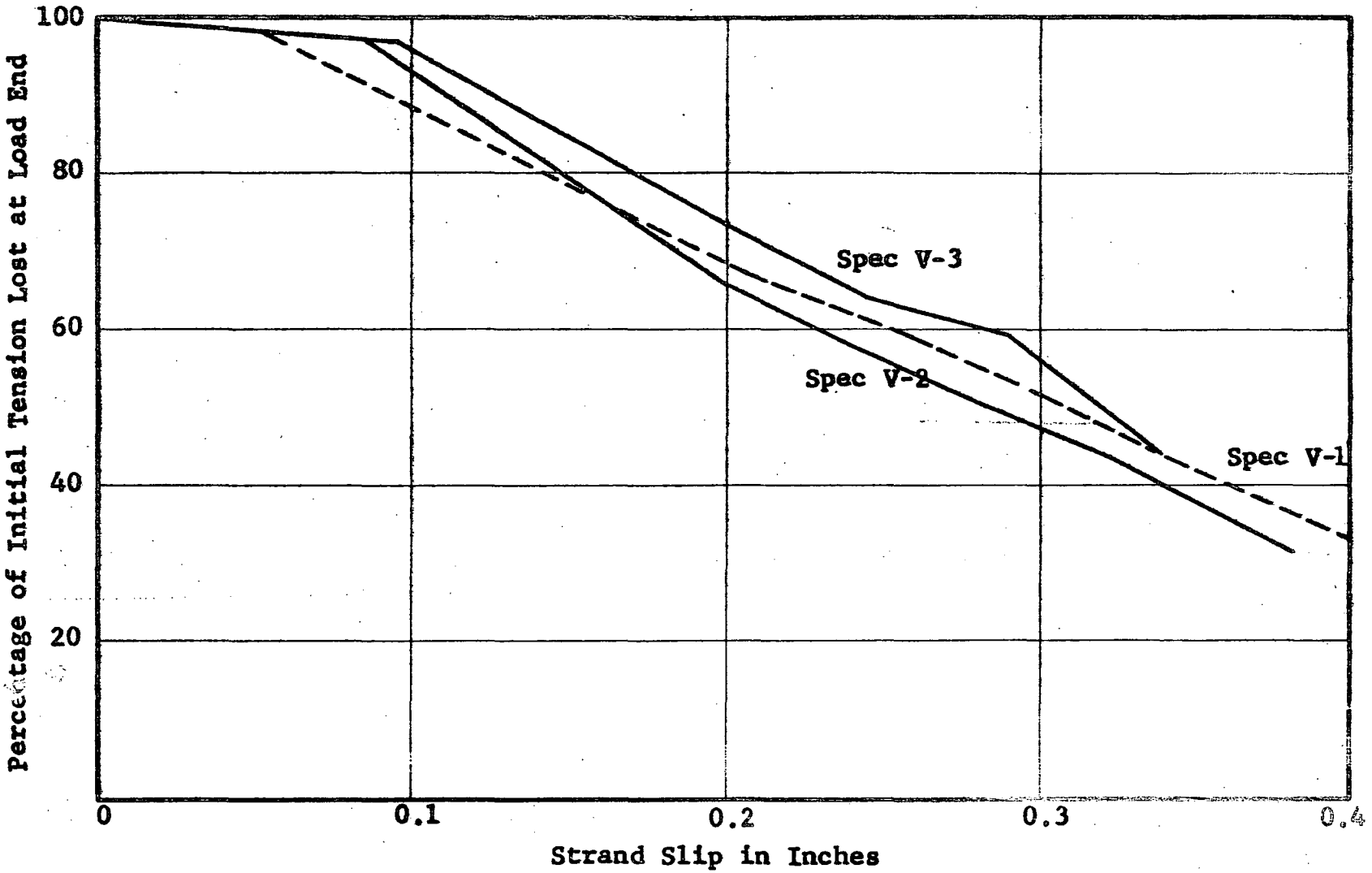

Figure B48 Strand Slip vs Prestress Lost To Strand Slip During Release of Series V Specimens

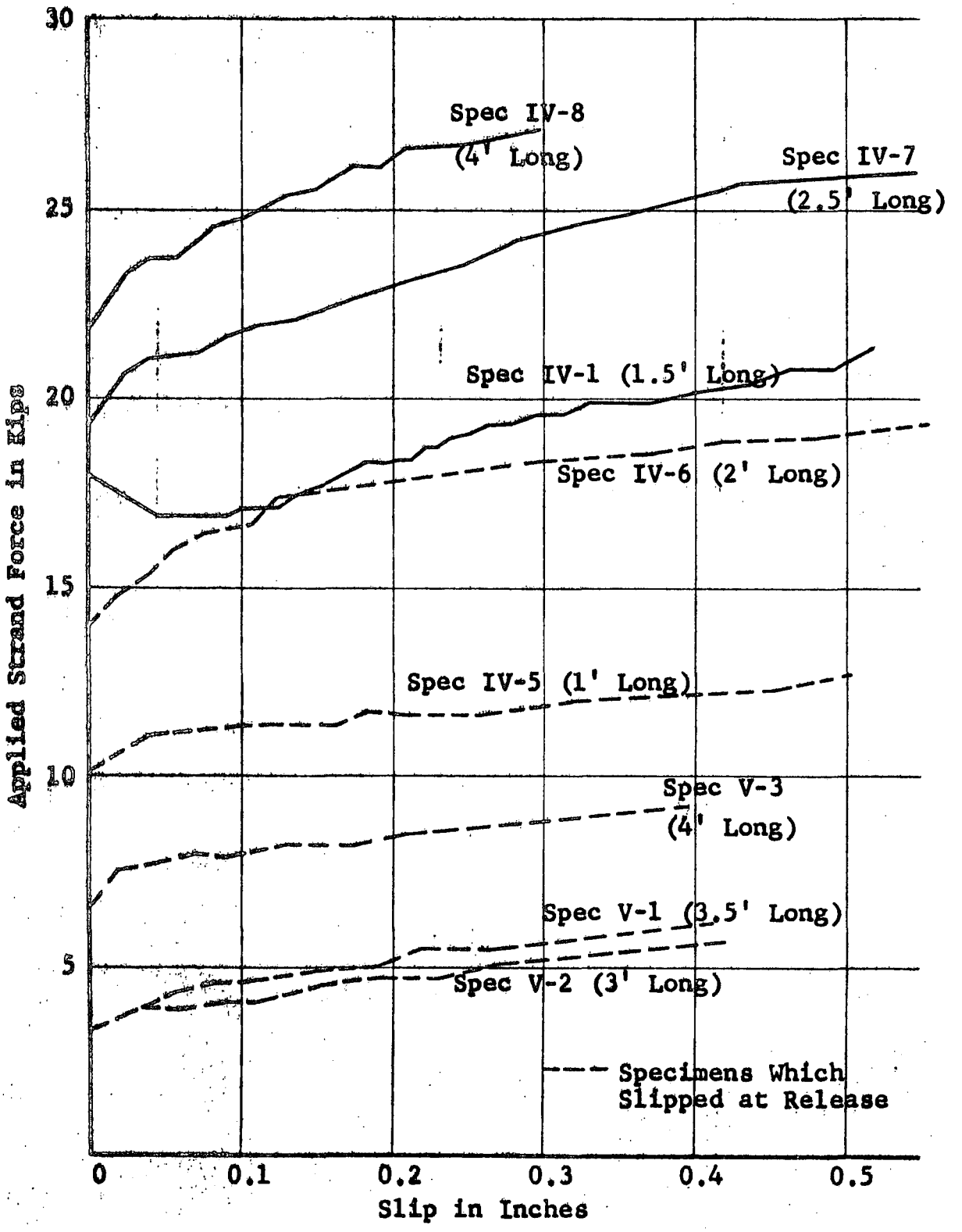

Figure B44 Slip of Specimens of Series IV and V Under Applied Load

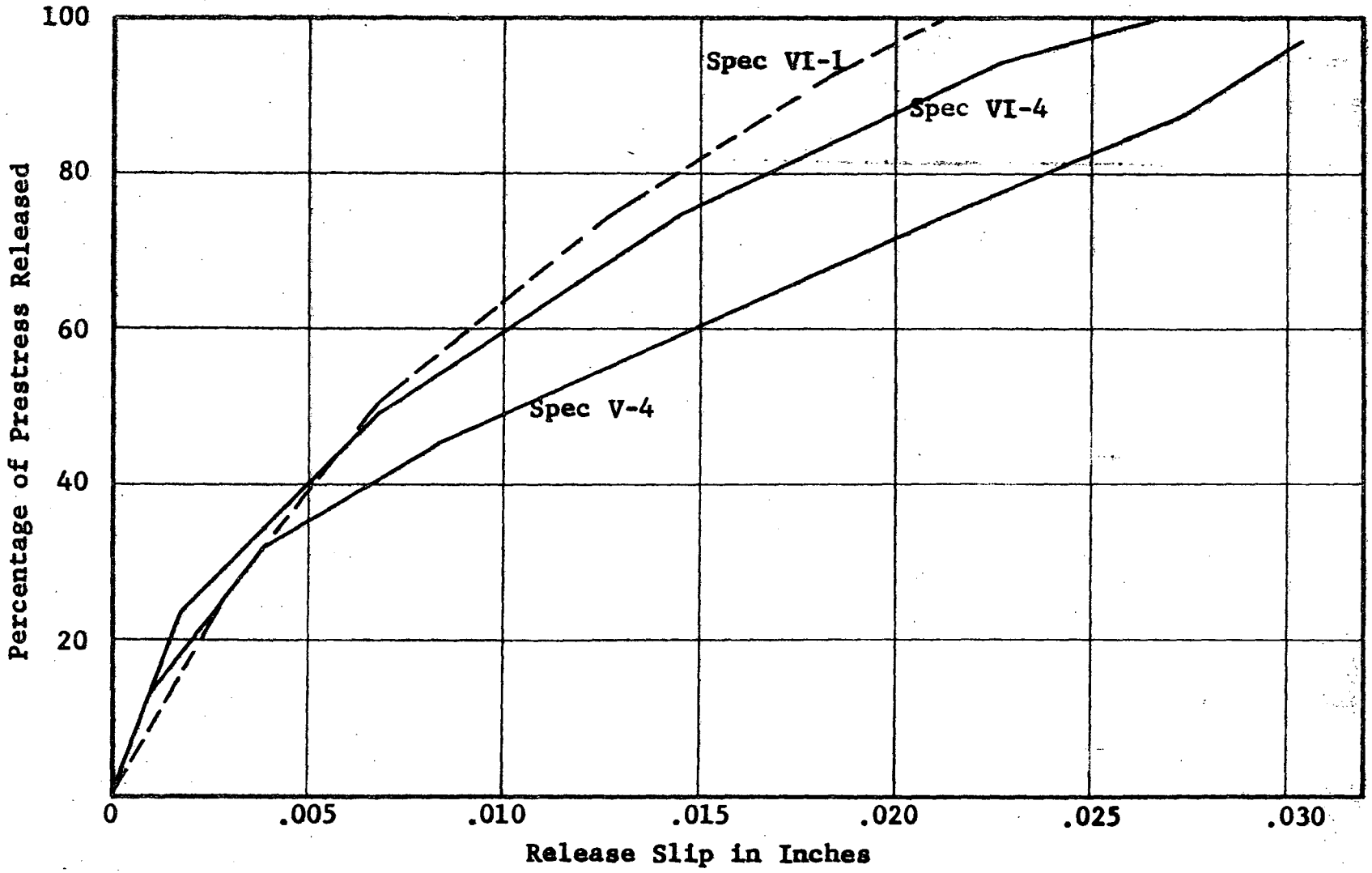

Figure B45 Progression of Release Slip During Gradual Release

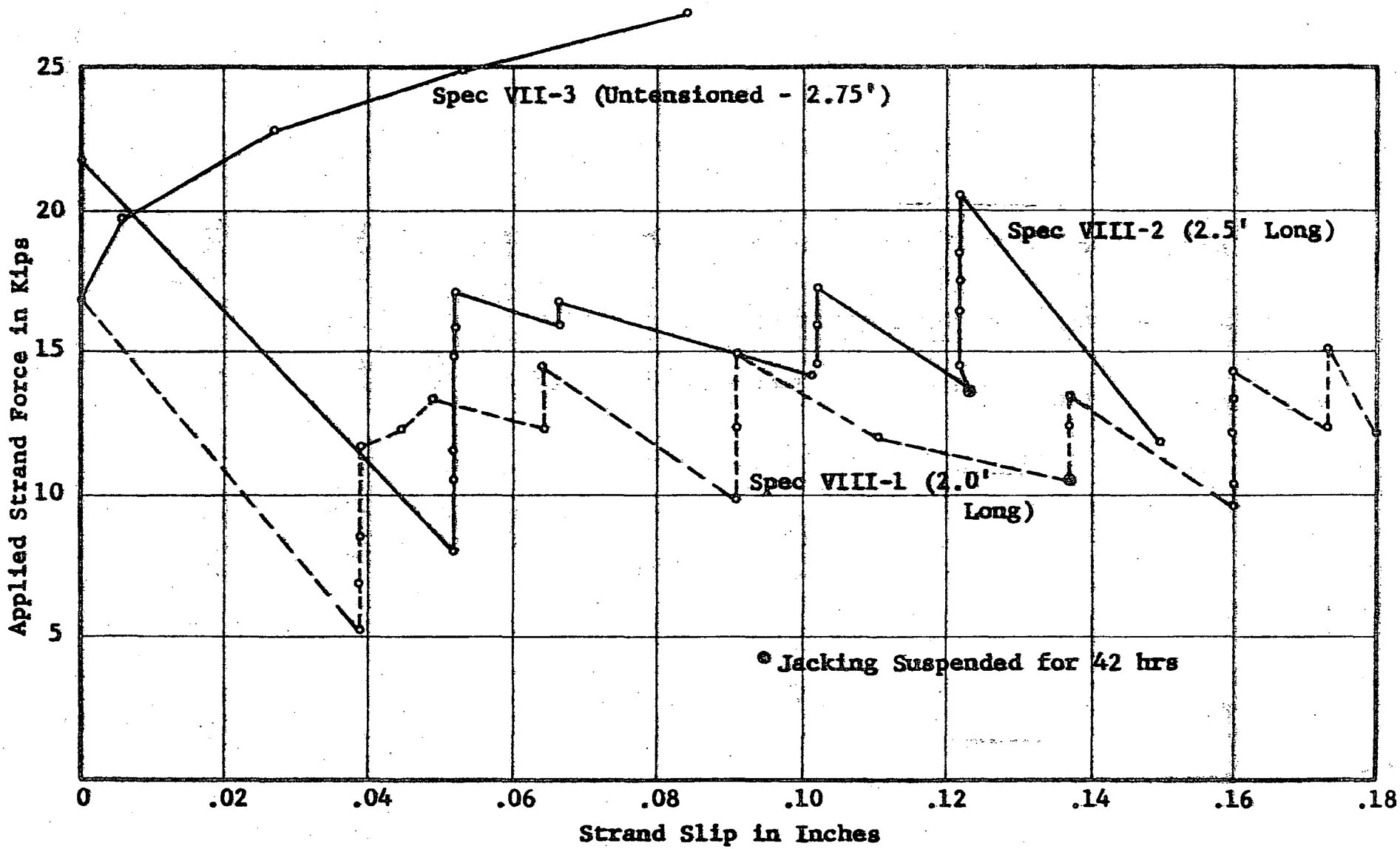

Figure B46 Slip of Specimens VII-3, VIII-1 and VIII-2 Under Applied Load

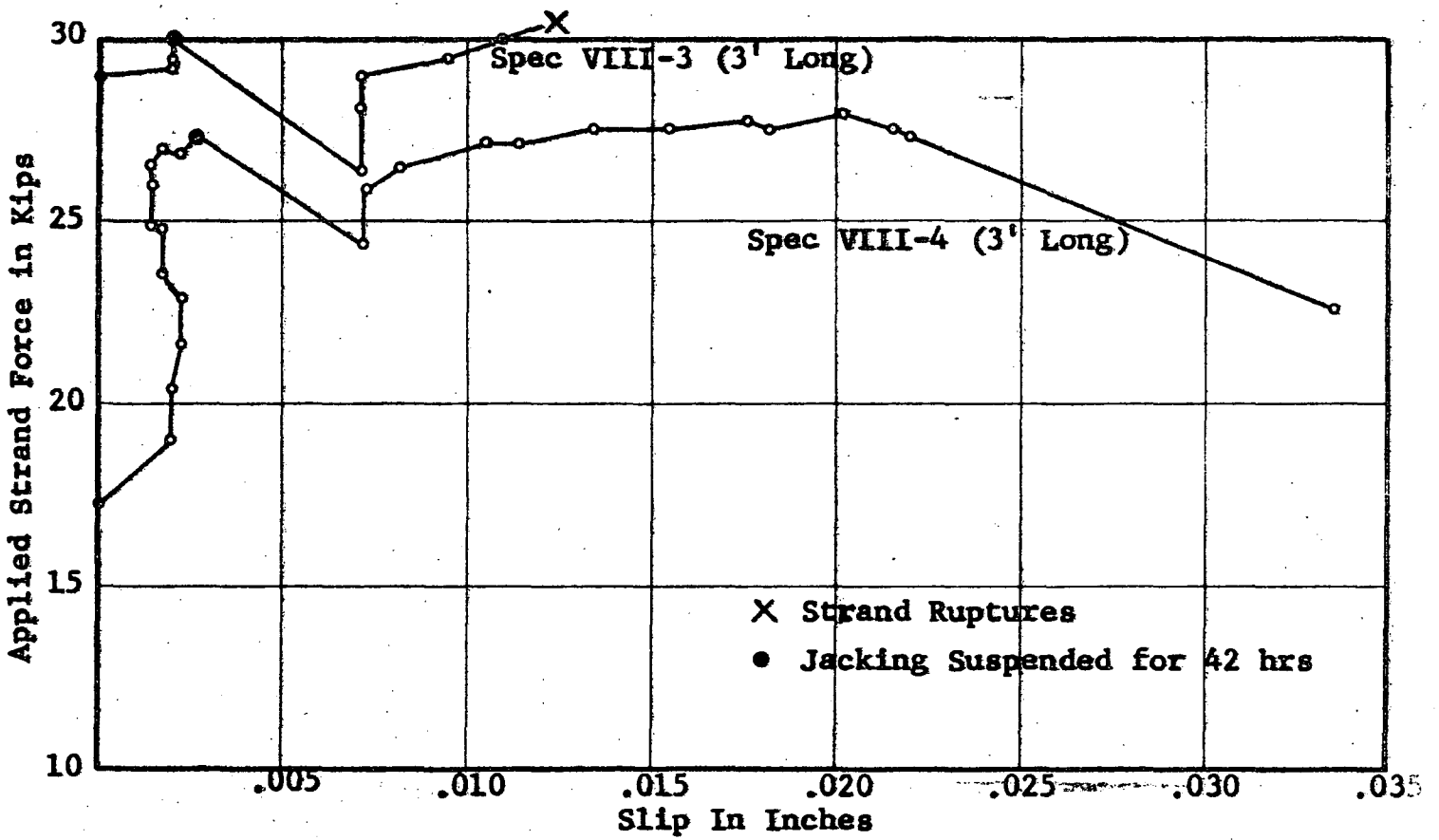

Figure B47 Slip of Specimens VIII-3 and VIII-4 While Under Sustained High Load

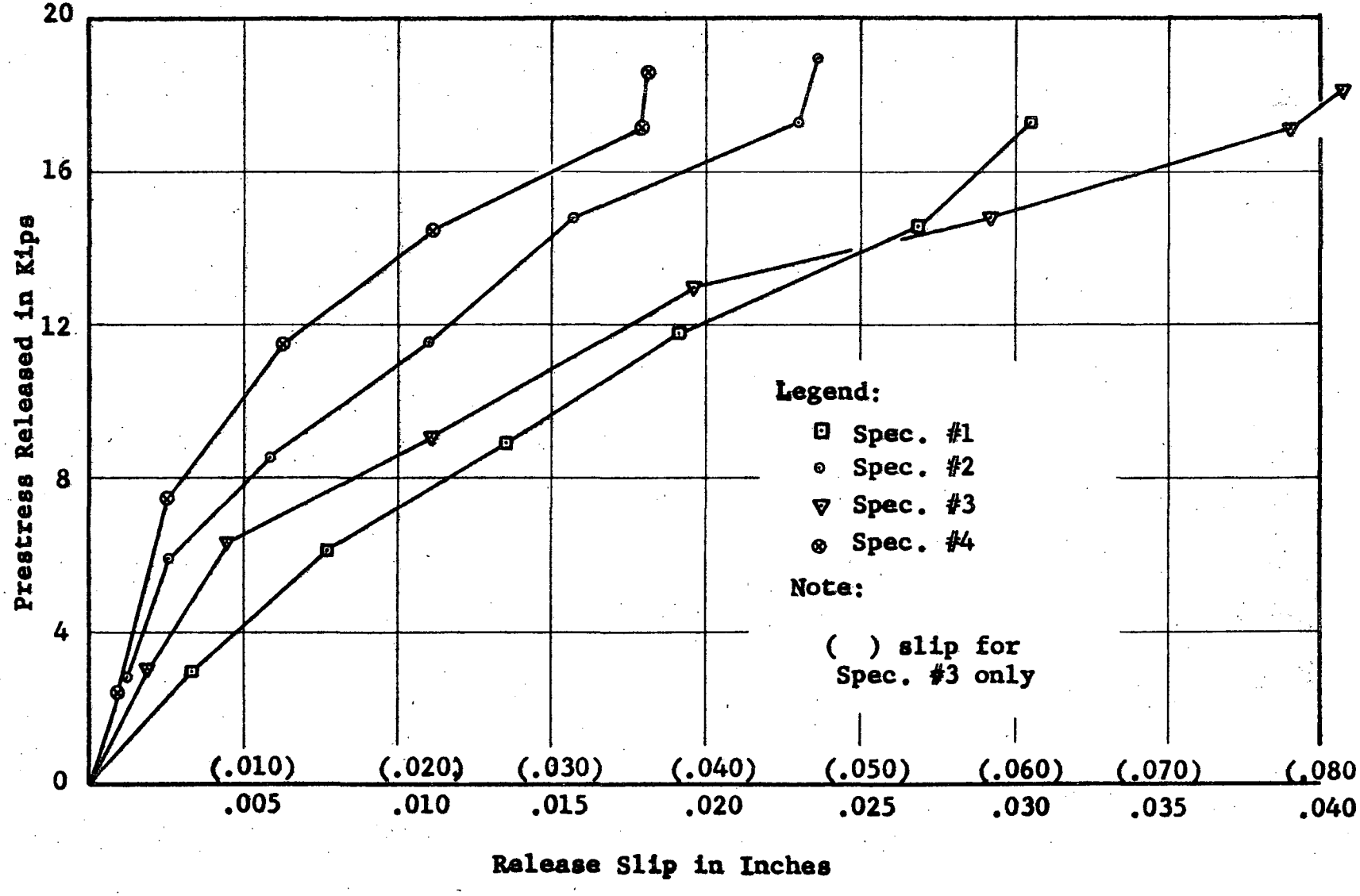

Figure B48 Progression of Release Slip During Gradual Release, Series IX

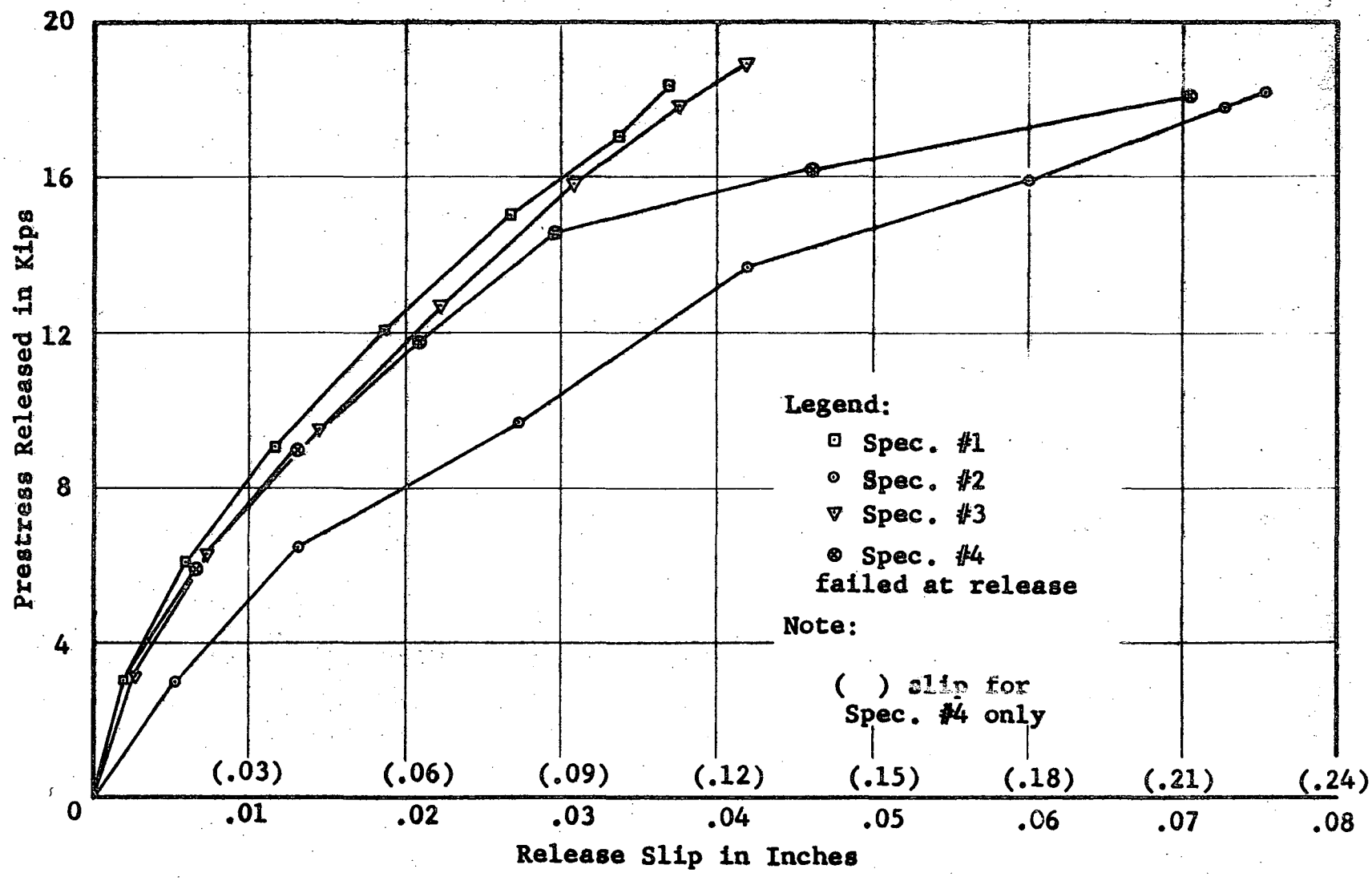

Figure B49. Progression of Release Slip During Gradual Release, Series X

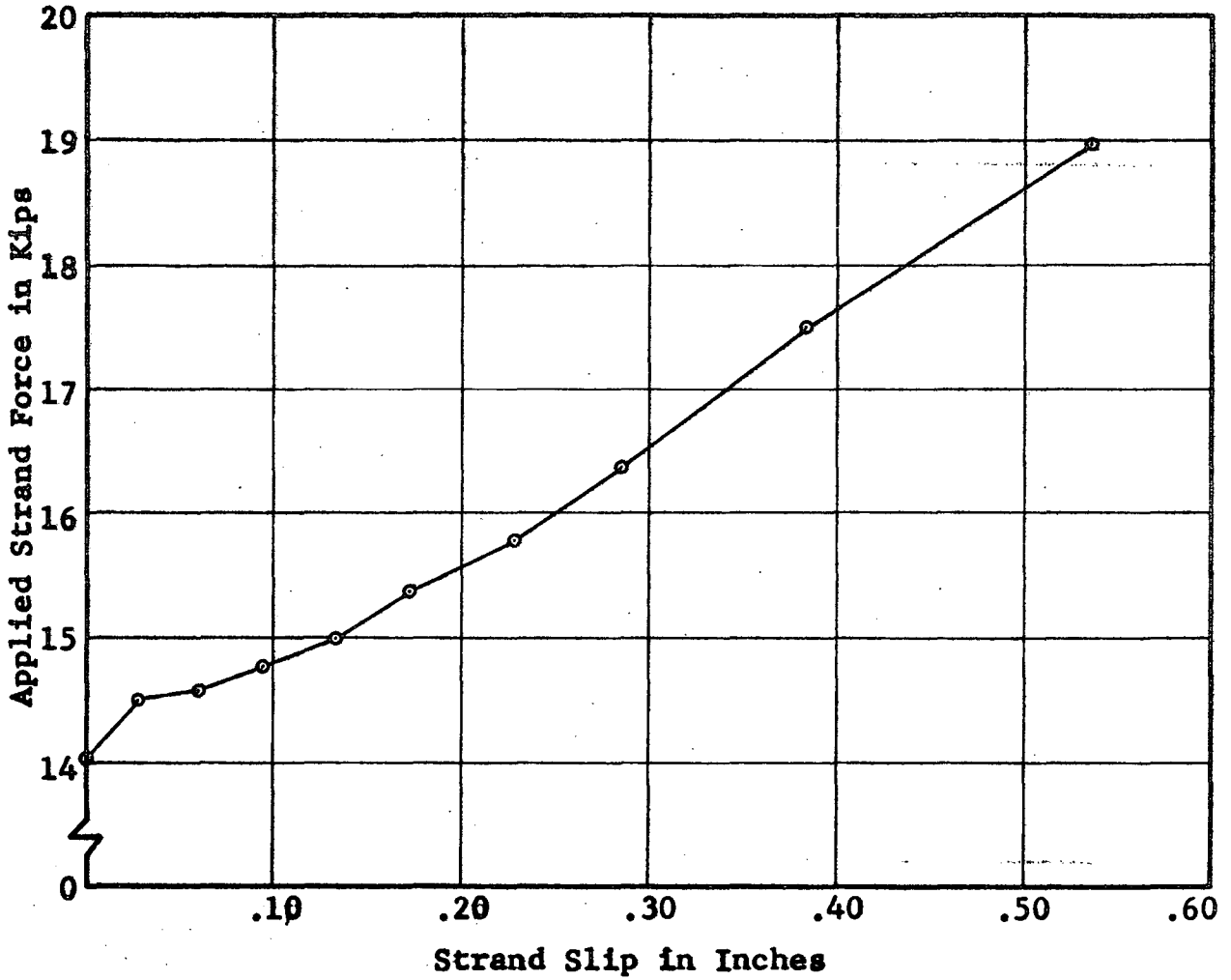

Figure 50 Slip of Specimen X-4 Under Applied Load

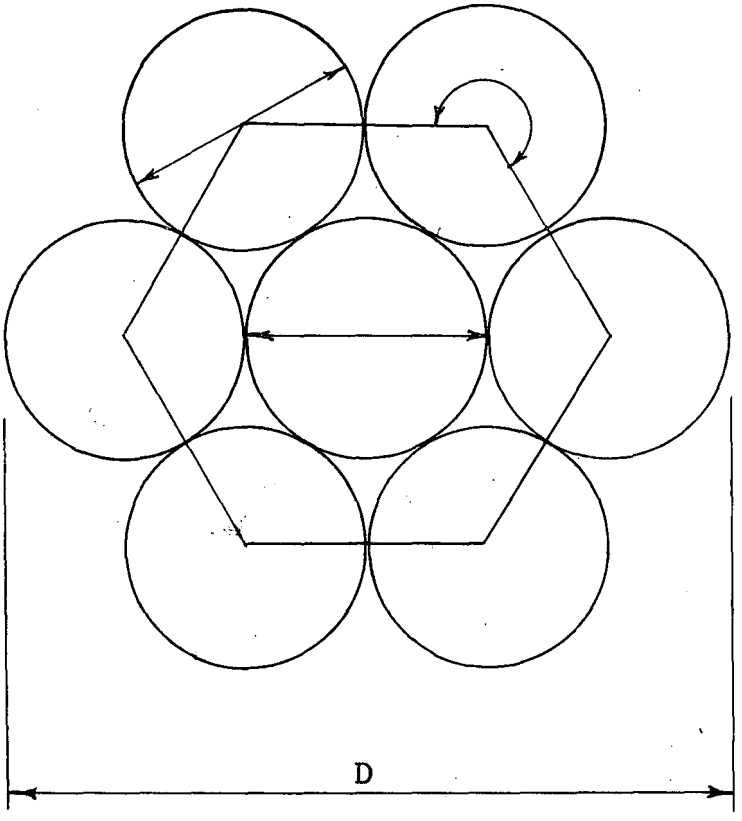

d_1 = 0.140 inches

d_2 = 0.145 inches

Nominal D = 0.4375 inches

Actual D = $2d_1 + d_2$ = 0.425 inches

$\Sigma_o = \frac{240°}{260°}$ 6 di = 4 d_1 = 1.76 inches

Figure B51. Physical Properties of 7/16 Inch Seven Wire Strand

APPENDIX C

FIGURES RELATING TO RELEASE OF BEAM TEST SPECIMENS

BY MONTEMAYOR

APPENDIX C

FIGURES RELATING TO RELEASE OF BEAM TEST SPECIMENS

BY MONTEMAYOR

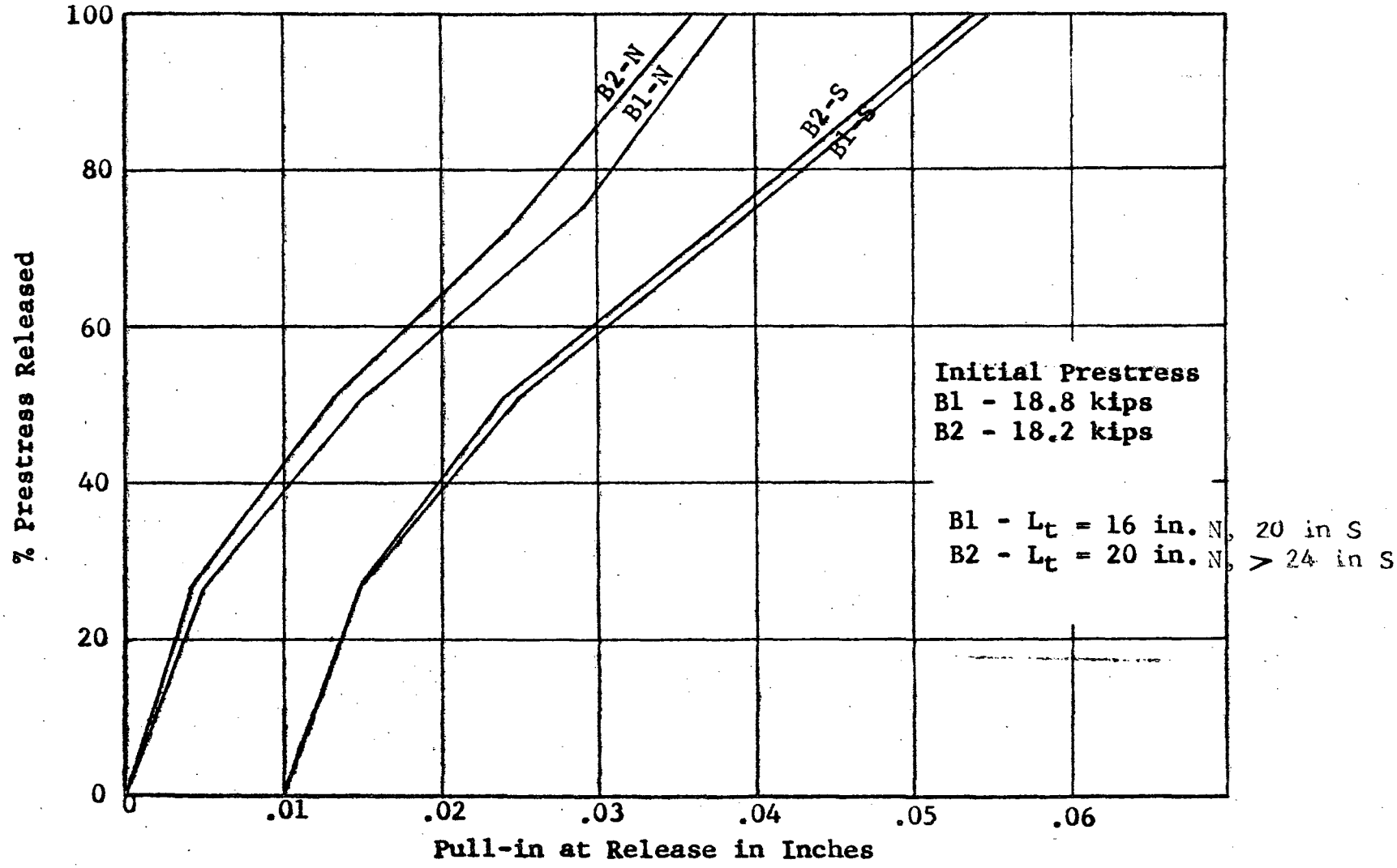

Figure 1. Progression of Slip During Release of Beams B1 and B2.

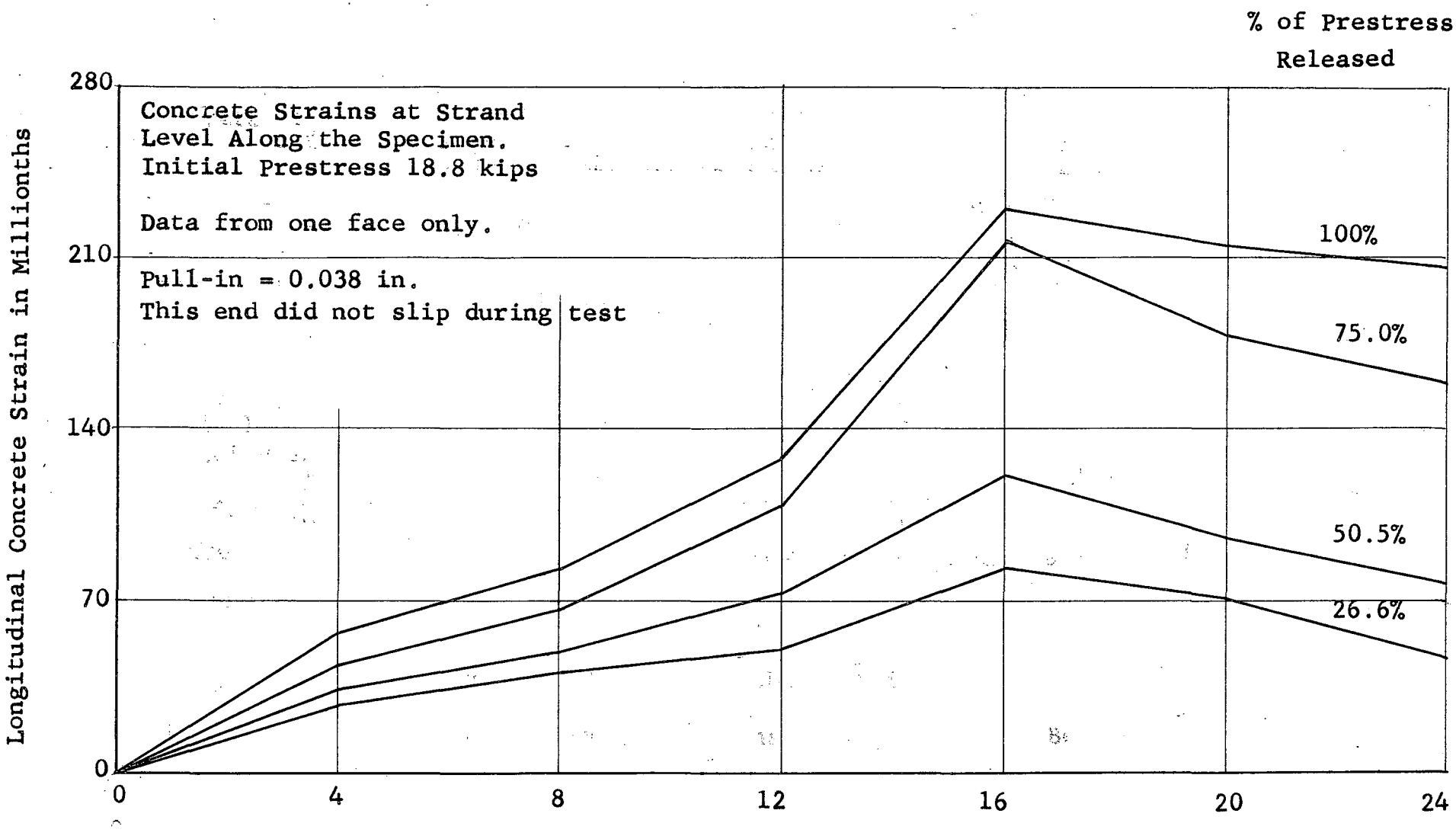

Figure C2. Development of Concrete Strains During Release. Beam B1 N-End.

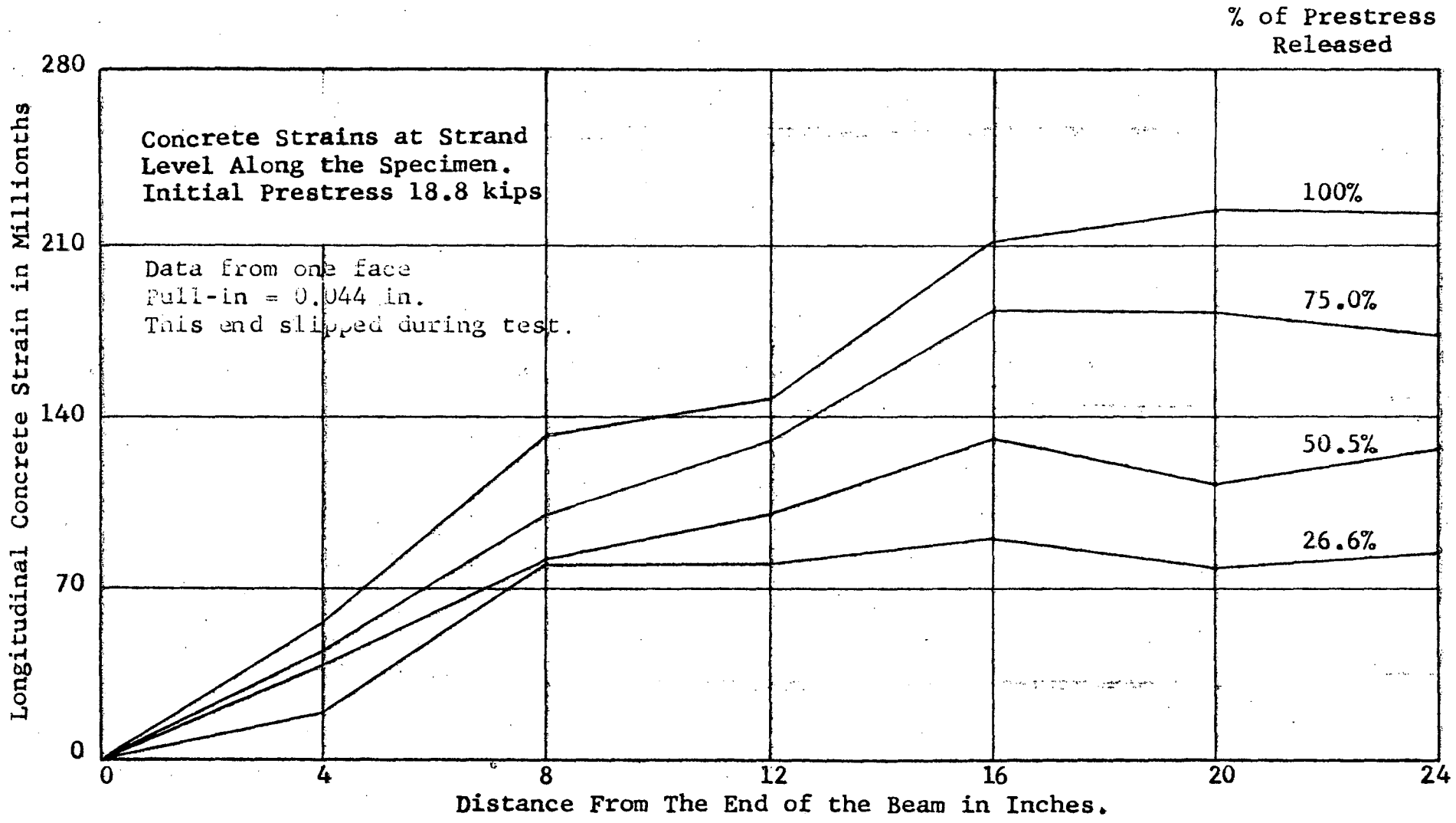

Figure C3. Development of Concrete Strains During Release. Beam B1 S-End.

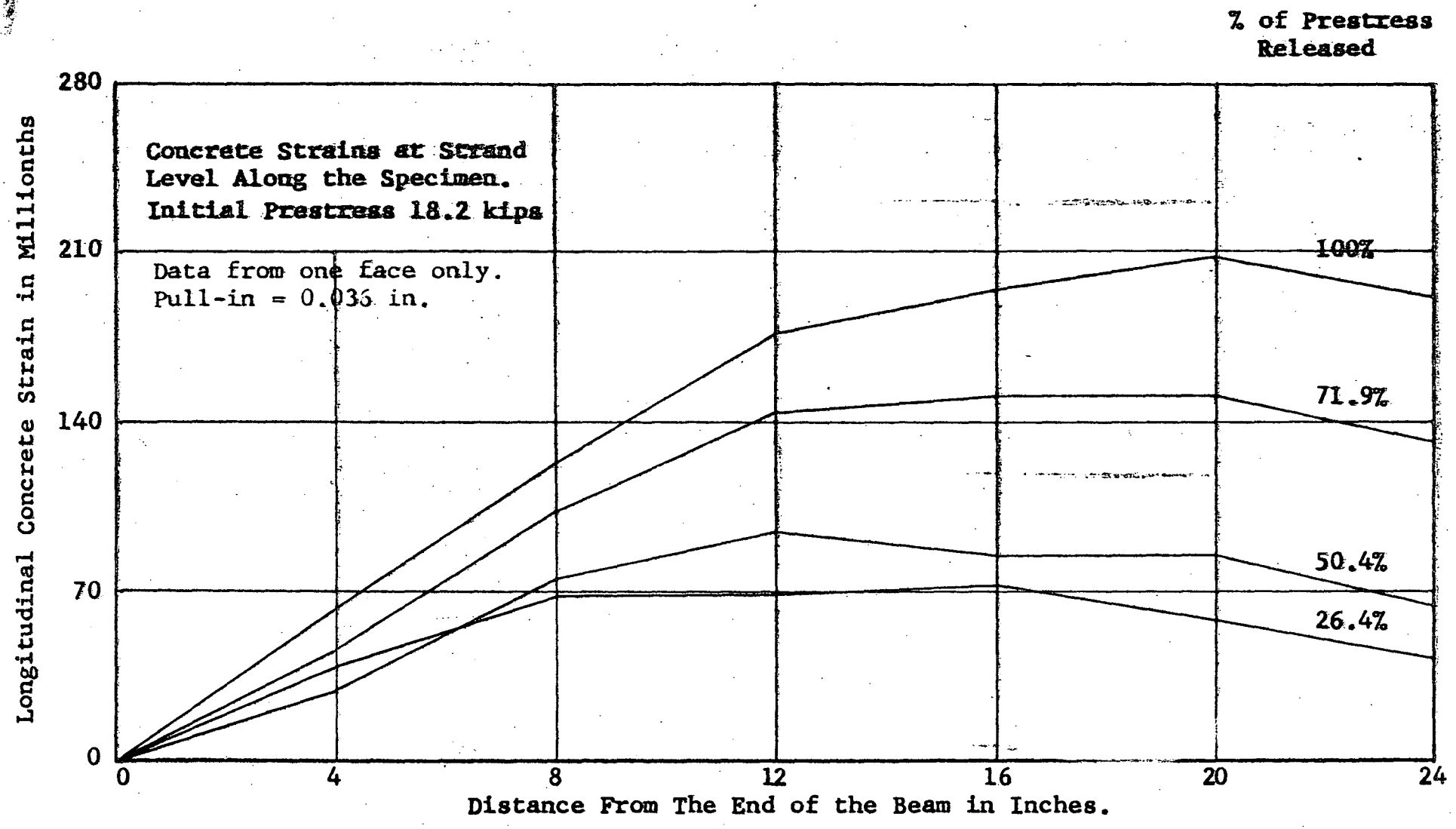

Figure 24 Development of Concrete Strains During Release. Beam B2 N-End

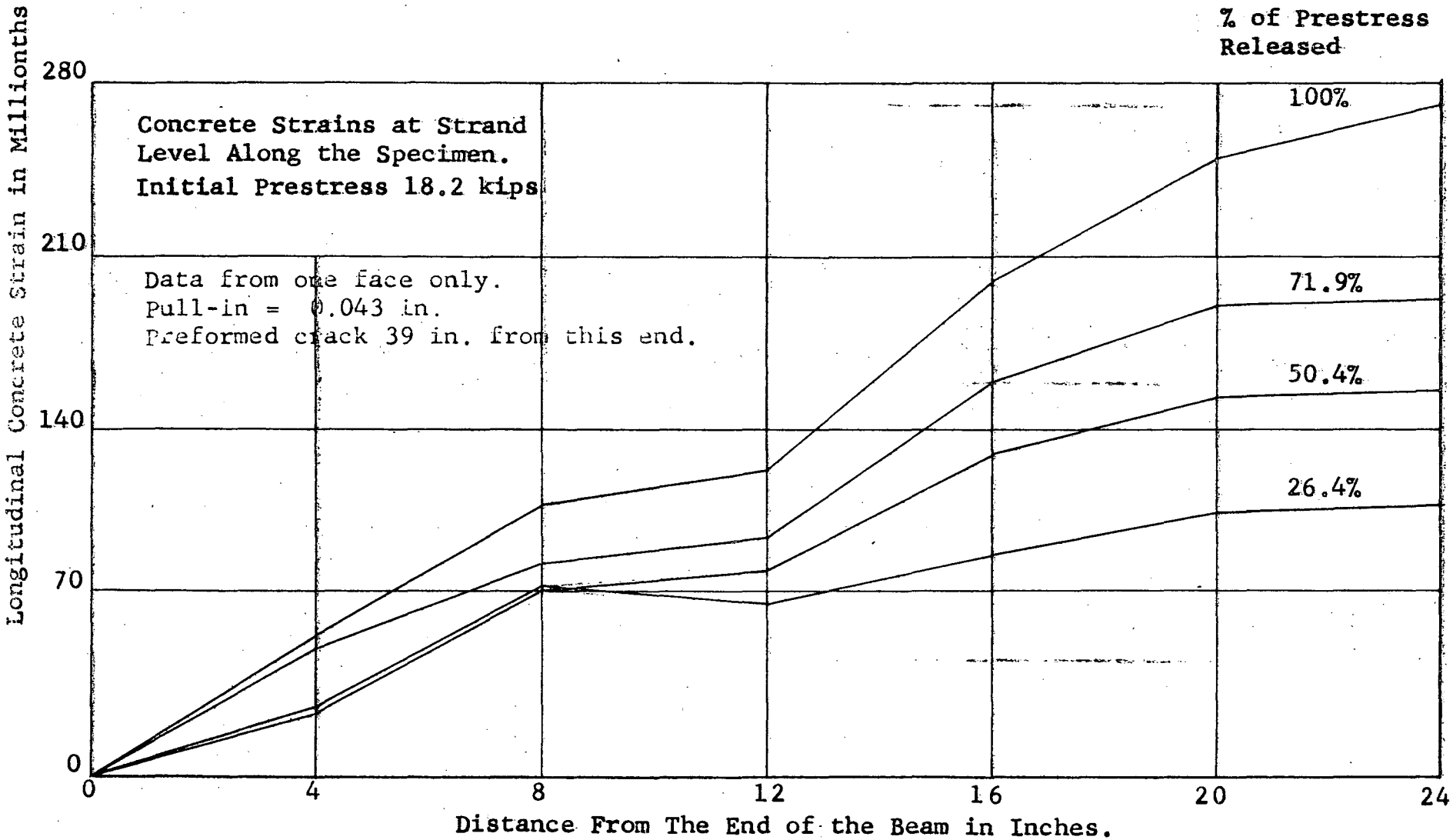

Figure C5. Development of Concrete Strains During Release. Beam B2 S-End

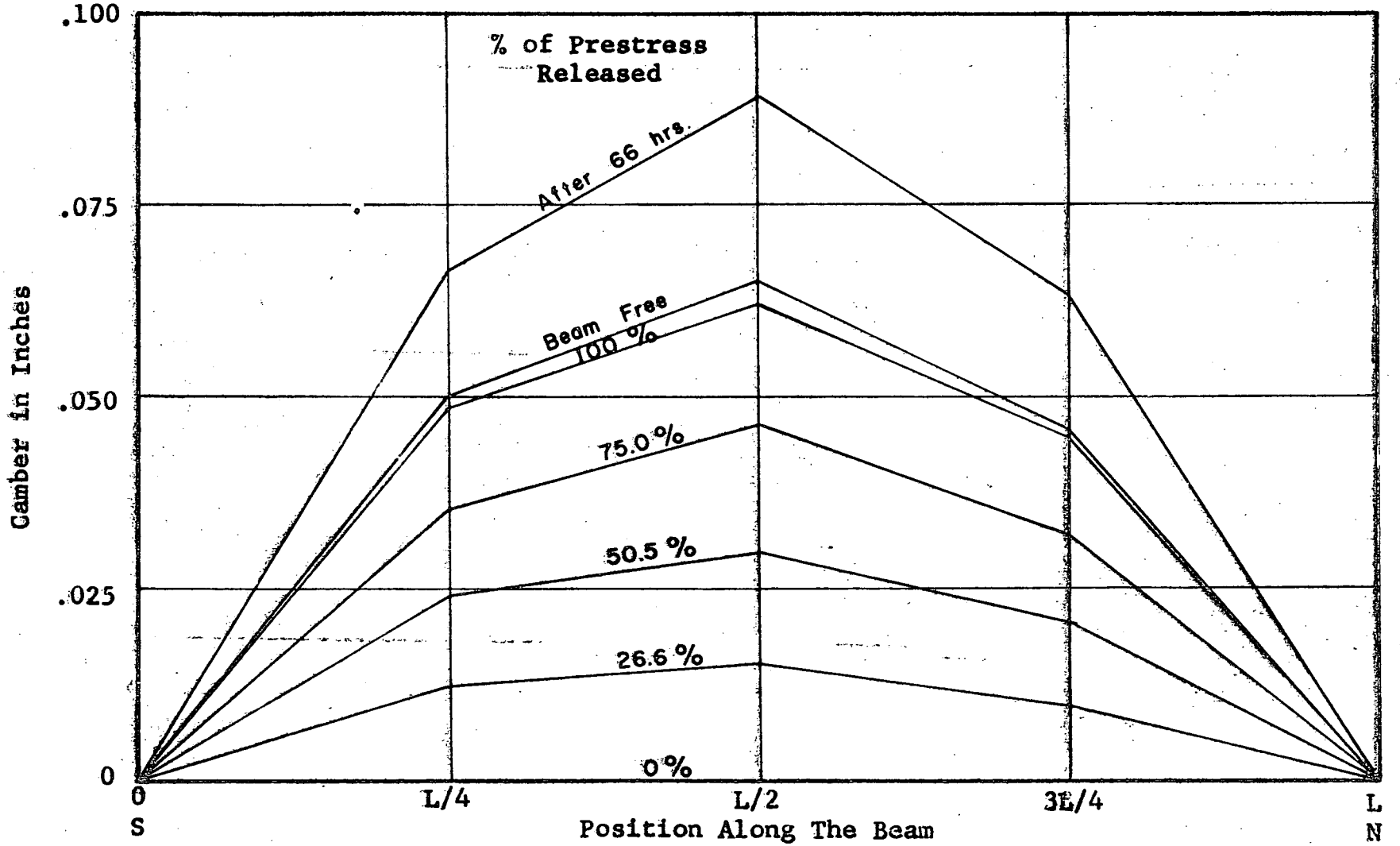

Figure 23 Camber Build-up of Beam B1 at Release.

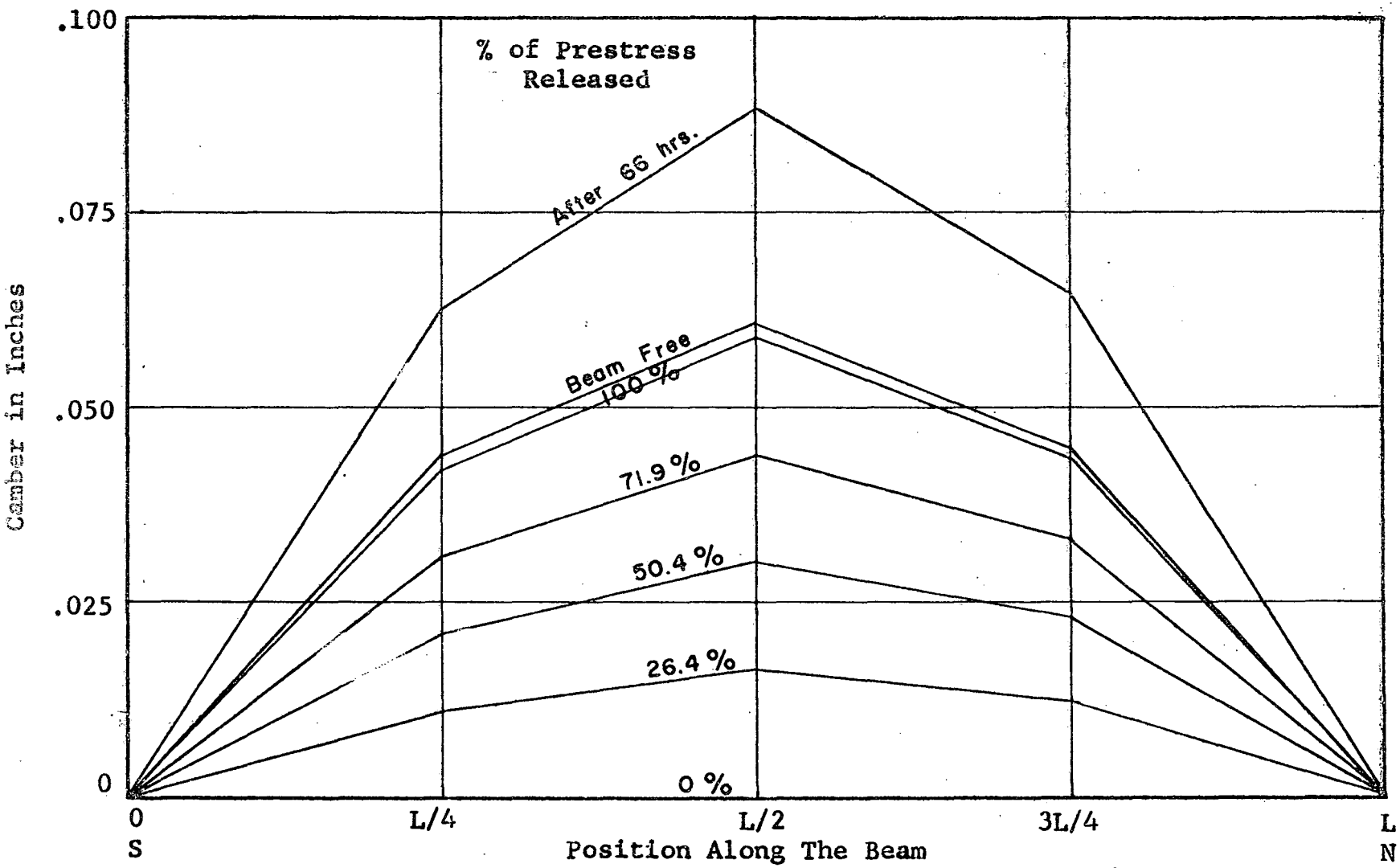

Figure C7. Camber Build-up of Beam B2 at Release.

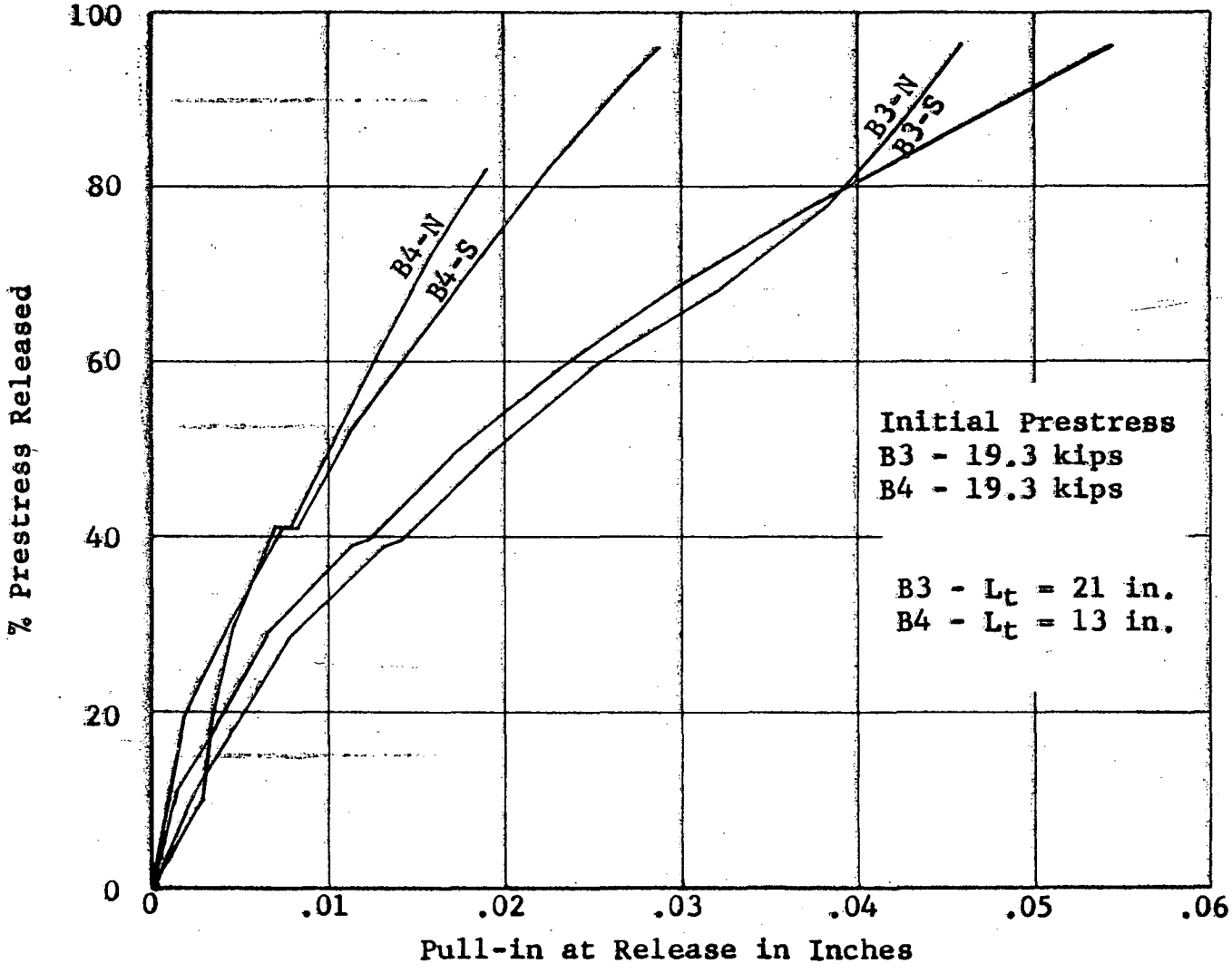

Figure 68 Progression of Slip During Release of Beams B3 and B4

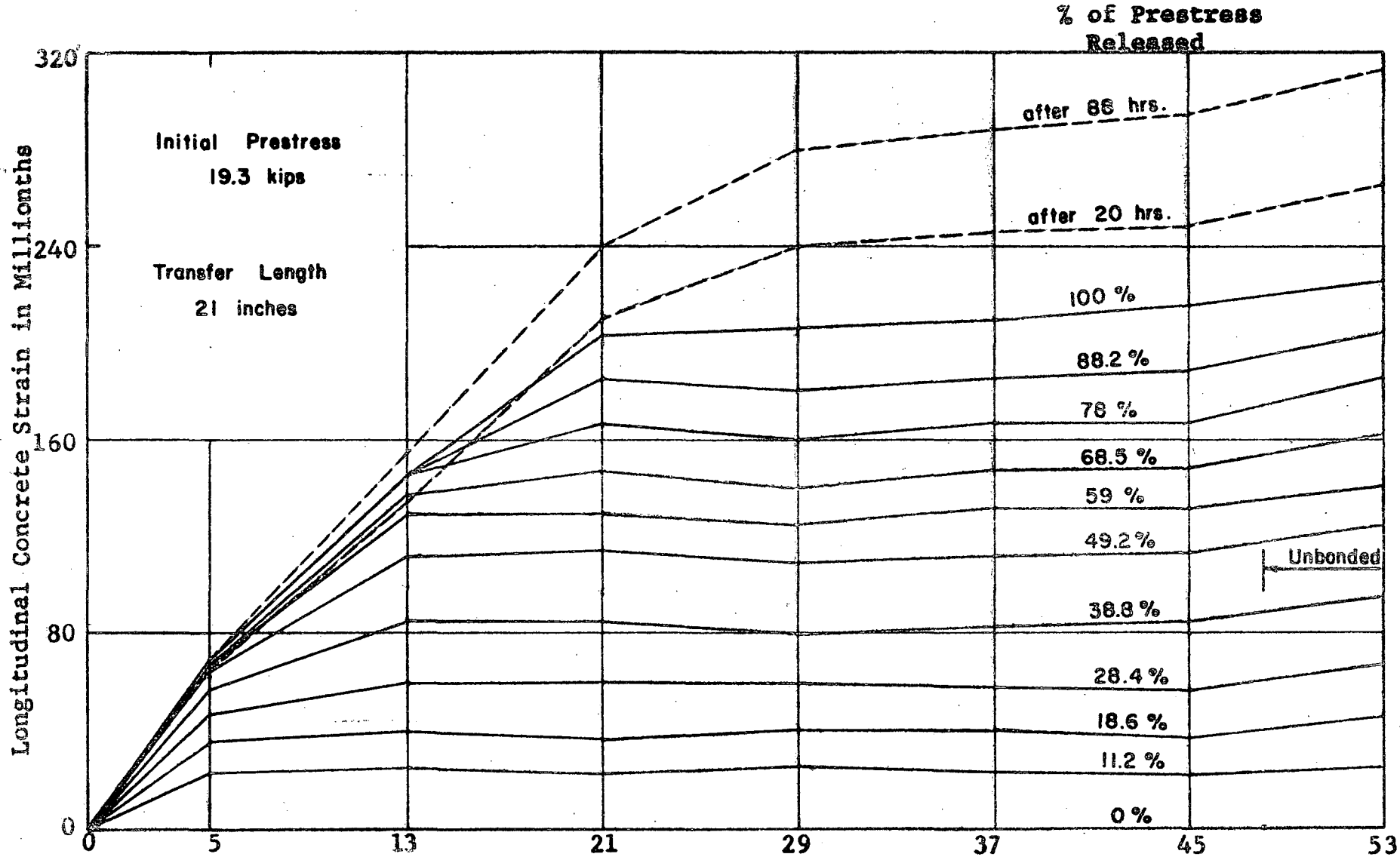

Figure 69 Development of Concrete Strains During Release, Beam B3 N-End.

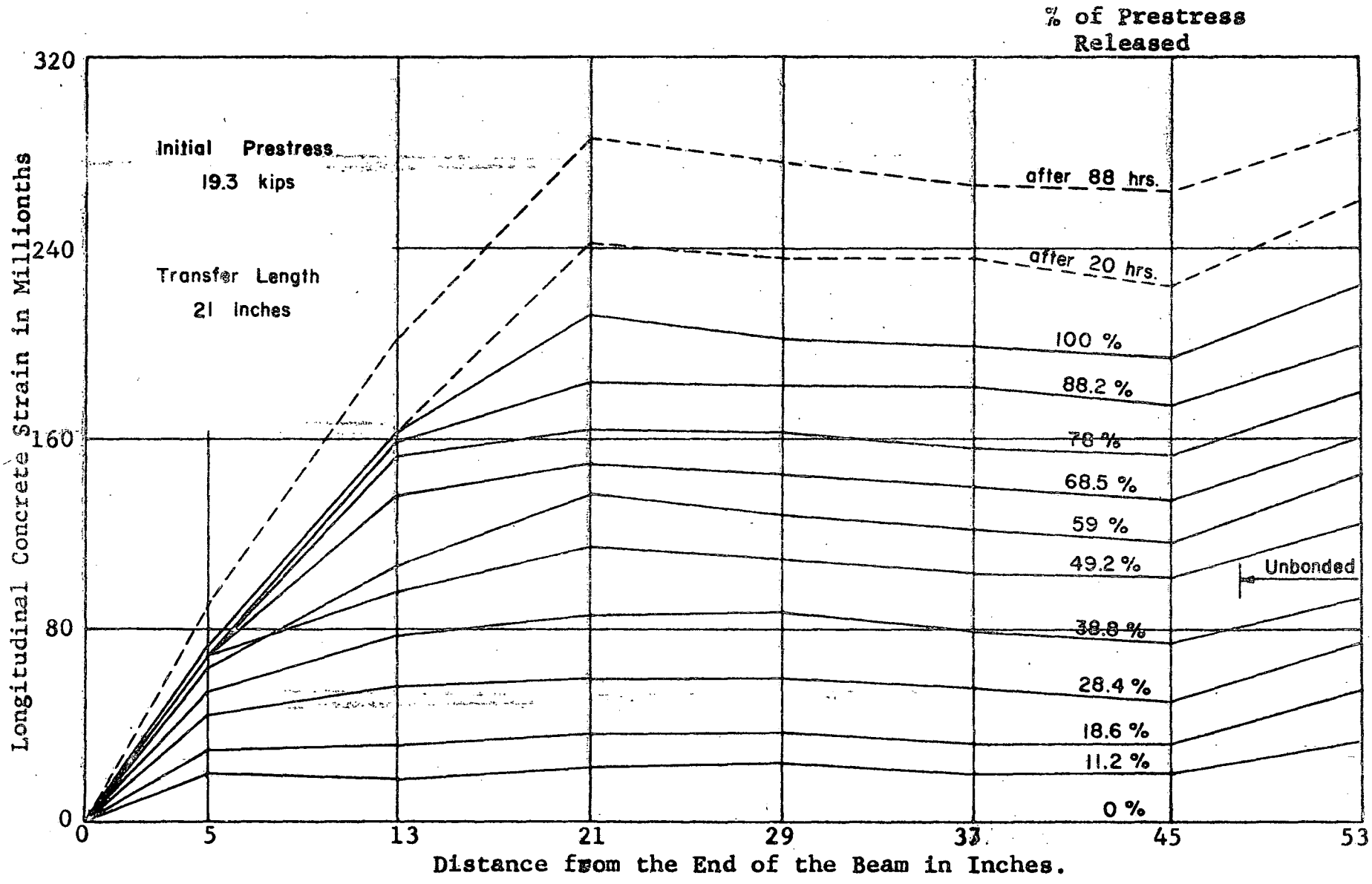

Figure C10 Development of Concrete Strains During Release
Beam B3 S-End.

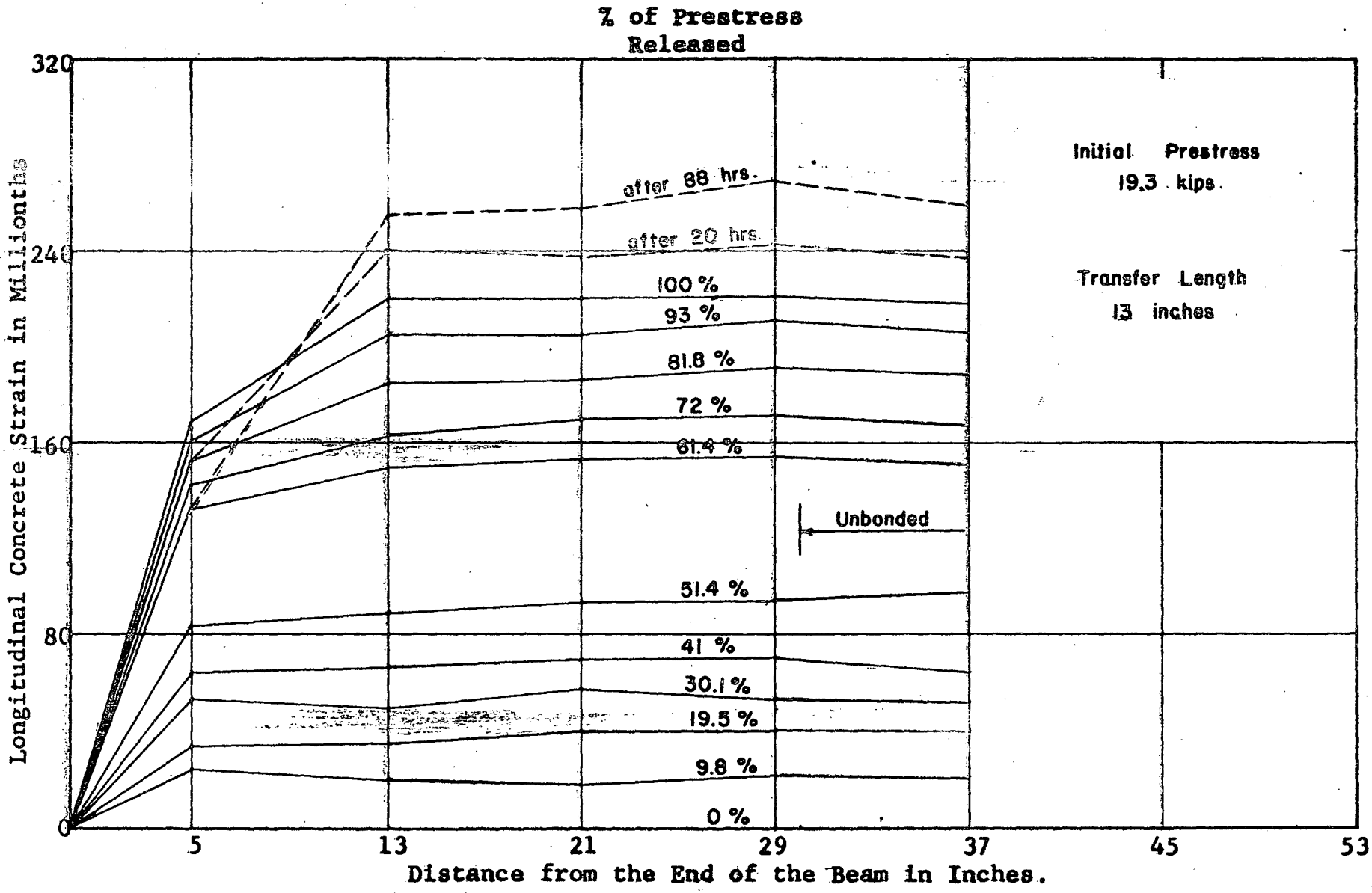

Figure C-1. Development of Concrete Strains During Release
Beam B4 N-End.

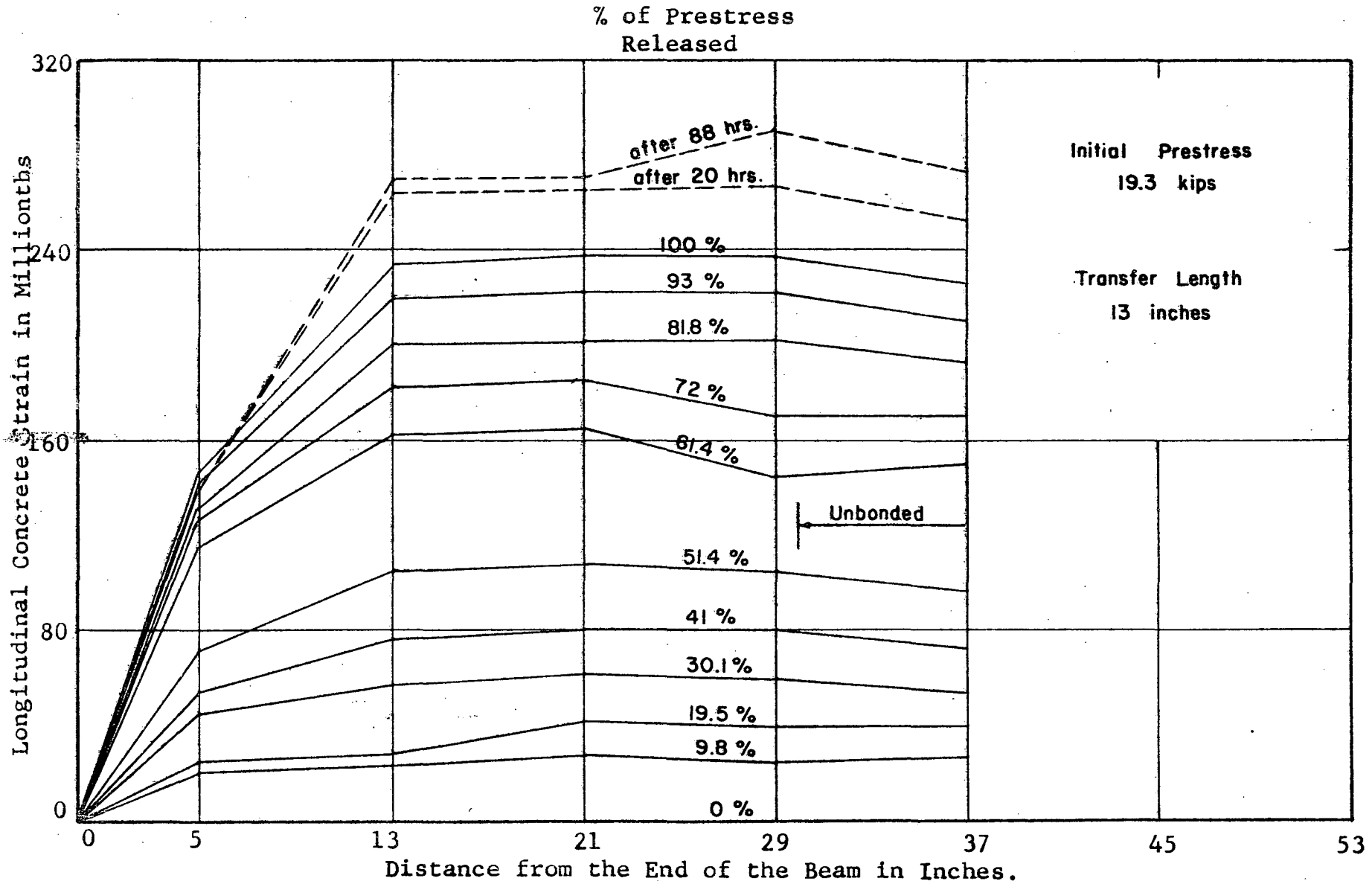

Figure 61. Development of Concrete Strains During Release
Beam B4 S-End.

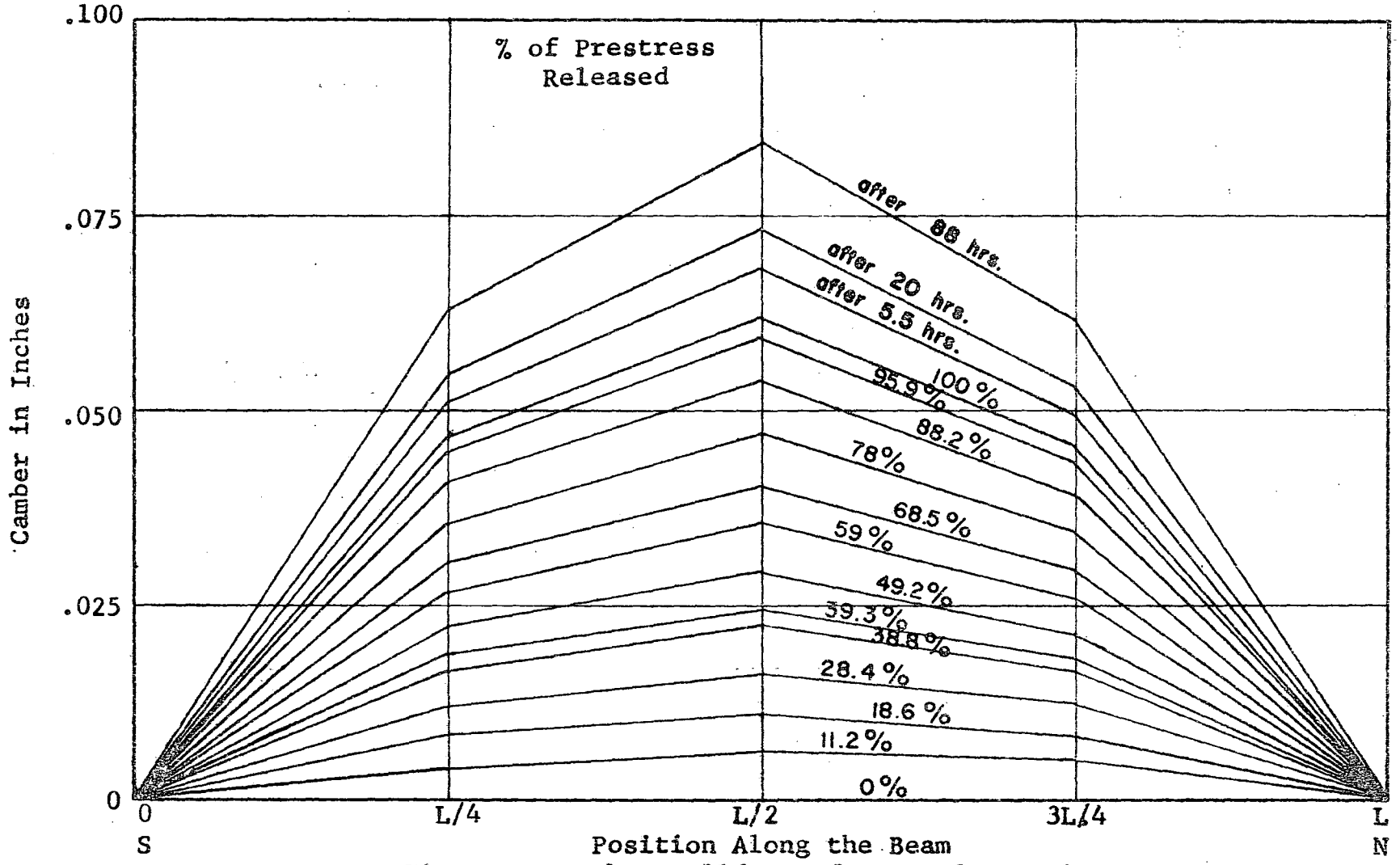

Figure C13 Camber Build-up of Beam B3 at Release.

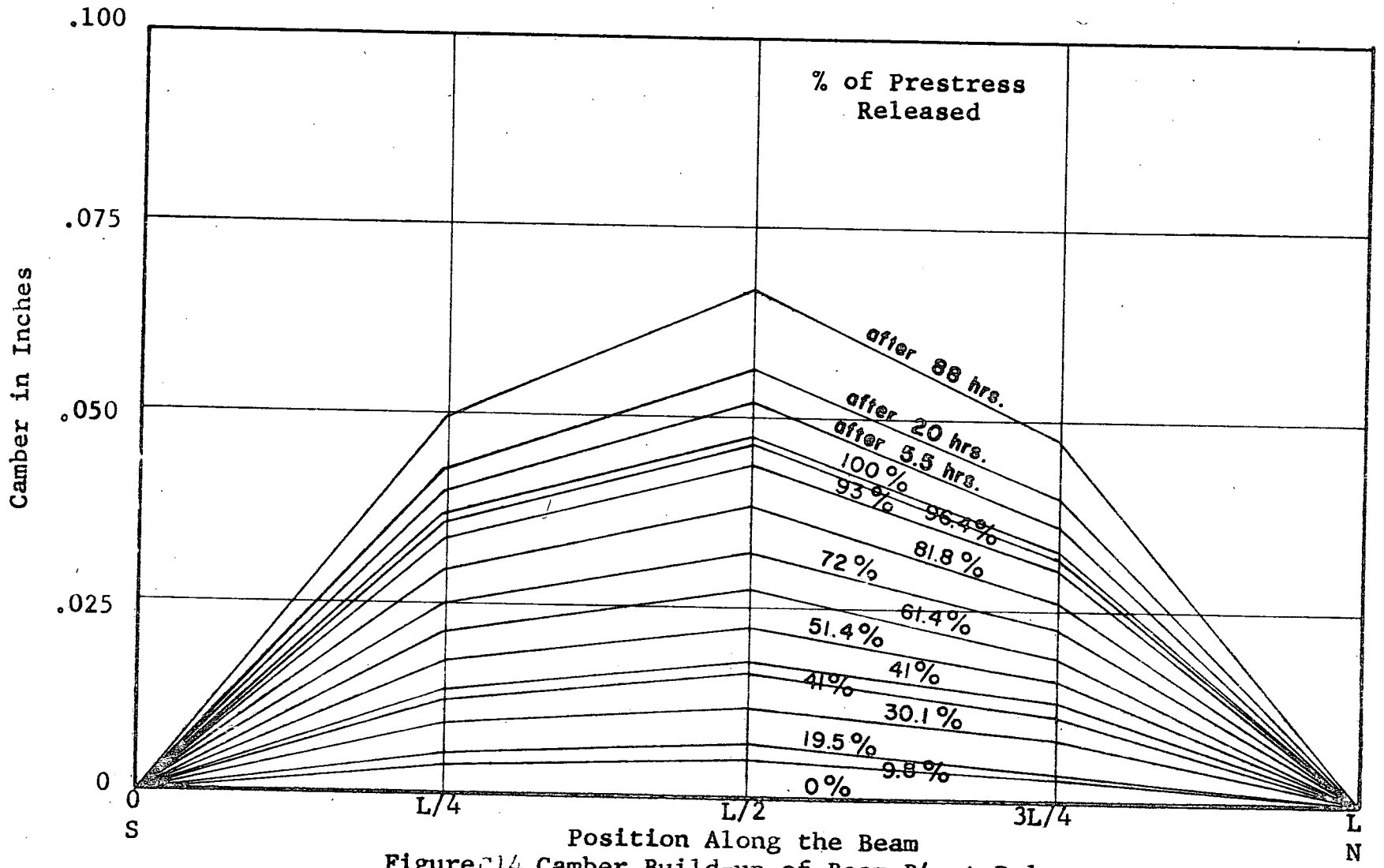

Figure 14 Camber Build-up of Beam B4 at Release.